THE UNIVERSITY OF HULL

Mitochondrial ATP production and energy-buffering in the human pathogen *Trypanosoma brucei*

being a Thesis submitted for the Degree of Doctor of Philosophy

in the University of Hull

by

Fei Gao

Bachelor in Biological Science

March 2013

Acknowledgements

I would like to give my gratitude to all those who gave me the possibility of this work.

Many thanks to:

Dr. Frank Voncken, my supervisor. I am deeply appreciate you invested so much time for help, encouragement and pushing me all the time for the research and writing. You are the one brought me to the research way.

Dr. Claudia Colasante, colleague and friend. Thanks for all your time to help me all kind experiments and data analysis. Miss your cakes.

Dr. Carmen Priscila Pena Diaz and Dr Ludovic Pelosi. Thanks for all your help for my work in the Chapter II including providing conditional ATP/ADP carrier knockout *T.brucei* cell lines and growth analysing for *T.brucei* under different nutritious condition; and the transport kinetic analysis done by Dr Ludovic Pelosi.

Mrs. Cath Wadforth, our lab mother. I would not finish my work without your preparation for all kinds of medium and solution.

Chan Kuan Yoow, Wen Liu, Mohammad Sherif and Klaus Ersfeld for sharing the lab and the talking.

All my family members and my friends for a long time support and encouragement.

Abstract

The mitochondrion plays a vital role in the cellular energy (ATP) provision of the human pathogen *Trypanosoma brucei*. ATP is produced in the mitochondrial matrix from ADP and inorganic phosphate by substrate-level and oxidative phosphorylation. To maintain the cellular energy provision, ATP has to be exported from the mitochondrial matrix, and ADP and Pi imported from the cytosol. This exchange is in eukaryotes facilitated by specific mitochondrial carrier family (MCF) proteins, i.e. the ADP/ATP carrier and the phosphate carrier located in the mitochondrial inner membrane.

The MCF protein inventory of *T. brucei* from our lab's previous study showed two putative ADP/ATP carriers, i.e. TbMCP5 and TbMCP15, and two putative phosphate carriers, i.e. TbMCP8 and TbMCP11. In order to confirm the mitochondrial carrier family proteins and further study mitochondrial energy metabolism, proteomic analysis of mitochondria in both bloodstream form and procyclic form *T. brucei* were performed. The preliminary results showed that many enzymes required for TCA cycle, lipid metabolism, amino acid metabolism, nucleotide metabolism exist in both bloodstream form and procyclic form *T.brucei.* (Data were not shown in this thesis). Functional characterisation of TbMCP5 and TbMCP15 (Chapter II) revealed that only TbMCP5 functions as a mitochondrial ADP/ATP carrier, while the function of TbMCP15 remains unknown. TbMCP5 is able to functionally complement growth of ADP/ATP-carrier deficient *Saccharomyces cerevisiae* on a non-fermentable carbon source, and mitochondrial transport experiments (done by Ludovic Pelosi) revealed that TbMCP5 has similar biochemical ADP/ATP transport kinetics to the prototypical ADP/ATP carrier ScAnc2p from yeast. Silencing of TbMCP5 expression confirmed that this MCF protein is essential for the survival of the procyclic form *T. brucei* and represents the only ADP/ATP exchanger present in the procyclic form mitochondrion. Functional characterisation of the putative mitochondrial phosphate carriers TbMCP8 and TbMCP11 (Chapter III) revealed that only TbMCP11 is expressed in the bloodstream form and procyclic form of *T. brucei*. Silencing of TbMCP11 expression in the bloodstream form had no effect on growth, whereas in the procyclic form it resulted in a lethal growth phenotype. Heterologous expression of TbMCP11 in mitochondrial phosphate carrier-deficient *S. cerevisiae* restored its

growth on a non-fermentable carbon source as well as the phosphate-dependent swelling of its mitochondria.

ATP exported from the mitochondrion is either directly used by the rest of the cell or stored as an energy buffer, which can be used during periods of high energy demand. The phosphoarginine/arginine kinase energy (ATP) buffering system of *T. brucei* consists of three different arginine kinase isoforms, i.e. TbAK1-3 (Chapter IV). The TbAK1-3 isoforms are localised in different subcellular compartments, here respectively the flagellum, glycosome and cytosol, and are dependent on the presence of specific organellar targeting signals. Silencing of total TbAK expression in the procyclic form of *T. brucei* resulted in a significant growth defect, and was even lethal in the presence of the oxidative challenging agent hydrogen peroxide. These results suggest an important role of the *T. brucei* phosphoarginine/arginine kinase energy-buffering system in oxidative stress defence. Additional roles of the TbAK isoforms in the different subcellular compartments are proposed.

In conclusion, the mitochondrial ADP/ATP carrier TbMCP5 and phosphate carrier TbMCP11, and the TbAK1-3-dependant energy buffering system play an essential role in the maintenance of the *T.brucei* energy metabolism.

Author's declaration

I hereby certify that the work presented in this thesis is entirely my own unless otherwise stated. I confirm that:

Where the published work of others has been consulted it has been clearly cited.

I have acknowledged all main sources of help.

Where the thesis work was done jointly with others, I have made clear what was done by others and what was contributed by myself.

This work was carried out in the University of Hull, Biological Science department, under the supervision of Dr. Frank Voncken, between September 2009 and February 2013.

Fei Gao

Table of contents

Abbreviations..... i

Chapter I Introduction…….…….....1

1. *Trypanosoma brucei* and African Sleeping Sickness.....2

2. Morphology of *Trypanosoma brucei* 3

3. Life cycle of *Trypanosoma brucei* 5

4. Overview of important cell biological peculiarities found in *T. brucei* 7

4.1. The kinetoplast and mitochondrial RNA editing 7

4.2. *Trans*- and *cis*-splicing in *T. brucei*.....9

4.3. Variant Surface Glycoprotein (VSG) and antigenic variation 10

4.4. Trypanothione and anti-oxidative defence 11

4.5. Purine salvage.....11

4.6. The glycosome 12

4.7. The T. brucei mitochondrion.....13

5. Treatment of Sleeping Sickness 15

6. The *T. brucei* energy metabolism 17

7. Mitochondrial Carrier Family proteins 24

8. The MCF protein inventory of *T.brucei*.....30

9. The mitochondrial ADP/ATP carrier 33

10. The mitochondrial phosphate carrier 36

11. Energy-buffering in *T. brucei* 40

12. Aim of the PhD project 43

References 44

Chapter II Functional Characterisation of TbMCP5, a Conserved and Essential ADP/ATP Carrier Present in the Mitochondrion of the Human Pathogen

***Trypanosoma brucei*.**……...……..….69

1. Introduction.....71

2. Materials and methods.....73

2.1 Chemicals.....73

2.2 Yeast complementation.....74

2.3 ADP/ATP transport assays for yeast mitochondria.....74

2.4 ATR and CATR binding assays.....75

2.5 Mitochondrial cytochrome *aa3* content.....76

2.6 TbMCP5 peptide-antibody.....76

2.7 Culture of *T. brucei* cell lines.....76

2.8 Protein quantification, western blot analysis and immunofluorescence Microscopy.....77

2.9 Northern blot analysis.....78

2.10 Generation of the conditional TbMCP5 double-knockout cell line.....78

2.11 ATP production by *T. brucei* mitochondria.....79

2.12 Metabolite analysis.....80

2.13 Depletion of TbMCP5 by RNA interference.....80

3. Results.....82

3.1 Sequence analysis of TbMCP5 and TbMCP15.....82

3.2 Functional complementation analysis of *S. cerevisiae JL1Δ2Δ3u-*.....86

3.3 Mitochondrial localisation and quantification of TbMCP5 in *JL1Δ2Δ3u-*.....91

3.4 ADP/ATP-transport kinetics of TbMCP5 in comparison to ScAnc2p.....93

3.5 TbMCP5 is exclusively mitochondrial and differentially expressed in *T. brucei* 95

3.6 Silencing and depletion of TbMCP5 in PCF trypanosomes.....96

3.7 TbMCP5-depletion eliminates mitochondrial ADP/ATP transport in *T. brucei*.....102

3.8 Depletion of TbMCP5 and its effect on the PCF energy metabolism.....103

4. Discussion.....106

References.....111

Chapter III The mitochondrial phosphate carrier TbMCP11 is essential for growth of procyclic form *Trypanosoma brucei*.....118

1. Introduction.....119

2. Material and Methods.....121

2.1 Cell culture and transfection.....121

2.2 Phylogenetic reconstruction and sequence analysis.....121

2.3 Northern blot analysis.....124

2.4 TbMCP11 polyclonal rabbit antibody and Western blot analysis.....124

2.5 *T. brucei* cell lines expressing recombinant myc-tagged TbMCP11.....125

2.6 Immunofluorescence microscopy.....126

2.7 Generation of the BSF ΔTbMCP11 double knockout cell line.....126

2.8 Generation of the PCF TbMCP11-RNAi cell line.....127

2.9 Growth analysis.....128

2.10 Mitochondrial ATP production assay.....128

2.11 Mitochondrial oxygen consumption.....129

2.12 Scanning electron microscopy (SEM).....130

2.13 Yeast complementation.....130

2.14 Mitochondrial swelling assay.....131

3. Results.....132

3.1 The *T. brucei* genome codes for two putative mitochondrial phosphate carriers.....132
3.2 Differential expression of TbMCP11 in *T. brucei*.....138
3.3 TbMCP11 is exclusively mitochondrial in BSF and PCF *T. brucei*.....141
3.4 TbMCP11 functionally complements mitochondrial Pi-carrier deficiency in the yeast Δ*mir1*Δ*pic2*.....141
3.5 TbMCP11 is essential for growth of PCF, but not BSF *T. brucei*.....146
3.6 Lack of Pi transport in mitochondria from TbMCP11-depleted PCF *T. brucei*.....149
3.7 Abnormal cell morphology and loss of mitochondrial membrane potential in TbMCP11-depleted PCF *T. brucei*.....150
3.8 TbMCP11 is required for mitochondrial respiration and ATP production.....154
4. Discussion.....157
References.....166
Chapter IV The phosphoarginine energy-buffering system of *Trypanosoma brucei* is essential for survival and involves multiple arginine kinase isoforms with different subcellular locations.....176
1. Introduction 178
2. Materials and methods.....180
2.1 Sequence analysis.....180
2.2 Isolation of recombinant TbAK1-nHis.....180
2.3 Measurement of arginine kinase activity.....181
2.4 Phosphoarginine synthesis and analysis.....182
2.5 Trypanosome culture.....183
2.6 Western blot analysis.....183

2.7 Northern blot analysis..... 184
2.8 Expression of myc-tagged TbAK1-3..... 184
2.9 Immunofluorescence microscopy..... 186
2.10 RNA interference..... 186
2.11 Growth analysis..... 187
3. Results..... 188
3.1 Sequence analysis..... 188
3.2 Arginine kinase activity of TbAK1..... 192
3.3 Subcellular location of TbAK1-3..... 195
3.4 Life cycle stage-dependent expression..... 203
3.5 Overexpression, oxidative stress and growth..... 205
3.6 Silencing of TbAK expression..... 208
4. Discussion..... 210
References..... 217
Chapter V Discussion and Conclusion.....224
Discussion.....225
Conclusions.....232
References.....234
Appendix 1, medium used for *T.brucei* culture.....238
Appendix 2, medium used for yeast culture.....241
Appendix 3, yeast strains used for transformation.....242

Abbreviation

ACH	Acetyl-CoA Thioesterase
ADP	Adenosine Diphosphate
ANC	Mitochondrial Adenine Nucleotide Carrier (ADP/ATP carrier) coding gene
Ancp	Adenine Nucleotide Carrier Protein (ADP/ATP carrier)
ASCT	Acetate:Succinate CoA-transferase
ATP	Adenosine Triphosphate
ATR	Atractyloside
Ap5A	Diadenosine 5'-pentaphosphate
BA	Bonkrekic Acid
BCA	Bicinchoninic Acid
BSD	Blasticidin
BSF	Bloodstream Form
CATR	Carboxyatractyloside
CBB	Coomassie Brilliant Blue
CCCP	Carbonyl Cyanide m-Chlorophenyl Hydrazine
CP	Contact Point
DAPI	4',6-Diamidino-2-phenyl-indole
DDM	*n*-Dodecyl-β-D-Maltoside
DNA	Deoxyribonucleic Acid
ECL	Enhanced Chemiluminescence
EDTA	Ethylenediaminetetraacetic Acid
ER	Endoplasmic Reticulum
FAD	Flavin Adenine Dinucleotide
FBS	Foetal Bovine Serum
GFP	Green Fluorescent Protein
GPI	Glycosylphosphatidylinositol
GSH	Glutathione
HMI	Hirumi's Modified Iscove's Medium
HPLC	High-performance liquid chromatography
HYG	Hygromycin
HRP	Horseradish Peroxidase

HSP60	Heat Shock Protein 60
IMS	Intermembrane Space
KO	Knockout
MCF	Mitochondrial Carrier Family
MEM	Minimum Essential Medium
MIM	Mitochondrial Inner Membrane
MOM	Mitochondrial Outer Membrane
MTP	Mitochondrial Transition Pore
NADH	Nicotinamide Adenine Dinucleotide Reduced
N-ADP	3'-*O*-(1-naphthoyl)-adenosine 5'-diphosphate
NEM	N-ethylmaleimide
NEO	Neomycin
OMIM	Online Mendelian Inheritance in Man
ORF	Open Reading Frame
PARP	Procyclic Acidic Repetitive Protein
PBS	Phosphate-buffered Saline
PCF	Procyclic Form
PCR	Polymerase Chain Reaction
PEP	Phosphoenolpyruvate
PEPCK	Phosphoenolpyruvate Carboxykinase
3-PGA	3-Phosphoglycerate
PGK	Phosphoglycerate Kinase
Pi	Inorganic Phosphate
PTS1	Type 1 Peroxisomal Targeting Signal
RNAi	RNA interference
ScAnc2p	Isoform 2 of *Saccharomyces cerevisiae* Ancp
SDM	Semi-defined Medium
SDS	Sodium Dodecyl Sulfate
SDS-PAGE	Sodium Dodecylsulfate-containing Polyacrylamide Gel
SEM	Scanning Electron Microscopy
SCoAS	Succinyl-CoA Synthase
SoTE-buffer	Sorbitol Tris EDTA buffer
SRP	Signal Recognition Particle

TAO	Trypanosome Alternative Oxidase
TbMCP	*Trypanosoma brucei* Mitochondrial Carrier Family Protein
TBS	Tris–buffered Saline
TBS-T	Tris–buffered Saline-Tween 20
TCA	Tricarboxylic Acid
TM	Transmembrane
TXN	Tryparedoxin
tet	Tetracycline
VSG	Variable Surface Glycoprotein
WB	Western Blot
WT	Wild Type
YNB	Yeast Nitrogen Broth medium
YPD	rich Yeast extract Peptone Dextrose medium
YPG	rich Yeast extract Peptone Glycerol medium
YPL	rich Yeast extract Peptone Lactate medium

Chapter I

Introduction

1. *Trypanosoma brucei* and African Sleeping Sickness

Trypanosoma brucei is a protozoan parasite belonging to the Order of Kinetoplastida (Embley and Martin, 2006). *T. brucei* branched very early in evolution and is one of the earliest known aerobic eukaryotes containing a functional mitochondrion (Cavalier-Smith, 1981, Embley and Martin, 2006, Bringaud et al., 2006). It is characterised by the presence of a large specialized mitochondrial DNA structure called the kinetoplast (Simpson, 1973). There are three different *T. brucei* subspecies that cause disease in mammals (Fevre et al., 2005). *T. b. gambiense* is the causative agent of West African Sleeping Sickness, a chronic disease mainly found in west and central Africa, while *T. b. rhodesiense* causes East African Sleeping Sickness, a more acute and virulent disease that is prevalent in eastern parts of Africa (Gibson, 1986). The third subspecies *T. b. brucei* does not affect humans, but causes the wasting disease 'Nagana' in vertebrate animals and is found in large parts of sub-Saharan Africa (http://www.who.int). Transmission of the different *T. brucei* subspecies takes place via a bite of the tsetse fly, a blood-sucking insect vector that predominantly inhabits woodland and savannah areas.

Before 2005, approximately 50,000 to 70,000 new infections occurred in Africa each year, whereas more recently the annual case numbers dropped to below 10,000 per year as a result of the continuing control efforts by the WHO (WHO, 2012). However, many *T. brucei*-related infection cases are not reported as a consequence of the lack of proficient health care provision in many African countries. The true number of *T. brucei*-infected patients is therefore expected to be much higher (http://www.who.int).

The development of Sleeping Sickness in humans can be divided into two main stages. During the first or hemolymphatic stage, trypanosomes multiply in the blood,

lymph and spinal fluids, which causes fever, headache, joint and muscle pains, as well as extreme fatigue in the patient (Apted, 1970). During the second stage, also called the meningoencephalitic or neurological stage, trypanosomes cross the blood-brain barrier and invade the central nervous system. Patients in this stage will suffer severe disturbances of the circadian sleeping rhythm (somnolence) and profound changes in behaviour, finally followed by loss of consciousness and coma. Infected patients invariably die within months when left untreated (Stich et al., 2002, Kennedy, 2006).

2. Morphology of *Trypanosoma brucei*

T. brucei is a motile, single celled eukaryote. It contains all major organelles like other eukaryote cells, such as a nucleus, endoplasmic reticulum (ER), golgi and mitochondrion (Figure 1 (Overath and Engstler, 2004)). Its motility is provided by a single flagellum, which for a large part is attached to the main cell body by an undulating membrane. The flagellum originates close to the flagellar pocket and the kinetoplast, a unique mitochondrial DNA structure found in all members of the Kinetoplastida Order (Parsons et al., 2001, Overath and Engstler, 2004). *T. brucei* further contains a peroxisome-like microbody called the glycosome, since it compartmentalises most of the glycolytic pathway (Parsons et al., 2001, Parsons, 2004).

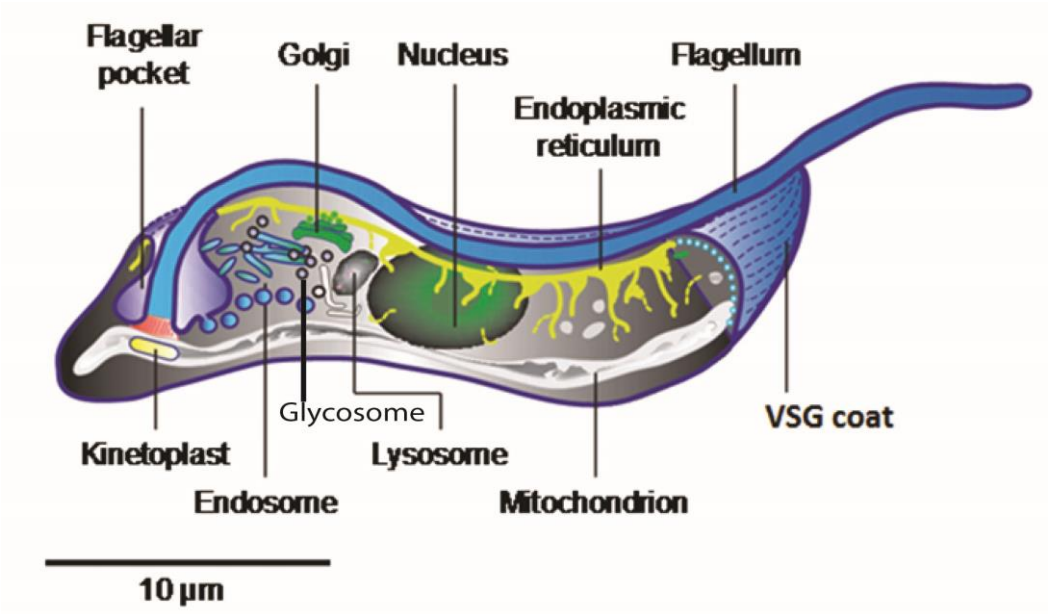

Figure 1: Schematic representation of the overall cell structure of bloodstream form *Trypanosoma brucei*. Abbreviations: VSG, Variable Surface Glycoprotein. (Source: (Overath and Engstler, 2004))

3. Life cycle of Trypanosoma brucei

Trypanosoma brucei has a complex life cycle and undergoes many developmental changes when alternating between the mammalian and the tsetse fly hosts. A schematic representation of the *T. brucei* life cycle is shown in Figure 2. The *T. brucei* life cycle starts with the infectious metacyclic trypanosomes, which are injected from the tsetse fly salivary gland into the mammalian bloodstream when the tsetse fly takes a blood meal (Matthews et al., 2004). In the mammalian bloodstream, the non-dividing metacyclic trypanosomes differentiate into long slender trypanosomes, also called the bloodstream form. This form multiplies by binary fission and is expressing an immuno-protective surface coat consisting of variable surface glycoprotein (VSG) (Barry and McCulloch, 2001, Vickerman and Luckins, 1969). The bloodstream form subsequently differentiates into the stumpy form, which is non-dividing and can again be taken up by another tsetse fly when taking a blood meal (Vassella et al., 1997, Tyler et al., 1997). In the tsetse fly, the stumpy form differentiates into the procyclic form, which multiplies in the midgut of the insect vector and is expressing a protective protein surface coat consisting of procyclin (Roditi et al., 1989). After differentiation into epimastigotes, they multiply by binary fission in the salivary gland of tsetse fly. The epimastigotes finally differentiate again into the infective metacyclic form, bringing us back to the start point of the life cycle (Matthews, 2005).

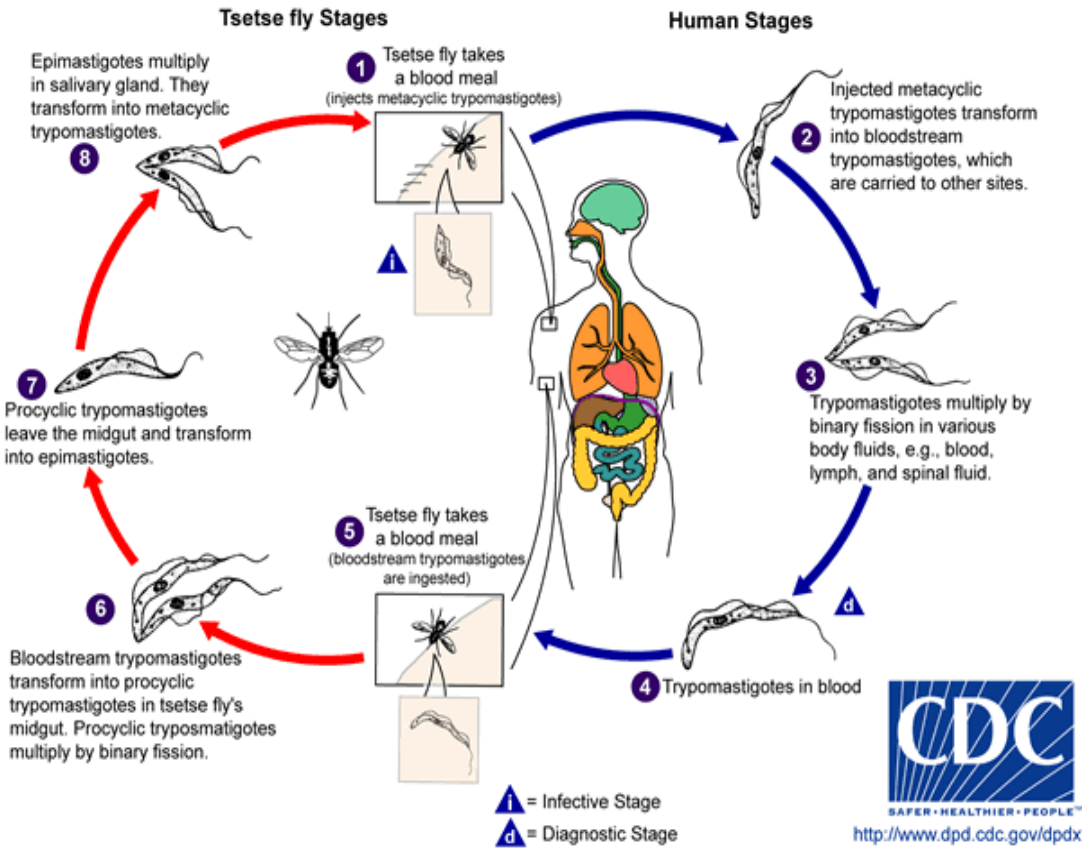

Figure 2: Life cycle of *Trypanosoma brucei* (Source: CDC). The life cycle of *T.brucei* start from a blood meal containing infectious metacyclic trypomastigotes token by tsetse fly. The metacyclic trypomastigotes were injected to host bloodstream and transform to bloodstream trypomastigotes. Bloodstream trypomastigotes then multiply in various host body fluids and enter the tsetse fly's midgut with procyclic trypomastigotes after taking a blood meal. After procyclic trypomastigotes multiply in the tsetse fly's midgut, they transform to epimastigotes and enter salivary gland. In salivary gland epimastigotes multiply and transform into metacyclic trypomastigotes which is ready for the next meal to inject into host bloodstream.

4. Overview of important cell biological peculiarities found in *T. brucei*

4.1. The kinetoplast and mitochondrial RNA editing

The kinetoplast is a hallmark of all Kinetoplastida and is located in the mitochondrion, near the base of the flagellum (see Fig. 1). It represents one the most unusual and complex mitochondrial DNA structures among eukaryotes , and is composed of ~50 DNA maxi circles and several thousand DNA mini circles (Simpson et al., 1980, Ray, 1987, Carpenter and Englund, 1995, Vago et al., 1996). The genes located on the DNA maxi circles mainly code for mitochondrial household proteins, while the mini circles predominantly code for guide RNAs. These guide RNAs play an essential role in mitochondrial RNA editing, a unique process initially described for subunit 2 of cytochrome *c* oxidase (Benne et al., 1986). Sequence analysis of mitochondrial mRNA revealed the insertion of four non-coding uridylates (U), leading to a "non-sense" messenger, and only upon removal of these insertions, the correct open reading frame was obtained. Later, abundant U insertions and U deletions were discovered in many other mitochondrial RNAs from *T. brucei* (Stuart, 1993). RNA editing is dependent on guide RNAs (gRNAs) and a specialised RNA-editing protein complex, called the 20S editosome (Pollard et al., 1992). A schematic representation of RNA-editing is shown in figure 3. Guide RNAs are short 3′ uridylated RNA transcripts that direct the sequence-specific endonucleolytic cleavage of precursor mRNA and subsequent U insertion/deletion by the 20S editosome (Sturm and Simpson, 1990, Blum et al., 1990). During RNA-editing, 5′ and 3′ cleaved RNA fragments are formed, which are subsequently ligated by a mitochondrial RNA ligase (Panigrahi et al., 2003, Aphasizhev and Aphasizheva, 2011). In addition and in contrast to other eukaryotes, the mitochondrial DNA of *T. brucei* does not code for

any transfer RNAs, which therefore have to be imported from the cytosol (Matthews, 2005).

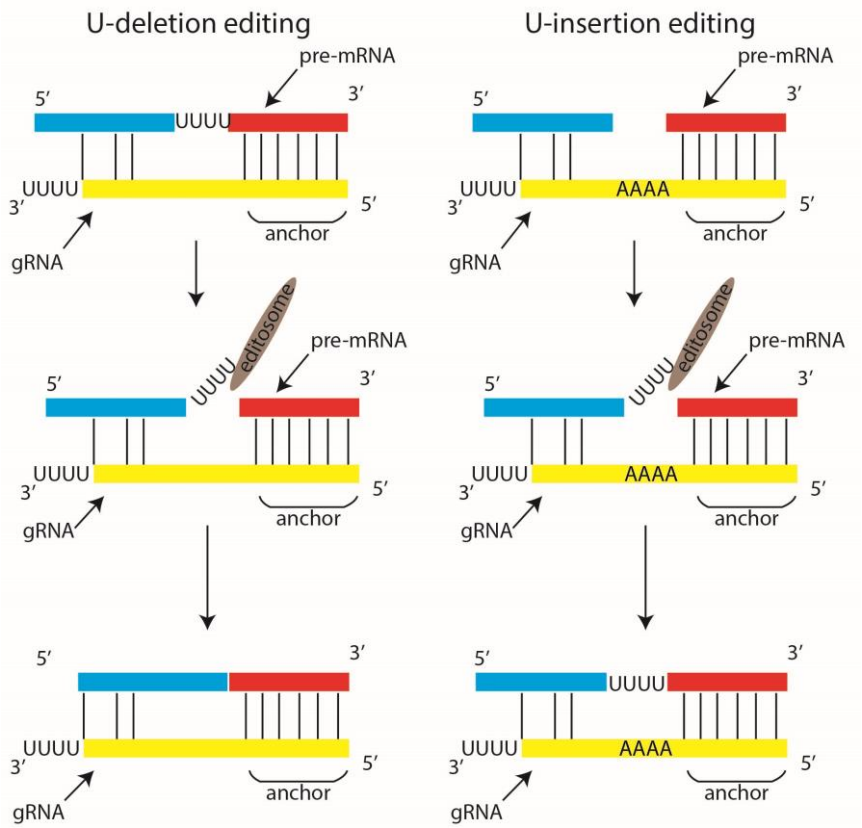

Figure 3: Schematic representation of RNA-editing in *Trypanosoma brucei*. The pre-mRNA was edited according to the guide RNA to insert or delete the uridines by editosome. Editosome is a larege protein complex which contains the enzymes for catalysing the editing and ligating the final nucleotide chain. Abbreviations: U, Uracil; A, Adenine; gRNA, guide RNA. (Adopted from (Aphasizhev and Aphasizheva, 2011)).

4.2. *Trans*- and *cis*-splicing in *T. brucei*

Another peculiarity of *T. brucei* is its ability for trans- and cis-splicing of mRNA. In general, the eukaryotes have monocistronic transcription such as *Drosophila* (Brogna and Ashburner, 1997), *Arabidopsis* (Thimmapuram et al., 2005). In contrast to other eukaryotes, expression in the *T. brucei* mitochondrion and nuclear RNA is predominantly polycistronic which is defined as one signal mRNA that encodes two or more peptides or proteins (Englund et al., 1982, Koslowsky and Yahampath, 1997, Grams et al., 2000, Daniels et al., 2010), with the resulting pre-mRNA molecules being processed into individual mRNAs via splicing (Sather and Agabian, 1985). Polycistronic transcripts are normally found in prokaryotes and rarely found in eukaryotes (Pi et al., 2009). Trans-splicing was discovered for the first time in *T. brucei* when comparing the nucleotide sequences of the 5′ ends of variant surface glycoprotein (VSG) mRNAs with those of the corresponding coding genes (Boothroyd and Cross, 1982). A schematic representation of trans-splicing is shown in figure 4. Key to this process is the addition (ligation) of a capped and 39-bp long spliced leader (SL) RNA sequence to the first exon at the 5' end of mRNA molecules during splicing (Sather and Agabian, 1985, Liang et al., 2003). The SL RNA sequences and the spliced genes are in general coded for in different parts of the *T. brucei* genome, hence the process is called "trans"-splicing (Agabian, 1990). Trans-splicing was later also found in some higher eukaryotes, including nematodes, plants and animals (reviewed in (Bonen, 1993)).

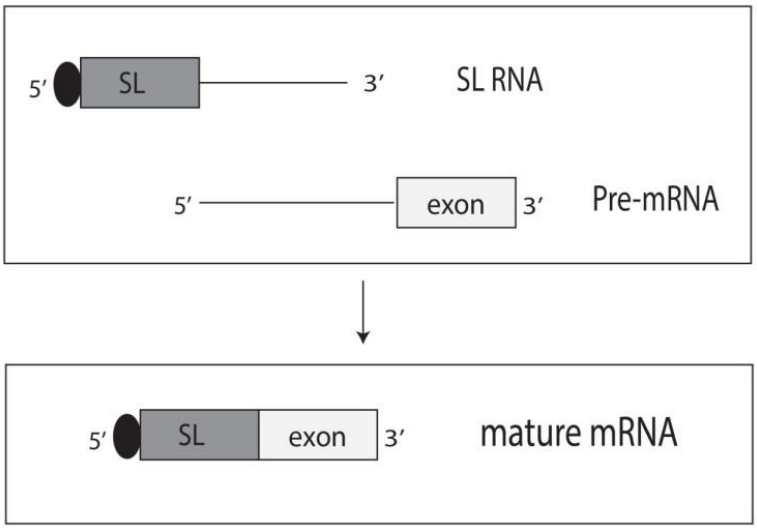

Figure 4: Schematic representation of trans-splicing in *T. brucei*. Spliced leader (SL) RNA sequence and pre-mRNA were ligated together and formed matured mRNA. SL RNA is composed with a 5' cap and a 39-bp long RNA sequence. Abbreviations: SL, Spliced Leader. (Adopted from (Liang et al., 2003))

4.3. Variant Surface Glycoprotein (VSG) and antigenic variation

T. brucei is constantly challenged by the immune system in the human bloodstream (Stockdale et al., 2008, Barry et al., 2005, Pays et al., 1989). To evade recognition by the human complement and subsequent immune response and destruction, the parasite expresses a dense coat of Variant Surface Glycoprotein (VSG) on its surface (Stockdale et al., 2008, Pays et al., 1989). These VSG proteins are attached to the plasma membrane by a glycosylphosphatidylinositol (GPI) anchor (Martin and Smith, 2006). The *T. brucei* genome contains a substantial number (up to 20% of total genome) of different VSG genes and pseudogenes, and through homologous recombination it is able to create an indefinite reservoir of novel VSG molecules (Marcello and Barry, 2007). *T. brucei* expresses only a single VSG at any given time, and upon an immunogenic challenge it can switch its VSG coat for another coat made

up of a different VSG molecule, a process called antigenic variation (Stockdale et al., 2008).

4.4. Trypanothione and anti-oxidative defence

In addition to the challenge by the immune system, *T. brucei* is continuously exposed to oxidative species in the human bloodstream (Docampo, 1995). To avoid oxidative stress an appropriate anti-oxidative defence is required, which in trypanosomes is primarily dependent on trypanothione (N^1, N^8-bis(glutathionyl)spermidine, $T(SH)_2$). Trypanothione is a glutathione-derived molecule that is only found in trypanosomes (Fairlamb et al., 1985). It plays a central role in the NADPH-dependent reduction of hydroperoxides and the maintenance of the cellular thiol redox balance, similar to glutathione (GSH) in mammals (Nogoceke et al., 1997). The electrons required for the reduction of hydroperoxides are donated by trypanothione or via the intermediate tryparedoxin (TXN) (Dormeyer et al., 2001). Next to its role in anti-oxidative defence, trypanothione is further involved in the detoxification of xenobiotics using the mercapturic acid pathway (Krauth-Siegel et al., 2003) and the trypanosomal glyoxalase system (Comini et al., 2004).

4.5. Purine salvage

Purines are essential building blocks required for the biosynthesis of DNA and RNA nucleotides, as well as for the biosynthesis of other important molecules like ATP, GTP, cyclic AMP, NADH and Coenzyme A (Rosemeyer, 2004). The majority of parasitic protozoa cannot synthesize purines *de novo*, but are dependent on the provision of purines by their mammalian hosts using a salvage pathway (Davies et al., 1983, Chaudhary et al., 2004, Baum et al., 1989). The way in which purines are salvaged from their hosts differs among parasites (Davies et al., 1983, Chaudhary et

al., 2004, Baum et al., 1989). The purine salvage pathway of *T. brucei* is dependent on phosphoribosyltransferases for the salvage of the purine bases and on nucleoside kinases for making nucleosides (Davies et al., 1983). In addition, an adenosine aminohydrolase is found in *T. brucei* (Davies et al., 1983).

4.6. The glycosome

Another peculiarity of *T. brucei* is that it contains the glycosome, a unique peroxisome-like organelle bound by a single membrane (Hart et al., 1984, Parsons, 2004). The biogenesis of this organelle is similar to that of peroxisomes and is dependent on peroxines (Parsons, 2004). Remarkably, the glycosome compartmentalises the first seven to nine enzymes of the glycolytic pathway, which in all other eukaryotes is exclusively located in the cytosol (Opperdoes and Borst, 1977). The bloodstream form *T. brucei* is completely dependent on glycolysis for its cellular ATP production, while the procyclic form *T. brucei* is dependent on a combination of both glycolysis and mitochondrial oxidative and substrate level phosphorylation (Bringaud et al., 2006, Michels et al., 2000, Bochud-Allemann and Schneider, 2002). Glucose, the main substrate for glycolysis, is in the glycosome degraded to the glycolytic intermediate glycerate 3-phosphate in the bloodstream form or glycerate 1,3-phosphate in procyclic form *T. brucei*. Both glycolytic intermediates are exported from the glycosome and further converted to pyruvate in the cytosol of *T. brucei* (Coley et al., 2011, Opperdoes and Borst, 1977, Colasante et al., 2006b). A more detailed description of the glycosomal energy metabolism of *T. brucei* can be found in section 1.6.

The glycosome participates further in degradation of lipids via β-oxidation, lipid biosynthesis, and the metabolism of sterols and isoprenoids (Parsons et al., 2001,

Parsons, 2004, Michels et al., 2000). The coprresponding pathways are present in all peroxisomes characterised so far (Opperdoes, 1984, Wiemer et al., 1996, Parsons, 2004, Colasante et al., 2006b). In addition, the *T. brucei* glycosome contains the first two enzymes of the pentose phosphate pathway, i.e. glucose-6-phosphate dehydrogenase and 6-phosphogluconate dehydrogenase, which are proposed to play an important role in the regeneration of reducing equivalents (Barrett, 1997, Colasante et al., 2006b, Opperdoes and Szikora, 2006). An extensive proteomic analysis of isolated *T. brucei* glycosomes revealed further the presence of enzymes and parts of pathways that are usually not found in other peroxisomes, including part of the purine salvage pathway, part of the Calvin-Benson cycle, different enzymes of the nucleotide metabolism, and phosphoenolpyruvate carboxykinse (PEPCK) and pyruvate kinase, which are involved in pyruvate metabolism (Colasante et al., 2006b).

4.7. The *T. brucei* mitochondrion

Virtually all information available regarding the structure and function of the *T. brucei* mitochondrion is derived from the procylic form of the parasite, whereas little is known about the bloodstream form mitochondrion (Panigrahi et al., 2009, Stephens et al., 2007, Schneider et al., 2007, Bringaud et al., 2006). In the procyclic form *T. brucei,* the mitochondrion plays an essential role in the cellular provision of ATP via oxidative and substrate level phosphorylation (Schneider et al., 2007, Bringaud et al., 2006, Bochud-Allemann and Schneider, 2002), but is also proposed to contribute to carbohydrate metabolism, the pentose phosphate pathway, the biosynthesis and conversion of lipids, amino acids, and nucleotides, and the maintenance of the cellular redox balance (Opperdoes, 1987, Barrett, 1997, Smith and Butikofer, 2010, Bringaud et al., 2012, Castro et al., 2010). Similar to mitochondria from other eukaryotes, its structure is composed of a mitochondrial outer membrane (MOM),

mitochondrial intermembrane space (IMS), mitochondrial inner membrane (MIM) and matrix (Panigrahi et al., 2009, Panigrahi et al., 2008). In contrast to other eukaryotes, *T. brucei* contains only a single tubular mitochondrion stretching over the whole length of the cell (Figure 1). The function and structure of the *T. brucei* mitochondrion can change in response to the different host environments and available substrates, which the parasite encounters during its life cycle (Bringaud et al., 2006, Matthews, 2005, Fenn and Matthews, 2007). The tubular structure of the mitochondrion can be more or less branched, and even form a cellular network depending on the *T. brucei* life cycle stage (Schneider, 2001). In procyclic form, *T. brucei*, most of its ATP is provided via proline degradation, and concomitant oxidative and substrate level phosphorylation in the mitochondrion (Bringaud et al., 2012, Bochud-Allemann and Schneider, 2002, Schneider et al., 2007). The mitochondrion contains further a functional mitochondrial respiratory chain (complexes I-IV), which is involved in the maintenance of the redox cellular balance and the production of ATP via an ATP synthase (complex V) located in the mitochondrial inner membrane (van Hellemondt et al., 2005). In agreement with its function in ATP production, the single procyclic form mitochondrion is highly branched to increase its functional membrane surface (Schneider, 2001).

This in contrast to the bloodstream form, where the single mitochondrion is reduced to a simple tubular structure with little or no branching at all (Schneider, 2001). This life cycle stage of the parasite dwells in the glucose-rich (about 3-5 mM) human bloodstream, and is exclusively dependent on the glycosomes and the compartmentalised glycolytic pathway for its cellular ATP provision (Michels et al., 2000, Bringaud et al., 2006). The redox balance in the bloodstream form is maintained by the combined action of a mitochondrial alternative oxidase (TAO) and

ATP synthase (Bienen et al., 1993, Chaudhuri et al., 2006, Schnaufer et al., 2005). These are the only mitochondrial functions described so far for this life cycle stage (van Hellemond et al., 2005). The bloodstream form mitochondrion further lacks a functional TCA cycle, respiratory chain and cytochrome *c*, and is proposed to not contribute to the cellular ATP production at all (van Hellemond et al., 2005).

5. Treatment of Sleeping Sickness

The treatment of Sleeping Sickness is dependent on the disease stage, here the hemolymphatic stage 1 or the neurological stage 2, and the different *T. brucei* subspecies causing the disease, i.e. *T. b. gambiense* and *T. b. rhodesiense* (Barrett et al., 2007, Kennedy, 2004, Rodgers, 2009). Since 1921, only 5 drugs successful against *T.brucei* have been developed, i.e. Pentamidine, Suramin, Melarsoprol, Eflornithine and Nifurtimox (Kennedy, 2004, Barrett et al., 2007, Ashley et al., 1942, Hall et al., 2011, Lourie, 1942). Each of these drugs is only effective against the first or second stage of Sleeping Sickness of a particular *T. brucei* subspecies. Pentamidine has been in use since 1941 and can only be used for the treatment of first stage West African Sleeping Sickness, which is caused by *T. b. gambiense* (Ashley et al., 1942). Although this drug is highly effective against *T. b. gambiense*, it also causes severe neurological side effects in some patients (Lourie, 1942, Rodgers, 2009). Suramin was discovered in 1921 and can only be used for the treatment of the more acute East African Sleeping Sickness caused by *T. b. rhodesiense* (Steverding, 2010). Melarsoprol was introduced in 1949 and is the only effective drug that can be used for treatment of second stage sleeping sickness caused by *T. b. rhodesiense*. Unfortunately, it also causes reactive encephalopathy in 5-10% of the treated patients (Kuzoe, 1993). Eflornithine (a-difluoromethylornithine or DFMO) was discovered in 1990, and can only be used for treatment of second stage sleeping sickness caused by

T. b. gambiense (Nightingale, 1991). Later on Nifurtimox was developed, which is also effective against second stage sleeping sickness caused by *T. b. gambiense* (Hall et al., 2011). Both Eflornithine and Nifurtimox are currently used as an effective combination therapy for second-stage *T. b. gambiense* sleeping sickness (Priotto et al., 2007).

Unfortunately, most of the drugs mentioned above show severe side effects, and can only be applied under controlled hospital conditions. In addition, they are rather expensive and are therefore not affordable for patients in the mainly poor, developing countries where Sleeping Sickness is endemic. Another problem is that *T. brucei* becomes more and more resistance against the existing drugs, rendering them less suitable for future treatment of Sleeping Sickness (Rodgers, 2009, Barrett et al., 2007, Matovu et al., 2001). Consequently, novel drug targets have to be identified as well as novel drugs developed. Currently several approaches are underway to identify new drug targets. They include the identification of essential metabolic pathways and their enzymes, which are only present in *T. brucei* and not the human host. For example, trypanothione-dependent enzymes such as trypanothione synthetase (Comini et al., 2004), trypanothione reductase, glyoxalase and different transferases (Spinks et al., 2009) are unique to Kinetoplastida and are vital for the survival of *T. brucei*, and are therefore regarding as a suitable targets for the development of novel drugs. Also the purine salvage pathway of *T. brucei* is considered as a suitable drug target, due to the absence of a *de novo* purine synthesis pathway in this parasite (Davies et al., 1983). Other potential drug targets are glycolytic enzymes found in the glycosomes, including triosephosphate isomerase (Wierenga et al., 1991), phosphoglycerate kinase (Bernstein et al., 1998) and aldolase (Chudzik et al., 2000).

6. The *T. brucei* energy metabolism

The energy metabolism of *Trypanosoma brucei* is highly adaptive and is dependent on the different host environments that the parasite encounters during its lifecycle (Bringaud et al., 2006, Vickerman, 1985, Matthews, 2005). The energy metabolism of bloodstream form of *T. brucei* is rather simple and is exclusively dependent on the glycolytic degradation of glucose (Michels et al., 2000, Opperdoes, 1987), which is abundantly present in the mammalian bloodstream (ter Kulle, 1993). A schematic representation of the bloodstream form energy metabolism is shown in figure 5. In the glycosome, glucose is oxidized to 3-phosphoglycerate (3-PGA), involving the first 7-9 enzymes of the glycolytic pathway (Parsons et al., 2001, Parsons, 2004, Michels et al., 2000). 3-PGA is subsequently exported from the glycosome and further metabolized to mainly pyruvate in the cytosol. It is postulated that ATP production and consumption is balanced in the glycosome and that no ATP is exported from this subcellular compartment (Opperdoes and Borst, 1977, Opperdoes, 1987, Hammond and Bowman, 1980). Instead, ATP is exclusively formed in the cytosolic part of the glycolytic pathway, here the pyruvate kinase-catalysed conversion of phosphoenolpyruvate (PEP) to the metabolic end product pyruvate (Opperdoes, 1987, Hammond and Bowman, 1980). The redox balance in the glycosome is maintained by the combined action of a glycerol 3-phosphate shuttle located in the glycosomal membrane and an alternative oxidase present at the mitochondrial membrane (Opperdoes and Borst, 1977). Depending on the glycosomal and cellular redox balance, glycerol can be produced in addition to pyruvate (Opperdoes and Borst, 1977, Hannaert et al., 2003). Current metabolic models regard both pyruvate and glycerol as the final metabolic end products of the bloodstream form energy metabolism (Tielens and Van Hellemond, 1998, Opperdoes, 1987).

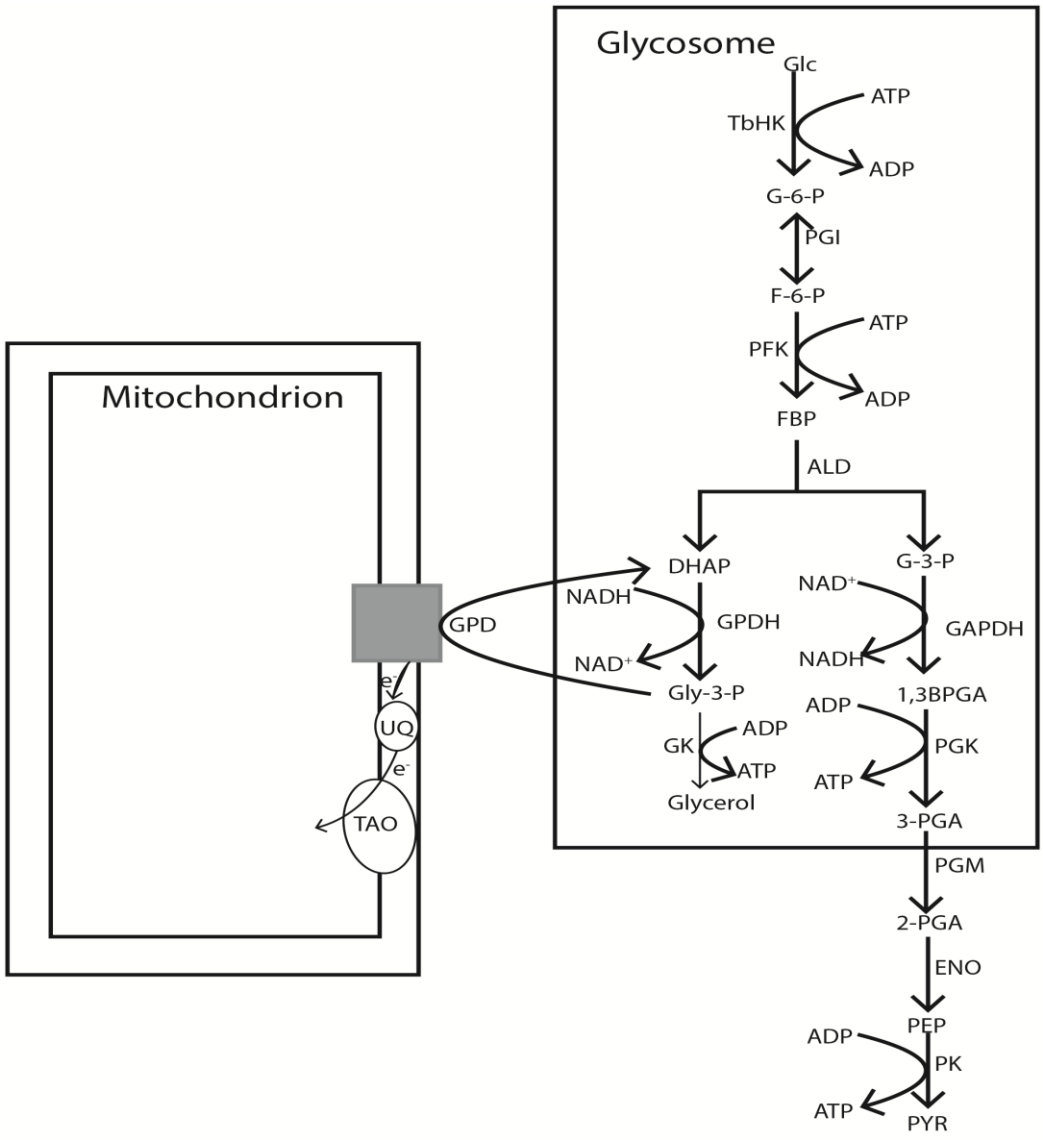

Figure 5: Schematic represenation of the bloodstream form *T. brucei* energy metabolism. Abbreviations used: Glc, glucose; TbHK, *T. brucei* hexokinase; G-6-P, glucose-6-phosphate; PGI, glucose-6-phosphate isomerase; F-6-P, fructose-6-phosphate; PFK, phosphofructokinase; FBP, fructose 1,6-bisphosphate; ALD, aldolase; DHAP, dihydroxyacetone phosphate; GPDH, glycerol 3-phosphate dehydrogenase; GK, glycerol kinase; Gly-3-p, glycerol-3-phosphate; G-3-P, glyceraldehyde 3-phosphate; GAPDH, glyceraldehyde-3-phosphate dehydrogenase, 1,3BPGA, 1,3-bisphosphoglycerate; PGK, phosphoglycerate kinase; 3-PGA, 3-phosphoglycerate; PGM, phosphoglycerate mutase; 2-PGA, 2-phosphoglycerate; ENO, enolase; PEP, phosphoenolpyruvate; PK, pyruvate kinase; PYR, pyruvate; TAO, alternative oxidase. UQ, ubiquinone, GPD, glycerol-3-phosphate dehydrogenase.

In contrast to the bloodstream form *T. brucei*, the energy metabolism of the procyclic form is more elaborate, and involves multiple metabolic pathways in different subcellular compartments, including the glycosome, cytosol and mitochondrion (Bringaud et al., 2012, Bochud-Allemann and Schneider, 2002, Opperdoes, 1987). The procyclic form parasite can not only use the glucose derived from the insect blood meal, but also the amino acid proline as a carbon sources for the production of ATP (Bringaud et al., 2012). Proline is abundantly present in the insect's hemolymph (Neufeld and Leader, 1998, Barrett, 1974, Arrese and Soulages, 2010). A simplified schematic presentation of the complex energy metabolism of the procyclic form *T. brucei* is shown in figure 6.

When comparing the glucose metabolism present in bloodstream form (Fig. 5) and procyclic form (Fig. 6) *T. brucei*, several important differences can be observed in terms of energy production. In the procyclic form, not 3-phosphoglycerate but 1,3-biphosphoglycerate is exported from the glycosome. 1,3-biphosphoglycerate is in the cytosol converted to 3-phosphoglycerate by a cytosolic phosphoglycerate kinase (PGK) with the concomitant formation of ATP (Opperdoes and Borst, 1977, Opperdoes, 1987, Hammond and Bowman, 1980). 3-phosphoglycerate is subsequently converted to phosphoenolpyruvate (PEP) by the combined action of phosphoglycerate mutase and enolase (Opperdoes and Borst, 1977, Opperdoes, 1987, Hammond and Bowman, 1980). PEP is a key metabolic intermediate and represents an important branching point of the procyclic form energy metabolism (Fig. 6). It can act as a substrate for the different energy producing pathways located in the cytosol, glycosome and mitochondrion (Coustou et al., 2003, Bringaud et al., 2006, Matthews, 2005). Re-direction of PEP to these different pathways is dependent on the ATP and redox (NAD^+/NADH) balances in the different subcellular compartments (Coustou et

al., 2005, Barnard and Pedersen, 1994). Part of the cytosolic PEP is converted to pyruvate in the cytosol with the concomitant production of ATP (Van Hellemond et al., 1998). The formed pyruvate can be imported into the mitochondrion, where it is converted to acetyl-CoA and the metabolic end product acetate, again with concomitant ATP production (Gilbert and Klein, 1984, Callens et al., 1991). Alternatively, pyruvate can remain in the cytosol, where it is converted to the metabolic end products lactate and alanine, which contributes to maintenance of the cytosolic redox balance, or pyruvate can be converted to the metabolic intermediate malate (Barnard and Pedersen, 1994). Malate can again enter the mitochondrion, where it is converted to succinate by part of the mitochondrial TCA cycle involving a NADH-dependent fumarate reductase (FRD) (Coustou et al., 2005), or after its conversion to fumarate in the cytosol, it can be imported into the glycosome where it is also converted to succinate using part of the succinic fermentation branch (Aranda et al., 2006). The remaining part of the PEP formed in the cytosol can re-enter the glycosome, where it is converted to succinate via the succinic fermentation pathway (Fig. 6, (Ebikeme et al., 2010)). This pathway not only plays an important role in the maintenance of the glycosomal redox balance, but also in ATP formation in this organelle (Ebikeme et al., 2010). The observed flexibility of the various glucose metabolising pathways and the transport of different metabolic intermediates in and out of the different subcellular compartments is most probably required for the maintenance of the cellular ATP and redox homeostasis in *T. brucei*.

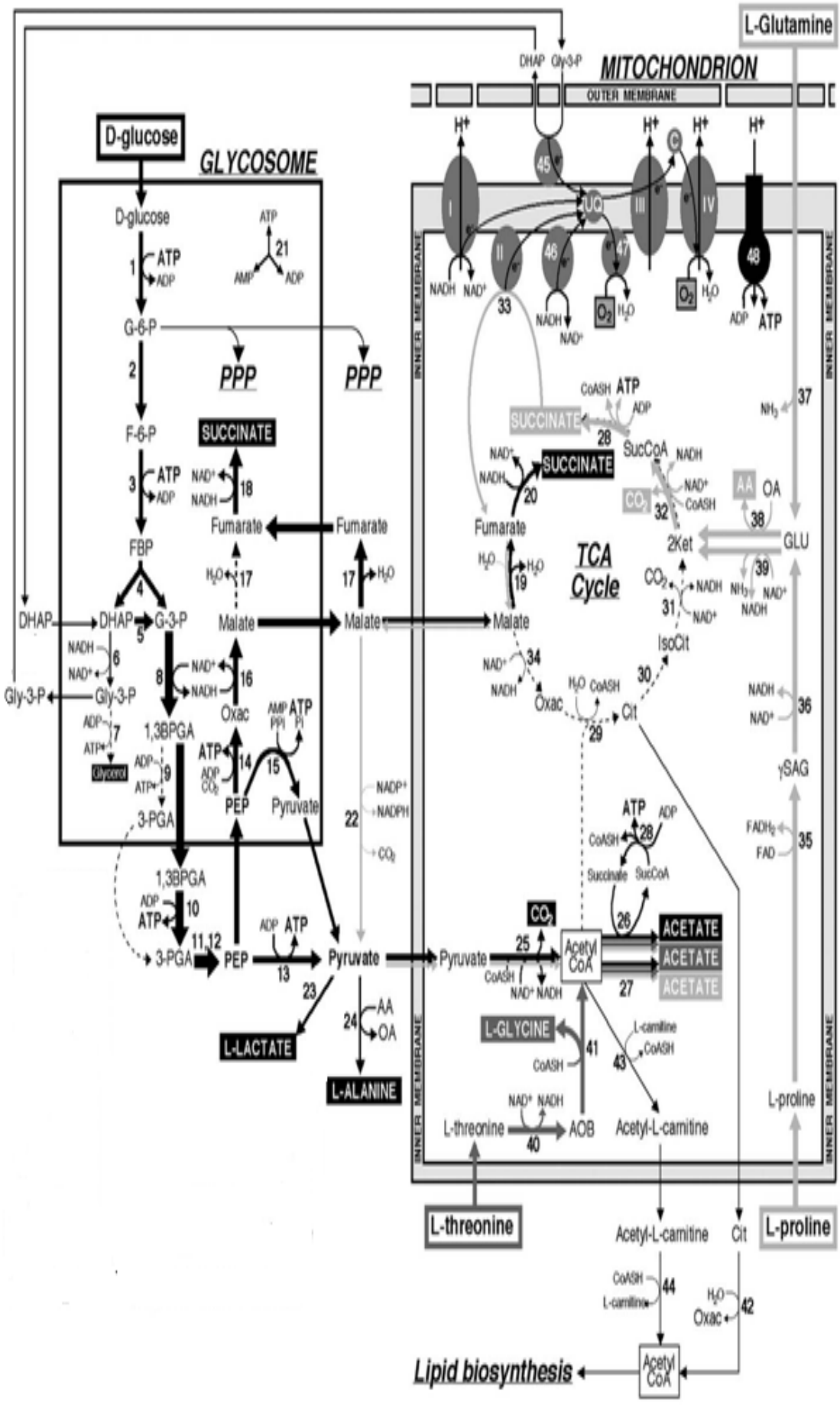
L-Glutamine
MITOCHONDRION
OUTER MEMBRANE
INNER MEMBRANE
D-glucose
GLYCOSOME
PPP
PPP
SUCCINATE
Fumarate
Malate
DHAP
G-3-P
Gly-3-P
1,3BPGA
3-PGA
PEP
Pyruvate
Oxac
Cit
IsoCit
2Ket
GLU
SucCoA
Acetyl CoA
ACETATE
ACETATE
ACETATE
L-LACTATE
L-ALANINE
L-GLYCINE
L-threonine
AOB
Acetyl-L-carnitine
L-proline
γSAG
TCA Cycle
Lipid biosynthesis

Figure 6: Schematic representation of the procyclic form *T. brucei* energy metabolism (Bringaud et al., 2006). Dark, grey and light grey arrows represent enzymatic steps of glucose, threonine and proline/glutamine metabolism, respectively. Excreted end products (acetate, alanine, glycerol, glycine, lactate, succinate and CO_2) derived from glucose, threonine and proline metabolism are in white characters on a black, grey and light grey background, respectively. Arrows with different thicknesses tentatively represent the metabolic flux at each enzymatic step, when *T. brucei* is cultured in the presence of both glucose and proline (glucose-rich medium). Dashed arrows indicate steps that are supposed to occur at a background level or not at all, under these growth conditions. The glycosomal and mitochondrial compartments, the tricarboxylic acid (TCA) cycle and the links to the pentose phosphate pathway (PPP) and lipid biosynthesis pathway are indicated. The mitochondrial outer membrane is permeable to metabolites and is only shown in the vicinity of the schematic electron-transport chain. Abbreviations used are: AA, amino acid; AOB, amino oxobutyrate; 1,3BPGA, 1,3-bisphosphoglycerate; C, cytochrome *c*; Cit, citrate; CoASH, coenzyme A; DHAP, dihydroxyacetone phosphate; F-6-P, fructose 6-phosphate; FBP, fructose 1,6-bisphosphate; G-3-P, glyceraldehyde 3-phosphate; G-6-P, glucose 6-phosphate; GLU, glutamate; Gly-3-P, glycerol 3-phosphate; IsoCit, isocitrate; 2Ket, 2-ketoglutarate; OA, 2-oxoacid; Oxac, oxaloacetate; PEP, phosphoenolpyruvate; 3-PGA, 3-phosphoglycerate; Pi, inorganic phosphate; PPi, inorganic pyrophosphate; SAG, glutamate -semialdehyde; SucCoA, succinyl-CoA; T[SH]2, reduced form of trypanothione; UQ, ubiquinone pool. Enzymes are: 1, hexokinase; 2, glucose-6-phosphate isomerase; 3, phosphofructokinase; 4, aldolase; 5, triose-phosphate isomerase; 6, glycerol-3-phosphate dehydrogenase; 7, glycerol kinase; 8, glyceraldehyde-3-phosphate dehydrogenase; 9, glycosomal phosphoglycerate kinase; 10, cytosolic phosphoglycerate kinase; 11, phosphoglycerate mutase; 12, enolase; 13, pyruvate kinase; 14, phosphoenolpyruvate carboxykinase; 15, pyruvate phosphate dikinase; 16, glycosomal malate dehydrogenase; 17, cytosolic (and glycosomal) fumarase (FHc); 18, glycosomal NADH-dependent fumarate reductase; 19, mitochondrial fumarase (FHm); 20, mitochondrial NADH-dependent fumarate reductase; 21, glycosomal adenylate kinase; 22, malic enzyme; 23, unknown enzyme; 24, alanine aminotransferase; 25, pyruvate dehydrogenase complex; 26, acetate:succinate, CoA-transferase; 27, unknown enzyme; 28, succinyl-CoA synthetase; 29, citrate synthase;

30, aconitase; 31, isocitrate dehydrogenase; 32, 2-ketoglutarate dehydrogenase complex; 33, succinate dehydrogenase (complex II of the respiratory chain); 34, mitochondrial malate dehydrogenase; 35, L-proline dehydrogenase; 36, pyrroline-5 carboxylate dehydrogenase; 37, L-glutamine deaminase; 38, glutamate aminotransferase; 39, glutamate dehydrogenase; 40, l-threonine dehydrogenase; 41, acetyl-CoA:glycine C-acetyltransferase; 42, citrate lyase; 43, acetyl-l-carnitine transferase; 44, acetyl-l-carnitine transferase; 45, FAD-dependent glycerol-3-phosphate dehydrogenase; 46, rotenone-insensitive NADH dehydrogenase; 47, alternative oxidase; 48, F0F1-ATP synthase; 49, spontaneous reaction; 50, glyoxalase I; 51, glyoxalase II; 52, pyruvate decarboxylase; 53, NAD-linked alcohol dehydrogenase; I, II, III and IV, complexes of the respiratory chain.

As mentioned above, the procyclic form *T. brucei* can also use proline for its energy generation (Bringaud et al., 2012). This is particularly the case when the glucose present in the blood meal becomes depleted (Bochud-Allemann and Schneider, 2002, Lamour et al., 2005). The proline-metabolising pathway is exclusively located in the *T. brucei* mitochondrion (Lamour et al., 2005). In contrast to the bloodstream form, the mitochondrion of the procyclic form is fully functional in terms of energy production (Bringaud et al., 2006). During proline degradation, α-ketoglutarate is formed, which subsequently enters the TCA cycle. Although all TCA cycle enzymes are present in the procyclic form of *T. brucei* mitochondrion, the cycle is only partly used, leading to the formation of succinate as the main end product from proline degradation (van Weelden et al., 2003). In the mitochondrion, ATP production from proline takes place by a combination of substrate-level and oxidative phosphorylation (Lamour et al., 2005), while the redox balance is maintained by a functional respiratory chain (Njogu et al., 1980, Castro et al., 2010).

7. Mitochondrial Carrier Family proteins

The mitochondrial inner membrane is impermeable and requires the presence of dedicated transporters to facilitate the transport of metabolites across this barrier (Schneider et al., 2007). The majority of the metabolite transporters found in the mitochondrial inner membrane are members of the mitochondrial carrier family (MCF) (Palmieri, 2004, Millar and Heazlewood, 2003). MCF proteins transport a wide range of metabolites, including nucleotides, phosphate, carboxylic acids, amino acids, protons and iron (Palmieri, 2004, Palmieri et al., 2006a, Kunji and Robinson, 2006, Colasante et al., 2009). As a consequence of their wide substrate range, they are involved in most of the metabolic pathways present in the mitochondrion, and form an essential metabolic link between the mitochondrion and the rest of the cell (Palmieri, 2004, Kunji, 2004). MCF proteins are characterised by a highly conserved protein structure composed of three homologous sequence repeats and a similar molecular mass of about 30-35 kDa (Millar and Heazlewood, 2003, Palmieri et al., 2006a, Picault et al., 2004). A schematic representation of the conserved MCF protein structure is shown in Figure 7. Each sequence repeat is about 100 amino acids long and includes two membrane-spanning alpha helices connected by a hydrophilic loop (Saraste and Walker, 1982). Each odd numbered hydrophilic loop contains a conserved MCF signature sequence, i.e. 'Px(D/E)x_2(K/R)x(K/R)/x_{20-30}/(D/E)Gx_{4-5}(W/F/Y)(K/R)G' with 'a' standing for an aromatic residue and 'x' for any amino acid (Aquila et al., 1987, Saraste and Walker, 1982). The N- and C-terminal ends of MCF proteins are facing the mitochondrial inter membrane space (Fig. 7).

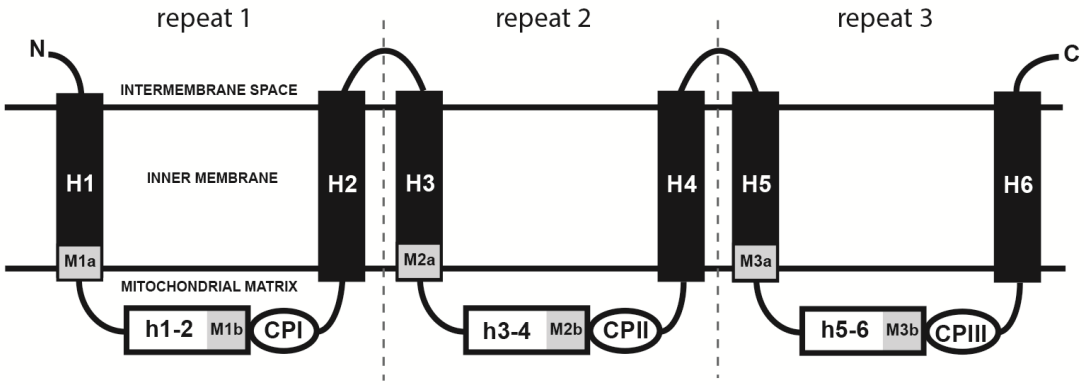

Figure 7: Schematic representation of mitochondrial carrier family proteins and their conserved protein structure (edited from Colasante et al., 2009). Abbreviations used: N, N-terminal; C, C-terminal; H1-6, transmembrane domains; h1-2, h3-4, h5-6, hydrophilic loops; M1-3a, the first part of canonical signature sequence motif ($Px(D/E)x_2(K/R)x(K/R)$); M1-3b, the second part of canonical signature sequence motif ($(D/E)Gx_{4-5}(W/F/Y)(K/R)G$); CPI-III, substrate contact points.

So far, about 30 MCF proteins have been identified in yeast, and more than 50 MCF proteins in humans and plants (Palmieri et al., 2000, Picault et al., 2004, Wohlrab, 2006). Functional characterisation showed that MCF proteins are involved in essential cellular processes (see Fig.8), including energy generation, the biosynthesis and degradation of amino acids, mitochondrial DNA replication, and the maintenance of the mitochondrial and cellular redox balance (Kunji, 2004). Pyruvate derived from glycolysis is transported into the mitochondrion for conversion to acetyl-CoA, which can be used as a substrate for the TCA cycle (Hildyard and Halestrap, 2003). Concomitant mitochondrial ATP production is dependent on the availability of ADP and inorganic phosphate as substrates, which have to be imported from the cytosol by two MCF proteins, the ADP/ATP carrier and the phosphate carrier (Knirsch et al., 1989). In addition, several MCF proteins are required for the exchange of TCA cycle intermediates between the cytosol and the mitochondrion, including the dicarboxylate

carrier, which exchanges malate and succinate with inorganic phosphate, sulphate and thiosulphate (Fiermonte et al., 1999), the tricarboxylate carrier, which transports citrate in exchange with malate or other anionic metabolites (Iacobazzi et al., 1996), and the oxoglutarate/malate carrier, which transports 2-oxoglutarate in an exchange for malate or other dicarboxylic acids (Iacobazzi et al., 1992). Also the mitochondrial biosynthesis and degradation of amino acids is dependent on different MCF proteins for the transport of substrates and intermediates (see (Kunji, 2004) and references therein). This includes the citrulline/ornithine carrier, which transports ornithine in exchange with citrulline (Fiermonte et al., 2003), the aspartate/glutamate exchanger, which transports glutamate in exchange with aspartate (Fiermonte et al., 2002, Palmieri et al., 2001), and the oxoglutarate carrier, which transports oxoglutarate in exchange for oxoadipate derived from cytosolic lysine and tryptophan degradation (Fiermonte et al., 2001). In addition, mitochondrial DNA replication is dependent on MCF proteins such as the deoxynucleotide carrier, which exchanges deoxynucleotides, and the *S*-adenosylmethionine carrier, which is required for the methylation of mitochondrial DNA (Dolce et al., 2001, Marobbio et al., 2003).

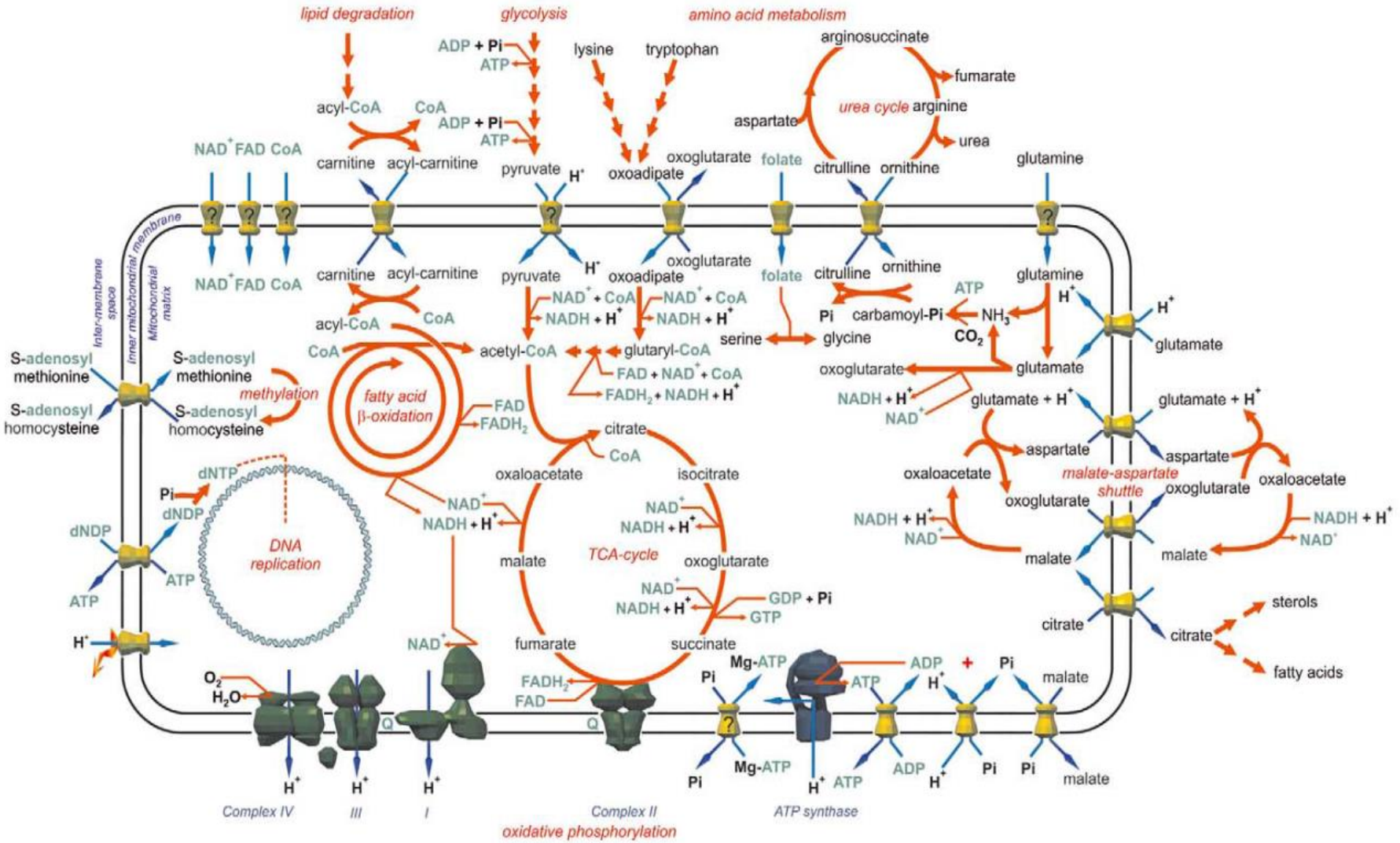
lipid degradation
glycolysis
amino acid metabolism
ADP + Pi
ATP
lysine
tryptophan
arginosuccinate
fumarate
urea cycle arginine
urea
aspartate
acyl-CoA
CoA
carnitine
acyl-carnitine
pyruvate
H+
oxoadipate
oxoglutarate
folate
citrulline
ornithine
glutamine
NAD+ FAD CoA
Inter-membrane space
Inner mitochondrial membrane
Mitochondrial matrix
NAD+ + CoA
NADH + H+
acetyl-CoA
glutaryl-CoA
FAD + NAD+ + CoA
FADH2 + NADH + H+
serine
glycine
Pi
carbamoyl-Pi
NH3
CO2
glutamate
oxoglutarate
S-adenosyl methionine
S-adenosyl homocysteine
methylation
fatty acid β-oxidation
FAD
FADH2
citrate
isocitrate
oxaloacetate
malate
TCA-cycle
malate-aspartate shuttle
dNTP
dNDP
DNA replication
GDP + Pi
GTP
succinate
fumarate
sterols
fatty acids
O2
H2O
Q
Mg-ATP
ADP
Complex IV
III
I
Complex II
ATP synthase
oxidative phosphorylation

Figure 8: Proposed transport functions of MCF proteins in the mitochondrial and cellular metabolism (adpted from (Kunji, 2004)). This schematic representation shows the mammalian mitochondrial inner membrane containing the ATP synthase, complexes I-IV of the respiratory chain, and various MCF proteins. Metabolic pathways are simplified to emphasise the transport of key metabolites, and are indicated by red arrows. Blue arrows indicate the main transport direction. Co-factors and high-energy intermediates are coloured green. Some metabolites can appear in different pathways, meaning that the corresponding pathways are linked. For CoA, glutamine, FAD, NAD^+, and pyruvate it is currently unknown (indicated by "?") whether they are transported by MCF proteins or by other transporters.

For the study of MCF proteins and their transport function, three different approaches have been used. The most common and widely used approach is the reconstitution of MCF proteins in artificial liposomes, and the subsequent analysis of transport function in the generated proteoliposomes by using radio-labelled substrates (Palmieri et al., 2006b, Palmieri, 2004, Picault et al., 2002, Hoyos et al., 2003, Segrest et al., 1974). However, reconstitution is notoriously difficult since many of the reconstituted MCF proteins do not function at all or transport at a very low rate due to problems associated with heterologous expression, purification, renaturation and refolding, and the correct insertion and orientation of the reconstituted protein in the liposomal membrane (Palmieri et al., 2006b, Rigaud et al., 1995, Rigaud, 2002). To circumvent the reconstitution problems, some of the MCF proteins have been studied upon expression in prokaryotes such as *Escherichia coli*, followed by the assessment of their transport function in the intact microorganism and radio-labelled substrates (Haferkamp et al., 2002, Tjaden et al., 2004, Leroch et al., 2005). Several studies confirmed that MCF proteins do not require post-translational modification for their function and that they indeed can correctly fold and integrate into the *Escherichia coli* membrane in a functional manner (Geigenberger et al., 2001, Haferkamp et al., 2002, Leroch et al., 2005, Mohlmann et al., 1998, Tjaden et al., 2004, Tjaden et al., 1998). A disadvantage of this approach is that it is limited to metabolites for which there are no other transporters present in the *E. coli* plasma membrane, such as the ADP/ATP carrier (Miroux and Walker, 1996).

Another, more successful approach is based on the expression of heterologous MCF proteins in *S. cerevisiae* knockout strains, which are deficient in specific MCF proteins (Klingenberg, 1993). Most of the MCF protein deficient yeast knockout

strains cannot grow on non-fermentable carbon sources such as glycerol or lactate medium, and can only grow on fermentable carbon source such as glucose (Clemencon et al., 2008, Kolarov et al., 1990b, Klingenberg, 1993). Subsequent expression of a homologous MCF protein into a mutant yeast strain can again complement its mitochondrial function and restore growth of the strain on a non-fermentable carbon source (Clemencon et al., 2008, Babot et al., 2012). This functional complementation method can however not be used for all MCF proteins since a knockout does not always results in an analysable growth defect on a non-fermentable carbon source (Nelson et al., 1998). In addition, functional complementation in a MCF protein deficient yeast strain is not always optimal, when compared to the wild type yeast (Mayr et al., 2011, De Marcos Lousa et al., 2002). This is most probably caused by problems with protein expression and mitochondrial protein targeting as a result of the absence of functional/yeast-specific mitochondrial targeting signals in the heterologous MCF protein (van Wilpe et al., 1999).

8. The MCF protein inventory of *T. brucei*

The *T. brucei* genome (www.genedb.org) harbours 26 genes coding for 24 different MCF proteins, called TbMCP1-24 (Colasante et al., 2009). Reciprocal database searches and sequence analysis confirmed that the identified *T. brucei* proteins are indeed members of the mitochondrial carrier family. All 24 TbMCPs show significant amino acid similarity (39–78%) to known human (SLC25A) and *S. cerevisiae* MCF proteins, and their sequence structure consists of three semi-conserved protein domains of about 100 amino acids, with each domain containing two transmembrane (TM) helices and a conserved MCF signature sequence motif (Colasante et al., 2009). Immunolocalisation studies confirmed that all TbMCPs have a mitochondrial

localisation, with the exception of TbMCP6, which seems to have a dual subcellular localisation (see below) (Colasante et al., 2009, Colasante et al., 2006a).

The putative transport function of the identified TbMCPs was predicted by reciprocal BLASTP database searches and phylogenetic reconstruction using functionally characterized MCF proteins from other eukaryotes. MCF proteins contain further several conserved residues downstream of the MCF signature sequences, which were previously shown to be involved in the recognition and binding of specific substrate classes (Kunji and Robinson, 2006, Robinson and Kunji, 2006). These conserved amino acids are predominantly located in 3 different substrate-contact points, i.e. CPI-III (figure 7). The first amino acid of each substrate contact point is located six amino acids downstream of the conserved glycine (G) residue at the end of each signature sequence motif (figure 7). CPI-III are conserved in MCF proteins that transport similar substrates (Kunji and Robinson, 2006, Robinson and Kunji, 2006). In particular CPII was proposed to play an important role in substrate discrimination, and is defined by the amino acid pair 'G(IVLM)' for nucleotide carriers, '(R/K)Q' for phosphate carriers, 'R(QHNT)' for dicarboxylic acid carriers, 'R(D/E)' for amino acid carriers, and 'MN' for iron carriers (Kunji and Robinson, 2006, Robinson and Kunji, 2006). Identification of CPI-III sequences in the 24 TbMCPs and comparison to those of functionally characterized MCF proteins allowed a more specific definition of their putative mitochondrial transport function (Colasante et al., 2009, Colasante et al., 2006a).

Of the 24 TbMCPs identified in *T. brucei*, only TbMCP6 has been studied in more detail (Colasante et al., 2009, Colasante et al., 2006a). Sequence analysis and phylogenetic reconstruction suggested that TbMCP6 could function as an ADP/ATP

or ATP-Mg/Pi exchanger (Colasante et al., 2009, Colasante et al., 2006a). Functional reconstitution of TbMCP6 in *E. coli* and using [α^{32}P]-labelled ATP, ADP and Mg^{2+}-ATP as substrates during transport assays revealed however that none of these substrates were transported (Colasante et al., 2006a). Knockout experiments revealed that TbMCP6 was essential for the survival of PCF *T. brucei* and its ablation had a detrimental effect on kinetoplast division and cytokinesis (Colasante et al., 2006a). These results indicated that TbMCP6 maybe functions as a mitochondrial nucleotide carrier, which is closely related to ADP/ATP and ATP-Mg/Pi carriers (Colasante et al., 2009, Colasante et al., 2006a). Remarkable is further the dual subcellular localisation of TbMCP6: this MCF protein was predominantly mitochondrial in PCF *T. brucei*, whereas in the BSF trypanosome, TbMCP6 was mainly found in the glycosome (Colasante et al., 2006a).

Next to TbMCP6, two other *T. brucei* MCF proteins have been predicted to play a role in mitochondrial ADP/ATP exchange, i.e. TbMCP5 and TbMCP15 (Colasante et al., 2009). Both most probably play an important role in the PCF *T. brucei* energy metabolism (Colasante et al., 2009), where the mitochondrion is the main source of ATP production during proline degradation and concomitant substrate level and oxidative phosphorylation (Bringaud et al., 2006, Schneider et al., 2007, Bochud-Allemann and Schneider, 2002). The mitochondrial ADP/ATP carrier is further dependent on the presence of one or more phosphate carriers for its function, requiring the replenishment of Pi consumed during ATP synthesis in the mitochondrial matrix (Kramer, 1996). The *T. brucei* MCF protein inventory indeed includes two predicted mitochondrial phosphate carriers, i.e. TbMCP11 and TbMCP8, which potentially could fulfil this role (Colasante et al., 2009).

9. The mitochondrial ADP/ATP carrier

The ADP/ATP carrier is one of the best-studied members of the mitochondrial carrier family, and represents the most abundant protein in the mitochondrial inner membrane (Klingenberg, 1993, Brandolin et al., 1993, Trezeguet et al., 2008). This MCF protein plays a central and essential role in the eukaryotic energy metabolism by exporting the ATP produced in the mitochondrial matrix to the cytosol in exchange for cytosolic ADP, thereby replenishing the matrix ADP pool and enabling a continuous mitochondrial energy production (Knirsch et al., 1989, Kramer and Klingenberg, 1985, Dahout-Gonzalez et al., 2006). The ADP/ATP exchange function is dependent on the presence of cardiolipin, a unique lipid only found in the mitochondrial inner membrane (Beyer and Klingenberg, 1985). In addition, the ADP/ATP carrier is part of the mitochondrial transition pore (MTP), which plays an essential role in cytochrome-*c* mediated apoptosis (Palmieri, 2004).

The important role of the ADP/ATP carrier in the eukaryotic energy production is particularly evident in humans, where dysfunction of this MCF protein leads to rather detrimental diseases, including mitochondrial myopathy and cardiomyopathy (Graham et al., 1997). Deficiency of the mitochondrial ADP/ATP carrier isoform 1 causes further progressive external ophthalmoplegia, accompanied by ptosis, exercise intolerance and large-scale deletion of mitochondrial DNA (Online Mendelian Inheritance in Man, OMIM 157640) (Kaukonen et al., 2000, Napoli et al., 2001). In other cases, the ADP/ATP carrier gene itself is not mutated but its protein expression (transcription) or mitochondrial import is affected, which leads to Sengers syndrome and some other symptoms, such as exercise intolerance, hypertrophic cardiomyopathy and lactic acidaemia (OMIM 103220) (Palmieri, 2004). In virtually all cases, a

substantially reduced energy production and oxidative phosphorylation capacity is observed in the affected tissues (Dahout-Gonzalez et al., 2006, Palmieri, 2004).

The protein structure of different ADP/ATP carriers, i.e. AAC3 from *Saccharomyces cerevisiae* (Kunji and Harding, 2003) and ANT1 from *Bos taurus* (Pebay-Peyroula et al., 2003) has been resolved by X-ray crystallography and is used as a model for the prediction of protein structures from other MCF proteins (Palmieri et al., 2011). In addition to the repetitive protein structure and conserved sequence motives of MCF proteins (see Section 1.7), the ADP/ATP carrier further contains a canonical hexapeptide sequence, i.e. 'RRRMMM'. This hexapeptide sequence is essential for ADP-binding and ADP/ATP exchange and is the hallmark of all ADP/ATP carriers (Nury et al., 2006, Clemencon et al., 2011). MCF proteins further contain several conserved amino acids that are involved in the selective binding and transport of substrates (see 1.7. and (Kunji and Robinson, 2006)). These amino acids are organized in three distinct substrate contact points (CP1-3, Fig. 6), which are conserved in MCF proteins transporting similar substrates (Kunji and Robinson, 2006, Robinson and Kunji, 2006). For ADP/ATP carriers, CP1 is composed of 3 conserved amino acids, i.e. arginine (R), threonine (T) and asparagine (N); CP2 is composed of a conserved glycine (G) and isoleucine (I); and CP3 is composed of only a single conserved amino acid and is in the case of ADP/ATP carriers represented by an arginine (R) (Kunji and Robinson, 2006). Mutations of these conserved amino acid residues decrease or ablate the ADP/ATP exchange function of this MCF protein (Kunji and Robinson, 2006, Robinson and Kunji, 2006).

All eukaryotic genomes studied to date contain at least one gene coding for a mitochondrial ADP/ATP carrier (Loytynoja and Milinkovitch, 2001). Multiple genes

coding for several ADP/ATP-carrier isoforms are predominantly found in the genomes of multicellular eukaryotes (Traba et al., 2011, Loytynoja and Milinkovitch, 2001). These isoforms are very similar in sequence and are thought to have arisen during evolution by recent gene duplication (Loytynoja and Milinkovitch, 2001). For example, 4 different isoforms of the ADP/ATP carrier were found in *Homo sapiens* (Battini et al., 1987, Houldsworth and Attardi, 1988, Cozens et al., 1989, Dolce et al., 2005) and *Bos taurus* ((Powell et al., 1989)REF), while *Saccharomyces cerevisae* contains 3 different isoforms (Kolarov et al., 1990b, Lawson and Douglas, 1988, Adrian et al., 1986). This is in contrast to protozoa, which in general contain only a single ADP/ATP carrier isoform (Tjaden et al., 2004, Williams et al., 2008, Chan et al., 2005). The expression of different isoforms is tissue dependent in multicellular eukaryotes (Powell et al., 1989, Dahout-Gonzalez et al., 2006). For example in *Homo sapiens*, ADP/ATP carrier isoform 1 is mainly expressed in heart and skeletal muscle and much less in brain, isoform 2 is expressed in most differentiated tissues during development, isoform 3 is expressed in all tissues with different levels, and isoform 4 is exclusively expressed in liver, testis and brain (Stepien et al., 1992, Dolce et al., 2005). This is in contrast to unicellular eukaryotes, where the expression of different isoforms is found to be dependent on the available substrates and the associated aerobic or fermentative metabolism (Kolarov et al., 1990b). For most unicellular eukaryotes the situation appears to be less complex, and in general their genomes code for only one single ADP/ATP carrier (for an overview, see (Traba et al., 2011) and references therein). A notable exception is *S. cerevisiae*, with its genome containing 3 different ADP/ATP carrier genes (*ScANC1-3*; (Lawson and Douglas, 1988). The expression and physiological function of the respective ScAnc1-3p isoforms has been extensively analysed, and was found to be dependent on the type of

metabolic substrate and the presence of specific environmental factors (Kolarov et al., 1990a, Lawson et al., 1990, Gawaz et al., 1990, Drgon et al., 1992, Sabova et al., 1996). For example, ScAnc2p is only required for aerobic growth on non-fermentable carbon sources such as lactate and glycerol, whereas ScAnc3p is essential for growth under fermentative or anaerobic conditions. Expression of both ScAnc2p and ScAnc3p is furthermore relying on the availability of heme (Betina et al., 1995, Sabova et al., 1993). This is in contrast to ScAnc1p, whose expression is down regulated under anaerobic conditions in a heme-independent fashion (Gavurnikova et al., 1996). The different ScAncp isoforms most probably evolved to accommodate the changing energy requirements of *S. cerevisiae*, when producing ATP by using different substrates and associated fermentative or non-fermentative pathways (Sabova et al., 1996).

Also *T. brucei* exhibits an adaptable energy metabolism – with substantial metabolic re-arrangements occurring during the various developmental life cycle stages (Matthews, 2005, Bringaud et al., 2006, Michels et al., 2006). The *T. brucei* MCF protein inventory includes only two predicted ADP/ATP carriers, i.e. TbMCP5 and TbMCP15, with significant sequence similarity to known and functionally characterised ADP/ATP carriers from other eukaryotes (Colasante et al., 2009). The transport function and physiological role(s) of TbMCP5 and TbMCP15 have not been determined yet.

10. The mitochondrial phosphate carrier

As mentioned above, also the phosphate carrier plays an important role in the mitochondrial energy metabolism by replenishing Pi that has been consumed during ATP synthesis in the mitochondrial matrix (Wohlrab, 1986, Stappen and Kramer,

1993, Wehrle and Pedersen, 1982). Three different transport mechanisms have been described for the phosphate carrier (see Figure 9), i.e. phosphate/phosphate or phosphate/hydroxyl antiport, phosphate/proton symport, and mercurial-induced uniport (see (Kramer, 1996) and references therein). Similar to the ADP/ATP carrier, also the phosphate carrier is dependent on the presence of cardiolipin (Kadenbach et al., 1982). Its Pi-exchange activity can be reversible inactivated by the addition of Triton X-100 or high concentrations of non-ionic detergents, which removes cardiolipin from the carrier (Mende et al., 1983). Vice versa, its Pi-exchange activity into rat liver mitochondria is stimulated by the addition of thyroid hormones, which substantially increases the cardiolipin concentration in the mitochondrial inner membrane, thus leading to a more favourable lipid microenvironment for the phosphate carrier (Paradies and Ruggiero, 1990).

The important role of the mitochondrial phosphate carrier in the eukaryotic energy production, and associated detrimental disease in case of its dysfunction, was recently described for human patients (Mayr et al., 2007). Dysfunction was mainly caused by specific detrimental mutations in the human phosphate carrier-coding genes, and was confirmed by functional complementation studies using mitochondrial phosphate carrier-deficient yeast strains (Mayr et al., 2007). In particular oxidative phosphorylation appears to be affected by mitochondrial phosphate carrier dysfunction (Mayr et al., 2007). The mitochondrial phosphate carrier plays further a key role in mitochondrial permeability transition, and was found to be a critical component of the mitochondrial permeability transition pore (MPTP) (Leung et al., 2008, Varanyuwatana and Halestrap, 2012). It further interacts with cyclophilin-D, which is a known regulator and component of the MPTP (Giorgio et al., 2010, Azzolin et al., 2010, Doczi et al., 2011).

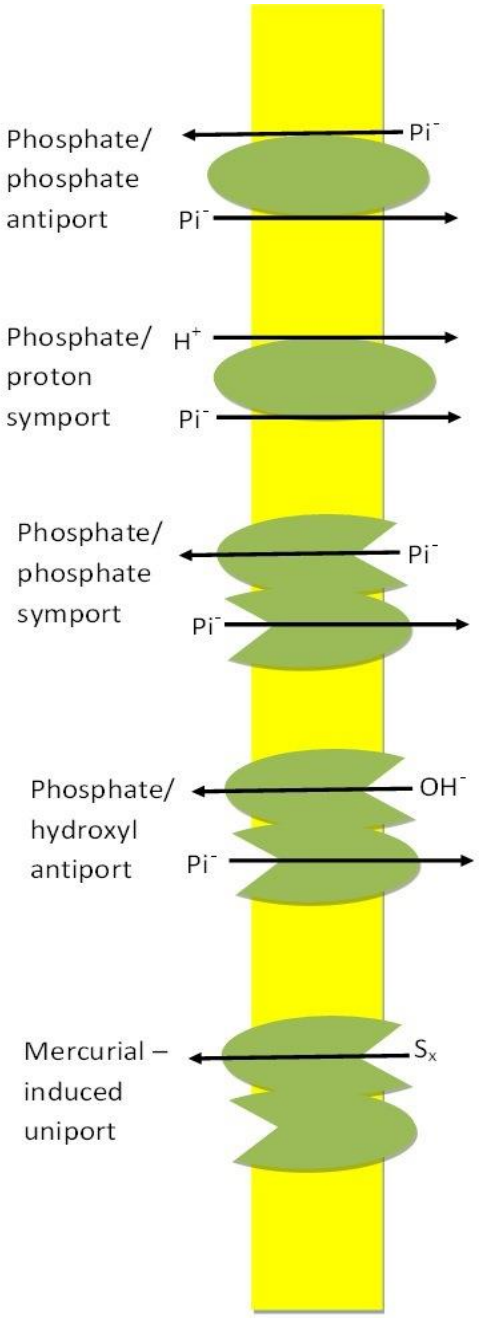

Figure 9: Proposed transport models for the mitochondrial phosphate carrier. The upper two models show a schematic representation of the antiport and symport transport modes, while the lower three models illustrate the transport of different substrates in exchange with phosphate. Adapted from (Kramer, 1996).

Of all known mitochondrial phosphate carriers, in particular those from bovine heart (SLC25A3) (Runswick et al., 1987), rat liver (SLC25A3) (Ferreira et al., 1989), human heart (SLC25A3) (Dolce et al., 1991) and yeast (Mir1p and Pic2p) (Phelps et al., 1991) have been well studied (Palmieri et al., 2011, Kramer, 1996). Their sequences show the typical repetitive protein structure and conserved sequence motives present in all MCF proteins (see Section 1.7) (Kuan and Saier, 1993). In addition, their substrate contact points (CP1-3, Fig. 6) are conserved, confirming the binding of similar substrates. All phosphate-transporting MCF proteins known so far contain the conserved amino acids glycine (G), glutamine (Q) and lysine (K) in CP1; the amino acids arginine (R) and glutamine (Q) in CP2; and a conserved methionine (M) in CP3 (Kunji and Robinson, 2006). In addition, different cysteine residues have been identified, which were shown to be involved in two different transport mechanisms, i.e. substrate-specific antiport, and uncoupled/unspecific uniport (Schroers et al., 1997). Reversible modification of two cysteine residues at position 28 of the functional dimers, resulted in a switch between these two transport modes (Schroers et al., 1997). The specific molecular mechanism behind this switch is still unclear. Other important amino residues are found in the first hydrophilic loop, i.e. the cysteine (C) position 42 of the beef heart phosphate carrier Mir1p and the threonine (T) found at position 43 in the case of yeast phosphate carrier Mir1p (Kramer, 1996). The cysteine 42 in beef, and threonine together with isoleucine 141 in yeast are responsible for high transport activity. (Wohlrab and Briggs, 1994, Guerin et al., 1990, Phelps and Wohlrab, 1991). Moreover, the glutamate (E) residue at position 126, the glutamate residue at position 137, and the histidine residue at position 31 of the yeast phosphate carrier Mir1p were reported to play an important role in proton transport (Wohlrab and Briggs, 1994). As mentioned above, two

putative mitochondrial phosphate carriers were predicted for *T. brucei*, i.e. TbMCP8 and TbMCP11 (Colasante et al., 2009). The transport function and physiological role(s) of these MCF proteins is yet unknown.

11. Energy-buffering in *T. brucei*

As mentioned above, *T. brucei* is a motile (flagellated) parasite with a complex life cycle alternating between the bloodstream in the mammalian host and the midgut of the vector, the tsetse fly (Matthews et al., 2004). In the mammalian bloodstream, and to some extent also in the tsetse fly midgut, the parasite will be exposed to substantial oxidative stress (see (Turrens, 2004) and references therein). When taken up by the insect vector during a blood meal or when injected with the saliva into the mammalian bloodstream, the parasite will enter a new host environment with different metabolic substrates. This change in environment requires differentiation, and a quick adaptation of the different metabolic pathways involved with these substrates. This process of adaptation will most probably be accompanied by a short period of ATP shortage. Also oxidative stress defence mechanisms and motility are known to consume large quantities of ATP (Tiwari et al., 2002, Agalakova and Gusev, 2012). Therefore, a rapid energy-phosphate buffer/regeneration system is required to maintain constant ATP levels in *T. brucei*.

Arginine kinase (ATP:arginine phosphotransferase) is one of the most widely distributed phosphagen kinases and catalyses the reversible phosphorylation of arginine using ATP (Ellington, 2001, Wallimann et al., 1992). The resulting product, phosphoarginine, does not interfere with the metabolism and can be stored in large quantities in the cell (Ellington, 2001, Wallimann et al., 1992). The phosphoarginine/arginine kinase system is predominantly found in crustaceans,

molluscs, insects, and different protozoa (Blethen and Kaplan, 1968, Suzuki et al., 2000, Werr et al., 2009, Pereira et al., 2002), and is analogous to the phosphocreatine/creatine kinase system, which is mainly found in vertebrates (Ellington, 2001, Wallimann et al., 1992). Creatine kinases and arginine kinases are evolutionarily related, and most probably share a common ancestral gene (Ellington, 2001).

Also trypanosomes were reported to contain a phosphoarginine/arginine kinase system (Pereira et al., 2011, Canepa et al., 2011, Pereira et al., 2000). In particular the arginine kinase from *Trypanosoma cruzi* has been well-studied, including its characterization, and functional and structural analysis (Fernandez et al., 2007, Pereira et al., 2000, Miranda et al., 2006, Pereira et al., 2003). *T. cruzi* expresses only a single arginine kinase (TcAK), which is exclusively located in its cytoplasm (Pereira et al., 2000, Miranda et al., 2009). Overexpression of TcAK was found to significantly increase the survival capability of *T. cruzi*, when exposed to low pH, high concentrations of hydrogen peroxide (oxidative stress) and nutritional stress (Pereira et al., 2003, Miranda et al., 2006). A similar phenotype, i.e. an increased survival capability in the presence of challenging conditions, was observed when expressing TcAK in the heterologous hosts *S. cerevisiae* and *E. coli*, which lack natural phosphagen kinases (Canonaco et al., 2003, Canonaco et al., 2002). It was therefore postulated that the *T. cruzi* arginine kinase plays an important role in the provision of a cellular energy buffer (phosphoarginine), which can be used as a source of ATP under stress conditions (Miranda et al., 2006, Pereira et al., 2003).

The *T. cruzi* arginine kinase has been structurally characterized by X-ray crystallography, and comparison revealed a high structural similarity with the only

other structurally characterised arginine kinase from the horseshoe crab *Limulus polyphemus* (Fernandez et al., 2007, Zhou et al., 1998). Sequence analysis showed that the *T. cruzi* arginine kinase is very similar (72%) to the arginine kinase from *Limulus polyphemus* and to creatine kinases (45-47%) from different vertebrates (Fernandez et al., 2007, Yousef et al., 2003). Arginine kinase and other phosphagen kinases, like creatine and guanidine kinases, share a common mechanism for substrate binding and the transfer of the γ-phosphoryl group from ATP (Yousef et al., 2002). The canonical arginine kinase structure from *L. polyphemus* has been extensively characterised and was shown to include two so-called 'specificity loop' at position 63-68 which mediate substrate specificity (Zhou et al., 1998, Azzi et al., 2004, Fernandez et al., 2007) and the residues 309-318 which form the second loop and are involved in closing the active site after binding of substrate analogues (Fernandez et al., 2007, Azzi et al., 2004); as well as two conserved amino acid residues required for substrate binding (Cys271) and catalysis (Glu225) (Pruett et al., 2003). The sequences found in the first corresponding 'specificity loop' of the *T. cruzi* (TcAK: 'LDSGIGVY') and *L. polyphemus* (LpAK: 'LDSGVGIY') arginine kinases are nearly identical (Fernandez et al., 2007). The *T. cruzi* arginine kinase however lacks a second amino acid residue, i.e. Glu314, which was proposed to be conserved and involved in catalysis for the *L. polyphemus* arginine kinase (Fernandez et al., 2007). In addition to the 'specificity loop', other amino acid residues were found to be conserved in both TcAK and LpAK, including the residues Ser122, His185 and His284, which are involved in interaction with the nucleotide ring; the residues Arg124, Arg126, Arg229 and Arg280, which are involved in the binding of ADP and ATP (Fernandez et al., 2007).

Next to *T. cruzi*, also *T. brucei* was reported to contain arginine kinase activity (Pereira et al., 2002). Genome analysis indicated further the presence of three different arginine kinase-coding genes in the *T. brucei* genome, whereas none could be identified for *Leishmania major* (Ivens et al., 2005, Berriman et al., 2005). The expression of the different arginine kinase isoforms in *T. brucei*, and their function and physiological roles in the different life cycle stages of this parasite, has not been elucidated yet.

12. Aim of the PhD project

The mitochondrion plays a vital role in the cellular energy (ATP) provision of the procyclic form of *Trypanosoma brucei*. ATP is produced in the mitochondrial matrix from ADP and inorganic phosphate by substrate-level and oxidative phosphorylation. To maintain the cellular energy provision, ATP has to be exported from the mitochondrial matrix, and ADP and Pi imported from the cytosol. This exchange is facilitated by ADP/ATP carriers and phosphate carriers located in the mitochondrial inner membrane. The exported ATP is either directly used by the rest of the cell or stored as phosphoarginine to provide an energy buffer during periods of high energy consumption. Virtually nothing is known about the mitochondrial ADP/ATP and Pi transport, and the phosphoarginine/arginine kinase energy (ATP) buffering system in *Trypanosoma brucei*. The aim of this PhD project is to improve our understanding of these two important cellular processes in *T. brucei*. To achieve this aim, I will functionally characterise the putative ADP/ATP carriers TbMCP5 and TbMCP15 (Chapter II), the putative phosphate carriers TbMCP8 and TbMCP11 (Chapter III), and the arginine kinases TbAK1-3 (Chapter IV) involved in the *T. brucei* energy-production and buffering system.

References

ADRIAN, G. S., MCCAMMON, M. T., MONTGOMERY, D. L. & DOUGLAS, M. G. 1986. Sequences required for delivery and localization of the ADP/ATP translocator to the mitochondrial inner membrane. *Mol Cell Biol,* 6**,** 626-34.

AGABIAN, N. 1990. Trans splicing of nuclear pre-mRNAs. *Cell,* 61**,** 1157-60.

AGALAKOVA, N. I. & GUSEV, G. P. 2012. Fluoride induces oxidative stress and ATP depletion in the rat erythrocytes in vitro. *Environ Toxicol Pharmacol,* 34**,** 334-7.

APHASIZHEV, R. & APHASIZHEVA, I. 2011. Uridine insertion/deletion editing in trypanosomes: a playground for RNA-guided information transfer. *Wiley Interdiscip Rev RNA,* 2**,** 669-85.

APTED, F. I. C. 1970. *Clinical Manifestations and Diagnosis of Sleeping Sickness. In The African Trypanosomiases.*

AQUILA, H., LINK, T. A. & KLINGENBERG, M. 1987. Solute carriers involved in energy transfer of mitochondria form a homologous protein family. *FEBS Lett,* 212**,** 1-9.

ARANDA, A., MAUGERI, D., UTTARO, A. D., OPPERDOES, F., CAZZULO, J. J. & NOWICKI, C. 2006. The malate dehydrogenase isoforms from *Trypanosoma brucei*: subcellular localization and differential expression in bloodstream and procyclic forms. *Int J Parasitol,* 36**,** 295-307.

ARRESE, E. L. & SOULAGES, J. L. 2010. Insect fat body: energy, metabolism, and regulation. *Annu Rev Entomol,* 55**,** 207-25.

ASHLEY, J. N., BARBER, H. J., EWINS, A. J., NEWBERY, G. & SELF, A. D. H. 1942. 20. A chemotherapeutic comparison of the trypanocidal action of some aromatic diamidines. *Journal of the Chemical Society (Resumed),* 0**,** 103-116.

AZZI, A., CLARK, S. A., ELLINGTON, W. R. & CHAPMAN, M. S. 2004. The role of phosphagen specificity loops in arginine kinase. *Protein Sci,* 13**,** 575-85.

AZZOLIN, L., VON STOCKUM, S., BASSO, E., PETRONILLI, V., FORTE, M. A. & BERNARDI, P. 2010. The mitochondrial permeability transition from yeast to mammals. *FEBS Lett,* 584**,** 2504-9.

BABOT, M., BLANCARD, C., PELOSI, L., LAUQUIN, G. J. & TREZEGUET, V. 2012. The transmembrane prolines of the mitochondrial ADP/ATP carrier are

involved in nucleotide binding and transport and its biogenesis. *J Biol Chem,* 287**,** 10368-78.

BARNARD, J. P. & PEDERSEN, P. L. 1994. Alteration of pyruvate metabolism in African trypanosomes during differentiation from bloodstream into insect forms. *Arch Biochem Biophys,* 313**,** 77-82.

BARRETT, F. M. 1974. Changes in the concentration of free amino acids in the haemolymph of Rhodnius prolixus during the fifth instar. *Comp Biochem Physiol B,* 48**,** 241-50.

BARRETT, M. P. 1997. The pentose phosphate pathway and parasitic protozoa. *Parasitol Today,* 13**,** 11-6.

BARRETT, M. P., BOYKIN, D. W., BRUN, R. & TIDWELL, R. R. 2007. Human African trypanosomiasis: pharmacological re-engagement with a neglected disease. *Br J Pharmacol,* 152**,** 1155-71.

BARRY, J. D., MARCELLO, L., MORRISON, L. J., READ, A. F., LYTHGOE, K., JONES, N., CARRINGTON, M., BLANDIN, G., BOHME, U., CALER, E., HERTZ-FOWLER, C., RENAULD, H., EL-SAYED, N. & BERRIMAN, M. 2005. What the genome sequence is revealing about trypanosome antigenic variation. *Biochem Soc Trans,* 33**,** 986-9.

BARRY, J. D. & MCCULLOCH, R. 2001. Antigenic variation in trypanosomes: enhanced phenotypic variation in a eukaryotic parasite. *Adv Parasitol,* 49**,** 1-70.

BATTINI, R., FERRARI, S., KACZMAREK, L., CALABRETTA, B., CHEN, S. T. & BASERGA, R. 1987. Molecular cloning of a cDNA for a human ADP/ATP carrier which is growth-regulated. *J Biol Chem,* 262**,** 4355-9.

BAUM, K. F., BERENS, R. L., MARR, J. J., HARRINGTON, J. A. & SPECTOR, T. 1989. Purine deoxynucleoside salvage in Giardia lamblia. *J Biol Chem,* 264**,** 21087-90.

BENNE, R., VAN DEN BURG, J., BRAKENHOFF, J. P., SLOOF, P., VAN BOOM, J. H. & TROMP, M. C. 1986. Major transcript of the frameshifted coxII gene from trypanosome mitochondria contains four nucleotides that are not encoded in the DNA. *Cell,* 46**,** 819-26.

BERNSTEIN, B. E., WILLIAMS, D. M., BRESSI, J. C., KUHN, P., GELB, M. H., BLACKBURN, G. M. & HOL, W. G. 1998. A bisubstrate analog induces

unexpected conformational changes in phosphoglycerate kinase from *Trypanosoma brucei*. *J Mol Biol,* 279**,** 1137-48.

BERRIMAN, M., GHEDIN, E., HERTZ-FOWLER, C., BLANDIN, G., RENAULD, H., BARTHOLOMEU, D. C., LENNARD, N. J., CALER, E., HAMLIN, N. E., HAAS, B., BOHME, U., HANNICK, L., ASLETT, M. A., SHALLOM, J., MARCELLO, L., HOU, L., WICKSTEAD, B., ALSMARK, U. C., ARROWSMITH, C., ATKIN, R. J., BARRON, A. J., BRINGAUD, F., BROOKS, K., CARRINGTON, M., CHEREVACH, I., CHILLINGWORTH, T. J., CHURCHER, C., CLARK, L. N., CORTON, C. H., CRONIN, A., DAVIES, R. M., DOGGETT, J., DJIKENG, A., FELDBLYUM, T., FIELD, M. C., FRASER, A., GOODHEAD, I., HANCE, Z., HARPER, D., HARRIS, B. R., HAUSER, H., HOSTETLER, J., IVENS, A., JAGELS, K., JOHNSON, D., JOHNSON, J., JONES, K., KERHORNOU, A. X., KOO, H., LARKE, N., LANDFEAR, S., LARKIN, C., LEECH, V., LINE, A., LORD, A., MACLEOD, A., MOONEY, P. J., MOULE, S., MARTIN, D. M., MORGAN, G. W., MUNGALL, K., NORBERTCZAK, H., ORMOND, D., PAI, G., PEACOCK, C. S., PETERSON, J., QUAIL, M. A., RABBINOWITSCH, E., RAJANDREAM, M. A., REITTER, C., SALZBERG, S. L., SANDERS, M., SCHOBEL, S., SHARP, S., SIMMONDS, M., SIMPSON, A. J., TALLON, L., TURNER, C. M., TAIT, A., TIVEY, A. R., VAN AKEN, S., WALKER, D., WANLESS, D., WANG, S., WHITE, B., WHITE, O., WHITEHEAD, S., WOODWARD, J., WORTMAN, J., ADAMS, M. D., EMBLEY, T. M., GULL, K., ULLU, E., BARRY, J. D., FAIRLAMB, A. H., OPPERDOES, F., BARRELL, B. G., DONELSON, J. E., HALL, N., FRASER, C. M., et al. 2005. The genome of the African trypanosome *Trypanosoma brucei*. *Science*, 309**,** 416-22.

BETINA, S., GAVURNIKOVA, G., HAVIERNIK, P., SABOVA, L. & KOLAROV, J. 1995. Expression of the AAC2 gene encoding the major mitochondrial ADP/ATP carrier in Saccharomyces cerevisiae is controlled at the transcriptional level by oxygen, heme and HAP2 factor. *European journal of biochemistry / FEBS,* 229**,** 651-7.

BEYER, K. & KLINGENBERG, M. 1985. ADP/ATP carrier protein from beef heart mitochondria has high amounts of tightly bound cardiolipin, as revealed by 31P nuclear magnetic resonance. *Biochemistry,* 24**,** 3821-6.

BIENEN, E. J., MATURI, R. K., POLLAKIS, G. & CLARKSON, A. B., JR. 1993. Non-cytochrome mediated mitochondrial ATP production in bloodstream form *Trypanosoma brucei brucei*. *Eur J Biochem,* 216**,** 75-80.

BLETHEN, S. L. & KAPLAN, N. O. 1968. Characteristics of arthropod arginine kinases. *Biochemistry,* 7**,** 2123-35.

BLUM, B., BAKALARA, N. & SIMPSON, L. 1990. A model for RNA editing in kinetoplastid mitochondria: "guide" RNA molecules transcribed from maxicircle DNA provide the edited information. *Cell,* 60**,** 189-98.

BOCHUD-ALLEMANN, N. & SCHNEIDER, A. 2002. Mitochondrial substrate level phosphorylation is essential for growth of procyclic *Trypanosoma brucei*. *J Biol Chem,* 277**,** 32849-54.

BONEN, L. 1993. Trans-splicing of pre-mRNA in plants, animals, and protists. *FASEB J,* 7**,** 40-6.

BOOTHROYD, J. C. & CROSS, G. A. 1982. Transcripts coding for variant surface glycoproteins of *Trypanosoma brucei* have a short, identical exon at their 5' end. *Gene,* 20**,** 281-9.

BRANDOLIN, G., LE SAUX, A., TREZEGUET, V., VIGNAIS, P. V. & LAUQUIN, G. J. 1993. Biochemical characterisation of the isolated Anc2 adenine nucleotide carrier from Saccharomyces cerevisiae mitochondria. *Biochem Biophys Res Commun,* 192**,** 143-50.

BRINGAUD, F., BARRETT, M. P. & ZILBERSTEIN, D. 2012. Multiple roles of proline transport and metabolism in trypanosomatids. *Front Biosci,* 17**,** 349-74.

BRINGAUD, F., RIVIERE, L. & COUSTOU, V. 2006. Energy metabolism of trypanosomatids: adaptation to available carbon sources. *Mol Biochem Parasitol,* 149**,** 1-9.

BROGNA, S. & ASHBURNER, M. 1997. The Adh-related gene of Drosophila melanogaster is expressed as a functional dicistronic messenger RNA: multigenic transcription in higher organisms. *EMBO J,* 16**,** 2023-31.

CALLENS, M., KUNTZ, D. A. & OPPERDOES, F. R. 1991. Characterization of pyruvate kinase of *Trypanosoma brucei* and its role in the regulation of carbohydrate metabolism. *Mol Biochem Parasitol,* 47**,** 19-29.

CANEPA, G. E., CARRILLO, C., MIRANDA, M. R., SAYE, M. & PEREIRA, C. A. 2011. Arginine kinase in Phytomonas, a trypanosomatid parasite of plants. *Comp Biochem Physiol B Biochem Mol Biol,* 160**,** 40-3.

CANONACO, F., SCHLATTNER, U., PRUETT, P. S., WALLIMANN, T. & SAUER, U. 2002. Functional expression of phosphagen kinase systems confers resistance to transient stresses in Saccharomyces cerevisiae by buffering the ATP pool. *J Biol Chem,* 277**,** 31303-9.

CANONACO, F., SCHLATTNER, U., WALLIMANN, T. & SAUER, U. 2003. Functional expression of arginine kinase improves recovery from pH stress of Escherichia coli. *Biotechnol Lett,* 25**,** 1013-7.

CARPENTER, L. R. & ENGLUND, P. T. 1995. Kinetoplast maxicircle DNA replication in Crithidia fasciculata and *Trypanosoma brucei*. *Mol Cell Biol,* 15**,** 6794-803.

CASTRO, H., ROMAO, S., CARVALHO, S., TEIXEIRA, F., SOUSA, C. & TOMAS, A. M. 2010. Mitochondrial redox metabolism in trypanosomatids is independent of tryparedoxin activity. *PLoS One,* 5**,** e12607.

CAVALIER-SMITH, T. 1981. Eukaryote kingdoms: seven or nine? *Biosystems,* 14**,** 461-81.

CHAN, K. W., SLOTBOOM, D. J., COX, S., EMBLEY, T. M., FABRE, O., VAN DER GIEZEN, M., HARDING, M., HORNER, D. S., KUNJI, E. R., LEON-AVILA, G. & TOVAR, J. 2005. A novel ADP/ATP transporter in the mitosome of the microaerophilic human parasite Entamoeba histolytica. *Curr Biol,* 15**,** 737-42.

CHAUDHARY, K., DARLING, J. A., FOHL, L. M., SULLIVAN, W. J., JR., DONALD, R. G., PFEFFERKORN, E. R., ULLMAN, B. & ROOS, D. S. 2004. Purine salvage pathways in the apicomplexan parasite Toxoplasma gondii. *J Biol Chem,* 279**,** 31221-7.

CHAUDHURI, M., OTT, R. D. & HILL, G. C. 2006. Trypanosome alternative oxidase: from molecule to function. *Trends Parasitol,* 22**,** 484-91.

CHUDZIK, D. M., MICHELS, P. A., DE WALQUE, S. & HOL, W. G. 2000. Structures of type 2 peroxisomal targeting signals in two trypanosomatid aldolases. *J Mol Biol,* 300**,** 697-707.

CLEMENCON, B., REY, M., DIANOUX, A. C., TREZEGUET, V., LAUQUIN, G. J., BRANDOLIN, G. & PELOSI, L. 2008. Structure-function relationships of

the C-terminal end of the Saccharomyces cerevisiae ADP/ATP carrier isoform 2. *J Biol Chem,* 283**,** 11218-25.

CLEMENCON, B., REY, M., TREZEGUET, V., FOREST, E. & PELOSI, L. 2011. Yeast ADP/ATP carrier isoform 2: conformational dynamics and role of the RRRMMM signature sequence methionines. *J Biol Chem,* 286**,** 36119-31.

COLASANTE, C., ALIBU, V. P., KIRCHBERGER, S., TJADEN, J., CLAYTON, C. & VONCKEN, F. 2006a. Characterization and developmentally regulated localization of the mitochondrial carrier protein homologue MCP6 from *Trypanosoma brucei*. *Eukaryot Cell,* 5**,** 1194-205.

COLASANTE, C., ELLIS, M., RUPPERT, T. & VONCKEN, F. 2006b. Comparative proteomics of glycosomes from bloodstream form and procyclic culture form *Trypanosoma brucei brucei*. *Proteomics,* 6**,** 3275-93.

COLASANTE, C., PENA DIAZ, P., CLAYTON, C. & VONCKEN, F. 2009. Mitochondrial carrier family inventory of *Trypanosoma brucei brucei*: Identification, expression and subcellular localisation. *Mol Biochem Parasitol,* 167**,** 104-17.

COLEY, A. F., DODSON, H. C., MORRIS, M. T. & MORRIS, J. C. 2011. Glycolysis in the african trypanosome: targeting enzymes and their subcellular compartments for therapeutic development. *Mol Biol Int,* 2011**,** 123702.

COMINI, M. A., GUERRERO, S. A., HAILE, S., MENGE, U., LUNSDORF, H. & FLOHE, L. 2004. Validation of *Trypanosoma brucei* trypanothione synthetase as drug target. *Free Radic Biol Med,* 36**,** 1289-302.

COUSTOU, V., BESTEIRO, S., BIRAN, M., DIOLEZ, P., BOUCHAUD, V., VOISIN, P., MICHELS, P. A., CANIONI, P., BALTZ, T. & BRINGAUD, F. 2003. ATP generation in the *Trypanosoma brucei* procyclic form: cytosolic substrate level is essential, but not oxidative phosphorylation. *J Biol Chem,* 278**,** 49625-35.

COUSTOU, V., BESTEIRO, S., RIVIERE, L., BIRAN, M., BITEAU, N., FRANCONI, J. M., BOSHART, M., BALTZ, T. & BRINGAUD, F. 2005. A mitochondrial NADH-dependent fumarate reductase involved in the production of succinate excreted by procyclic *Trypanosoma brucei*. *J Biol Chem,* 280**,** 16559-70.

COZENS, A. L., RUNSWICK, M. J. & WALKER, J. E. 1989. DNA sequences of two expressed nuclear genes for human mitochondrial ADP/ATP translocase. *J Mol Biol,* 206**,** 261-80.

DAHOUT-GONZALEZ, C., NURY, H., TREZEGUET, V., LAUQUIN, G. J., PEBAY-PEYROULA, E. & BRANDOLIN, G. 2006. Molecular, functional, and pathological aspects of the mitochondrial ADP/ATP carrier. *Physiology (Bethesda),* 21**,** 242-9.

DANIELS, J. P., GULL, K. & WICKSTEAD, B. 2010. Cell biology of the *trypanosome* genome. *Microbiol Mol Biol Rev,* 74**,** 552-69.

DAVIES, M. J., ROSS, A. M. & GUTTERIDGE, W. E. 1983. The enzymes of purine salvage in *Trypanosoma cruzi*, *Trypanosoma brucei* and *Leishmania mexicana*. *Parasitology,* 87 (Pt 2)**,** 211-7.

DE MARCOS LOUSA, C., TREZEGUET, V., DIANOUX, A. C., BRANDOLIN, G. & LAUQUIN, G. J. 2002. The human mitochondrial ADP/ATP carriers: kinetic properties and biogenesis of wild-type and mutant proteins in the yeast *S. cerevisiae*. *Biochemistry,* 41**,** 14412-20.

DOCAMPO, R. 1995. *Antioxidant Mechanisms. In "Biochemistry and Molecular Biology of Parasites ".* , London, Academic Press.

DOCZI, J., TURIAK, L., VAJDA, S., MANDI, M., TOROCSIK, B., GERENCSER, A. A., KISS, G., KONRAD, C., ADAM-VIZI, V. & CHINOPOULOS, C. 2011. Complex contribution of cyclophilin D to Ca2+-induced permeability transition in brain mitochondria, with relation to the bioenergetic state. *J Biol Chem,* 286**,** 6345-53.

DOLCE, V., FIERMONTE, G., MESSINA, A. & PALMIERI, F. 1991. Nucleotide sequence of a human heart cDNA encoding the mitochondrial phosphate carrier. *DNA Seq,* 2**,** 133-5.

DOLCE, V., FIERMONTE, G., RUNSWICK, M. J., PALMIERI, F. & WALKER, J. E. 2001. The human mitochondrial deoxynucleotide carrier and its role in the toxicity of nucleoside antivirals. *Proc Natl Acad Sci U S A,* 98**,** 2284-8.

DOLCE, V., SCARCIA, P., IACOPETTA, D. & PALMIERI, F. 2005. A fourth ADP/ATP carrier isoform in man: identification, bacterial expression, functional characterization and tissue distribution. *FEBS Lett,* 579**,** 633-7.

DORMEYER, M., RECKENFELDERBAUMER, N., LUDEMANN, H. & KRAUTH-SIEGEL, R. L. 2001. Trypanothione-dependent synthesis of

deoxyribonucleotides by *Trypanosoma brucei* ribonucleotide reductase. *J Biol Chem,* 276**,** 10602-6.

DRGON, T., SABOVA, L., GAVURNIKOVA, G. & KOLAROV, J. 1992. Yeast ADP/ATP carrier (AAC) proteins exhibit similar enzymatic properties but their deletion produces different phenotypes. *FEBS letters,* 304**,** 277-80.

EBIKEME, C., HUBERT, J., BIRAN, M., GOUSPILLOU, G., MORAND, P., PLAZOLLES, N., GUEGAN, F., DIOLEZ, P., FRANCONI, J. M., PORTAIS, J. C. & BRINGAUD, F. 2010. Ablation of succinate production from glucose metabolism in the procyclic *trypanosomes* induces metabolic switches to the glycerol 3-phosphate/dihydroxyacetone phosphate shuttle and to proline metabolism. *J Biol Chem,* 285**,** 32312-24.

ELLINGTON, W. R. 2001. Evolution and physiological roles of phosphagen systems. *Annu Rev Physiol,* 63**,** 289-325.

EMBLEY, T. M. & MARTIN, W. 2006. Eukaryotic evolution, changes and challenges. *Nature,* 440**,** 623-30.

ENGLUND, P. T., HAJDUK, S. L. & MARINI, J. C. 1982. The molecular biology of *trypanosomes*. *Annu Rev Biochem,* 51**,** 695-726.

FAIRLAMB, A. H., BLACKBURN, P., ULRICH, P., CHAIT, B. T. & CERAMI, A. 1985. Trypanothione: a novel bis(glutathionyl)spermidine cofactor for glutathione reductase in *trypanosomatids*. *Science,* 227**,** 1485-7.

FENN, K. & MATTHEWS, K. R. 2007. The cell biology of *Trypanosoma brucei* differentiation. *Curr Opin Microbiol,* 10**,** 539-46.

FERNANDEZ, P., HAOUZ, A., PEREIRA, C. A., AGUILAR, C. & ALZARI, P. M. 2007. The crystal structure of *Trypanosoma cruzi* arginine kinase. *Proteins,* 69**,** 209-12.

FERREIRA, G. C., PRATT, R. D. & PEDERSEN, P. L. 1989. Energy-linked anion transport. Cloning, sequencing, and characterization of a full length cDNA encoding the rat liver mitochondrial proton/phosphate symporter. *J Biol Chem,* 264**,** 15628-33.

FEVRE, E. M., PICOZZI, K., FYFE, J., WAISWA, C., ODIIT, M., COLEMAN, P. G. & WELBURN, S. C. 2005. A burgeoning epidemic of sleeping sickness in Uganda. *Lancet,* 366**,** 745-7.

FIERMONTE, G., DOLCE, V., ARRIGONI, R., RUNSWICK, M. J., WALKER, J. E. & PALMIERI, F. 1999. Organization and sequence of the gene for the human

mitochondrial dicarboxylate carrier: evolution of the carrier family. *Biochem J,* 344 Pt 3**,** 953-60.

FIERMONTE, G., DOLCE, V., DAVID, L., SANTORELLI, F. M., DIONISI-VICI, C., PALMIERI, F. & WALKER, J. E. 2003. The mitochondrial ornithine transporter. Bacterial expression, reconstitution, functional characterization, and tissue distribution of two human isoforms. *J Biol Chem,* 278**,** 32778-83.

FIERMONTE, G., DOLCE, V., PALMIERI, L., VENTURA, M., RUNSWICK, M. J., PALMIERI, F. & WALKER, J. E. 2001. Identification of the human mitochondrial oxodicarboxylate carrier. Bacterial expression, reconstitution, functional characterization, tissue distribution, and chromosomal location. *J Biol Chem,* 276**,** 8225-30.

FIERMONTE, G., PALMIERI, L., TODISCO, S., AGRIMI, G., PALMIERI, F. & WALKER, J. E. 2002. Identification of the mitochondrial glutamate transporter. Bacterial expression, reconstitution, functional characterization, and tissue distribution of two human isoforms. *J Biol Chem,* 277**,** 19289-94.

GAVURNIKOVA, G., SABOVA, L., KISSOVA, I., HAVIERNIK, P. & KOLAROV, J. 1996. Transcription of the AAC1 gene encoding an isoform of mitochondrial ADP/ATP carrier in *Saccharomyces cerevisiae* is regulated by oxygen in a heme-independent manner. *European journal of biochemistry / FEBS,* 239**,** 759-63.

GAWAZ, M., DOUGLAS, M. G. & KLINGENBERG, M. 1990. Structure-function studies of adenine nucleotide transport in mitochondria. II. Biochemical analysis of distinct AAC1 and AAC2 proteins in yeast. *The Journal of biological chemistry,* 265**,** 14202-8.

GEIGENBERGER, P., STAMME, C., TJADEN, J., SCHULZ, A., QUICK, P. W., BETSCHE, T., KERSTING, H. J. & NEUHAUS, H. E. 2001. Tuber physiology and properties of starch from tubers of transgenic potato plants with altered plastidic adenylate transporter activity. *Plant Physiol,* 125**,** 1667-78.

GIBSON, W. C. 1986. Will the real *Trypanosoma b. gambiense* please stand up. *Parasitol Today,* 2**,** 255-7.

GILBERT, R. J. & KLEIN, R. A. 1984. Pyruvate kinase: a carnitine-regulated site of ATP production in *Trypanosoma brucei brucei*. *Comp Biochem Physiol B,* 78**,** 595-9.

GIORGIO, V., SORIANO, M. E., BASSO, E., BISETTO, E., LIPPE, G., FORTE, M. A. & BERNARDI, P. 2010. Cyclophilin D in mitochondrial pathophysiology. *Biochim Biophys Acta,* 1797**,** 1113-8.

GRAHAM, B. H., WAYMIRE, K. G., COTTRELL, B., TROUNCE, I. A., MACGREGOR, G. R. & WALLACE, D. C. 1997. A mouse model for mitochondrial myopathy and cardiomyopathy resulting from a deficiency in the heart/muscle isoform of the adenine nucleotide translocator. *Nat Genet,* 16**,** 226-34.

GRAMS, J., MCMANUS, M. T. & HAJDUK, S. L. 2000. Processing of polycistronic guide RNAs is associated with RNA editing complexes in *Trypanosoma brucei. EMBO J,* 19**,** 5525-32.

GUERIN, B., BUKUSOGLU, C., RAKOTOMANANA, F. & WOHLRAB, H. 1990. Mitochondrial phosphate transport. N-ethylmaleimide insensitivity correlates with absence of beef heart-like Cys42 from the *Saccharomyces cerevisiae* phosphate transport protein. *J Biol Chem,* 265**,** 19736-41.

HAFERKAMP, I., HACKSTEIN, J. H., VONCKEN, F. G., SCHMIT, G. & TJADEN, J. 2002. Functional integration of mitochondrial and hydrogenosomal ADP/ATP carriers in the Escherichia coli membrane reveals different biochemical characteristics for plants, mammals and anaerobic chytrids. *Eur J Biochem,* 269**,** 3172-81.

HALL, B. S., BOT, C. & WILKINSON, S. R. 2011. Nifurtimox activation by trypanosomal type I nitroreductases generates cytotoxic nitrile metabolites. *J Biol Chem,* 286**,** 13088-95.

HAMMOND, D. J. & BOWMAN, I. B. 1980. Studies on glycerol kinase and its role in ATP synthesis in *Trypanosoma brucei. Mol Biochem Parasitol,* 2**,** 77-91.

HANNAERT, V., BRINGAUD, F., OPPERDOES, F. R. & MICHELS, P. A. 2003. Evolution of energy metabolism and its compartmentation in Kinetoplastida. *Kinetoplastid Biol Dis,* 2**,** 11.

HART, D. T., MISSET, O., EDWARDS, S. W. & OPPERDOES, F. R. 1984. A comparison of the glycosomes (microbodies) isolated from *Trypanosoma brucei* bloodstream form and cultured procyclic trypomastigotes. *Mol Biochem Parasitol,* 12**,** 25-35.

HILDYARD, J. C. & HALESTRAP, A. P. 2003. Identification of the mitochondrial pyruvate carrier in Saccharomyces cerevisiae. *Biochem J,* 374**,** 607-11.

HOULDSWORTH, J. & ATTARDI, G. 1988. Two distinct genes for ADP/ATP translocase are expressed at the mRNA level in adult human liver. *Proc Natl Acad Sci U S A,* 85**,** 377-81.

HOYOS, M. E., PALMIERI, L., WERTIN, T., ARRIGONI, R., POLACCO, J. C. & PALMIERI, F. 2003. Identification of a mitochondrial transporter for basic amino acids in *Arabidopsis thaliana* by functional reconstitution into liposomes and complementation in yeast. *Plant J,* 33**,** 1027-35.

IACOBAZZI, V., DE PALMA, A. & PALMIERI, F. 1996. Cloning and sequencing of the bovine cDNA encoding the mitochondrial tricarboxylate carrier protein. *Biochim Biophys Acta,* 1284**,** 9-12.

IACOBAZZI, V., PALMIERI, F., RUNSWICK, M. J. & WALKER, J. E. 1992. Sequences of the human and bovine genes for the mitochondrial 2-oxoglutarate carrier. *DNA Seq,* 3**,** 79-88.

IVENS, A. C., PEACOCK, C. S., WORTHEY, E. A., MURPHY, L., AGGARWAL, G., BERRIMAN, M., SISK, E., RAJANDREAM, M. A., ADLEM, E., AERT, R., ANUPAMA, A., APOSTOLOU, Z., ATTIPOE, P., BASON, N., BAUSER, C., BECK, A., BEVERLEY, S. M., BIANCHETTIN, G., BORZYM, K., BOTHE, G., BRUSCHI, C. V., COLLINS, M., CADAG, E., CIARLONI, L., CLAYTON, C., COULSON, R. M., CRONIN, A., CRUZ, A. K., DAVIES, R. M., DE GAUDENZI, J., DOBSON, D. E., DUESTERHOEFT, A., FAZELINA, G., FOSKER, N., FRASCH, A. C., FRASER, A., FUCHS, M., GABEL, C., GOBLE, A., GOFFEAU, A., HARRIS, D., HERTZ-FOWLER, C., HILBERT, H., HORN, D., HUANG, Y., KLAGES, S., KNIGHTS, A., KUBE, M., LARKE, N., LITVIN, L., LORD, A., LOUIE, T., MARRA, M., MASUY, D., MATTHEWS, K., MICHAELI, S., MOTTRAM, J. C., MULLER-AUER, S., MUNDEN, H., NELSON, S., NORBERTCZAK, H., OLIVER, K., O'NEIL, S., PENTONY, M., POHL, T. M., PRICE, C., PURNELLE, B., QUAIL, M. A., RABBINOWITSCH, E., REINHARDT, R., RIEGER, M., RINTA, J., ROBBEN, J., ROBERTSON, L., RUIZ, J. C., RUTTER, S., SAUNDERS, D., SCHAFER, M., SCHEIN, J., SCHWARTZ, D. C., SEEGER, K., SEYLER, A., SHARP, S., SHIN, H., SIVAM, D., SQUARES, R., SQUARES, S., TOSATO, V., VOGT, C., VOLCKAERT, G., WAMBUTT, R., WARREN, T., WEDLER, H., WOODWARD, J., ZHOU, S., ZIMMERMANN, W., SMITH, D. F.,

BLACKWELL, J. M., STUART, K. D., BARRELL, B., et al. 2005. The genome of the kinetoplastid parasite, *Leishmania major*. *Science,* 309**,** 436-42.

KADENBACH, B., MENDE, P., KOLBE, H. V., STIPANI, I. & PALMIERI, F. 1982. The mitochondrial phosphate carrier has an essential requirement for cardiolipin. *FEBS Lett,* 139**,** 109-12.

KAUKONEN, J., JUSELIUS, J. K., TIRANTI, V., KYTTALA, A., ZEVIANI, M., COMI, G. P., KERANEN, S., PELTONEN, L. & SUOMALAINEN, A. 2000. Role of adenine nucleotide translocator 1 in mtDNA maintenance. *Science,* 289**,** 782-5.

KENNEDY, P. G. 2004. Human African trypanosomiasis of the CNS: current issues and challenges. *J Clin Invest,* 113**,** 496-504.

KENNEDY, P. G. E. 2006. Human African trypanosomiasis–neurological aspects. *Journal of neurology,* 253**,** 411-416.

KLINGENBERG, M. 1993. Dialectics in carrier research: the ADP/ATP carrier and the uncoupling protein. *J Bioenerg Biomembr,* 25**,** 447-57.

KNIRSCH, M., GAWAZ, M. P. & KLINGENBERG, M. 1989. The isolation and reconstitution of the ADP/ATP carrier from wild-type *Saccharomyces cerevisiae*. Identification of primarily one type (AAC-2). *FEBS Lett,* 244**,** 427-32.

KOLAROV, J., KOLAROVA, N. & NELSON, N. 1990a. A third ADP/ATP translocator gene in yeast. *The Journal of biological chemistry,* 265**,** 12711-6.

KOLAROV, J., KOLAROVA, N. & NELSON, N. 1990b. A third ADP/ATP translocator gene in yeast. *J Biol Chem,* 265**,** 12711-6.

KOSLOWSKY, D. J. & YAHAMPATH, G. 1997. Mitochondrial mRNA 3' cleavage/polyadenylation and RNA editing in are independent events. *Mol Biochem Parasitol,* 90**,** 81-94.

KRAMER, R. 1996. Structural and functional aspects of the phosphate carrier from mitochondria. *Kidney Int,* 49**,** 947-52.

KRAMER, R. & KLINGENBERG, M. 1985. Structural and functional asymmetry *Trypanosoma brucei* of the ADP/ATP carrier from mitochondria. *Ann N Y Acad Sci,* 456**,** 289-90.

KRAUTH-SIEGEL, R. L., MEIERING, S. K. & SCHMIDT, H. 2003. The parasite-specific trypanothione metabolism of trypanosoma and leishmania. *Biol Chem,* 384**,** 539-49.

KUAN, J. & SAIER, M. H., JR. 1993. The mitochondrial carrier family of transport proteins: structural, functional, and evolutionary relationships. *Crit Rev Biochem Mol Biol,* 28**,** 209-33.

KUNJI, E. R. 2004. The role and structure of mitochondrial carriers. *FEBS Lett,* 564**,** 239-44.

KUNJI, E. R. & HARDING, M. 2003. Projection structure of the atractyloside-inhibited mitochondrial ADP/ATP carrier of *Saccharomyces cerevisiae*. *J Biol Chem,* 278**,** 36985-8.

KUNJI, E. R. & ROBINSON, A. J. 2006. The conserved substrate binding site of mitochondrial carriers. *Biochim Biophys Acta,* 1757**,** 1237-48.

KUZOE, F. A. 1993. Current situation of African trypanosomiasis. *Acta Trop,* 54**,** 153-62.

LAMOUR, N., RIVIERE, L., COUSTOU, V., COOMBS, G. H., BARRETT, M. P. & BRINGAUD, F. 2005. Proline metabolism in procyclic *Trypanosoma brucei* is down-regulated in the presence of glucose. *J Biol Chem,* 280**,** 11902-10.

LAWSON, J. E. & DOUGLAS, M. G. 1988. Separate genes encode functionally equivalent ADP/ATP carrier proteins in *Saccharomyces cerevisiae*. Isolation and analysis of AAC2. *J Biol Chem,* 263**,** 14812-8.

LAWSON, J. E., GAWAZ, M., KLINGENBERG, M. & DOUGLAS, M. G. 1990. Structure-function studies of adenine nucleotide transport in mitochondria. I. Construction and genetic analysis of yeast mutants encoding the ADP/ATP carrier protein of mitochondria. *The Journal of biological chemistry,* 265**,** 14195-201.

LEROCH, M., KIRCHBERGER, S., HAFERKAMP, I., WAHL, M., NEUHAUS, H. E. & TJADEN, J. 2005. Identification and characterization of a novel plastidic adenine nucleotide uniporter from *Solanum tuberosum*. *J Biol Chem,* 280**,** 17992-8000.

LEUNG, A. W., VARANYUWATANA, P. & HALESTRAP, A. P. 2008. The mitochondrial phosphate carrier interacts with cyclophilin D and may play a key role in the permeability transition. *J Biol Chem,* 283**,** 26312-23.

LIANG, X. H., HARITAN, A., ULIEL, S. & MICHAELI, S. 2003. trans and cis splicing in trypanosomatids: mechanism, factors, and regulation. *Eukaryot Cell,* 2**,** 830-40.

LOURIE, E. M. 1942. Treatment of sleeping sickness in Sierra Leone. *Trop. Med. Parasitol,* 36**,** 113-131.

LOYTYNOJA, A. & MILINKOVITCH, M. C. 2001. Molecular phylogenetic analyses of the mitochondrial ADP-ATP carriers: the Plantae/Fungi/Metazoa trichotomy revisited. *Proceedings of the National Academy of Sciences of the United States of America,* 98**,** 10202-7.

MARCELLO, L. & BARRY, J. D. 2007. Analysis of the VSG gene silent archive in Trypanosoma brucei reveals that mosaic gene expression is prominent in antigenic variation and is favored by archive substructure. *Genome Res,* 17**,** 1344-52.

MAROBBIO, C. M., AGRIMI, G., LASORSA, F. M. & PALMIERI, F. 2003. Identification and functional reconstitution of yeast mitochondrial carrier for S-adenosylmethionine. *EMBO J,* 22**,** 5975-82.

MARTIN, K. L. & SMITH, T. K. 2006. The glycosylphosphatidylinositol (GPI) biosynthetic pathway of bloodstream-form *Trypanosoma brucei* is dependent on the de novo synthesis of inositol. *Mol Microbiol,* 61**,** 89-105.

MATOVU, E., SEEBECK, T., ENYARU, J. C. & KAMINSKY, R. 2001. Drug resistance in *Trypanosoma brucei* spp., the causative agents of sleeping sickness in man and nagana in cattle. *Microbes Infect,* 3**,** 763-70.

MATTHEWS, K. R. 2005. The developmental cell biology of *Trypanosoma brucei. J Cell Sci,* 118**,** 283-90.

MATTHEWS, K. R., ELLIS, J. R. & PATEROU, A. 2004. Molecular regulation of the life cycle of African trypanosomes. *Trends Parasitol,* 20**,** 40-7.

MAYR, J. A., MERKEL, O., KOHLWEIN, S. D., GEBHARDT, B. R., BOHLES, H., FOTSCHL, U., KOCH, J., JAKSCH, M., LOCHMULLER, H., HORVATH, R., FREISINGER, P. & SPERL, W. 2007. Mitochondrial phosphate-carrier deficiency: a novel disorder of oxidative phosphorylation. *Am J Hum Genet,* 80**,** 478-84.

MAYR, J. A., ZIMMERMANN, F. A., HORVATH, R., SCHNEIDER, H. C., SCHOSER, B., HOLINSKI-FEDER, E., CZERMIN, B., FREISINGER, P. & SPERL, W. 2011. Deficiency of the mitochondrial phosphate carrier presenting as myopathy and cardiomyopathy in a family with three affected children. *Neuromuscul Disord,* 21**,** 803-8.

MENDE, P., HUTHER, F. J. & KADENBACH, B. 1983. Specific and reversible activation and inactivation of the mitochondrial phosphate carrier by cardiolipin and nonionic detergents, respectively. *FEBS Lett,* 158**,** 331-4.

MICHELS, P. A., BRINGAUD, F., HERMAN, M. & HANNAERT, V. 2006. Metabolic functions of glycosomes in trypanosomatids. *Biochimica et biophysica acta,* 1763**,** 1463-77.

MICHELS, P. A., HANNAERT, V. & BRINGAUD, F. 2000. Metabolic aspects of glycosomes in trypanosomatidae - new data and views. *Parasitol Today,* 16**,** 482-9.

MILLAR, A. H. & HEAZLEWOOD, J. L. 2003. Genomic and proteomic analysis of mitochondrial carrier proteins in Arabidopsis. *Plant Physiol,* 131**,** 443-53.

MIRANDA, M. R., BOUVIER, L. A., CANEPA, G. E. & PEREIRA, C. A. 2009. Subcellular localization of *Trypanosoma cruzi* arginine kinase. *Parasitology,* 136**,** 1201-7.

MIRANDA, M. R., CANEPA, G. E., BOUVIER, L. A. & PEREIRA, C. A. 2006. *Trypanosoma cruzi:* Oxidative stress induces arginine kinase expression. *Exp Parasitol,* 114**,** 341-4.

MIROUX, B. & WALKER, J. E. 1996. Over-production of proteins in *Escherichia coli*: mutant hosts that allow synthesis of some membrane proteins and globular proteins at high levels. *J Mol Biol,* 260**,** 289-98.

MOHLMANN, T., TJADEN, J., SCHWOPPE, C., WINKLER, H. H., KAMPFENKEL, K. & NEUHAUS, H. E. 1998. Occurrence of two plastidic ATP/ADP transporters in *Arabidopsis thaliana L.*--molecular characterisation and comparative structural analysis of similar ATP/ADP translocators from plastids and Rickettsia prowazekii. *Eur J Biochem,* 252**,** 353-9.

NAPOLI, L., BORDONI, A., ZEVIANI, M., HADJIGEORGIOU, G. M., SCIACCO, M., TIRANTI, V., TERENTIOU, A., MOGGIO, M., PAPADIMITRIOU, A., SCARLATO, G. & COMI, G. P. 2001. A novel missense adenine nucleotide translocator-1 gene mutation in a Greek adPEO family. *Neurology,* 57**,** 2295-8.

NELSON, D. R., FELIX, C. M. & SWANSON, J. M. 1998. Highly conserved charge-pair networks in the mitochondrial carrier family. *J Mol Biol,* 277**,** 285-308.

NEUFELD, D. S. & LEADER, J. P. 1998. Cold inhibition of cell volume regulation during the freezing of insect malpighian tubules. *J Exp Biol,* 201**,** 2195-204.

NIGHTINGALE, S. 1991. Drug for sleeping sickness approved. *JAMA,* 265**,** 1229.

NJOGU, R. M., WHITTAKER, C. J. & HILL, G. C. 1980. Evidence for a branched electron transport chain in *Trypanosoma brucei. Mol Biochem Parasitol,* 1**,** 13-29.

NOGOCEKE, E., GOMMEL, D. U., KIESS, M., KALISZ, H. M. & FLOHE, L. 1997. A unique cascade of oxidoreductases catalyses trypanothione-mediated peroxide metabolism in *Crithidia fasciculata*. *Biol Chem,* 378**,** 827-36.

NURY, H., DAHOUT-GONZALEZ, C., TREZEGUET, V., LAUQUIN, G. J., BRANDOLIN, G. & PEBAY-PEYROULA, E. 2006. Relations between structure and function of the mitochondrial ADP/ATP carrier. *Annu Rev Biochem,* 75**,** 713-41.

OPPERDOES, F. R. 1984. Localization of the initial steps in alkoxyphospholipid biosynthesis in glycosomes (microbodies) of *Trypanosoma brucei*. *FEBS Lett,* 169**,** 35-9.

OPPERDOES, F. R. 1987. Compartmentation of carbohydrate metabolism in trypanosomes. *Annu Rev Microbiol,* 41**,** 127-51.

OPPERDOES, F. R. & BORST, P. 1977. Localization of nine glycolytic enzymes in a microbody-like organelle in *Trypanosoma brucei*: the glycosome. *FEBS Lett,* 80**,** 360-4.

OPPERDOES, F. R. & SZIKORA, J. P. 2006. In silico prediction of the glycosomal enzymes of *Leishmania major* and *trypanosomes. Mol Biochem Parasitol,* 147**,** 193-206.

OVERATH, P. & ENGSTLER, M. 2004. Endocytosis, membrane recycling and sorting of GPI-anchored proteins: *Trypanosoma brucei* as a model system. *Mol Microbiol,* 53**,** 735-44.

PALMIERI, F. 2004. The mitochondrial transporter family (SLC25): physiological and pathological implications. *Pflugers Arch,* 447**,** 689-709.

PALMIERI, F., AGRIMI, G., BLANCO, E., CASTEGNA, A., DI NOIA, M. A., IACOBAZZI, V., LASORSA, F. M., MAROBBIO, C. M., PALMIERI, L., SCARCIA, P., TODISCO, S., VOZZA, A. & WALKER, J. 2006a. Identification of mitochondrial carriers in *Saccharomyces cerevisiae* by transport assay of reconstituted recombinant proteins. *Biochim Biophys Acta,* 1757**,** 1249-62.

PALMIERI, F., PIERRI, C. L., DE GRASSI, A., NUNES-NESI, A. & FERNIE, A. R. 2011. Evolution, structure and function of mitochondrial carriers: a review with new insights. *Plant J,* 66**,** 161-81.

PALMIERI, L., ARRIGONI, R., BLANCO, E., CARRARI, F., ZANOR, M. I., STUDART-GUIMARAES, C., FERNIE, A. R. & PALMIERI, F. 2006b. Molecular identification of an Arabidopsis S-adenosylmethionine transporter. Analysis of organ distribution, bacterial expression, reconstitution into liposomes, and functional characterization. *Plant Physiol,* 142**,** 855-65.

PALMIERI, L., PARDO, B., LASORSA, F. M., DEL ARCO, A., KOBAYASHI, K., IIJIMA, M., RUNSWICK, M. J., WALKER, J. E., SAHEKI, T., SATRUSTEGUI, J. & PALMIERI, F. 2001. Citrin and aralar1 are Ca(2+)-stimulated aspartate/glutamate transporters in mitochondria. *EMBO J,* 20**,** 5060-9.

PALMIERI, L., RUNSWICK, M. J., FIERMONTE, G., WALKER, J. E. & PALMIERI, F. 2000. Yeast mitochondrial carriers: bacterial expression, biochemical identification and metabolic significance. *J Bioenerg Biomembr,* 32**,** 67-77.

PANIGRAHI, A. K., OGATA, Y., ZIKOVA, A., ANUPAMA, A., DALLEY, R. A., ACESTOR, N., MYLER, P. J. & STUART, K. D. 2009. A comprehensive analysis of *Trypanosoma brucei* mitochondrial proteome. *Proteomics,* 9**,** 434-50.

PANIGRAHI, A. K., SCHNAUFER, A., ERNST, N. L., WANG, B., CARMEAN, N., SALAVATI, R. & STUART, K. 2003. Identification of novel components of *Trypanosoma brucei* editosomes. *RNA,* 9**,** 484-92.

PANIGRAHI, A. K., ZIKOVA, A., DALLEY, R. A., ACESTOR, N., OGATA, Y., ANUPAMA, A., MYLER, P. J. & STUART, K. D. 2008. Mitochondrial complexes in *Trypanosoma brucei*: a novel complex and a unique oxidoreductase complex. *Mol Cell Proteomics,* 7**,** 534-45.

PARADIES, G. & RUGGIERO, F. M. 1990. Stimulation of phosphate transport in rat-liver mitochondria by thyroid hormones. *Biochim Biophys Acta,* 1019**,** 133-6.

PARSONS, M. 2004. Glycosomes: parasites and the divergence of peroxisomal purpose. *Mol Microbiol,* 53**,** 717-24.

PARSONS, M., FURUYA, T., PAL, S. & KESSLER, P. 2001. Biogenesis and function of peroxisomes and glycosomes. *Mol Biochem Parasitol,* 115**,** 19-28.

PAYS, E., TEBABI, P., PAYS, A., COQUELET, H., REVELARD, P., SALMON, D. & STEINERT, M. 1989. The genes and transcripts of an antigen gene expression site from T. brucei. *Cell,* 57**,** 835-45.

PEBAY-PEYROULA, E., DAHOUT-GONZALEZ, C., KAHN, R., TREZEGUET, V., LAUQUIN, G. J. & BRANDOLIN, G. 2003. Structure of mitochondrial ADP/ATP carrier in complex with carboxyatractyloside. *Nature,* 426**,** 39-44.

PEREIRA, C. A., ALONSO, G. D., IVALDI, S., SILBER, A. M., ALVES, M. J., TORRES, H. N. & FLAWIA, M. M. 2003. Arginine kinase overexpression improves *Trypanosoma cruzi* survival capability. *FEBS Lett,* 554**,** 201-5.

PEREIRA, C. A., ALONSO, G. D., PAVETO, M. C., IRIBARREN, A., CABANAS, M. L., TORRES, H. N. & FLAWIA, M. M. 2000. *Trypanosoma cruzi* arginine kinase characterization and cloning. A novel energetic pathway in protozoan parasites. *J Biol Chem,* 275**,** 1495-501.

PEREIRA, C. A., ALONSO, G. D., TORRES, H. N. & FLAWIA, M. M. 2002. Arginine kinase: a common feature for management of energy reserves in African and American flagellated trypanosomatids. *J Eukaryot Microbiol,* 49**,** 82-5.

PEREIRA, C. A., BOUVIER, L. A., CAMARA MDE, L. & MIRANDA, M. R. 2011. Singular features of trypanosomatids' phosphotransferases involved in cell energy management. *Enzyme Res,* 2011**,** 576483.

PHELPS, A., SCHOBERT, C. T. & WOHLRAB, H. 1991. Cloning and characterization of the mitochondrial phosphate transport protein gene from the yeast *Saccharomyces cerevisiae*. *Biochemistry,* 30**,** 248-52.

PHELPS, A. & WOHLRAB, H. 1991. Mitochondrial phosphate transport. *The Saccharomyces cerevisiae* (threonine 43 to cysteine) mutant protein explicitly identifies transport with genomic sequence. *J Biol Chem,* 266**,** 19882-5.

PI, H., LEE, L. W. & LO, S. J. 2009. New insights into polycistronic transcripts in eukaryotes. *Chang Gung Med J,* 32**,** 494-8.

PICAULT, N., HODGES, M., PALMIERI, L. & PALMIERI, F. 2004. The growing family of mitochondrial carriers in *Arabidopsis*. *Trends Plant Sci,* 9**,** 138-46.

PICAULT, N., PALMIERI, L., PISANO, I., HODGES, M. & PALMIERI, F. 2002. Identification of a novel transporter for dicarboxylates and tricarboxylates in

plant mitochondria. Bacterial expression, reconstitution, functional characterization, and tissue distribution. *J Biol Chem,* 277**,** 24204-11.

POLLARD, V. W., HARRIS, M. E. & HAJDUK, S. L. 1992. Native mRNA editing complexes from *Trypanosoma brucei* mitochondria. *EMBO J,* 11**,** 4429-38.

POWELL, S. J., MEDD, S. M., RUNSWICK, M. J. & WALKER, J. E. 1989. Two bovine genes for mitochondrial ADP/ATP translocase expressed differences in various tissues. *Biochemistry,* 28**,** 866-73.

PRIOTTO, G., KASPARIAN, S., NGOUAMA, D., GHORASHIAN, S., ARNOLD, U., GHABRI, S. & KARUNAKARA, U. 2007. Nifurtimox-eflornithine combination therapy for second-stage *Trypanosoma brucei* gambiense sleeping sickness: a randomized clinical trial in Congo. *Clin Infect Dis,* 45**,** 1435-42.

PRUETT, P. S., AZZI, A., CLARK, S. A., YOUSEF, M. S., GATTIS, J. L., SOMASUNDARAM, T., ELLINGTON, W. R. & CHAPMAN, M. S. 2003. The putative catalytic bases have, at most, an accessory role in the mechanism of arginine kinase. *J Biol Chem,* 278**,** 26952-7.

RAY, D. S. 1987. Kinetoplast DNA minicircles: high-copy-number mitochondrial plasmids. *Plasmid,* 17**,** 177-90.

RIGAUD, J. L. 2002. Membrane proteins: functional and structural studies using reconstituted proteoliposomes and 2-D crystals. *Braz J Med Biol Res,* 35**,** 753-66.

RIGAUD, J. L., PITARD, B. & LEVY, D. 1995. Reconstitution of membrane proteins into liposomes: application to energy-transducing membrane proteins. *Biochim Biophys Acta,* 1231**,** 223-46.

ROBINSON, A. J. & KUNJI, E. R. 2006. Mitochondrial carriers in the cytoplasmic state have a common substrate binding site. *Proc Natl Acad Sci U S A,* 103**,** 2617-22.

RODGERS, J. 2009. Human African trypanosomiasis, chemotherapy and CNS disease. *J Neuroimmunol,* 211**,** 16-22.

ROSEMEYER, H. 2004. The chemodiversity of purine as a constituent of natural products. *Chem Biodivers,* 1**,** 361-401.

RUNSWICK, M. J., POWELL, S. J., NYREN, P. & WALKER, J. E. 1987. Sequence of the bovine mitochondrial phosphate carrier protein: structural relationship

to ADP/ATP translocase and the brown fat mitochondria uncoupling protein. *EMBO J,* 6**,** 1367-73.

SABOVA, L., GAVURNIKOVA, G. & KOLAROV, J. 1996. Regulation of AAC isogenes encoding mitochondrial ADP/ATP translocator in the yeast *Saccharomyces cerevisiae. Folia microbiologica,* 41**,** 124-6.

SABOVA, L., ZEMAN, I., SUPEK, F. & KOLAROV, J. 1993. Transcriptional control of AAC3 gene encoding mitochondrial ADP/ATP translocator in *Saccharomyces cerevisiae* by oxygen, heme and ROX1 factor. *European journal of biochemistry / FEBS,* 213**,** 547-53.

SARASTE, M. & WALKER, J. E. 1982. Internal sequence repeats and the path of polypeptide in mitochondrial ADP/ATP translocase. *FEBS Lett,* 144**,** 250-4.

SATHER, S. & AGABIAN, N. 1985. A 5' spliced leader is added in trans to both alpha- and beta-tubulin transcripts in *Trypanosoma brucei*. *Proc Natl Acad Sci U S A,* 82**,** 5695-9.

SCHNAUFER, A., CLARK-WALKER, G. D., STEINBERG, A. G. & STUART, K. 2005. The F1-ATP synthase complex in bloodstream stage trypanosomes has an unusual and essential function. *EMBO J,* 24**,** 4029-40.

SCHNEIDER, A. 2001. Unique aspects of mitochondrial biogenesis in trypanosomatids. *Int J Parasitol,* 31**,** 1403-15.

SCHNEIDER, A., BOUZAIDI-TIALI, N., CHANEZ, A. L. & BULLIARD, L. 2007. ATP production in isolated mitochondria of procyclic *Trypanosoma brucei. Methods Mol Biol,* 372**,** 379-87.

SCHROERS, A., KRAMER, R. & WOHLRAB, H. 1997. The reversible antiport-uniport conversion of the phosphate carrier from yeast mitochondria depends on the presence of a single cysteine. *J Biol Chem,* 272**,** 10558-64.

SEGREST, J. P., GULIK-KRZYWICKI, T. & SARDET, C. 1974. Association of the membrane-penetrating polypeptide segment of the human erythrocyte MN-glycoprotein with phospholipid bilayers. I. Formation of freeze-etch intramembranous particles. *Proc Natl Acad Sci U S A,* 71**,** 3294-8.

SIMPSON, L. 1973. Structure and function of kinetoplast DNA. *J Protozool,* 20**,** 2-8.

SIMPSON, L., SIMPSON, A. M., KIDANE, G., LIVINGSTON, L. & SPITHILL, T. W. 1980. The kinetoplast DNA of the hemoflagellate protozoa. *Am J Trop Med Hyg,* 29**,** 1053-63.

SMITH, T. K. & BUTIKOFER, P. 2010. Lipid metabolism in *Trypanosoma brucei. Mol Biochem Parasitol,* 172**,** 66-79.

SPINKS, D., SHANKS, E. J., CLEGHORN, L. A., MCELROY, S., JONES, D., JAMES, D., FAIRLAMB, A. H., FREARSON, J. A., WYATT, P. G. & GILBERT, I. H. 2009. Investigation of trypanothione reductase as a drug target in *Trypanosoma brucei. ChemMedChem,* 4**,** 2060-9.

STAPPEN, R. & KRAMER, R. 1993. Functional properties of the reconstituted phosphate carrier from bovine heart mitochondria: evidence for asymmetric orientation and characterization of three different transport modes. *Biochim Biophys Acta,* 1149**,** 40-8.

STEPHENS, J. L., LEE, S. H., PAUL, K. S. & ENGLUND, P. T. 2007. Mitochondrial fatty acid synthesis in *Trypanosoma brucei*. *J Biol Chem,* 282**,** 4427-36.

STEPIEN, G., TORRONI, A., CHUNG, A. B., HODGE, J. A. & WALLACE, D. C. 1992. Differential expression of adenine nucleotide translocator isoforms in mammalian tissues and during muscle cell differentiation. *J Biol Chem,* 267**,** 14592-7.

STEVERDING, D. 2010. The development of drugs for treatment of sleeping sickness: a historical review. *Parasit Vectors,* 3**,** 15.

STICH, A., ABEL, P. M. & KRISHNA, S. 2002. Human African trypanosomiasis. *BMJ,* 325**,** 203-6.

STOCKDALE, C., SWIDERSKI, M. R., BARRY, J. D. & MCCULLOCH, R. 2008. Antigenic variation in *Trypanosoma brucei:* joining the DOTs. *PLoS Biol,* 6**,** e185.

STUART, K. 1993. The RNA editing process in Trypanosoma brucei. *Semin Cell Biol,* 4**,** 251-60.

STURM, N. R. & SIMPSON, L. 1990. Partially edited mRNAs for cytochrome b and subunit III of cytochrome oxidase from *Leishmania tarentolae* mitochondria: RNA editing intermediates. *Cell,* 61**,** 871-8.

SUZUKI, T., FUKUTA, H., NAGATO, H. & UMEKAWA, M. 2000. Arginine kinase from Nautilus pompilius, a living fossil. Site-directed mutagenesis studies on the role of amino acid residues in the Guanidino specificity region. *J Biol Chem,* 275**,** 23884-90.

TER KULLE, B. H. 1993. Glucose and proline transport in kinetoplastids. *Parasitol Today,* 9**,** 206-10.

THIMMAPURAM, J., DUAN, H., LIU, L. & SCHULER, M. A. 2005. Bicistronic and fused monocistronic transcripts are derived from adjacent loci in the *Arabidopsis* genome. *RNA,* 11**,** 128-38.

TIELENS, A. G. & VAN HELLEMOND, J. J. 1998. Differences in energy metabolism between trypanosomatidae. *Parasitol Today,* 14**,** 265-72.

TIWARI, B. S., BELENGHI, B. & LEVINE, A. 2002. Oxidative stress increased respiration and generation of reactive oxygen species, resulting in ATP depletion, opening of mitochondrial permeability transition, and programmed cell death. *Plant Physiol,* 128**,** 1271-81.

TJADEN, J., HAFERKAMP, I., BOXMA, B., TIELENS, A. G., HUYNEN, M. & HACKSTEIN, J. H. 2004. A divergent ADP/ATP carrier in the hydrogenosomes of *Trichomonas gallinae* argues for an independent origin of these organelles. *Mol Microbiol,* 51**,** 1439-46.

TJADEN, J., SCHWOPPE, C., MOHLMANN, T., QUICK, P. W. & NEUHAUS, H. E. 1998. Expression of a plastidic ATP/ADP transporter gene in Escherichia coli leads to a functional adenine nucleotide transport system in the bacterial cytoplasmic membrane. *J Biol Chem,* 273**,** 9630-6.

TRABA, J., SATRUSTEGUI, J. & DEL ARCO, A. 2011. Adenine nucleotide transporters in organelles: novel genes and functions. *Cellular and molecular life sciences : CMLS,* 68**,** 1183-206.

TREZEGUET, V., PELOSI, L., LAUQUIN, G. J. & BRANDOLIN, G. 2008. The mitochondrial ADP/ATP carrier: functional and structural studies in the route of elucidating pathophysiological aspects. *J Bioenerg Biomembr,* 40**,** 435-43.

TURRENS, J. F. 2004. Oxidative stress and antioxidant defenses: a target for the treatment of diseases caused by parasitic protozoa. *Mol Aspects Med,* 25**,** 211-20.

TYLER, K. M., MATTHEWS, K. R. & GULL, K. 1997. The bloodstream differentiation-division of *Trypanosoma brucei* studied using mitochondrial markers. *Proc Biol Sci,* 264**,** 1481-90.

VAGO, A. R., MACEDO, A. M., OLIVEIRA, R. P., ANDRADE, L. O., CHIARI, E., GALVAO, L. M., REIS, D., PEREIRA, M. E., SIMPSON, A. J., TOSTES, S.

& PENA, S. D. 1996. Kinetoplast DNA signatures of *Trypanosoma cruzi* strains obtained directly from infected tissues. *Am J Pathol,* 149**,** 2153-9.

VAN HELLEMOND, J. J., OPPERDOES, F. R. & TIELENS, A. G. 1998. Trypanosomatidae produce acetate via a mitochondrial acetate:succinate CoA transferase. *Proc Natl Acad Sci U S A,* 95**,** 3036-41.

VAN HELLEMOND, J. J., OPPERDOES, F. R. & TIELENS, A. G. 2005. The extraordinary mitochondrion and unusual citric acid cycle in *Trypanosoma brucei. Biochem Soc Trans,* 33**,** 967-71.

VAN HELLEMONDT, G. G., SONNEVELD, H., SCHREUDER, M. H., KOOIJMAN, M. A. & DE KLEUVER, M. 2005. Triple osteotomy of the pelvis for acetabular dysplasia: results at a mean follow-up of 15 years. *J Bone Joint Surg Br,* 87**,** 911-5.

VAN WEELDEN, S. W., FAST, B., VOGT, A., VAN DER MEER, P., SAAS, J., VAN HELLEMOND, J. J., TIELENS, A. G. & BOSHART, M. 2003. Procyclic *Trypanosoma brucei* do not use Krebs cycle activity for energy generation. *J Biol Chem,* 278**,** 12854-63.

VAN WILPE, S., BOUMANS, H., LOBO-HAJDU, G., GRIVELL, L. A. & BERDEN, J. A. 1999. Functional complementation analysis of yeast bc1 mutants. A study of the mitochondrial import of heterologous and hybrid proteins. *Eur J Biochem,* 264**,** 825-32.

VARANYUWATANA, P. & HALESTRAP, A. P. 2012. The roles of phosphate and the phosphate carrier in the mitochondrial permeability transition pore. *Mitochondrion,* 12**,** 120-5.

VASSELLA, E., STRAESSER, K. & BOSHART, M. 1997. A mitochondrion-specific dye for multicolour fluorescent imaging of *Trypanosoma brucei*. *Mol Biochem Parasitol,* 90**,** 381-5.

VICKERMAN, K. 1985. Developmental cycles and biology of pathogenic trypanosomes. *Br Med Bull,* 41**,** 105-14.

VICKERMAN, K. & LUCKINS, A. G. 1969. Localization of variable antigens in the surface coat of *Trypanosoma brucei* using ferritin conjugated antibody. *Nature,* 224**,** 1125-6.

WALLIMANN, T., WYSS, M., BRDICZKA, D., NICOLAY, K. & EPPENBERGER, H. M. 1992. Intracellular compartmentation, structure and function of creatine kinase isoenzymes in tissues with high and fluctuating energy demands: the

'phosphocreatine circuit' for cellular energy homeostasis. *Biochem J,* 281 (Pt 1)**,** 21-40.

WEHRLE, J. P. & PEDERSEN, P. L. 1982. Characteristics of phosphate uptake by Ehrlich ascites tumor cells. *J Biol Chem,* 257**,** 9698-703.

WERR, M., CRAMER, J. & ILG, T. 2009. Identification and characterization of two arginine kinases from the parasitic insect *Ctenocephalides felis*. *Insect Biochem Mol Biol,* 39**,** 634-45.

WHO. 2012. *African trypanosomiasis (sleeping sickness)* [Online]. Available: http://www.who.int/mediacentre/factsheets/fs259/en/index.html.

WIEMER, E. A., L, I. J., VAN ROY, J., WANDERS, R. J. & OPPERDOES, F. R. 1996. Identification of 2-enoyl coenzyme A hydratase and NADP(+)-dependent 3-hydroxyacyl-CoA dehydrogenase activity in glycosomes of procyclic *Trypanosoma brucei*. *Mol Biochem Parasitol,* 82**,** 107-11.

WIERENGA, R. K., NOBLE, M. E., VRIEND, G., NAUCHE, S. & HOL, W. G. 1991. Refined 1.83 A structure of trypanosomal triosephosphate isomerase crystallized in the presence of 2.4 M-ammonium sulphate. A comparison with the structure of the trypanosomal triosephosphate isomerase-glycerol-3-phosphate complex. *J Mol Biol,* 220**,** 995-1015.

WILLIAMS, B. A., HAFERKAMP, I. & KEELING, P. J. 2008. An ADP/ATP-specific mitochondrial carrier protein in the microsporidian *Antonospora locustae*. *J Mol Biol,* 375**,** 1249-57.

WOHLRAB, H. 1986. Molecular aspects of inorganic phosphate transport in mitochondria. *Biochim Biophys Acta,* 853**,** 115-34.

WOHLRAB, H. 2006. The human mitochondrial transport/carrier protein family. Nonsynonymous single nucleotide polymorphisms (nsSNPs) and mutations that lead to human diseases. *Biochim Biophys Acta,* 1757**,** 1263-70.

WOHLRAB, H. & BRIGGS, C. 1994. Yeast mitochondrial phosphate transport protein expressed in *Escherichia coli.* Site-directed mutations at threonine-43 and at a similar location in the second tandem repeat (isoleucine-141). *Biochemistry,* 33**,** 9371-5.

YOUSEF, M. S., CLARK, S. A., PRUETT, P. K., SOMASUNDARAM, T., ELLINGTON, W. R. & CHAPMAN, M. S. 2003. Induced fit in guanidino kinases--comparison of substrate-free and transition state analog structures of arginine kinase. *Protein Sci,* 12**,** 103-11.

YOUSEF, M. S., FABIOLA, F., GATTIS, J. L., SOMASUNDARAM, T. & CHAPMAN, M. S. 2002. Refinement of the arginine kinase transition-state analogue complex at 1.2 A resolution: mechanistic insights. *Acta Crystallogr D Biol Crystallogr,* 58**,** 2009-17.

ZHOU, G., SOMASUNDARAM, T., BLANC, E., PARTHASARATHY, G., ELLINGTON, W. R. & CHAPMAN, M. S. 1998. Transition state structure of arginine kinase: implications for catalysis of bimolecular reactions. *Proc Natl Acad Sci U S A,* 95**,** 8449-54.

Chapter II

Functional Characterisation of TbMCP5, a Conserved and Essential ADP/ATP Carrier Present in the Mitochondrion of the Human Pathogen *Trypanosoma brucei.*

The contents of this chapter have been published.
Pena-Diaz, P., Pelosi, L., Ebikeme, C., Colasante, C., Gao, F., Bringaud, F. & Voncken, F. 2012. The Journal of Biological Chemistry, 287, 41861-74.

The work presented in this chapter was started during the time Dr Priscilla Pena-Diaz was doing her PhD under the supervision of Dr Frank Voncken in this laboratory. She made efforts to generating the double-knockout Δ*TbMCP5::NEO/*Δ*TbMCP5:: BSD* cell line. Unfortunately, it was not possible. Later, she successfully generated the conditional TbMCP5 double-knockout cell line Δ*TbMCP5::NEO/*Δ*TbMCP5:: BSD/TbMCP5-cmyc*^{ti}. After that, Dr Priscilla Pena-Diaz also did part of the following analysis including growth analysis under different culture conditions, the ATP production assay, protein quantification and localisation analysis. After she finished her PhD, I continued the work. After I received the conditional double-knockout cell line, with the help of Dr Claudia Colasante in this laboratory I repeated most of the analysis experiments and got convincing results presented in this chapter. Later, for the TbMCP5 functional study, the work was a collaboration with two other labs, Dr Ludovic Pelosi's lab and Dr Frederic Bringaud's lab. I made the construct for yeast complementation analysis, and Dr Ludovic Pelosi did the yeast transformation and later ADP/ATP transport kinetic analysis. I did the TbMCP5 RNA interference in the *T.brucei* cell line and Dr Charles Ebikeme and Dr Frederic Bringaud did the RNA interference in PCF *T. brucei* knockout mutant Δ*pepck*-cl1 cell line.

1. Introduction

The Kinetoplastida are the earliest-branching unicellular eukaryotes to possess 'classical' mitochondria (Embley and Martin, 2006). They include the closely related trypanosomatid protozoa *Trypanosoma brucei*, *Trypanosoma cruzi* and *Leishmania* sp., which have been well studied mainly because of their significant medical and veterinary importance (http://www.who.int). *T. brucei* is predominantly found in sub-Saharan Africa and its subspecies are the etiological agents of Sleeping Sickness in humans and the wasting disease 'Nagana' in cattle (http://www.who.int). The complex lifecycle of *T. brucei* includes two replicating forms that can be grown *in vitro*: the bloodstream form (BSF) found in the blood and tissue fluids of the mammalian host, and the procyclic form (PCF) in the intestinal tract and salivary glands of the bloodsucking insect vector, the tsetse fly. The energy metabolism of the parasite is subject to substantial rearrangements in order to adapt to the distinct host environments (Michels et al., 2006b). BSF trypanosomes rely exclusively on glucose and its degradation by glycolysis for their cellular energy (ATP) provision, with pyruvate and glycerol excreted as incomplete fermentation products. Most of the glycolytic pathway is compartmentalised in a specialised peroxisome, the glycosome (Michels et al., 2006a). ATP production and consumption in the glycosome is balanced, and it has been postulated that this organelle does not provide ATP to the rest of the cell (Michels et al., 2006a). Instead, net production of ATP occurs in the final and cytosolic part of the glycolytic pathway, during the conversion of phosphoenolpyruvate (PEP) to pyruvate. The BSF mitochondrion lacks key enzymes and components of the Krebs cycle, and its role in the energy metabolism is restricted to the re-oxidation of glycosome-derived glycerol-3-phosphate by an alternative oxidase located at the inner mitochondrial membrane (van Hellemond et al., 2005,

Chaudhuri et al., 2006). The procyclic form (PCF) of *T. brucei* has a more elaborate energy metabolism predominantly depending on the mitochondrion (Bringaud et al., 2012). Remarkably, PCF trypanosomes do not use the Krebs cycle for the generation of ATP (van Weelden et al., 2003). Instead, ATP is mainly generated by the incomplete aerobic fermentation of glucose present in the blood meal or from proline found in the insect vector (Bochud-Allemann and Schneider, 2002, Lamour et al., 2005). During glycolysis the metabolic intermediate phosphoenolpyruvate (PEP) is produced in the cytosol. Depending on the cellular redox and ATP balances, PEP is converted to pyruvate and further metabolised in the mitochondrion to acetate, or it enters the glycosome where it is converted to succinate via the succinic fermentation branch (Ebikeme et al., 2010). Under glucose-depleted conditions, which reflect the insect midgut environment, proline is catabolised in the mitochondrion where ATP is mainly produced from oxidative phosphorylation (Lamour et al., 2005, Coustou et al., 2008). However, under glucose-rich conditions ATP is primarily produced by substrate-level phosphorylation, whereas oxidative phosphorylation becomes essential in the absence of glucose (Coustou et al., 2005, Bochud-Allemann and Schneider, 2002, Coustou et al., 2008, Ebikeme et al., 2010, Lamour et al., 2005)

The inner mitochondrial membrane of *Trypanosoma brucei* is thought to be impermeable to metabolites (Schneider et al., 2007), implying the presence of specific membrane-bound transporters. Mitochondrial carrier family (MCF) proteins are located in the inner mitochondrial membrane and mediate the transport of a wide range of metabolic intermediates (see (Palmieri et al., 2011) and references therein). As the predominant mitochondrial metabolite transporters, they exert flux control on metabolic pathways and are involved in the maintenance of cellular redox and ATP balances (Palmieri et al., 2011). In particular the mitochondrial ADP/ATP carrier

plays an important role in sustaining the cellular ATP homeostasis by facilitating the 1:1 counter-exchange of mitochondrial ATP for cytosolic ADP (Dahout-Gonzalez et al., 2006). The evolution of the ADP/ATP-carrier has been key to the evolution of the eukaryotic cell by enabling the establishment of the mitochondrion as an ATP-generating organelle. ADP/ATP carriers have been extensively and predominantly studied in a wide range of higher eukaryotes (Palmieri et al., 2011, Trezeguet et al., 2008), whereas virtually nothing is known about their homologues from earlier branching eukaryotes such as the Kinetoplastida. We previously reported that the genome of *T. brucei* codes for 24 different MCF proteins (Colasante et al., 2009). Two of the identified MCF proteins, here TbMCP5 and TbMCP15, showed significant sequence similarity to functionally characterised ADP/ATP carriers from other eukaryotes (Colasante et al., 2009). In this thesis, I analysed these MCF proteins regarding their predicted function as mitochondrial ATP/ADP carriers, and assessed the importance of TbMCP5 for the energy metabolism of *T. brucei*.

2. Materials and methods

2.1 Chemicals

[^{3}H]-ATR, 6'-*O*-naphthoyl-atractyloside (N-ATR), [^{3}H]-ATR and 3'-*O*-(1-naphthoyl)-adenosinev5'-diphosphate (N-ADP) were synthesized as described previously (Block et al., 1982, Boulay et al., 1983). Succinate, α-ketoglutarate, ADP, ATP, ATR, bonkrekic acid (BA), carboxyatractyloside (CATR) and digitonin were purchased from Sigma-Aldrich. Luciferase and luciferin were from Roche, and diadenosine 5'-pentaphosphate (Ap5A) and *n*-dodecyl-β-D-maltoside (DDM) were from Calbiochem.

2.2 Yeast complementation (this work has been done jointly with Dr Ludovic Pelosi)

The ADP/ATP carrier (*ANC*) deficient *Saccharomyces cerevisiae* strain *JL1Δ2Δ3u*$^-$ was cultured as described previously (De Marcos Lousa et al., 2002, Clemencon et al., 2008). The complete open reading frames of *TbMCP5* (GeneDB Tb927.10.14820) and *TbMCP15* (GeneDB Tb927.8.1310) were PCR-amplified using the primer combination 5'-ggcgaattcatgacggataaaa agcgggaaccgg-3' (sense) and 5'-gcggatccttaattc gatctgcgccactccacataaatgg-3' (antisense) for *TbMCP5*, and the primer combination 5'-ggcgaattcatggttggtggcgatggtgaggagc-3' (sense) and 5'-gccggatccttaggcagccggtaaaaaccacatataga gtgac-3' (antisense) for *TbMCP15*. Restriction enzyme sites used for subsequent cloning into the yeast centromeric expression vector *pRS314* (http://seq.yeastgenome.org/vectordb) are under-lined. Expression from *pRS314* takes place under the control of included *ScANC2* regulatory sequences (Le Saux et al., 1996). The resulting *TbMCP5-pRS314* and *TbMCP15-pRS314* constructs were used to transform *JL1Δ2Δ3u*$^-$ using a standard LiCl method (Ito et al., 1983). The rescue of non-fermentative growth of *JL1Δ2Δ3u*$^-$ by expression of ScANC2p (positive control), TbMCP5 or TbMCP15 was assessed on solid YPL medium (glucose-free, lactate-containing rich medium) and compared to the fermentative growth on YNB Glc W$^-$ medium (tryptophan-free, glucose-supplemented minimal medium) (Clemencon et al., 2008).

2.3 ADP/ATP transport assays for yeast mitochondria (this work has been done jointly with Dr Ludovic Pelosi)

Yeast mitochondria were prepared by differential centrifugation (Daum et al., 1982). Briefly, yeast cells grown in YPL medium were harvested in the late log phase (OD_{600nm} ~5). Spheroplasts obtained after enzymatic digestion by Zymolyase 20T

were disrupted by Dounce homogenization in 0.6 M mannitol, 10 mM Tris-HCl, pH 7.4, 1 mM EDTA, 0.1% (w/v) BSA and 1 mM PMSF. Mitochondria were isolated by differential centrifugation, washed in the same buffer devoid of BSA and PMSF, and stored in liquid nitrogen. Mitochondrial ADP/ATP-transport was measured using a luminescence assay as detailed in Dassa *et al*. (Dassa et al., 2005). Briefly, freshly prepared mitochondria were incubated for 5 min at 25°C in 10 mM Tris-HCl pH 7.4, 10 mM KH_2PO_4, 0.6 M mannitol, 0.1 mM EGTA, 2 mM $MgCl_2$, 10 µM Ap5A and 1 mM α-ketoglutarate, in the presence of 0.1% (w/v) luciferin and 0.1% (w/v) luciferase. ADP was added to initiate the mitochondrial ATP efflux. ATP production was determined by measuring the luciferase/luciferin-related light emission using a luminometer. Control experiments were carried out in the presence of the inhibitors CATR and BA, which specifically inhibit nucleotide exchange in ADP/ATP carriers.

2.4 ATR and CATR binding assays (performed by Dr Ludovic Pelosi)

[^{3}H]-ATR binding assays with isolated yeast mitochondria were carried out as described previously (Brandolin et al., 1993). Mitochondria were diluted (1 mg protein.mL^{-1}) in 1 mL MKE buffer (0.12 M KCl, 10 mM MOPS pH 6.8, 1 mM EDTA), and [^{3}H]-ATR was added at concentrations up to 6 µM. After incubation for 1 h at 4°C, mitochondria were pelleted by centrifugation and radioactivity associated with the pellet was determined using a liquid scintillation counter. Control experiments were performed in the presence of 20 µM CATR to correct for minor nonspecific [^{3}H]-ATR binding. Fluorescence back-titration of CATR-binding sites was performed on mitochondria in MKE buffer in the presence of 1 µM of N-ATR (Roux et al., 1996). The time course of the CATR-induced release of bound N-ADP was studied by incubating isolated mitochondria at 20°C in MKE buffer (1 mg protein.mL^{-1}) and fluorescence was measured as described in (David et al., 2008).

2.5 Mitochondrial cytochrome *aa3* content (performed by Dr Ludovic Pelosi)

The *aa*3 cytochrome content of the isolated yeast mitochondrial fractions was determined by calculating the difference between recorded reduced and oxidized spectra at 550 to 650 nm (Dassa et al., 2008). Briefly, mitochondria were diluted to 2 mg protein.mL^{-1} in 100 mM Na_2SO_4, 10 mM Tris-HCl pH 7.3, 1 mM EDTA, and 0.5% (w/v) DDM. Cytochromes were oxidized or reduced by adding solid potassium ferricyanide or sodium dithionite, respectively. The extinction coefficient used for cytochrome *aa*3 was 24,000 $M^{-1}.cm^{-1}$.

2.6 TbMCP5 peptide-antibody

The peptide 'VDALKPIYVEWRRSN' (amino acids 293-307 of TbMCP5) was coupled to KLH and used for the immunization of rabbits following a standard immunization protocol (EZBiolab, USA). The αTbMCP5 antiserum was collected 9 weeks after first immunization and showed an antibody titre of 1/1,192,000. Western blot analysis (1/2,000 dilution) revealed a singly cross-reacting protein band with a molecular weight of 34 kDa, as predicted for TbMCP5 (Colasante et al., 2009).

2.7 Culture of T. brucei cell lines

BSF and PCF *T. brucei* cell lines were cultured in HMI9 (Hirumi and Hirumi, 1989) and glucose-rich SDM79 medium (Brun and Schonenberger, 1979), respectively. For growth experiments in the absence of glucose, PCF trypanosomes were cultured in glucose-depleted SDM80 medium (Lamour et al., 2005). PCF *T. brucei* strains 449 and EATRO1125.T7T were used as 'wildtype' cell lines for all experiments and were cultured in the continuous presence of phleomycin (5 μg.mL^{-1}) to maintain stable expression of the tetracycline repressor from plasmid pHD449 (Biebinger et al., 1997) or in the presence of G418 (10 μg.mL^{-1}) and hygromycin (25 μg.mL^{-1}) to

maintain stable expression of the tetracycline repressor and T7 RNA polymerase from plasmids pLew90/Neo and pHD328, respectively (Bringaud et al., 2000). Trypanosomes were transfected as described previously (Biebinger et al., 1997, Clayton, 1999). The PCF cell line *TbMCP5-cmyc*^{ti} (Colasante et al., 2009) was cultured in the presence of hygromycin (50 μg.mL^{-1}), the conditional TbMCP5 double-knockout cell line Δ*TbMCP5/TbMCP5-cmyc*^{ti} was cultured in the presence of hygromycin (50 μg.mL^{-1}), G418 (15 μg.mL^{-1}) and blasticidin (10 μg.mL^{-1}), and the EATRO1125.T7T RNAi mutant cell lines were cultured in the presence of hygromycin (25 μg.mL^{-1}), G418 (10 μg.mL^{-1}) and phleomycin (5 μg.mL^{-1}). Cells were harvested at mid-logarithmic phase densities of 1x10^{6} cells.mL^{-1} (BSF) and 1x10^{7} cells.mL^{-1} (PCF) for protein and RNA analysis.

2.8 Protein quantification, western blot analysis and immunofluorescence microscopy

Protein concentrations were determined using the bicinchoninic acid (BCA) reagent kit (Sigma-Aldrich) and BSA as the protein standard. The raised TbMCP5 antibody (this thesis), an antibody against full-length ScAnc2p (Clemencon et al., 2008), and an antibody against heat shock protein 60 (HSP60) (Bringaud et al., 1995) were used for Western blot analysis at a dilution of 1/2,000, 1/1,500 and 1/10,000, respectively. Immunodetection was performed using horseradish peroxidase (HRP)-coupled protein A (Biorad) or HRP-coupled myc-antibody (Santa Cruz Biosciences), and the enhanced chemiluminescence (ECL) kit from GE Healthcare. Immunofluorescence microscopy using paraformaldehyde-fixed trypanosomes was performed as described previously (Colasante et al., 2006, Colasante et al., 2009). 4',6-Diamidino-2-phenyl-indole (DAPI) was used for the specific staining of nuclear and kinetoplastid

(mitochondrial) DNA, the mitochondrial marker MitoTracker (Invitrogen) for the specific labelling of *T. brucei* mitochondria (Vassella et al., 1997), and the TbMCP5 antibody for the specific labelling of TbMCP5.

2.9 Northern blot analysis

Total RNA was isolated from trypanosomes using the RNeasy mini kit (Qiagen). Northern blot analysis was performed as described by Sambrook *et al*. (Sambrook J, 1989). The complete open reading frame of *TbMCP5* was labelled with [^{32}P]-dCTP (PerkinElmer) using a standard PCR procedure. The RNA blot was pre-hybridised in hybridisation buffer (5xSSC, 0.1% w/v SDS, 5xDenhardt's, 100 μg.mL^{-1} denatured and sheared salmon sperm DNA) for 30 min at 60°C, after which the [^{32}P]-dCTP labelled DNA probe was added. After overnight hybridisation at 60°C, the blots were washed for 30 min in 1xSSC/0.1% (w/v) SDS at room temperature, for 45 min in 1xSSC/0.5% (w/v) SDS at 42°C and for 30 min in 0.1xSSC/0.2% (w/v) SDS at 42°C, followed by auto-radiographic detection.

2.10 Generation of the conditional TbMCP5 double-knockout cell line (performed by Dr Priscilla Pena-Diaz in this laboratary)

The previously generated PCF *T. brucei* cell line *TbMCP5-cmyc*^{ti} (Colasante et al., 2009) allows the ectopic and tetracycline-inducible expression of recombinant N-terminal 2xmyc-tagged TbMCP5, and was used as parental cell line for generation of the conditional TbMCP5 double-knockout cell line. The 5'-UTR of *TbMCP5a* (GeneDB Tb927.10.14820) and 3'-UTR of *TbMCP5c* (GeneDB Tb927.10.14840) were inserted on either side of the *NEO* (G418) or *BSD* (blasticidin) antibiotic resistance cassettes bearing actin 5'-splice sites and actin 3'-untranslated regions (Voncken et al., 2003). The different UTRs were obtained by PCR from isolated *T.*

brucei genomic DNA: the primer combination 5'-agggtgagctcgttctcagaagtgacttctgtcgcc-3' (sense) and 5'-accgcactagtgtccatatgcaccagacgcggctagtcg -3' (antisense) was used for the 678 bp 5'-UTR of *TbMCP5a*, whereas the primer combination 5'-ctcaccaggatccgtgccgttgctggtttttatttg-3' (sense) and 5'-ccttgggcccctcctcaggc acag c cttaccgtttt-3' (antisense) was used for the 724 bp 3'-UTR of *TbMCP5c*. The underlined restriction enzyme sites were used for subsequent cloning in the different *NEO*- and *BSD*-containing knockout (KO) plasmids. After transfection of *TbMCP5-cmyc*^{ti} with the *NEO-TbMCP5*-KO construct and clonal selection with 15 µg.mL^{-1} G418, the half-knockout cell line Δ*TbMCP5::NEO/TbMCP5/ TbMCP5-cmyc*^{ti} was isolated. The double-knockout cell line Δ*TbMCP5::NEO/*Δ*TbMCP5:: BSD/TbMCP5-cmyc*^{ti}, further referred to as Δ*TbMCP5/TbMCP5-cmyc*^{ti} in this paper, was obtained after subsequent transfection with the *BSD-TbMCP5*-KO plasmid, followed by clonal selection with 15 µg.mL^{-1} G418 and 10 µg.mL^{-1} blasticidin. The *TbMCP5a-c* half- and double knockout cell lines were cultured in the continuous presence of tetracycline (1 µg.mL^{-1}) in order to maintain TbMCP5-nmyc expression and cell viability. Correct integration of the different *NEO*/*BSD-TbMCP5*-KO constructs and deletion of the two native *TbMCP5a-c* gene clusters was confirmed by southern blot analysis and PCR (results not shown), as well as by western blot analysis for the TbMCP5 gene product (this chapter).

2.11 ATP production by T. brucei mitochondria

Mitochondrial ATP production in *T. brucei* was analysed according to Schneider *et al*. (Schneider et al., 2007). Briefly, 1x10^{8} trypanosomes were harvested and permeabilized with 0.008% (w/v) digitonin. A mitochondria-enriched subcellular

fraction was obtained after centrifugation and extensive washing in SoTE buffer (20 mM Tris-HCl pH 7.5, 2 mM EDTA, 0.6 M Sorbitol). The mitochondria-enriched subcellular fraction was resuspended in ATP Assay Buffer (20 mM Tris-HCl pH 7.4, 15 mM KH_2PO_4, 5 mM $MgSO_4$, 0.6 M Sorbitol), and mitochondrial ATP production was initiated by addition of 67 μM ADP and 5mM succinate or 5 mM α-ketoglutarate (Schneider et al., 2007). The specific ADP/ATP carrier inhibitor CATR (4 $\mu g.mL^{-1}$) was added during control experiments. ATP formation was quantified using the ATP Bioluminescence Assay Kit CLS II (Roche) in combination with a luminometer.

2.12 Metabolite analysis (performed by Dr Charles Ebikeme and Dr Frederic Bringaud)

'Wildtype' and TbMCP5-depleted Δ*TbMCP5/TbMCP5-cmyc*^{ti} trypanosomes were cultured for 72 h in glucose-depleted SDM80 medium. Culture aliquots were collected every 24 h for the determination of cell density ($cells.mL^{-1}$). Proline consumption was determined as previously described (Bates, 1977), whereas product formation, here succinate and acetate, was determined using corresponding detection kits from Megazyme.

2.13 Depletion of TbMCP5 by RNA interference

Inhibition of *TbMCP5* gene expression was performed in PCF *T. brucei* by using RNA-interference (RNAi) (Bellofatto and Palenchar, 2008). The 563 bp sense and 624 bp antisense sequences of *TbMCP5* were PCR-amplified and cloned into the *T. brucei* expression vector *pLew100* (Wirtz et al., 1999). The primer combination 5'-gtgtataagctttggcgaggtaacctgtca-3' and 5'-gtcatcctcgagcgccggcgaacggtgtccaa-3' was used for amplification of the 563 bp sense *TbMCP5* sequence, and the primer combination 5'-gggcgtggatccgctttggcgaggtaacctgtc-3' and 5'-

tgcaacaagctttccctcgagttcttgtacttcacagcagc-3' was used for the 624 bp antisense *TbMCP5* sequence. The underlined restriction enzyme sites were used for cloning into *pLew100*. The resulting *pLew100-TbMCP5* RNAi construct harbors a phleomycin resistance gene, and contains the consecutively cloned sense and antisense *TbMCP5* target sequences separated by a 50 bp spacer fragment. Inducible expression is under control of the procyclic acidic repetitive protein (PARP) promoter linked to a prokaryotic tetracycline (tet) operator (Wirtz et al., 1999). The *pLew100-TbMCP5* RNAi construct was used for transfection of procyclic form *T. brucei* EATRO1125-T7T (Bringaud et al., 2000). The mutant ^{RNAi}*TbMCP5* cell line was obtained after clonal selection in glucose-rich SDM79 medium containing hygromycin (25 μg.mL^{-1}), neomycin (10 μg.mL^{-1}) and phleomycin (5 μg.mL^{-1}). This cell line enables inducible depletion of TbMCP5 on a 'wildtype' PCF background. The *pLew100-TbMCP5* RNAi construct was further used for transfection of the previously generated PCF *T. brucei* knockout mutant Δ*pepck*-cl1 (this part has been performed by Dr Charles Ebikeme and Dr Frederic Bringaud), which lacks the gene coding for phosphoenolpyruvate carboxykinase (PEPCK) (Ebikeme et al., 2010). The mutant cell line Δ*pepck*/^{RNAi}*TbMCP5* was obtained after clonal selection in glucose-rich SDM79 medium containing puromycin (1 μg.mL^{-1}), hygromycin (25 μg.mL^{-1}), neomycin (10 μg.mL^{-1}) and phleomycin (5 μg.mL^{-1}). This cell line enables inducible depletion of TbMCP5 on a *pepck* null background. The obtained mutant cell lines were subsequently adapted to glucose-depleted SDM80 medium, containing the same antibiotics. Addition of tetracycline to the PCF ^{RNAi}*TbMCP5* and Δ*pepck*/^{RNAi}*TbMCP5* cell lines will lead to the expression of double-stranded *TbMCP5* RNA molecules and the concomitant down-regulation (silencing) of TbMCP5 expression.

3. Results

3.1 Sequence analysis of TbMCP5 and TbMCP15

TbMCP5 and TbMCP15 have previously been identified as novel members of the *T. brucei* mitochondrial carrier family (MCF) (Colasante et al., 2009). The *T. brucei* genome contains three identical and consecutive arranged genes coding for TbMCP5, i.e. *TbMCP5a-c* (GeneDB Tb927.10.14820/830/840), while TbMCP15 is coded for by a single gene (GeneDB Tb927.8.1310) (Colasante et al., 2009). TbMCP5 and TbMCP15 contain sequence features that are conserved in all MCF proteins (Palmieri et al., 2011), including the presence of 6 trans-membrane helices, a tripartite protein domain structure with semi-conserved sequence repeats of approximately 100 amino acids, and the canonical signature sequence motif 'Px(D/E)x_2(K/R)x(K/R)x_{20-30}(D/E)Gx_{4-5}(W/F/Y) (K/R)G' at the end of each odd-numbered trans-membrane helix (Fig. 1A). They are further the only two members of the *T. brucei* MCF inventory that share significant sequence similarity (67-84% amino acid identity (Colasante et al., 2009)) with functionally characterised ADP/ATP carriers from other eukaryotes, such as *Saccharomyces cerevisiae* Anc2p (Brandolin et al., 1993) and *Homo sapiens* Anc1p (De Marcos Lousa et al., 2002).

The hallmark of ADP/ATP carriers is the presence of the conserved hexapeptide sequence 'RRRMMM' (Nury et al., 2006). Mutation analysis confirmed that this motif is involved in ADP-binding and is essential for ADP/ATP exchange (Clemencon et al., 2011). Also TbMCP5 contains a conserved 'RRRMMM' motif (Fig. 1B), supporting the prediction that this MCF protein functions as an ADP/ATP carrier. MCF proteins further contain several conserved amino acids that are involved in the selective binding and transport of substrates. These amino acids are organised in three distinct substrate contact points (CP1-3, Fig. 1B) and are conserved for MCF

proteins that transport similar substrates (Kunji and Robinson, 2006). For ADP/ATP carriers, CP1 is composed of the 3 conserved amino acids arginine (R), threonine (T) and asparagine (N), corresponding to respectively R96, T100 and N104 of the ScAnc2p reference sequence; CP2 is composed of a conserved glycine (G) and isoleucine (I), here G199 and I200 in ScAnc2p; and CP3 is composed of only a single amino acid and is in the case of ADP/ATP carriers represented by a conserved arginine (R), R294 in ScAnc2p (Fig. 1B). Sequence comparison revealed that in TbMCP5 the amino acid compositions of the 3 different substrate contact points were identical to those of ScAnc2p and HsAnc1p (Fig. 1B). In addition, TbMCP5 contains a well-conserved aromatic ladder, corresponding to Y203, Y207, F208 and Y211 in the ScAnc2p reference sequence (Fig. 1B), which is crucial for ADP/ATP-exchange in ADP/ATP carriers (David et al., 2008). All these observations reinforced the predicted ADP/ATP carrier function of TbMCP5.

In contrast, TbMCP15 contains a degenerated version of the ‘RRRMMM’ motif, with a single amino acid substitution (‘M’ to ‘I’) at position 3 of the methionine cluster (Fig. 1B). A similar mutation of the methionine cluster in ScAnc2p resulted in the elimination of ADP/ATP exchange activity (Clemencon et al., 2011). In addition, the amino acid compositions of CP1-3 are different from those of conventional ADP/ATP carriers - in particular CP1 is not conserved at all (Fig. 1B). TbMCP15 further contains a degenerated aromatic ladder (Fig. 1B). Overall, these deviations strongly suggest that TbMCP15 is not a classical ADP/ATP exchanger, despite its overall sequence similarity to ADP/ATP carriers from other eukaryotes.

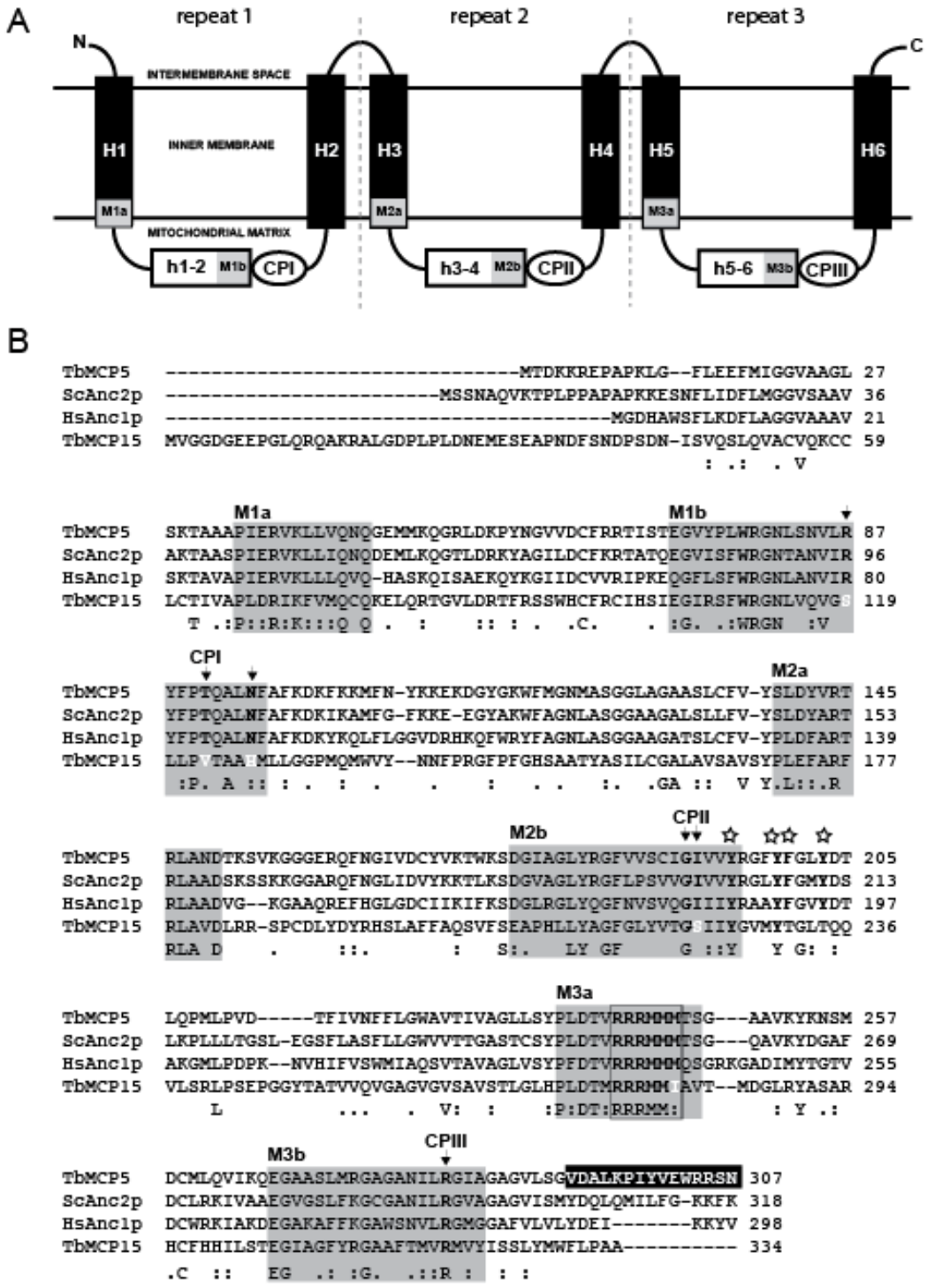

Figure 1: TbMCP5 contains conserved ADP/ATP carrier sequence features. A. Schematic representation of MCF protein sequence structure (adapted from Pena-Diaz et al., 2012). Transmembrane (TM) helices are represented by H1-6, while the connecting hydrophilic loops are represented by h1-2, h3-4 and h5-6, respectively. M1-3a indicate the first part (Px[D/E]xx[K/R]x[K/R]) and M1-3b the second part

([D/E]Gx$_n$[K/R]G) of the canonical MCF signature sequence. The different conserved substrate contact points are indicated by CP1-3. B. Sequence alignment of TbMCP5 and TbMCP15 with *S. cerevisiae* Anc2p (ScAnc2p) and *H. sapiens* Anc1p (HsAnc1p). The different parts of the canonical signature sequence (see A) are indicated by grey backgrounds. Open stars indicate conserved amino acids of the aromatic ladder. Conserved amino acids of the different substrate contact points (CP1-3) are printed black bold face and indicated by arrows, whereas deviating amino acids are printed white bold face. The conserved hexapeptide sequence 'RRRMMM' found in all ADP/ATP carriers is boxed. The carboxy-terminal peptide sequence of TbMCP5 used for immunisation is printed white on a black background.

3.2 Functional complementation analysis of *S. cerevisiae JL1Δ2Δ3u⁻*

The *S. cerevisiae* deletion strain *JL1*Δ*2*Δ*3u⁻* is deficient in mitochondrial ADP/ATP carriers (*ANC*-deficient) and is only viable on a fermentable carbon source such as glucose (Clemencon et al., 2008). The putative ADP/ATP-exchange function of *TbMCP5* and *TbMCP15* can therefore be directly assessed *in vivo* by testing their ability to restore growth of *JL1*Δ*2*Δ*3u⁻* cells on glucose-depleted YPL medium, containing lactate as a non-fermentable carbon source (Clemencon et al., 2008, Babot et al., 2012). The open reading frames of *TbMCP5* and *TbMCP15* were cloned into the low copy-number yeast expression vector *pRS314* containing *ScANC2* regulatory regions (Le Saux et al., 1996). *pRS314* containing the *ScANC2* ORF was used as a positive control, whereas *pRS314* without any insert was used as a negative control. The *JL1*Δ*2*Δ*3u⁻* strain was transformed with the various constructs to produce the *JL-TbMCP5*, *JL-TbMCP15*, and *JL-ScANC2* strains. Growth of these strains was examined on solid YPL medium and glucose-rich tryptophan-free YNB medium (YNB Glc W⁻). As expected, growth of all strains was similar when plated on YNB Glc W⁻ medium, whereas growth of *JL1*Δ*2*Δ*3u⁻* on YPL medium was restored to wild-type level with the expression of ScAnc2p (*JL-ScANC2*), but not with the empty *pRS314* vector (Fig. 2A). TbMCP15 could not restore growth of *JL1*Δ*2*Δ*3u⁻* (*JL-TbMCP15*) on YPL medium, which confirmed the *in silico* prediction that TbMCP15 is not an ADP/ATP carrier (Fig. 2A). Unfortunately, there is no antibody available for TbMCP15, which could confirm the presence of this protein in the *JL-TbMCP15* mitochondria. Expression of TbMCP5 in *JL1*Δ*2*Δ*3u⁻* yeast cells (*JL-TbMCP5*) resulted in a significant rescue of growth on YPL medium (Fig. 2A). This result confirmed that TbMCP5 is able to functionally complement the mitochondrial ADP/ATP carrier deficiency of yeast. However, the functional complementation is

not optimal: for *JL-TbMCP5* a doubling time of 6 h was found at the plateau phase of its growth, whereas for *JL-ScANC2* the doubling time was significantly shorter, here 2.5 h at the same growth phase (Table 1).

Table 1: Yeast growth properties, ligand-binding data for carriers, and kinetic parameters of ADP/ATP transport activity measured in mitochondria isolated from *JL-ScANC2* and *JL-TbMCP5* (Taken from Pena-Diaz et al., 2012).

Yeast strains	*JL- ScANC2*	*JL-TbMCP5*
Cell culture in YPL[a]		
Doubling time (h)	2.5	6
Growth yield $A_{600\ nm}$	12	11
[^{3}H]-ATR binding [b]		
B_{max} (pmol.mg protein $^{-1}$)	698±51	149±17
K_d (nM)	396±23	503±15
cyt aa_3 (pmol.mg^{-1})[c]	200±23	188±32
ADP/ATP exchange [d]		
V_{max} (nmol ATP.min^{-1}.mg protein^{-1})	1046±173	240±17
K_{cat} (min^{-1})	1424±101	1619±85
K_M external ADP (µM)	4.6±0.8	4.2±0.1
N-ADP dissociation constant [e]		
$K_{1/2}$	6.2±0.7	5.1±0.5

[a] Cells were cultivated on liquid YPL medium

[b] [^{3}H]-ATR binding parameters: number of binding sites, B_{max} and K_d values were calculated from Scatchard plots of [^{3}H]-ATR-binding data.

[c] The cytochrome *aa*3 content of isolated mitochondria was measured by recording the reduced minus oxidized visible spectrum. Δ_{aa3} = 24 000 M^{-1}.cm^{-1}.

[d] V_{max} and apparent K_m for external free ADP were calculated from kinetic data using the Michaelis-Menten and Lineweaver-Burk equations. k_{cat} refers to carrier turnover, calculated based on the carrier content determined by [^{3}H]-ATR-binding experiments, assuming that 1 mol of ATR binds to 1 mol of transport unit.

[e] The $K_{1/2}$ value was determined by plotting $\Delta F/\Delta F_{max}$ as a function of added N-ADP. All the values are the means of three independent experiments.

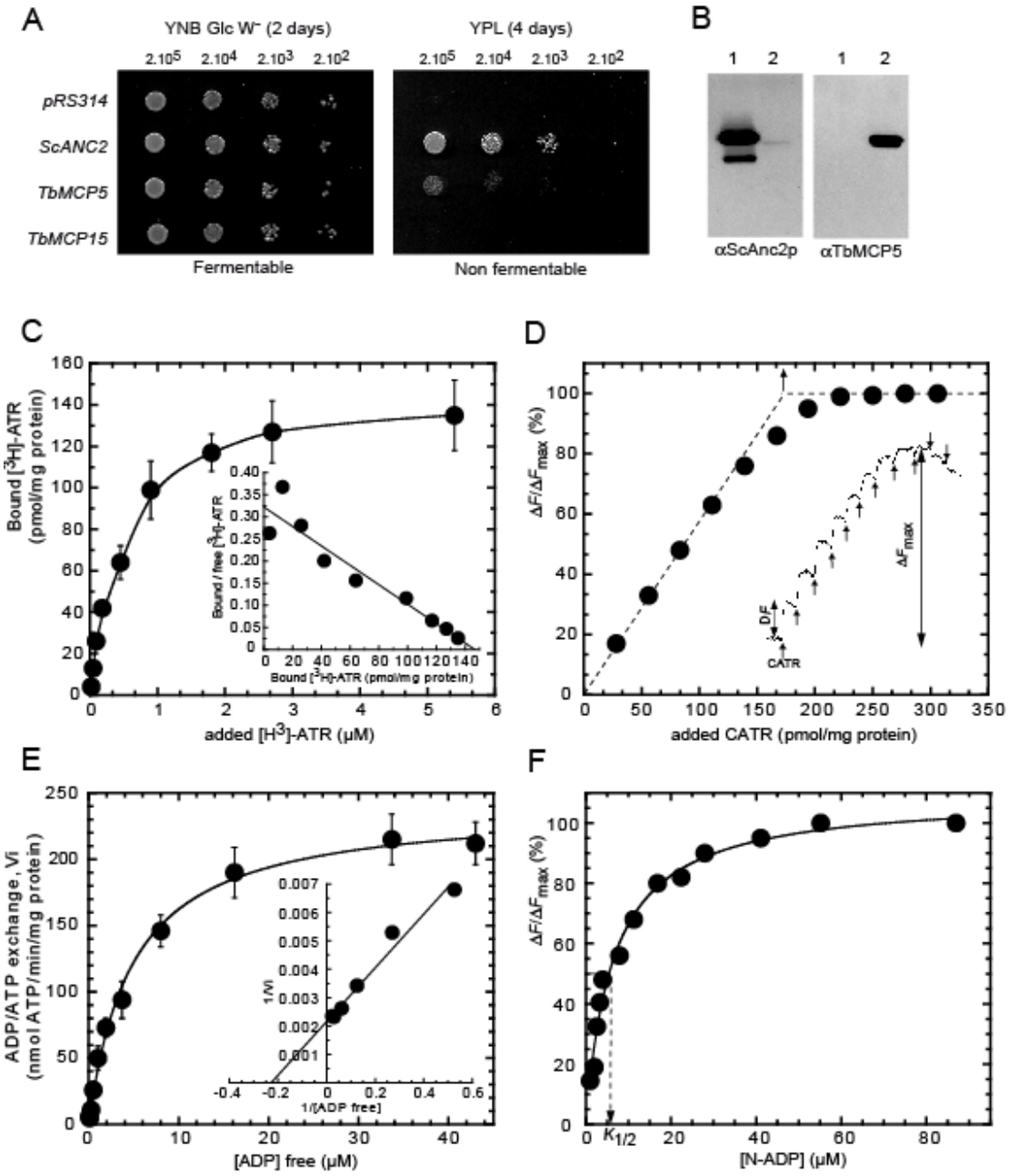

Figure 2: TbMCP5 functions as a mitochondrial ADP/ATP carrier (adapted from Pena-Diaz et al., 2012). A. Yeast growth phenotype associated with the expression of TbMCP5 and TbMCP15. The *ANC*-deficient *S. cerevisiae* strain *JL1Δ2Δ3u*$^-$ was transformed with *pRS314* (no insert) and *pRS314* containing *ScANC2*, *TbMCP5* or *TbMCP15*. Yeast cell lines were isolated and inoculated in liquid minimum tryptophan-free medium containing 2% (v/v) glucose as carbon source (YNB Glc W$^-$

). Log phase cultures were diluted to $2x10^3$-$2x10^5$ cells per 5 mL before spotting onto YNB Glc W^- or lactate-containing medium (YPL) plates, and incubated at 28°C for 2 days (YNB) or 4 days (YPL). B. Immunodetection of TbMCP5 and ScAnc2p in yeast mitochondria. Mitochondrial extracts (20 mg protein per lane) prepared from *JL-ScANC2* (lanes 1) and *JL-TbMCP5* (lanes 2) strains were subjected to SDS-PAGE (12.5% w/v acrylamide) and western blot analysis using a polyclonal rabbit antibody (αScAnc2p) directed against the complete ScAnc2p sequence and the TbMCP5 peptide antibody (αTbMCP5, this paper). C. Specific binding of [^{3}H]-ATR to mitochondria expressing TbMCP5. Isolated mitochondria (1 mg total protein) from yeast cells expressing TbMCP5 were incubated with increasing concentrations of [^{3}H]-ATR. After centrifugation, the radioactivity associated with the mitochondrial pellet was estimated by scintillation counting. Data were corrected for unspecific binding from parallel experiments carried out in the presence of 20 µM CATR. The inset shows the Scatchard plot of the binding data. Error bars were calculated from three independent experiments. D. Fluorescence back-titration of CATR-binding sites to quantify the amount of TbMCP5 in mitochondria. Mitochondria (0.9 mg protein.mL^{-1}) were suspended at 20°C in 2 mL of MKE buffer containing 1 µM of N-ATR. Fluorescence variations (ΔF) induced by additions of CATR (25 pmol for each addition) were recorded as a function of time and are shown as inset. $\Delta F/\Delta F_{max}$ was plotted as a function of added CATR per mg of total proteins. E. ADP/ATP transport activity of TbMCP5 in isolated mitochondria. ADP/ATP transport was measured by means of a luciferase-based ATP assay. Freshly prepared mitochondria were energized in the presence of 5 µM of α-ketoglutarate (as respiratory substrate), the adenylate kinase inhibitor Ap5A, and of 0.1% (w/v) luciferin and 0.1% (w/v) luciferase. After a 3 min incubation period, free ADP (0.06–43 µM final concentration calculated using the WinMaxc v2.05 software) was added to initiate the ATP efflux and the related light emission was recorded. The time course of ATP efflux was monitored over a 5 min period. Control experiments were carried out in the presence of 20 µM CATR, to ensure that the ADP/ATP exchange was mediated by ADP/ATP carriers. Quantification of released ATP was performed on the basis of the signal amplitude corresponding to additions of 0.5 nmol ATP as a standard. Kinetic data were plotted using the graphical representations of Michaelis-Menten and Lineweaver-Burk (inset). The shown values are the means of three independent

experiments. F. Fluorescence titration of N-ADP-binding sites. The time course of CATR-induced release of bound N-ADP was studied by incubating isolated mitochondria (1 mg of mitochondrial proteins.mL^{-1}) in presence of N-ADP (0.5-87 µM). Thereafter, the fluorescence level was set to zero. The increase in fluorescence induced upon addition of 5 µL of 2 mM CATR (ΔF) was recorded until it became stable. The apparent dissociation constant $K_{1/2}$ was determined after plotting $\Delta F/\Delta F_{max}$ as a function of added N-ADP concentration.

3.3 Mitochondrial localisation and quantification of TbMCP5 in *JL1Δ2Δ3u*$^-$

Growth of *JL-TbMCP5* on YPL medium was completely inhibited by addition of the specific ADP/ATP-carrier inhibitors CATR and BA (not shown). These results not only confirmed that TbMCP5 functions as an ADP/ATP carrier, but also implied that TbMCP5 has the expected mitochondrial localisation in *JL-TbMCP5*. The mitochondrial location of TbMCP5 was further investigated by subcellular fractionation and western blot analysis, using a polyclonal antibody directed against ScAnc2p (Clemencon et al., 2008) and the TbMCP5 antibody described in this paper (see below). Mitochondria were isolated by differential centrifugation from the *JL-TbMCP5* and *JL-ScANC2* strains (Daum et al., 1982). As expected, the ScAnc2p antibody readily detected the Anc2p protein in the mitochondrial fraction of *JL-ScANC2* (Fig. 2B, left panel, lane 1). In addition, a smaller cross-reacting protein band was observed (Fig. 2B, left panel, lane 1), which most probably represents a ScAnc2p degradation product resulting from the mitochondrial preparation. The ScAnc2p antibody was further able to stain the heterologous TbMCP5 protein in the *JL-TbMCP5* mitochondria, although the observed signal was rather faint (Fig. 2B, left panel, lane 2). Staining with the TbMCP5 antibody resulted in a single strong signal of the expected size and confirmed the presence of TbMCP5 in the mitochondrial fraction of *JL-TbMCP5* (Fig. 2B, right panel, lane 2). These results unambiguously correlated the restoration of *JL1*Δ*2*Δ*3u*$^-$ growth on YPL medium with the presence of TbMCP5 protein in the yeast mitochondria.

The amount of TbMCP5 present in *JL-TbMCP5* mitochondria was estimated by determining the number of ATR-binding sites via titration using specific ADP/ATP carrier inhibitors (Roux et al., 1996). Interaction parameters were measured directly

using the specific high-affinity labelled radioactive ligand [^{3}H]-atractyloside ([^{3}H]-ATR) or indirectly via a fluorescence back-titration assay with 6'-*O*-naphthoyl-atractyloside (N-ATR), assuming that 1 mol of ATR binds to 1 mol of analysed ADP/ATP carrier (Roux et al., 1996). As expected, the binding of [^{3}H]-ATR to *JL-TbMCP5* mitochondria increased as a function of the concentration of [^{3}H]-ATR added and finally reached saturation (Fig. 2C). The binding isotherm was deduced from the Scatchard plot (Fig. 2C, inset). The maximum number of ATR-binding sites (B_{max}^{ATR}) and the ATR dissociation constant (K_D^{ATR}) were determined for TbMCP5 and compared to those obtained for ScAnc2p (Table 1). The K_D^{ATR} measured for ScAnc2p and TbMCP5 were in the same range, here respectively 396±23 nM and 503±15 nM (Table 1), indicating that both carriers have similar ATR-binding properties. However, the B_{max}^{ATR} of TbMCP5 (149±17 pmol.mg^{-1} protein) is about 5 times lower than the B_{max}^{ATR} of ScAnc2p (698 ±51 pmol.mg^{-1} protein) (Table 1). To exclude the possibility that the observed difference in B_{max}^{ATR} is due to differences in protein concentration, cytochrome aa_3 was quantified for the different mitochondrial fractions. Analysis revealed that the cytochrome aa_3 concentrations were similar for the different mitochondrial fractions, i.e. 200 ± 23 *versus* 188±32 pmol.mg^{-1} of cytochrome aa_3, respectively (Table 1). Binding of ATR to isolated mitochondria was estimated by measuring fluorescence variation of bound N-ATR in competition with added CATR (Fig. 2D). The maximum amount of CATR-binding sites was estimated to be 160 pmol.mg^{-1}, which is in agreement with the obtained [^{3}H]-ATR titration data (149 pmol.mg^{-1} protein). These results indicated that TbMCP5 was about 4-fold less abundant than ScAnc2p in the isolated mitochondrial fractions, which in turn could account for the reduced growth of *JL-TbMCP5* on YPL medium.

3.4 ADP/ATP-transport kinetics of TbMCP5 in comparison to *ScAnc2p*

The ADP/ATP-exchange activity of TbMCP5 in JL-TbMCP5 mitochondria was determined as described previously (Dassa et al., 2005). Mitochondria isolated from ScAnc2p-expressing yeast cells (*JL-ScANC2*) were used for comparison. As expected, no ADP/ATP exchange was found for both mitochondrial preparations in the presence of the specific ADP/ATP-carrier inhibitors CATR and BA (not shown). The obtained Michaelis-Menten and Lineweaver-Burk plots (Fig. 2E) were used to determine the variation in exchange rate as a function of ADP concentration for TbMCP5 and ScAnc2p **(**Table 1). Comparison of the obtained kinetic parameters revealed that the V_{max} of TbMCP5 was about 4.5 times lower than the V_{max} of ScAnc2p (Table 1). This result is in agreement with the lower amount of TbMCP5 present in yeast mitochondria compared to ScAnc2p. Comparison revealed further that the k_{cat} values and K_M values of external free ADP were similar for TbMCP5 and ScAnc2p (Table 1). The fluorescent compound 3'-*O*-(1-naphthoyl)-adenosine 5'-diphosphate (N-ADP) is a non-transportable ADP analogue. Its fluorescence is quenched upon binding to ADP/ATP carriers, so specific binding to the mitochondrial ScAnc2p or TbMCP5 can be measured by the enhancement of fluorescence upon dissociation after addition of CATR (Fig. 2F). ADP-binding experiments revealed that the $K_{1/2}$ value of N-ADP binding to TbMCP5 is 6.2 µM, which is similar to the value found for ScAnc2p, here 5.1 µM (Table 1). This similarity in ADP-binding is further in agreement with the observed small difference in K_M value for external free ADP (Table 1). Overall, ScAnc2p and TbMCP5 present comparable biochemical properties with regard to their ADP/ATP-exchange activity in yeast mitochondria.

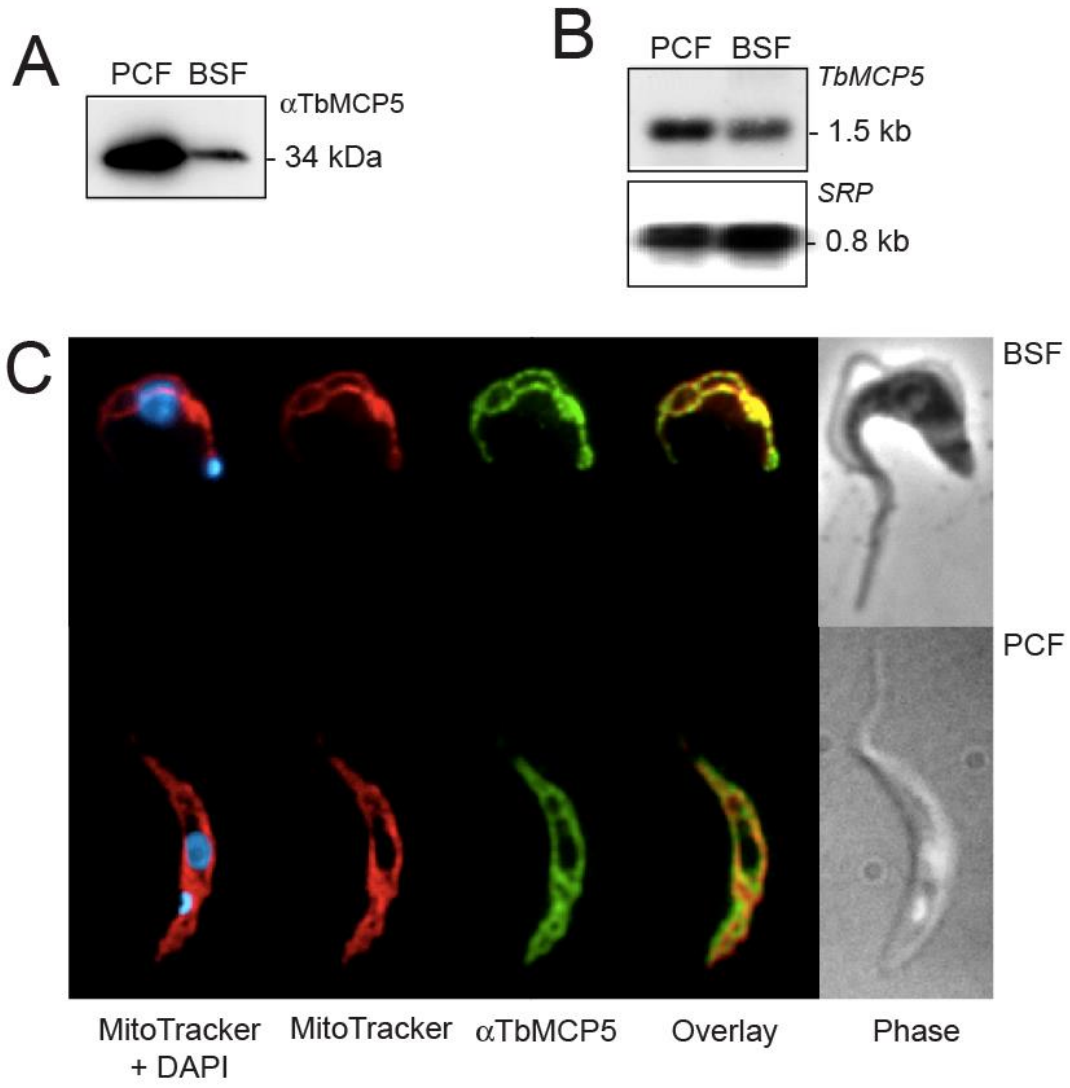

Figure 3: TbMCP5 is exclusively mitochondrial and differentially expressed (adapted from Pena-Diaz et al., 2012). A. Western blotting analysis of 'wildtype' PCF and BSF *T. brucei* using the αTbMCP5 antibody (diluted 1:2000). Each lane contained $2x10^6$ trypanosomes. B. Northern blot analysis of total RNA from PCF and BSF *T. brucei* using [α^{32}P]-dCTP labelled *TbMCP5* DNA as probe for hybridization. Each lane contained 20 μg total RNA. C. Immunofluorescence microscopy of 'wildtype' BSF and PCF *T. brucei* confirming the exclusive mitochondrial localisation of TbMCP5. TbMCP5 was stained (green) using the αTbMCP5 antibody (diluted 1:500). Mitochondria were stained (red) with the specific mitochondrial

marker Mitotracker, whereas nuclear and kinetoplast DNA (blue) was stained with DAPI.

3.5 TbMCP5 is exclusively mitochondrial and differentially expressed in *T. brucei*

We previously reported that TbMCP5 has an exclusive mitochondrial localisation in the procyclic life cycle stage of *T. brucei* (Colasante et al., 2009). This subcellular localisation was determined by immunofluorescence microscopy using a *T. brucei* cell line expressing recombinant N-terminal myc-tagged TbMCP5 (*TbMCP5-nmyc*^{ti}) and a commercial myc-antibody (Colasante et al., 2009). To assess the expression and subcellular localisation of the native protein, a polyclonal rabbit antiserum was raised against the C-terminal peptide AA293-307 of TbMCP5. Western blot analysis using the TbMCP5 peptide antibody revealed a single cross-reacting protein band with the expected molecular size of 34 kDa in both the procyclic (PCF) and bloodstream (BSF) forms of *T. brucei* strain 449 (Fig. 3A). Quantification of the obtained western blot signals revealed that about 4.5-fold more TbMCP5 is present in PCF *T. brucei* compared to the BSF parasite. This differential expression of TbMCP5 is supported by northern blot analysis, which revealed about 2.5-fold more *TbMCP5* mRNA in PCF *T. brucei* (Fig. 3B). Immunofluorescence microscopy showed specific tubular staining patterns for both PCF and BSF *T. brucei* when using the TbMCP5 peptide antibody (Fig. 3C). These staining patterns were identical to those obtained for the mitochondrial marker MitoTracker (Fig. 3C, (Vassella et al., 1997)). These results confirmed the expression and mitochondrial localization of TbMCP5 in the two different life cycle stages of *T. brucei* and indicated further that TbMCP5 is more abundant in PCF *T. brucei.*

3.6 Silencing and depletion of TbMCP5 in PCF trypanosomes

Different approaches were used to silence TbMCP5 expression in PCF *T. brucei*. Initially, a conventional targeted gene replacement method was used to replace the two chromosomal *TbMCP5a-c* gene clusters (diploid organism) through consecutive homologous recombination using different antibiotic resistant cassettes. The upstream *TbMCP5a* 5'-UTR and downstream *TbMCP5c* 3'-UTR were used for homologous recombination, allowing each *TbMCP5a-c* gene cluster to be removed in a single recombination event. However, using this conventional method no viable *TbMCP5a-c* double-knockout clones could be obtained on glucose-rich SDM79 or glucose-depleted SDM80 medium, suggesting that expression of TbMCP5 is essential for growth. To overcome the apparent lethal phenotype, a recombinant tetracycline-inducible and nmyc-tagged version of *TbMCP*5 (inducible rescue copy) was inserted into the *T. brucei* genome prior to the deletion of the two endogenous *TbMCP5a-c* gene clusters. Addition of tetracycline to the obtained *TbMCP5-nmyc*^{ti} cell line resulted in the expression of recombinant myc-tagged TbMCP5 (TbMCP5-nmyc, 37 kDa), whereas tetracycline withdrawal resulted in the absence (below detection limit of the used method) of the same protein (Fig. 4A). The tetracycline-induced *TbMCP5-nmyc*^{ti} cell line was subsequently used to generate the conditional TbMCP5 double-knockout cell line Δ*TbMCP5/TbMCP5-nmyc*^{ti}. Western blot analysis (Fig. 4B) of the tetracycline-induced Δ*TbMCP5/TbMCP5-nmyc*^{ti} cell line confirmed the absence of endogenous TbMCP5a-c (34 kDa) and the presence of recombinant TbMCP5-nmyc (37 kDa). Subsequent withdrawal of tetracycline resulted in the depletion (below detection limit) of *TbMCP5-nmyc* mRNA within 24 h (Fig. 4C). As expected, also the corresponding TbMCP5-nmyc protein level decreased significantly, although still some recombinant protein could be detected at 72 h (Fig.

4C). Withdrawal of tetracycline for more than 72 h resulted in loss of expression control and an increased expression of TbMCP5-nmyc (not shown). This loss of expression control upon gene deletion or silencing is common for *T. brucei*, especially if the target gene is essential for growth/survival of the parasite (Clayton, 1999).

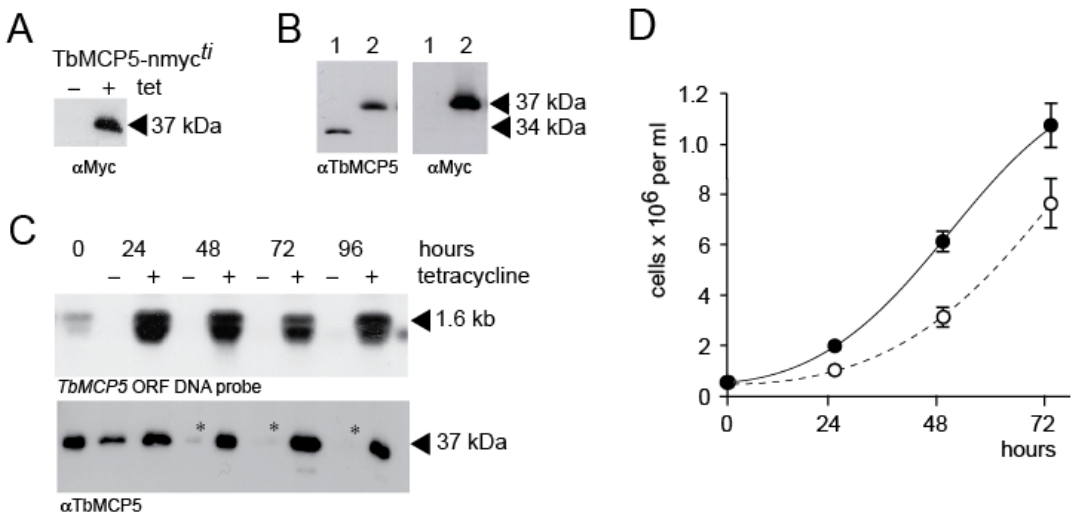

Figure 4: Analysis of the conditional Δ*TbMCP5/MCP5-nmyc*^{ti} cell line (adapted from Pena-Diaz et al., 2012). A. Western blot analysis of *TbMCP5-nmyc*^{ti} cells grown without (-) or in the presence (+) of tetracycline. Each lane contained 2x10^6 trypanosomes. TbMCP5-nmyc protein was stained with a myc-antibody (αMyc). B. Western blot analysis of protein extracts from 'wildtype' (lanes 1) and tetracycline-induced Δ*TbMCP5/TbMCP5-nmyc*^{ti} (TbMCP5-nmyc expressing, lanes 2) trypanosomes, using the TbMCP5 antibody (αTbMCP5) and αMyc. Each lane contained 2x10^6 trypanosomes. C. The conditional Δ*TbMCP5/MCP5-nmyc*^{ti} cell line was cultured in SDM80 medium with (+, induced) or without (-, non-induced) tetracycline. Samples were taken every 24 h for northern blot analysis (upper panel) using the [α^{32}P]-dCTP labelled *TbMCP5* ORF DNA as hybridisation probe, and for western blot analysis using αTbMCP5. Each lane contained 20 μg total RNA (upper panel, northern blot analysis) or 2x10^6 trypanosomes (lower panel, western blot analysis). Asterisks indicate residual TbMCP5-nmyc protein. D. Cumulative growth

curve of ‘wildtype’ (solid line) and non-induced Δ*TbMCP5/MCP5-nmyc*^{ti} trypanosomes (TbMCP5-depleted, dashed line) grown in glucose-depleted SDM80 medium. Cell densities (cells.mL^{-1}) were determined every 24 h and means are derived from 6 independent experiments.

Analysis of the non-induced Δ*TbMCP5/TbMCP5-nmyc*^{ti} cell line revealed a partial growth defect in glucose-depleted medium (SDM80), compared to growth of the ‘wildtype’ cell line in the same medium (Fig. 4D). This result was somewhat unexpected since TbMCP5 was proposed to be essential for trypanosome growth, thus its deletion should lead to a severe and probably lethal growth defect. However, the residual TbMCP5-nmyc protein observed for the non-induced Δ*TbMCP5/TbMCP5-nmyc*^{ti} cell line (Fig. 4C) is apparently sufficient to support substantial growth of the parasite.

Alternatively to the above described conventional and conditional gene replacement methods, we down-regulated the expression of TbMCP5 in ‘wildtype’ *T. brucei* through RNA interference (RNAi). Western blot analysis of the obtained ^{RNAi}*TbMCP5* cell line showed that when cultured on glucose-rich SDM79 or glucose-depleted SDM80 medium, TbMCP5 was completely depleted (below detection limit of the used method) within 48 h after induction of the RNAi (Fig. 5C). TbMCP5 remained depleted for up to 7 days after which it slowly re-appeared (Fig. 5C). In glucose-rich SDM79 medium, growth of the ^{RNAi}*TbMCP5* cell line was reduced until day 7 after induction (arrow in Figs 5A). However, with the re-appearance of TbMCP5 after day 7 (Fig 5C) it reverted to ‘wildtype’ growth, suggesting that TbMCP5 is essential for growth under glucose-rich conditions. Interestingly, the same cell line was unable to grow in glucose-depleted SDM80 medium (Fig. 5B), although TbMCP5 was re-expressed after day 7 **(**Fig 5C). This result suggested that

TbMCP5 plays a more important role when glucose is absent from the medium. In the absence of glucose, ATP can only be generated via mitochondrial oxidative phosphorylation from proline degradation (Lamour et al., 2005, Coustou et al., 2008, Ebikeme et al., 2010). This process is in turn dependent on the presence of a functional ADP/ATP carrier in the inner mitochondrial membrane, which replenishes ADP in the mitochondrion and provides essential ATP to the rest of the cell. The inability of TbMCP5-depleted PCF *T. brucei* to grow on glucose-depleted SDM80 medium was therefore expected. In the presence of glucose, however, ATP can be produced in the cytosol during the final two steps (phosphoglycerate kinase and pyruvate kinase) of the cytosolic part of the glycolytic pathway. PCF *T. brucei* is therefore not exclusively dependent on the mitochondrion for its cellular ATP provision (Lamour et al., 2005, Coustou et al., 2008).

To confirm this hypothesis, we subsequently down-regulated TbMCP5 expression on a phosphoenolpyruvate carboxykinase (PEPCK) null background. PEPCK is the first enzyme in the glycosomal succinic fermentation branch and is required for sustaining the ADP/ATP and redox balances in the glycosome (Ebikeme et al., 2010). Deletion of the PEPCK-coding gene in PCF *T. brucei* was previously shown to ablate the glycosomal production of succinate (Ebikeme et al., 2010). The resulting Δ*pepck* cell line is primarily dependent on the mitochondrial degradation of proline as consequence of a substantial decrease in glucose consumption, even under glucose-rich conditions (Ebikeme et al., 2010). RNAi-mediated depletion of TbMCP5 on a *PEPCK* null background (Δ*pepck/* ^{RNAi}*TbMCP5*) resulted in cell death 7 days after induction in both glucose-rich and glucose-depleted media (Fig. 5D and E). The absence of TbMCP5 in both experiments was confirmed by western blot analysis (Fig. 5F). The rapid death of the TbMCP5-depleted Δ*pepck/*^{RNAi}*TbMCP5* cell line

under both growth conditions reflects its now proline-dependent metabolism, irrespective of the glucose concentrations in the different culture media, i.e. 6 mM in SDM79 *versus* <0.15 mM in SDM80. Remarkably, the Δ*pepck* cell line is more sensitive to RNAi-mediated depletion of TbMCP5 than 'wildtype' cells, even under glucose-depleted conditions. This may be due to the presence of the residual <0.15 mM glucose in SDM80, which could be used for growth by the ^{RNAi}*TbMCP5* single mutant, but not by the Δ*pepck*/^{RNAi}*TbMCP5* double mutant. Altogether, these data showed that TbMCP5 is essential for PCF *T. brucei*, particularly in a glucose-depleted environment where ATP is primarily produced in the mitochondrion from proline metabolism.

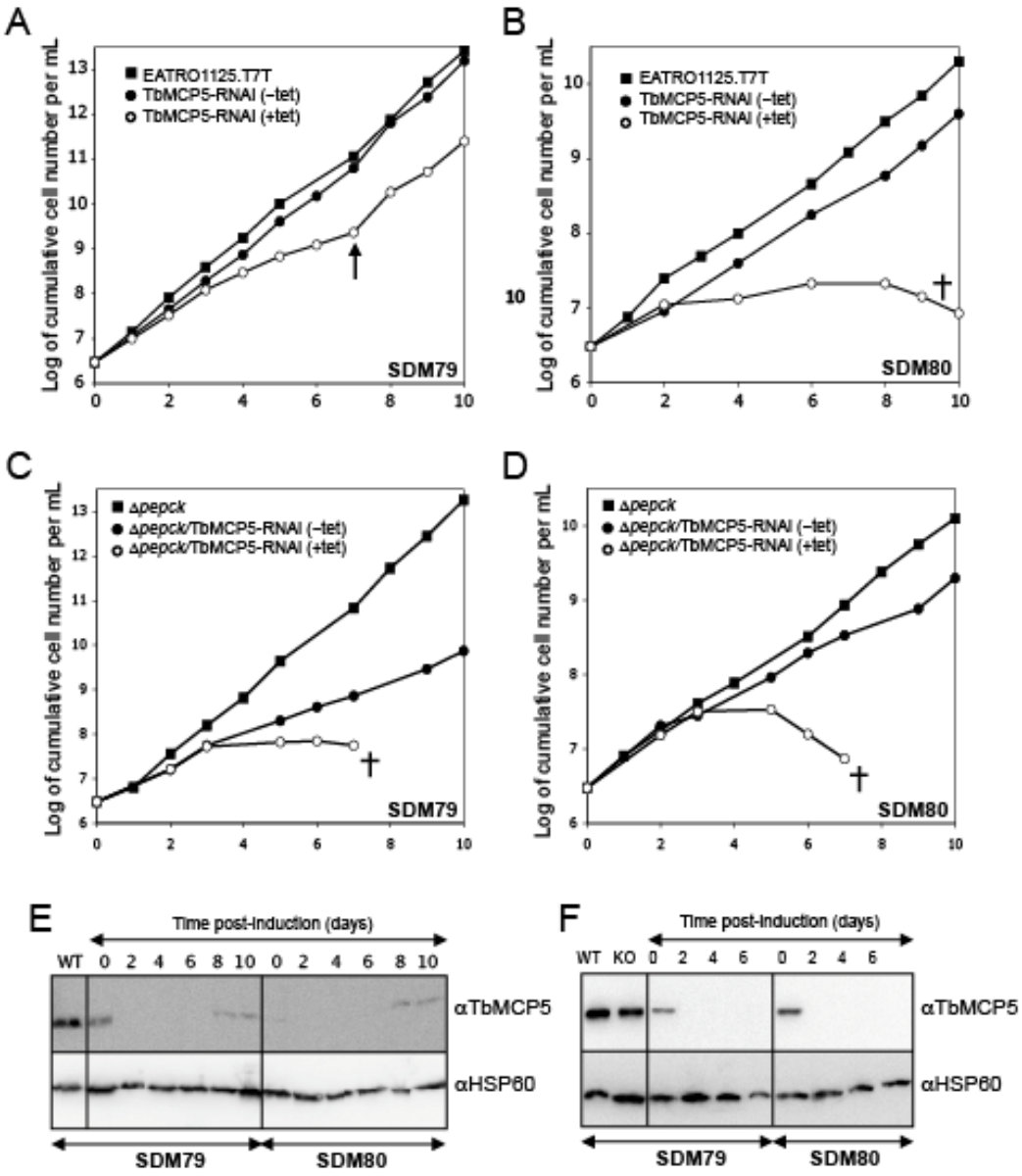

Figure 5: Growth phenotype analysis of *[RNAi]TbMCP5* and *Δpepck/[RNAi]TbMCP5* cell lines (adapted from Pena-Diaz et al., 2012). Growth curves of 'wildtype' EATRO1125.T7T (WT) and tetracyclic induced (+tet) and non-induced (-tet) *[RNAi]TbMCP5* cell lines cultured in glucose-rich SDM79 (A) and glucose-depleted SDM80 (B) culture medium. Trypanosome growth was kept exponential (between 10^6 and 10^7 cells.mL^{-1}) and the shown cumulative cell numbers include normalization for dilution during cultivation. The arrows indicate the estimated time of TbMCP5 re-expression. C. Western blot analysis of 'wildtype' (WT) EATRO1125.T7T and non-induced (0 days) and tetracycline induced (2-10 days) *[RNAi]TbMCP5* cell lines, using

αTbMCP5 and a polyclonal *T. brucei* HSP60 antibody (αHSP60, loading control). Each lane contained $2x10^6$ trypanosomes. D-F. Like A-C, but now with the Δ*pepck/*^{RNAi}*TbMCP5* cell line. The Δ*pepck* double knockout cell line is in panel F labeled as 'KO'.

3.7 TbMCP5-depletion eliminates mitochondrial ADP/ATP transport in *T. brucei*

Isolated *T. brucei* mitochondria were previously shown to produce ATP in a ΔΨ-dependent manner, and in the presence of ADP, free phosphate and suitable respiratory substrates such as succinate or α-ketoglutarate (Allemann and Schneider, 2000, Schneider et al., 2007). The efflux of mitochondrial ATP in exchange for cytosolic ADP is in all eukaryotes exclusively catalysed by ADP/ATP carriers (Klingenberg, 2008). A mitochondrial ATP production assay (Schneider et al., 2007) was used to determine whether TbMCP5 is fully or partially responsible for the mitochondrial ADP/ATP exchange in *T. brucei*. Mitochondrial ATP production was determined for the conditional Δ*TbMCP5/TbMCP5-nmyc*^{ti} cell line, grown for 72 h in the presence (TbMCP5-nmyc expression) or absence (no TbMCP5-nmyc expression) of tetracycline. Mitochondria isolated from 'wildtype' PCF trypanosomes were used as control. Comparison revealed a major reduction (>90%) in mitochondrial ATP production for the TbMCP5-nmyc depleted cell line at 72 h, when using succinate or α-ketoglutarate as mitochondrial substrates (Fig. 6A). Expression of TbMCP5-nmyc upon tetracycline addition restored the mitochondrial ATP production to 'wildtype' levels (Fig. 6A). These results indicated that TbMCP5 is responsible for the observed ADP/ATP-exchange activity in *T. brucei* mitochondria, and that the recombinant version of TbMCP5, here TbMCP5-nmyc, can functionally complement the lack of native TbMCP5. Addition of the specific ADP/ATP carrier inhibitor CATR

completely eliminated mitochondrial ATP production in all cell lines (Fig. 6A). This confirmed that in *T. brucei* the exchange of mitochondrial ATP for cytoplasmic ADP is exclusively facilitated by ADP/ATP-carrier activity. The observed ADP/ATP-exchange activity (<10%, Fig. 6A) in the non-induced Δ*TbMCP5/TbMCP5-nmyc*^{ti} cell line at 72 h is most probably catalysed by residual TbMCP5-nmyc protein **(**Fig. 4C, lower panel).

3.8 Depletion of TbMCP5 and its effect on the PCF energy metabolism

As demonstrated above, the contribution of TbMCP5 to the energy metabolism is particularly important for PCF trypanosomes grown with proline as their main substrate for ATP production. The effect of TbMCP5-depletion on the mitochondrial proline degradation pathway was analysed by quantifying the consumption of proline and the formation of succinate and acetate under glucose-depleted conditions. The results revealed that proline consumption is 2-fold decreased in the TbMCP5-depleted cell line, while succinate production is 8.7-fold increased, when compared to 'wildtype' trypanosomes (Fig. 6B). Interestingly, a similar reduction of proline consumption and increased succinate production was also observed when changing culture conditions for 'wildtype' PCF *T. brucei*, from a glucose-depleted (proline-only) SDM80 medium to a glucose-rich SDM79 medium (Lamour et al., 2005, Coustou et al., 2008). Indeed, the presence of glucose in the medium was shown to have an immediate effect on the proline metabolism (Lamour et al., 2005, Coustou et al., 2008). The substantial reduction in ADP/ATP-exchange activity in the TbMCP5-depleted cell line (>90%, see Fig. 6A) most probably leads to an aberrant mitochondrial ADP/ATP ratio, with a limited availability of ADP and the accumulation of ATP in the mitochondrial matrix. This in turn reduces the activity of

ADP-dependent enzymes, thereby causing ATP-dependent feedback inhibition of the electron transport chain and coupled oxidative phosphorylation. The increased production of the metabolic intermediate succinate would be the direct consequence of this inhibition.

In contrast to proline and succinate, no significant differences were found in the production of acetate when comparing 'wildtype' and TbMCP5-depleted trypanosomes (Fig. 6B). This result is in agreement with previously published data indicating that no or very low amounts of acetate are produced from proline, while the degradation of threonine is the main source of acetate production under glucose depleted-conditions (Coustou et al., 2003, Lamour et al., 2005). Acetate can be produced in the mitochondrion from threonine-derived acetyl-CoA via acetate:succinate CoA-transferase (ASCT) (Van Hellemond et al., 1998, Riviere et al., 2004) and by acetyl-CoA thioesterase (ACH) dependent pathways (Millerioux et al., 2012). An important difference between these pathways is that ASCT, forming the ASCT/SCoAS cycle in association with succinyl-CoA synthase (SCoAS), results in the production of ATP via substrate-level phosphorylation, whereas the ACH pathway does not lead to ATP production (61-63). Silencing of SCoAS expression by RNAi confirmed that acetate could be exclusively produced from threonine by ACH (63). This pathway does not result in ATP production and is thus not dependent on a functional mitochondrial ADP/ATP carrier. Our results are in agreement with this observation, since acetate production was apparently not affected by the depletion of the mitochondrial ADP/ATP carrier TbMCP5.

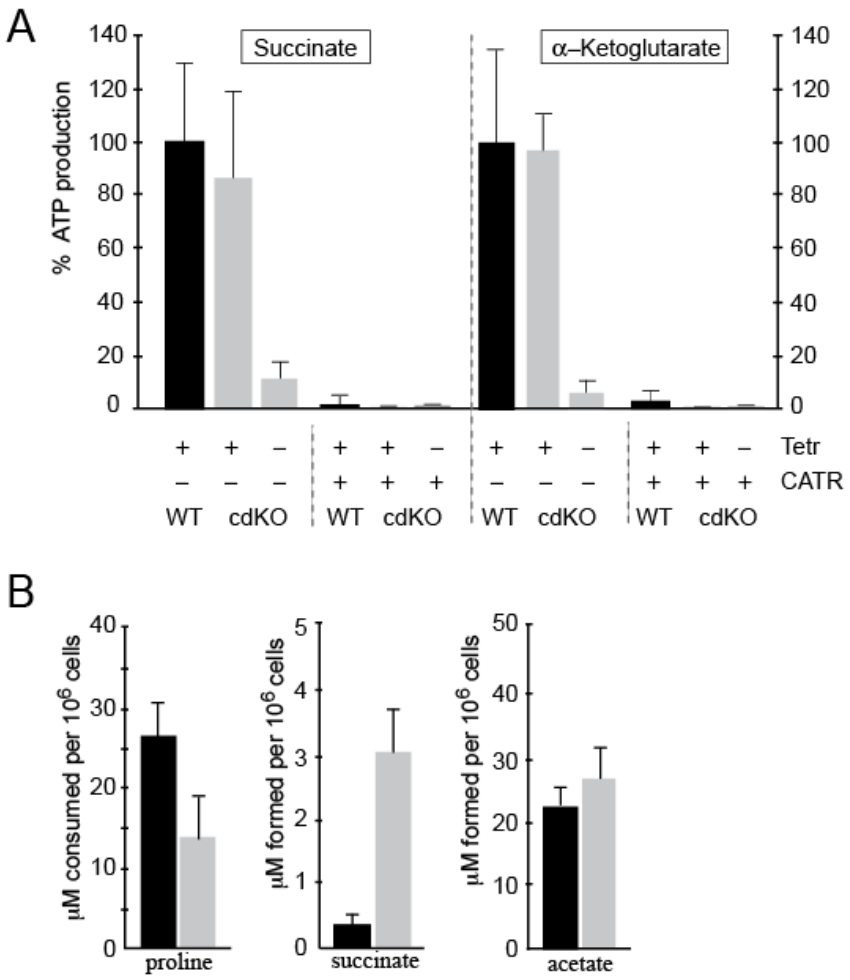

Figure 6: Mitochondrial ATP production (taken from Pena-Diaz et al., 2012). A. Intact mitochondria were isolated from 'wildtype' PCF *T. brucei* (WT), and from non-induced (-tet) and tetracycline-induced (+tet) Δ*TbMCP5/TbMCP5-nmyc*^{ti} (cdKO, conditional double knockout) trypanosomes at 72 h. Mitochondrial ATP production was initiated by addition of succinate (left panel) or α-ketoglutarate (right panel). ATP production in WT mitochondria from succinate or α-ketoglutarate was set to 100%. Mitochondrial ATP production (export) was completely inhibited by addition of carboxyatractyloside (CATR). Data shown are means of >3 independent experiments. B. Proline consumption and product formation (succinate, acetate) for 'wildtype' and non-induced Δ*TbMCP5/TbMCP5-nmyc*^{ti} (TbMCP5-depleted) PCF *T. brucei*, cultured in glucose-depleted SDM80 medium for 72 h. Black and grey bars represent substrate-consumption and product-formation values for 'wildtype' and TbMCP5-depleted trypanosomes, respectively. Data means are derived from >4 independent experiments.

4. Discussion

Comprehensive sequence analysis and functional complementation experiments in the *ANC*-deficient *S. cerevisiae* mutant *JL1*Δ*2*Δ*3u*$^-$ indicated that TbMCP5 functions as a mitochondrial ADP/ATP carrier. This was further reinforced by the results from the mitochondrial ATP-production assays, which revealed elimination of mitochondrial ADP/ATP-exchange activity in PCF *T. brucei* upon depletion of TbMCP5. Heterologous expression in *JL1*Δ*2*Δ*3u*$^-$ and mitochondrial transport assays revealed that the biochemical properties and ADP/ATP-exchange kinetics of TbMCP5 are similar to those of Anc2p, the prototypical ADP/ATP-carrier from *S. cerevisiae.* We therefore expected that both TbMCP5 and ScAnc2p would restore growth of *JL1*Δ*2*Δ*3u*$^-$ on YPL medium to the same extent. However, the functional complementation of *JL1*Δ*2*Δ*3u*$^-$ with TbMCP5 was found to be suboptimal, with *JL-TbMCP5* having a significantly higher doubling time than *JL*-ScANC2. The different B_{max}^{ATR} and V_{max} values (Table 1) obtained during the mitochondrial transport assays indicated that TbMCP5 was about 4-fold less abundant in yeast mitochondria than ScAnc2p, probably accounting for the reduced growth rate of *JL-TbMCP5*. Possible explanation could be the inefficient sorting of TbMCP5 to the yeast mitochondrion due to species-specific mitochondrial targeting signal requirements (van Wilpe et al., 1999). In particular the first 26 amino acid residues of ScAnc2p are important for efficient mitochondrial sorting in *S. cerevisiae* (Adrian et al., 1986, Hashimoto et al., 1999). Sequence comparison (see Fig. 1B) confirmed that TbMCP5 contains an N-terminal extension that is shorter and not homologous to the one from ScAnc2p. A more detailed molecular analysis of the sequences required for the specific mitochondrial targeting of TMCP5, and of *T. brucei* MCF proteins in general, is currently underway.

The higher abundance of TbMCP5 in PCF *T. brucei* argues for a more prominent role of the ADP/ATP carrier in this life cycle stage of the parasite. This is supported by the targeted gene replacement and RNAi studies, which confirmed that expression of TbMCP5 is indeed essential for growth and survival of PCF *T. brucei*, particularly when depending on proline for mitochondrial ATP production. This is exemplified by the stronger growth phenotype of the TbMCP5-depleted ^{RNAi}*TbMCP5* mutant in glucose-depleted medium. Indeed, the TbMCP5 mutant died under this culture condition although TbMCP5 is re-expressed before cell death, whereas in the presence of glucose re-expression of TbMCP5 immediately rescued growth (Fig. 5). This loss of expression control by the tetracycline inducible system upon RNAi-mediated silencing is common for *T. brucei*, especially if the target gene is essential for growth/survival of the parasite (Clayton, 1999). However, loss of expression control could not be observed when TbMCP5 is depleted on a *PEPCK* null background (Δ*pepck*/^{RNAi}*TbMCP5*), since the double mutant died (faster than the ^{RNAi}*TbMCP5* single mutant) before re-expression of TbMCP5 could occur. These differences between the ^{RNAi}*TbMCP5* and Δ*pepck*/^{RNAi}*TbMCP5* cell lines confirmed that the impact of TbMCP5 RNAi-mediated depletion on cell growth is more important when proline, instead of glucose, is the main carbon source for ATP production. It was previously shown that deletion of the *PEPCK* gene in the Δ*pepck* cell line strongly affects glycolysis, and leads to a metabolic shift toward proline catabolism (Ebikeme et al., 2010). This proline-dependency upon *PEPCK* deletion explains why the Δ*pepck*/^{RNAi}*TbMCP5* double mutant dies more rapidly regardless of the glucose concentration. The stronger growth phenotype observed for the Δ*pepck*/^{RNAi}*TbMCP5* cell line compared to the ^{RNAi}*TbMCP5* cell line in the SDM80 glucose-depleted medium may be due to the residual glucose (<0.15 mM) coming

from foetal calf serum, which could be used by the single mutant, but not by the double mutant for energy production and thus growth. The essential role of TbMCP5 during PCF growth under glucose-depleted conditions is obviously due to the exclusively mitochondrial production of ATP through proline and threonine degradation, the contribution of the latter being modest (Bringaud et al., 2006, Bringaud et al., 2012). Indeed, in the absence of glucose, these two amino acids become the major carbon sources and are metabolised in the mitochondrion (Lamour et al., 2005). Degradation of proline into alanine generates ATP by substrate level phosphorylation (via SCoAS) and several reduced cofactors, here NADH and $FADH_2$, which feed into the respiratory chain and may lead to an additional production of ATP by oxidative phosphorylation. Degradation of threonine into glycine and acetate generates ATP only via the ASCT/SCoAS cycle, in addition to NADH (Bringaud et al., 2006, Bringaud et al., 2010). The absence of significant ATP production in the cytosol needs to be overcome by exporting ATP from the mitochondria to supply energy for anabolic pathways in the cytosol and other compartments. As expected, TbMCP5 depletion strongly affects proline catabolism by provoking a reduction of its consumption rate as well as its conversion into succinate. This is certainly a consequence of ATP accumulation and ADP depletion inside the mitochondrion, which would considerably down-regulate this pathway. However, the rate of acetate production is not affected, suggesting that catabolism of threonine, the main source of acetate in glucose-depleted conditions, is functional without ATP production. Millerioux *et al*. (63) recently showed that acetate can be produced from acetyl-CoA by two enzymes, one involved in ATP production (ASCT) the other not (ACH) and proposed that this redundancy may be useful to modulate ATP production within this pathway. Here, we observed that when ATP production is

impaired, the acetate branch is still functional, which strengthens the essential role of acetate production in the procyclic trypanosomes (Riviere et al., 2009).

Two lines of evidences indicate that TbMCP5 is also essential for PCF trypanosomes grown under glucose-rich conditions: we did not succeed to delete both TbMCP5 alleles via a conventional double knockout approach, and depletion of TbMCP5 by RNAi leads to an important reduction of the growth rate until re-expression of the proteins after 7 days of induction (Fig. 5A). These results suggest that mitochondrial ADP/ATP-exchange is also required under glucose-rich conditions to provide the cytosol or the mitochondrion with ATP produced in the other compartment. However, both compartments have a high capacity to produce their own ATP in glucose-rich conditions, i.e. glycolysis provides cytosolic ATP by phosphoglycerate kinase and pyruvate kinase, while F_0/F_1-ATP synthase and the ASCT/SCoAS cycle are essential for ATP production in the mitochondrion, as demonstrated by the lethal phenotype induced by inactivation of the F_0/F_1-ATP synthase on a ASCT null background (Millerioux et al., 2012) or in 'wildtype' PCF *T. brucei* (Zikova et al., 2009). Further investigations are necessary to determine whether the cytosol or the mitochondrion requires additional ATP produced in the other subcellular compartment.

Western blot analysis revealed that in comparison to PCF *T. brucei,* substantially less but still a significant level of TbMCP5 is present in BSF trypanosomes. The current metabolic model of BSF trypanosomes excludes a role of the mitochondrion in the cellular provision of ATP (van Hellemond et al., 2005, Michels et al., 2006a). Instead, BSF trypanosomes rely exclusively on glycolysis with a concomitant net ATP-production in the cytosol of the parasite (Michels et al., 2006a, Gualdron-Lopez

et al., 2012). The BSF mitochondrion lacks a functional respiratory chain and key enzymes of the TCA cycle (Priest and Hajduk, 1994). Also its ATP-synthase level is reduced in comparison to PCF *T. brucei* (Brown et al., 2006), which argues for a less significant role of the BSF mitochondrion in cellular ATP provision. Depletion of the BSF F_1-ATPase α and β subunits by RNA interference revealed that this enzyme is essential and plays a critical role in the maintenance of the mitochondrial membrane potential in this life cycle stage (Brown et al., 2006). This in turn implies a mitochondrial requirement for ATP and the presence of a functional ADP/ATP carrier. An alternative role for TbMCP5 in BSF trypanosomes could be the import of cytosolic glycolysis-derived ATP into the mitochondrial matrix - such import would not only support the maintenance of the mitochondrial membrane potential, but would also provide energy for essential anabolic metabolism taking place in the mitochondrion (van Hellemond et al., 2005). The physiological role of TbMCP5 as a mitochondrial ADP/ATP-exchanger in BSF *T. brucei* is currently under investigation.

References

ADRIAN, G. S., MCCAMMON, M. T., MONTGOMERY, D. L. & DOUGLAS, M. G. 1986. Sequences required for delivery and localization of the ADP/ATP translocator to the mitochondrial inner membrane. *Molecular and cellular biology,* 6**,** 626-34.

ALLEMANN, N. & SCHNEIDER, A. 2000. ATP production in isolated mitochondria of procyclic *Trypanosoma brucei*. *Molecular and biochemical parasitology,* 111**,** 87-94.

BABOT, M., BLANCARD, C., PELOSI, L., LAUQUIN, G. J. & TREZEGUET, V. 2012. The transmembrane prolines of the mitochondrial ADP/ATP carrier are involved in nucleotide binding and transport and its biogenesis. *The Journal of biological chemistry,* 287**,** 10368-78.

BATES, C. J. 1977. Proline and hydroxyproline excretion and vitamin C status in elderly human subjects. *Clin Sci Mol Med,* 52**,** 535-43.

BELLOFATTO, V. & PALENCHAR, J. B. 2008. RNA interference as a genetic tool in trypanosomes. *Methods in molecular biology,* 442**,** 83-94.

BIEBINGER, S., WIRTZ, L. E., LORENZ, P. & CLAYTON, C. E. 1997. Vectors for inducible expression of toxic gene products in bloodstream and procyclic *Trypanosoma brucei*. *Mol. Biochem. Parasit.,* 85**,** 99-112.

BLOCK, M. R., LAUQUIN, G. J. & VIGNAIS, P. V. 1982. Interaction of 3'-O-(1-naphthoyl)adenosine 5'-diphosphate, a fluorescent adenosine 5'-diphosphate analogue, with the adenosine 5'-diphosphate/adenosine 5'-triphosphate carrier protein in the mitochondrial membrane. *Biochemistry,* 21**,** 5451-7.

BOCHUD-ALLEMANN, N. & SCHNEIDER, A. 2002. Mitochondrial substrate level phosphorylation is essential for growth of procyclic *Trypanosoma brucei. J Biol Chem,* 277**,** 32849-54.

BOULAY, F., BRANDOLIN, G., LAUQUIN, G. J. & VIGNAIS, P. V. 1983. Synthesis and properties of fluorescent derivatives of atractyloside as potential probes of the mitochondrial ADP/ATP carrier protein. *Analytical biochemistry,* 128**,** 323-30.

BRANDOLIN, G., LE SAUX, A., TREZEGUET, V., VIGNAIS, P. V. & LAUQUIN, G. J. 1993. Biochemical characterisation of the isolated Anc2

adenine nucleotide carrier from *Saccharomyces cerevisiae* mitochondria. *Biochemical and biophysical research communications,* 192**,** 143-50.

BRINGAUD, F., BARRETT, M. P. & ZILBERSTEIN, D. 2012. Multiple roles of proline transport and metabolism in trypanosomatids. *Frontiers in bioscience : a journal and virtual library,* 17**,** 349-74.

BRINGAUD, F., EBIKEME, C. & BOSHART, M. 2010. Acetate and succinate production in amoebae, helminths, diplomonads, trichomonads and trypanosomatids: common and diverse metabolic strategies used by parasitic lower eukaryotes. *Parasitology,* 137**,** 1315-31.

BRINGAUD, F., PEYRUCHAUD, S., BALTZ, D., GIROUD, C., SIMPSON, L. & BALTZ, T. 1995. Molecular characterization of the mitochondrial heat shock protein 60 gene from *Trypanosoma brucei. Molecular and biochemical parasitology,* 74**,** 119-23.

BRINGAUD, F., RIVIERE, L. & COUSTOU, V. 2006. Energy metabolism of trypanosomatids: adaptation to available carbon sources. *Molecular and biochemical parasitology,* 149**,** 1-9.

BRINGAUD, F., ROBINSON, D. R., BARRADEAU, S., BITEAU, N., BALTZ, D. & BALTZ, T. 2000. Characterization and disruption of a new *Trypanosoma brucei* repetitive flagellum protein, using double-stranded RNA inhibition. *Molecular and biochemical parasitology,* 111**,** 283-97.

BROWN, S. V., HOSKING, P., LI, J. & WILLIAMS, N. 2006. ATP synthase is responsible for maintaining mitochondrial membrane potential in bloodstream form *Trypanosoma brucei*. *Eukaryotic cell,* 5**,** 45-53.

BRUN, R. & SCHONENBERGER 1979. Cultivation and in vitro cloning or procyclic culture forms of *Trypanosoma brucei* in a semi-defined medium. Short communication. *Acta tropica,* 36**,** 289-92.

CHAUDHURI, M., OTT, R. D. & HILL, G. C. 2006. Trypanosome alternative oxidase: from molecule to function. *Trends Parasitol,* 22**,** 484-91.

CLAYTON, C. E. 1999. Genetic manipulation of Kinetoplastida. *Parasitol. Today,* 15**,** 372-378.

CLEMENCON, B., REY, M., DIANOUX, A. C., TREZEGUET, V., LAUQUIN, G. J., BRANDOLIN, G. & PELOSI, L. 2008. Structure-function relationships of the C-terminal end of the *Saccharomyces cerevisiae* ADP/ATP carrier isoform 2. *The Journal of biological chemistry,* 283**,** 11218-25.

CLEMENCON, B., REY, M., TREZEGUET, V., FOREST, E. & PELOSI, L. 2011. Yeast ADP/ATP carrier isoform 2: conformational dynamics and role of the RRRMMM signature sequence methionines. *The Journal of biological chemistry,* 286**,** 36119-31.

COLASANTE, C., ALIBU, V. P., KIRCHBERGER, S., TJADEN, J., CLAYTON, C. & VONCKEN, F. 2006. Characterization and developmentally regulated localization of the mitochondrial carrier protein homologue MCP6 from *Trypanosoma brucei. Eukaryot Cell,* 5**,** 1194-205.

COLASANTE, C., PENA DIAZ, P., CLAYTON, C. & VONCKEN, F. 2009. Mitochondrial carrier family inventory of *Trypanosoma brucei brucei:* Identification, expression and subcellular localisation. *Molecular and biochemical parasitology,* 167**,** 104-17.

COUSTOU, V., BESTEIRO, S., BIRAN, M., DIOLEZ, P., BOUCHAUD, V., VOISIN, P., MICHELS, P. A., CANIONI, P., BALTZ, T. & BRINGAUD, F. 2003. ATP generation in the *Trypanosoma brucei* procyclic form: cytosolic substrate level is essential, but not oxidative phosphorylation. *The Journal of biological chemistry,* 278**,** 49625-35.

COUSTOU, V., BESTEIRO, S., RIVIERE, L., BIRAN, M., BITEAU, N., FRANCONI, J. M., BOSHART, M., BALTZ, T. & BRINGAUD, F. 2005. A mitochondrial NADH-dependent fumarate reductase involved in the production of succinate excreted by procyclic *Trypanosoma brucei. The Journal of biological chemistry,* 280**,** 16559-70.

COUSTOU, V., BIRAN, M., BRETON, M., GUEGAN, F., RIVIERE, L., PLAZOLLES, N., NOLAN, D., BARRETT, M. P., FRANCONI, J. M. & BRINGAUD, F. 2008. Glucose-induced remodeling of intermediary and energy metabolism in procyclic *Trypanosoma brucei*. *The Journal of biological chemistry,* 283**,** 16342-54.

DAHOUT-GONZALEZ, C., NURY, H., TREZEGUET, V., LAUQUIN, G. J., PEBAY-PEYROULA, E. & BRANDOLIN, G. 2006. Molecular, functional, and pathological aspects of the mitochondrial ADP/ATP carrier. *Physiology,* 21**,** 242-9.

DASSA, E. P., DAHOUT-GONZALEZ, C., DIANOUX, A. C. & BRANDOLIN, G. 2005. Functional characterization and purification of a *Saccharomyces*

cerevisiae ADP/ATP carrier-iso 1 cytochrome c fusion protein. *Protein expression and purification,* 40**,** 358-69.

DASSA, E. P., PAUPE, V., GONCALVES, S. & RUSTIN, P. 2008. The mtDNA NARP mutation activates the actin-Nrf2 signaling of antioxidant defenses. *Biochemical and biophysical research communications,* 368**,** 620-4.

DAUM, G., BOHNI, P. C. & SCHATZ, G. 1982. Import of proteins into mitochondria. Cytochrome b2 and cytochrome c peroxidase are located in the intermembrane space of yeast mitochondria. *The Journal of biological chemistry,* 257**,** 13028-33.

DAVID, C., ARNOU, B., SANCHEZ, J. F., PELOSI, L., BRANDOLIN, G., LAUQUIN, G. J. & TREZEGUET, V. 2008. Two residues of a conserved aromatic ladder of the mitochondrial ADP/ATP carrier are crucial to nucleotide transport. *Biochemistry,* 47**,** 13223-31.

DE MARCOS LOUSA, C., TREZEGUET, V., DIANOUX, A. C., BRANDOLIN, G. & LAUQUIN, G. J. 2002. The human mitochondrial ADP/ATP carriers: kinetic properties and biogenesis of wild-type and mutant proteins in the yeast *S. cerevisiae*. *Biochemistry,* 41**,** 14412-20.

EBIKEME, C., HUBERT, J., BIRAN, M., GOUSPILLOU, G., MORAND, P., PLAZOLLES, N., GUEGAN, F., DIOLEZ, P., FRANCONI, J. M., PORTAIS, J. C. & BRINGAUD, F. 2010. Ablation of succinate production from glucose metabolism in the procyclic trypanosomes induces metabolic switches to the glycerol 3-phosphate/dihydroxyacetone phosphate shuttle and to proline metabolism. *The Journal of biological chemistry,* 285**,** 32312-24.

EMBLEY, T. M. & MARTIN, W. 2006. Eukaryotic evolution, changes and challenges. *Nature,* 440**,** 623-30.

GUALDRON-LOPEZ, M., BRENNAND, A., HANNAERT, V., QUINONES, W., CACERES, A. J., BRINGAUD, F., CONCEPCION, J. L. & MICHELS, P. A. 2012. When, how and why glycolysis became compartmentalised in the Kinetoplastea. A new look at an ancient organelle. *International journal for parasitology,* 42**,** 1-20.

HASHIMOTO, M., SHINOHARA, Y., MAJIMA, E., HATANAKA, T., YAMAZAKI, N. & TERADA, H. 1999. Expression of the bovine heart mitochondrial ADP/ATP carrier in yeast mitochondria: significantly enhanced expression by replacement of the N-terminal region of the bovine

carrier by the corresponding regions of the yeast carriers. *Biochimica et biophysica acta*, 1409**,** 113-24.

HIRUMI, H. & HIRUMI, K. 1989. Continuous cultivation of *Trypanosoma brucei* bloodstream forms in a medium containing a low concentration of serum protein without feeder cell layers. *J. Parasitol.*, 75**,** 985-9.

ITO, H., FUKUDA, Y., MURATA, K. & KIMURA, A. 1983. Transformation of intact yeast cells treated with alkali cations. *J Bacteriol*, 153**,** 163-8.

KLINGENBERG, M. 2008. The ADP and ATP transport in mitochondria and its carrier. *Biochim Biophys Acta*, 1778**,** 1978-2021.

KUNJI, E. R. & ROBINSON, A. J. 2006. The conserved substrate binding site of mitochondrial carriers. *Biochim Biophys Acta*, 1757**,** 1237-48.

LAMOUR, N., RIVIERE, L., COUSTOU, V., COOMBS, G. H., BARRETT, M. P. & BRINGAUD, F. 2005. Proline metabolism in procyclic *Trypanosoma brucei* is down-regulated in the presence of glucose. *The Journal of biological chemistry*, 280**,** 11902-10.

LE SAUX, A., ROUX, P., TREZEGUET, V., FIORE, C., SCHWIMMER, C., DIANOUX, A. C., VIGNAIS, P. V., BRANDOLIN, G. & LAUQUIN, G. J. 1996. Conformational changes of the yeast mitochondrial adenosine diphosphate/adenosine triphosphate carrier studied through its intrinsic fluorescence. 1. Tryptophanyl residues of the carrier can be mutated without impairing protein activity. *Biochemistry*, 35**,** 16116-24.

MICHELS, P. A., BRINGAUD, F., HERMAN, M. & HANNAERT, V. 2006a. Metabolic functions of glycosomes in trypanosomatids. *Biochimica et biophysica acta*, 1763**,** 1463-77.

MICHELS, P. A., BRINGAUD, F., HERMAN, M. & HANNAERT, V. 2006b. Metabolic functions of glycosomes in trypanosomatids. *Biochim Biophys Acta*, 1763**,** 1463-77.

MILLERIOUX, Y., MORAND, P., BIRAN, M., MAZET, M., MOREAU, P., WARGNIES, M., EBIKEME, C., DERAMCHIA, K., GALES, L., PORTAIS, J. C., BOSHART, M., FRANCONI, J. M. & BRINGAUD, F. 2012. ATP synthesis-coupled and -uncoupled acetate production from acetyl-CoA by mitochondrial acetate:succinate CoA-transferase and acetyl-CoA thioesterase in Trypanosoma. *The Journal of biological chemistry*, 287**,** 17186-97.

NURY, H., DAHOUT-GONZALEZ, C., TREZEGUET, V., LAUQUIN, G. J., BRANDOLIN, G. & PEBAY-PEYROULA, E. 2006. Relations between structure and function of the mitochondrial ADP/ATP carrier. *Annu Rev Biochem,* 75**,** 713-41.

PALMIERI, F., PIERRI, C. L., DE GRASSI, A., NUNES-NESI, A. & FERNIE, A. R. 2011. Evolution, structure and function of mitochondrial carriers: a review with new insights. *The Plant journal : for cell and molecular biology,* 66**,** 161-81.

PRIEST, J. W. & HAJDUK, S. L. 1994. Developmental regulation of mitochondrial biogenesis in *Trypanosoma brucei. Journal of bioenergetics and biomembranes,* 26**,** 179-91.

RIVIERE, L., MOREAU, P., ALLMANN, S., HAHN, M., BIRAN, M., PLAZOLLES, N., FRANCONI, J. M., BOSHART, M. & BRINGAUD, F. 2009. Acetate produced in the mitochondrion is the essential precursor for lipid biosynthesis in procyclic trypanosomes. *Proceedings of the National Academy of Sciences of the United States of America,* 106**,** 12694-9.

RIVIERE, L., VAN WEELDEN, S. W., GLASS, P., VEGH, P., COUSTOU, V., BIRAN, M., VAN HELLEMOND, J. J., BRINGAUD, F., TIELENS, A. G. & BOSHART, M. 2004. Acetyl:succinate CoA-transferase in procyclic *Trypanosoma brucei.* Gene identification and role in carbohydrate metabolism. *The Journal of biological chemistry,* 279**,** 45337-46.

ROUX, P., LE SAUX, A., FIORE, C., SCHWIMMER, C., DIANOUX, A. C., TREZEGUET, V., VIGNAIS, P. V., LAUQUIN, G. J. & BRANDOLIN, G. 1996. Fluorometric titration of the mitochondrial ADP/ATP carrier protein in muscle homogenate with atractyloside derivatives. *Analytical biochemistry,* 234**,** 31-7.

SAMBROOK J, F. E., AND MANIATIS T. 1989. *Molecular cloning: A Laboratory Manual,* Cold Spring Harbour, New York, Cold Spring Harbour Laboratory.

SCHNEIDER, A., BOUZAIDI-TIALI, N., CHANEZ, A. L. & BULLIARD, L. 2007. ATP production in isolated mitochondria of procyclic *Trypanosoma brucei. Methods Mol Biol,* 372**,** 379-87.

TREZEGUET, V., PELOSI, L., LAUQUIN, G. J. & BRANDOLIN, G. 2008. The mitochondrial ADP/ATP carrier: functional and structural studies in the route

of elucidating pathophysiological aspects. *Journal of bioenergetics and biomembranes,* 40**,** 435-43.

VAN HELLEMOND, J. J., OPPERDOES, F. R. & TIELENS, A. G. 1998. Trypanosomatidae produce acetate via a mitochondrial acetate:succinate CoA transferase. *Proceedings of the National Academy of Sciences of the United States of America,* 95**,** 3036-41.

VAN HELLEMOND, J. J., OPPERDOES, F. R. & TIELENS, A. G. 2005. The extraordinary mitochondrion and unusual citric acid cycle in *Trypanosoma brucei. Biochem Soc Trans,* 33**,** 967-71.

VAN WEELDEN, S. W., FAST, B., VOGT, A., VAN DER MEER, P., SAAS, J., VAN HELLEMOND, J. J., TIELENS, A. G. & BOSHART, M. 2003. Procyclic *Trypanosoma brucei* do not use Krebs cycle activity for energy generation. *The Journal of biological chemistry,* 278**,** 12854-63.

VAN WILPE, S., BOUMANS, H., LOBO-HAJDU, G., GRIVELL, L. A. & BERDEN, J. A. 1999. Functional complementation analysis of yeast bc1 mutants. A study of the mitochondrial import of heterologous and hybrid proteins. *European journal of biochemistry / FEBS,* 264**,** 825-32.

VASSELLA, E., STRAESSER, K. & BOSHART, M. 1997. A mitochondrion-specific dye for multicolour fluorescent imaging of *Trypanosoma brucei. Molecular and biochemical parasitology,* 90**,** 381-5.

VONCKEN, F., VAN HELLEMOND, J. J., PFISTERER, I., MAIER, A., HILLMER, S. & CLAYTON, C. 2003. Depletion of GIM5 causes cellular fragility, a decreased glycosome number, and reduced levels of ether-linked phospholipids in trypanosomes. *J Biol Chem,* 278**,** 35299-310.

WIRTZ, E., LEAL, S., OCHATT, C. & CROSS, G. A. 1999. A tightly regulated inducible expression system for conditional gene knock-outs and dominant-negative genetics in *Trypanosoma brucei. Molecular and biochemical parasitology,* 99**,** 89-101.

ZIKOVA, A., SCHNAUFER, A., DALLEY, R. A., PANIGRAHI, A. K. & STUART, K. D. 2009. The F(0)F(1)-ATP synthase complex contains novel subunits and is essential for procyclic *Trypanosoma brucei. PLoS pathogens,* 5**,** e1000436.

Chapter III

The mitochondrial phosphate carrier TbMCP11 is essential for growth of the procyclic form of *Trypanosoma brucei.*

All the work presented in this chapter is my own independent contribution.

1. Introduction

The mitochondrion compartmentalises a large number of important cellular processes (Palade, 1952, Ernster and Schatz, 1981). Its best-known function is the provision of the eukaryotic cell with ATP (Kennedy and Lehninger, 1949, Schneider et al., 2007). Mitochondria are further involved in the biosynthesis of complex biological compounds, and the regulation of cell signalling, differentiation, growth, differentiation and apoptosis (McBride et al., 2006). The kinetoplastid *Trypanosoma brucei* is one of the earliest eukaryotes branching in evolution, possesing a true mitochondrion (Embley and Martin, 2006, Barrett et al., 2007). Its subspecies *T. b. rhodesiense* and *T. b. gambiense* cause sleeping sickness in sub-saharan Africa, an invariably lethal disease when left untreated (WHO).

T. brucei has a complex digenetic life cycle and alternates between the bloodstream form in the mammalian host and the procyclic form in the insect vector, the tsetse fly (Matthews et al., 2004). The bloodstream form lacks mitochondrial ATP production and relies exclusively on the glycolytic degradation of glucose for its cellular ATP provision (Michels et al., 2006, Bringaud et al., 2006). This in contrast to the procyclic form, which is mainly dependent on the mitochondrial degradation of amino acids such as proline, and the concomitant production of ATP via substrate-level and oxidative phosphorylation (Bringaud et al., 2012, Bochud-Allemann and Schneider, 2002, Lamour et al., 2005).

Protein mass spectrometry indicated the presence of up to 1000 proteins in the procyclic form of the *T. brucei* mitochondrion, with most of them having a function in respiration, electron transport, mRNA editing, nucleic acid and amino acid metabolism, DNA and protein processing, lipid and TCA metabolism (Panigrahi et

al., 2008, Panigrahi et al., 2009). Maintenance of a functional mitochondrion requires the transport of metabolites, cofactors and nucleotides across the 'impermeable' mitochondrial inner membrane. Mitochondrial Carrier Family (MCF) proteins facilitate this exchange and form an indispensible metabolic link between the mitochondrion and the cytoplasm, thereby exerting flux control on virtually all mitochondrial pathways (Kunji, 2004, Colasante et al., 2009, Palmieri et al., 2011). In particular the ATP/ADP carrier and the phosphate carrier play a key role in mitochondrial ATP synthesis (Pena-Diaz et al., 2012, Kramer, 1996, Stappen and Kramer, 1993, Knirsch et al., 1989). The mitochondrial ATP/ADP carrier exchanges ATP produced in the mitochondrial matrix for cytosolic ADP, while the phosphate carrier replenishes the consumed intramitochondrial Pi (Knirsch et al., 1989, Stappen and Kramer, 1993). Both ADP and Pi are essential substrates for steady state oxidative phosphorylation and their supply from the cytosol to the mitochondrial matrix may be a rate-limiting step (see (Brown, 1992) and references therein). Mitochondrial ATP production is further dependent on the proton motive force (pmf), which is generated across the mitochondrial inner membrane by the proton-pumping activities of the respiratory complexes I, III and IV, and is driving F_1F_0-ATP synthase activity (Brown, 1992). The mitochondrial F_1F_0-ATP synthase of *T. brucei* has been functionally characterised and was shown to be dependent on the mitochondrial membrane potential for its function (Brown et al., 2006, Zikova et al., 2009). Its activity is essential for mitochondrial ATP synthesis in procyclic form *T. brucei* (Zikova et al., 2009), as well as the maintenance of the membrane potential in the bloodstream form mitochondrion (Brown et al., 2006).

We previously identified 24 different genes coding for MCF proteins in *T. brucei* (Colasante et al., 2009). Amongst these we identified one potential ADP/ATP carrier

coding gene, i.e. TbMCP5, and two potential phosphate carrier coding genes, namely TbMCP8 and TbMCP11 (Colasante et al., 2009). Functional analysis of TbMCP5 confirmed that this MCF protein indeed represents the only mitochondrial ADP/ATP carrier in *T. brucei* (Pena-Diaz et al., 2012). Its ADP/ATP exchange activity is essential for mitochondrial ATP production and export, as well as parasite survival (Pena-Diaz et al., 2012). In this chapter, we functionally characterised the putative phosphate carrier TbMCP11, and assessed its importance for the energy metabolism of bloodstream form and procyclic form *T. brucei*.

2. Material and Methods

2.1 Cell culture and transfection

Procyclic form (PCF) and bloodstream form (BSF) *Trypanosoma brucei* strain 449 were cultured in respectively MEM-PROS medium (Overath et al., 1986) and HMI-9 medium (Hirumi and Hirumi, 1989), and in the presence of phleomycin (5 μg ml^{-1}) to maintain expression of the tetracycline (tet) repressor from plasmid pHD449 (*TETR BLE*). The PCF *T. brucei* cell line EATRO1125.T7T was cultured in semi-defined medium (SDM-79) (Brun and Schonenberger, 1979), and in the presence of 10 μg ml^{-1} G418 and 25 μg ml^{-1} hygromycin to maintain expression of the tetracycline repressor and T7 RNA polymerase from plasmids pLew90/Neo and pHD328, respectively (Bringaud et al., 2000). All media were supplemented with 10% v/v foetal calf serum (Sigma-Aldrich) to support trypanosome growth.

2.2 Phylogenetic reconstruction and sequence analysis

Multiple sequence alignments were generated using ClustalW2 (Chenna et al., 2003) and manually optimized using the Sequence Alignment Editor (SE-AL v2.0a11) software. Phylogenetic trees were constructed using PHYLIP v3.67: pairwise

sequence distance matrices were calculated with Protdist (Dayhoff and Orcutt, 1979) and unrooted trees generated using the neighbor-joining method (Saitou and Nei, 1987). The final phylogenetic tree was drawn with SplitsTree4 v.4.8 (Huson, 1998). The statistical relevance was assessed by bootstrap re-sampling analysis (PHYLIP, SEQBOOT) generating 1000 reiterated data sets, with bootstrap values expressed as percentage for each node. Only bootstrap values above 50% are shown. The Genebank and GeneDB accession numbers for the different protein sequences used for the sequence alignment and phylogenetic reconstruction are XP_827321.1, Tb927.9.10310, TbMCP11 mitochondrial carrier protein [*Trypanosoma brucei TREU927*]; XP_823265.1, Tb927.10.10440, TbMCP8 mitochondrial carrier protein [*Trypanosoma brucei TREU927*]; NP_012611, Mir1p [*Saccharomyces cerevisiae S288c*]; NP_002626.1, phosphate carrier protein, mitochondrial isoform b precursor [*Homo sapiens*]; NP_777082, phosphate carrier protein, mitochondrial precursor [*Bos taurus*]; NP_620800, phosphate carrier protein, mitochondrial precursor [*Rattus norvegicus*]; NP_001076672, hypothetical protein F01G4.6 [*Caenorhabditis elegans*]; NP_598429.1, phosphate carrier protein, mitochondrial precursor [*Mus musculus*]; O61703.1, mitochondrial phosphate carrier protein [*Choristoneura fumiferana*]; CCC92988.1, putative mitochondrial phosphate transporter [*Trypanosoma congolense*]; EFZ26338.1, mitochondrial phosphate transporter, putative [*Trypanosoma cruzi*]; XP_001469252.1, putative mitochondrial phosphate transporter [*Leishmania infantum JPCM5*]; EGD81797.1, phosphate carrier protein [S*alpingoeca rosetta ATCC 50818*]; CBZ56276.1, mitochondrial phosphate carrier protein, related [*Neospora caninum Liverpool*]; XP_002370602.1, phosphate carrier protein, putative [*Toxoplasma gondii ME49*]; XP_766621.1, mitochondrial phosphate carrier [*Theileria parva strain Muguga*]; XP_001350431.1, mitochondrial phosphate

carrier protein [*Plasmodium falciparum 3D7*]; XP_001609505.1, mitochondrial phosphate transporter [*Babesia bovis T2Bo*]; XP_001703470.1, mitochondrial phosphate carrier 1, minor isoform [C*hlamydomonas reinhardtii*]; XP_002946967.1, mitochondrial phosphate carrier 1 [*Volvox carteri f. nagariensis*]; AAL66293.1, phosphate transporter [*Glycine max*]; XP_002318765.1, mitochondrial phosphate carrier protein [*Populus trichocarpa*]; NP_001104842.1, mitochondrial phosphate transporter [*Zea mays*]; ABW74474.1, mitochondrial phosphate transporter [*Paeonia suffruticosa*]; NP_001057115.1, Os06g0210500 [*Oryza sativa Japonica Group*]; XP_002511108.1, mitochondrial phosphate carrier protein, putative [*Ricinus communis*]; XP_001744152.1, hypothetical protein [*Monosiga brevicollis MX1*]; CAH59632.1, mitochondrial phosphate translocator [*Medicago truncatula*]; XP_002873645.1, mitochondrial phosphate transporter [*Arabidopsis lyrata subsp. lyrata*]; BAB83689.1, mitochondrial phosphate transporter [*Lotus japonicus*]; CAA69726.1, mitochondrial phosphate translocator [*Betula pendula*]; AAI49997.1, SLC25A3 protein [*Bos taurus*]; NP_001126257.1, phosphate carrier protein, mitochondrial precursor [*Pongo abelii*]; XP_001661491.1, mitochondrial phosphate carrier protein [*Aedes aegypti*]; XP_001459326.1, hypothetical protein [*Paramecium tetraurelia strain d4-2*]; NP_524069.2, mitochondrial phosphate carrier protein, isoform A [*Drosophila melanogaster*]; XP_001559432.1, mitochondrial phosphate carrier protein [*Botryotinia fuckeliana B05.10*]; XP_001598707.1, mitochondrial phosphate carrier protein [*Sclerotinia sclerotiorum 1980*]; XP_002579471.1, mitochondrial phosphate carrier protein [*Schistosoma mansoni*]; XP_002622090.1, mitochondrial phosphate carrier protein [*Ajellomyces dermatitidis SLH14081*]; XP_001818148.1, phosphate carrier protein 2 [*Aspergillus oryzae RIB40*]; ACN10336.1, phosphate carrier protein, mitochondrial precursor [*Salmo salar*];

ADD20494.1, mitochondrial phosphate carrier protein [*Glossina morsitans morsitans*]; ACO12540.1, phosphate carrier protein, mitochondrial precursor [*Lepeophtheirus salmonis*]; ACY69956.1, mitochondrial phosphate carrier protein [*Cimex lectularius*]; EFN66191.1, phosphate carrier protein, mitochondrial [*Camponotus floridanus*]; ACO09144.1, phosphate carrier protein, mitochondrial precursor [*Osmerus mordax*]; CAB61741.1, mitochondrial phosphate transporter [*Cicer arietinum*].

2.3 Northern blot analysis

Total RNA was isolated from BSF and PCF *T. brucei* strain 449 using TriFast (PeqLab Biotechnology GmbH). Northern blot analysis was performed as described by Sambrook (Sambrook J, 1989). The complete open reading frame of *TbMCP11* (Tb927.9.10310) was labelled with [^{32}P]dCTP using PCR, and 5'-ggacggaagcttaccatgagcgcaaagaacaaaact-3' (sense) and 5'-gcttgcaggatccatacttctttccggaaccaccac-3' (antisense) as primers. Blots were pre-hybridized in hybridization solution (5xSSC, 5x Denhardt´s reagent and 0.5% w/v SDS) for 1 h at 65 °C, after which the [^{32}P]dCTP-labelled DNA probe was added. Following overnight hybridization at 65 °C, the blots were washed in subsequently 1xSSC, 0.1% w/v SDS and 0.1xSSC, 0.1% w/v SDS, followed by exposure to X-ray film (Kodak).

2.4 TbMCP11 polyclonal rabbit antibody and Western blot analysis

Peptide synthesis and immunisation were performed by EZBiolab (USA). The peptide 'KNKTWDARYANPD' (N-terminal amino acids 4-16 of TbMCP11) was coupled to keyhole limpet hemocyanin (KLH) and used for the immunization of two rabbits. Immunisation was initiated by injection with 1.0 mg KLH-coupled peptide emulsified in complete Freund's adjuvant, followed by 3 subsequent boosts in weeks

2, 4 and 7, with 0.5 mg of KLH-coupled peptide emulsified in incomplete Freund's adjuvant. The polyclonal antisera were collected in week 9 after determination of the TbMCP11 antibody titer, which was about 1:1,500,000 for both rabbits (EZBiolab, USA). 2×10^6 trypanosomes were used per lane for SDS-PAGE (12% gel) and western blot analysis. Western blot analysis using the pre-immune sera confirmed the absence of cross-reacting protein bands (not shown), whereas the final TbMCP11 antiserum (1:5,000 dilution) stained a single 34 kDa protein band as expected for TbMCP11 (see results).

2.5 *T. brucei* cell lines expressing recombinant myc-tagged TbMCP11

The open reading frame (ORF) of *TbMCP11* (Tb927.9.10310) was PCR-amplified using 5'-ggacggaagcttaccatgagcgcaaagaacaaaact-3' (sense) and 5'-gcttgcaggatccatacttctttccggaaccaccac-3' (antisense) as primers, and isolated genomic DNA from *T. brucei* strain 449 as template. The added *Hind*III and *Bam*HI restriction enzyme sites (underlined) were used for subsequent cloning into the *T. brucei* expression vectors pHD1700 and pHD1701 (Colasante et al., 2009). Comparison of the cloned *TbMCP11* sequence from *T. brucei* strain 449 to the corresponding sequence from *T. brucei* strain 927 (http://www.genedb.org) revealed only a few sequence differences at the DNA level, but none in the predicted amino acid sequence. Tetracycline-inducible expression from pHD1700 and pHD1701 will result in the addition of a 2x-myc tag to either the C-terminal (pHD1700) or N-terminal (pHD1701) end of TbMCP11. BSF and PCF *T. brucei* strains 449 were transfected and hygromycin-resistant (50 μg mL^{-1} for PCF and 10 μg mL^{-1} for BSF) clones were isolated as described previously (Biebinger et al., 1997, Colasante et al., 2006). The genotype of the resulting cell lines is *TbMCP11*/*TbMCP11 TETR BLE TbMCP11-myc^{ti} HYG*, further referred to as PCF *TbMCP11-myc^{ti}* or BSF *TbMCP11-myc^{ti}*,

depending on the parental cell lines used. Expression of N-terminal (nmyc) or C-terminal (cmyc) myc-tagged TbMCP11 was induced by the addition of tetracycline (0.5 μg mL^{-1}) and assessed by western blotting analysis using a commercial myc-tag antibody (Roche Applied Science).

2.6 Immunofluorescence microscopy

Trypanosomes were collected from culture medium by centrifugation at 2,000x g, and immediately resuspended in phosphate-buffered saline (PBS) containing 4% w/v paraformaldehyde. Cells were fixed for 20 min at room temperature and allowed to settle down and attach to poly-L-lysine-coated microscope slides. Staining with 4',6'-diamidino-2-phenylindole (DAPI), the mitochondrion-specific probe MitoTracker, and the different antibodies (see Fig. Legends) was performed as described previously (Voncken et al., 2003). Cells were examined using a Leica DM RXA digital deconvolution microscope, and images were taken with a Hamamatsu digital camera.

2.7 Generation of the BSF Δ*TbMCP11* double knockout cell line

The BSF double-knockout cell line ΔTbMCP11::NEO/ΔTbMCP11::BSD (abbreviated to BSF ΔTbMCP11) was generated using the 'targeted gene replacement' approach (Eid and Sollner-Webb, 1991, Voncken et al., 2003, Colasante et al., 2006). The 5'- and 3'-UTRs of TbMCP11 (Tb927.9.10310) were inserted on either side of NEO (G418) or BSD (blasticidin) antibiotic resistance cassettes bearing actin 5'-splice sites and the actin 3'-untranslated region (Voncken et al., 2003, Colasante et al., 2006). The different TbMCP11 UTRs were obtained by PCR from isolated *T. brucei* genomic DNA: the primers 5'-gttgagctcggttggtgtgatatcgtatggtgtgtttc-3' (sense) and 5'-caaactagtgtattgatattggactcgtatgtggc-3' (antisense) were used for the amplification of

the 631 bp 5'-UTR, and the primers 5'-gaggatccgataacatgtaaggaggatgaacgggtgacgg-3' (sense) and 5'-ctgggcccgagatccctccacctcacactctacaatgac-3' (antisense) for the 385 bp 3'-UTR. The underlined restriction enzyme sites were used for subsequent cloning in the different NEO- and BSD-containing knockout (KO) plasmids (Voncken et al., 2003, Colasante et al., 2006). After transfection of BSF *T. brucei* strain 449 with the NEO-TbMCP11-KO construct and clonal selection with 2 µg.mL–1 G418, the half-knockout cell line ΔTbMCP11::NEO/TbMCP11 was isolated. The double-knockout cell line ΔTbMCP11::NEO/ ΔTbMCP11::BSD (BSF ΔTbMCP11) was obtained after subsequent transfection with the BSD-TbMCP11-KO plasmid, followed by clonal selection with 2 µg.ml-1 G418 and 20 µg. ml-1 blasticidin. Correct integration of the different NEO/BSD-TbMCP11-KO constructs and deletion of the two native TbMCP11 genes was confirmed by RT-PCR, as well as by southern blot and western blot analysis for the TbMCP11 gene product (Fig. 5).

2.8 Generation of the PCF *TbMCP11-RNAi* cell line

Expression of *TbMCP11* was silenced in PCF *T. brucei* by using RNA-interference (RNAi) (Bellofatto and Palenchar, 2008). The required sense and antisense sequences of *TbMCP11* were PCR-amplified and cloned into the *T. brucei* expression vector *pLew100* (Wirtz et al., 1999). The primers 5'-ggaagcttaaacttgggacgcacgttac-3' and 5'-cactcgaggcatggtggcaactgcagctc-3' were used for amplification of the 494 bp sense sequence, and the primers 5'-caggatccaaacttgggacgcacgttac-3' and 5'-cgaagctttccctcgagaacttcgccattgtgtaggg-3' were used for the 576 bp antisense sequence. The added restriction enzyme sites (underlined) were used for cloning. The resulting *pLew100-TbMCP11* RNAi construct harbors a phleomycin resistance gene, and contains the consecutively cloned sense and antisense *TbMCP11* target sequences separated by a 80 bp spacer fragment. Inducible expression is under control of the

procyclic acidic repetitive protein (PARP) promoter linked to a prokaryotic tetracycline (tet) operator (Wirtz et al., 1999). The *pLew100-TbMCP11* RNAi construct was used for transfection of the PCF *T. brucei* EATRO1125.T7T cell line (Wirtz et al., 1999). The PCF *TbMCP11-RNAi* cell line was obtained after clonal selection in standard SDM79 medium supplemented with phleomycin (50 $\mu g.ml^{-1}$). This cell line enables tetracycline-inducible (0.5 $\mu g\ ml^{-1}$) depletion of TbMCP11. Silencing of *TbMCP11* expression upon tetracycline induction was confirmed by RT-PCR as well as by western blot analysis using the raised TbMCP11 peptide antibody.

2.9 Growth analysis

At the start of each growth experiment, cell cultures of BSF Δ*TbMCP11* and PCF *TbMCP11-RNAi*, and the corresponding parental cell lines BSF 449 and PCF EATRO1125.T7T, were diluted to cell densities of 0.25×10^6 cells ml^{-1} (BSF) and 0.1×10^6 cells ml^{-1} (PCF), respectively. Cell densities (cells ml^{-1}) were determined every 24 hours using a Neubauer haemocytometer. BSF 449 and BSF Δ*TbMCP11* trypanosomes were continuously cultured for 72 h, while PCF EATRO1125.T7T and PCF *TbMCP11-RNAi* trypanosomes were cultured for 9 days, with subculturing into fresh medium at 48 h intervals. For the induced PCF *TbMCP11-RNAi* cell line, tetracycline was added to the culture medium (0.5 $\mu g\ ml^{-1}$) at the start of the experiment and every 48 h interval, to maintain RNA interference.

2.10 Mitochondrial ATP production assay

The mitochondrial ATP production assay was performed as described by Schneider *et al*. (Schneider et al., 2007). For each assay, $1x10^8$ trypanosomes were collected by centrifugation at 1500x g for 10 min, washed once with SoTE-buffer (20 mM Tris-HCl pH 7.5, 2 mM EDTA, 0.6 M Sorbitol), and finally resuspended in 1 ml of SoTE-buffer containing 0.008% w/v digitonin for PCF and 0.022% w/v digitonin for BSF

trypanosomes. Permeabilisation with digitonin was allowed to take place for exactly 5 minutes on ice, followed by immediate centrifugation for 3 minutes at 8000x g at 4 °C. The supernatant was removed and the pellet washed twice with 1 ml SoTE-buffer. The pellet, representing the mitochondria-enriched fraction, was resuspended in 0.5 ml of Assay Buffer (20 mM Tris-HCl pH 7.4, 15 mM KH_2PO_4, 0.6 M sorbitol, 5 mM $MgSO_4$). Mitochondrial ATP production was initiated by the addition 75 µl of Assay Buffer, containing 67 µM ADP and 5 mM substrate (succinate or α-ketoglutarate), to the mitochondria-enriched fraction. The inhibitors carboxyatractyloside (CATR) and azide were added to a final concentration of 5.2 µM and 6.8 mM, respectively, and incubated for 15 min at 30 °C prior to the addition of the substrates. Mitochondrial ATP production was initiated by the addition of substrate and was allowed to take place for 30 min at 30 °C. The reaction was terminated by the addition of 10 µl TE (10 mM Tris-HCl, 1 mM EDTA, pH 8.0), followed by denaturation at 100 °C for 3 min. Formed protein precipitate was removed by centrifugation for 1 min at 1,000x g. The ATP concentration in the supernatant was measured according to the protocol of the ATP Bioluminescence Assay Kit CLS II kit (Roche Applied Science) and using a Junior LB9509 tube luminometer (Berthold Technologies).

2.11 Mitochondrial oxygen consumption

Mitochondrial oxygen consumption was measured at 30 °C using a closed Clark-type oxygen electrode (Bienen et al., 1993), and mitochondria-enriched fractions from 2×10^8 PCF EATRO1125.T7T and tetracycline-induced PCF *TbMCP11-RNAi* trypanosomes. The assay buffer (20 mM Tris-HCl pH 7.4, 15 mM KH_2PO_4, 0.6 M sorbitol, 5 mM $MgSO_4$) was supplemented with salicylhydroxamic acid (SHAM, 2.5mM) to inhibit mitochondrial alternative oxidase (TAO) activity (Chaudhuri et al., 2006). After 15 min of baseline stabilization, oxygen consumption was initiated by

the addition of 5 mM succinate. Oxygen consumption was further analysed in the presence of different inhibitors, i.e. azide (6.8 mM), carbonyl cyanide m-chlorophenyl hydrazone (CCCP, 1 mM) and N-ethylmaleimide (NEM, 1.5 mM).

2.12 Scanning electron microscopy (SEM)

Trypanosomes were fixed with 2.5% w/v glutaraldehyde in 0.1 M cacodylate buffer (pH 7.2) and allowed to settle for 15 min onto glass cover slips coated with 0.1% w/v poly-L-lysine. The cover slips were extensively washed with 0.1 M cacodylate buffer (pH 7.2), and post-fixed for 30 min with 1% w/v osmium tetroxide in the same buffer. The trypanosomes were dehydrated in acetone, critical point dried, mounted onto SEM stubs, and coated with an approximately 20 nm thick gold layer. The cells were examined and digital images taken using a Zeiss DSM940 scanning electron microscopy.

2.13 Yeast complementation

The open reading frame of *TbMCP11* was PCR-amplified using 5'-tacgagctcatgagcgcaaagaacaaaa cttgggac-3' (sense) and 5'-gcttgcaggatcc ttacttctttccggaaccaccacttgtg-3' (antisense) as primers. The *TbMCP11-PIC2*^{nterm} fusion gene was generated by PCR-amplification using the sense primer 5'-gggagctcatggagtccaataaacaaccacgtaaaatccaattatatacgaaagagttttatctgaaatgcataggtgggg-3' and the *TbMCP11* antisense primer 5'-ctaggatcc ttacttctttccggaaccaccacttgtg-3'. The sense primer is chimeric and contains nt 1-51 of the *S.cerevisiae PIC2* ORF, followed by nt 70-91 of the *TbMCP11* ORF. This PCR approach will replace the first 69 nucleotides (coding for the first 23 amino acids) of *TbMCP11* with the first 51 nucleotides (coding for the first 17 amino acids) of *PIC2* (see Fig. 1). The included *Sac*I and *Bam*HI restriction enzyme sites (underlined) were used for subsequent cloning into the yeast multicopy (2μ) shuttle vector *pYPGK18*, containing a

phosphoglycerol kinase *PGK1* promoter and *LEU2* (Swiegers et al., 2002, Vaz et al., 2003). The *Saccharomyces cerevisiae* BY4741 reference strain (Euroscarf) and phosphate carrier-deficient deletion strain Δ*mir1*Δ*pic2* (Hamel et al., 2004) were maintained on YPD agar plates (1% w/v yeast extract, 2% w/v peptone, 2% w/v glucose) at 30 °C. The deletion strain Δ*mir1*Δ*pic2* was transformed with *pYPGK18/TbMCP11* and *pYPGK18/TbMCP11-PIC2*^{nterm} using the rapid lithium acetate/polyethyleen glycol method (Gietz and Woods, 2002). Transformants were selected on synthetic glucose-rich minimal agar medium (6.7 g yeast nitrogen base without amino acids (Difco), 20 mg adenine, 20 mg arginine, 20 mg histidine, 230 mg lysine, 20 mg methionine, 300 mg threonine, 20 mg tryptophan and 40 mg uracil per L) that lacked leucine and contained glucose (30 g L^{-1}) as a fermentative carbon source. The growth phenotypes of the Δ*mir1*Δ*pic2* yeast deletion strain, and derived strains containing *pYPGK18/TbMCP11* or *pYPGK18/TbMCP11-PIC2*^{nterm} were analyzed by streaking onto agar plates containing 1% yeast extract, 2% peptone, and either 2% glucose (YPD), 3% glycerol (YPG) or 2% lactate (YPL, adjusted to pH 5.5 using KOH). The parental BY4741 strain was used for comparison. The plates were incubated at 30 °C for 3–6 days.

2.14 Mitochondrial swelling assay

Intact *S. cerevisiae* mitochondria were prepared by using the lyticase and differential centrifugation method described by (Daum et al., 1982), while *T. brucei* mitochondria were prepared according to the digitonin method as previously described by (Schneider et al., 2007). Phosphate-dependent mitochondrial swelling was determined according to (Manon and Guerin, 1988) method with modifications from (Hamel et al., 2004). Briefly, freshly prepared yeast or *T. brucei* mitochondria were resuspended in 1 ml buffer containing 0.2 M potassium phosphate (pH7.4), 38 mM oligomycin

and 0.2 mM antimycin, to final protein concentrations of 0.1 mg/ml and 0.8 mg/ml, respectively. The mitochondrial swelling was induced by addition of valinomycin (final concentraion: 0.04 mM). The absorbance changes were monitored by spectrophotometer at 546 nm.

3. Results

3.1 The *T. brucei* genome codes for two putative mitochondrial phosphate carriers

Two MCF proteins, TbMCP8 (GeneDB: Tb927.10.10440) and TbMCP11 (Tb927.9.10310) were previously identified with significant sequence similarity (58-66%) to the functionally characterised mitochondrial phosphate (Pi) carriers Mir1p and Pic2p from *S. cerevisiae*, and to SLC25A3 from *H. sapiens* (Colasante et al., 2009, Schroers et al., 1998, Dolce et al., 1994). Both display features that are conserved in MCF proteins (Palmieri, 2004, Palmieri et al., 2011), including the presence of 6 trans-membrane helices, a tripartite protein domain structure with semi-conserved sequence repeats of approximately 100 amino acids, and the signature sequence motif 'Px(D/E)x_2(K/R)x(K/R)x_{20-30}(D/E)Gx_{4-5}(W/F/Y)(K/R)G' at the end of each odd-numbered trans-membrane helix (Fig. 1A, (Colasante et al., 2009)). Amino acids involved in the selective binding and transport of specific substrates are in MCF proteins conserved and organized in three distinct substrate contact points (CP1-3) (Robinson and Kunji, 2006). In all known Pi carriers, CP1 is represented by the 3 conserved amino acids glycine (G), glutamine (Q) and lysine (K); CP2 by a conserved arginine (R) and glutamine (Q); and CP3 by a conserved methionine (M) (Fig. 1B) (Robinson and Kunji, 2006). The amino acid compositions of CP1-3 in

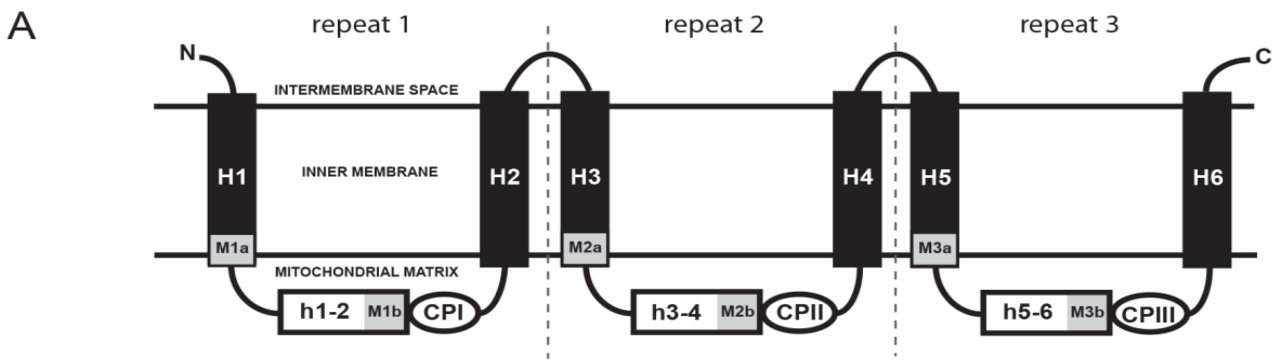

B

```
                                                                                                M1a
TbMCP11  -----------------------------------------MSAKNKTWDARYANPDIPHNNSYYLKCIGGGVLSCGLTHTAVCPLDVVKCNMQVNPEKFRGIGSG 65
TbMCP8   ----MLGRFDFLGKCRLYFVVVSRLFSFEGDYVAYRLFFVYFVFFTLSFLFVWSRRVVVEFSAFYFFCCFLGGVISGLAHTSMTPVDLVKCGVQVG--LYNSMTDG- 100
ScPic2p  -----------------------------------------------MESNKQPRKIQLYTKEFYATCTLGGIIACGPTHSSITPLDLVKCRLQVNPKLYTSNLQG- 59
ScMir1p  ------------------------------------------------MSVSAAPAIPQYSVSDYMKFALAGAIGCGSTHSSMVPIDVVKTRIQLEPTVYNKGMVGS 59
SLC25A3  MFSSVAHLARANPFNTPHLQLVHDGLGDLRSSSPGPTGQPRRPRNLAAAAVEE-YSCEFGSAKYYALCGFGGVLSCGLTHTAVVPLDLVKCRMQVDPQKY-KGIFNG 105
Btau     MYSSVVHLARANPFNAPHLQLVHDGLAGPRSDPAGPPGPPRRSRNLAAAAVEEQYSCDYGSGRFFILCGLGGIISCGTTHTALVPLDLVKCRMQVDPQKY-KSIFNG 106
                                                     :      G : .G :H::: P:D:VK  :Q:    :     .

                                     CP1
                   M1b            ▼   ▼   ▼                                                   M2a
TbMCP11  FKVLAAEDG----FGAKGIWKGWLPTLIGYSMQGACKFGLYEVFKDFYANLAGQKA------AKEYEGLIWLAGSASAEFFADVALCPMEMVKVKVQTSPSGTFPTSLGAAVATMRADPA 175
TbMCP8   FRSLWRNCGGCWFRSISVFTRGWVPTFFGYSSQGGLKFLLYELLKFWFCSRLEGSAASPMVLSYVSKLGIFVVSSGVAEIFADVALAPWEAVKIIIQTSN--VAHTELSYFFPLVYSSEG 218
ScPic2p  FRKIIAN------EGWKKVYTGFGATFVGYSLQGAGKYGGYEYFKHLYSSWLS------------PGVTVYLMASATAEFLADIMLCPFEAIKVKQQTTMPPFCNNVVDGWKKMYAESGG 161
ScMir1p  FKQIIA-------GEGAGALLTFGPTLLGYSIQGAFKFGGYEVFKKFFIDNLGYDT------ASRYKNSVYMGSAAMAEFLADIALCPLEATRIRLVSQPQ--FANGLVGGFSRILKEEG 164
SLC25A3  FSVTLKE------DGVRGLAKGWAPTFLGYSMQGLCKFGFYEVFKVLYSNMLGEEN------TYLWRTSLYLAASASAEFFADIALAPMEAAKVRIQTQPG--YANTLRDAAPKMYKEEG 211
Btau     FSVTLKE------DGFRGLAKGWAPTFIGYSLQGLCKFGFYEVFKVLYSNMLGEEN------AYLWRTSLYLAASASAEFFADIALAPMEAAKVRIQTQPG--YANTLRDAAPKMYKEEG 212
         F                    : .T:.GYS QG  K:  YE :K  : .                  ::: .:. AE::AD: L.P E  ::   :        . :          . .

                 CP2                                                                                            CP3
         M2b     ▼▼                                                    M3a                         M3b           ▼
TbMCP11  AGFPFKSLVPLWSRQIPYTMAKFFFFEKVVRFFYSNVFTKPKEEYSKGTQLSITFASGYIAGIVCAIVSHPADMLVSARGKASNV-GKSYG----QIANEIGYGNLCTKGLMARIIMIGT 290
TbMCP8   IYGFYKGLPALWCRQVPYTVVKFLSFEVIVRLAYRYLLTSPSDPAPKYVQLLVSVISGVLAGFLCAAVSHPADTVVSKLNQRVEGSPAADKRKVVQIVRELGWSGLW-KGVELRMMMTGA 337
ScPic2p  MKAFYKGIVPLWCRQIPYTMCKFTSFEKIVQKIYS-VLPKKKEEMNALQQISVSFVGGYLAGILCAAVSHPADVMVSKINSERKANESMS-VASKRIYQKIGFTGLW-NGLMVRIVMIGT 278
ScMir1p  IGSFYSGFTPILFKQIPYNIAKFLVFERASEFYYG--FAGPKEKLSSTSTTLLNLLSGLTAGLAAAIVSQPADTLLSKVNKTKKAPGQSTVGLLAQLAKQLGFFGSF-AGLPTRLVMVGT 281
SLC25A3  LKAFYKGVAPLWMRQIPYTMMKFACFERTVEALYKFVVPKPRSECSKPEQLVVTFVAGYIAGVFCAIVSHPADSVVSVLNKEK---GSSAS----LVLKRLGFKGVW-KGLFARIIMIGT 323
Btau     LKAFYKGVAPLWMRQIPYTMMKFACFERTVEALYKFVVPKPRSECSKPEQLVVTFVAGYIAGVFCAIVSHPADSVVSVLNKEK---GSSAS----EVLKRLGFRGVW-KGLFARIIMIGT 324
             :... .:  RQ:PY.: KF  FE    .  Y   ..   .          :.. .G  AG. .A VS:PAD ::S  ..                 : ..:G: .     G:  R::M G:

TbMCP11  LTGLQWWIYDTYKSTLGLGTSGGSGKK---------------- 317
TbMCP8   LTALQWLLYDSFKVSVGLSATGGNGVRISNHVDSDGRPPGDNK 380
ScPic2p  LTSFQWLIYDSFKAYVGLPTTG--------------------- 300
ScMir1p  LTSLQFGIYGSLKSTLGCPPTIEIGGGGH-------------- 310
SLC25A3  LTALQWFIYDSVKVYFRLPRPPPPEMPESLKKKLGLTQ----- 361
Btau     LTALQWFIYDSVKVYFRLPRPPPPEMPESLKKKLGYTQ----- 362
         LT.:Q: :Y.: K  .
```

Figure 1: TbMCP11 and TbMCP8 contain phosphate carrier features. A. Schematic representation of MCF protein sequence structure. H1-6 represents transmembrane helices; h1-2, h3-4 and h5-6 represent the connecting hydrophilic loops; M1-3a represent the first part (Px[D/E]xx[K/R]x[K/R]) and M1-3b represent the second part ([D/E]Gx_n[K/R]G) of the canonical MCF signature sequence; CP1-3 indicate the different conserved substrate contact points. B. Sequence alignment of TbMCP11 and TbMCP8 with *S. cerevisiae* Mir1p (ScMir1p), Pic2p (ScPic2p), *H. sapiens* SLC25A3 (SLC25A3) and *Bos. taurus* (Btau). The different parts of the canonical signature sequence are indicated by grey backgrounds. N-terminal signaling part of TbMCP11 (amino acids 1-23) and ScPic2p (amino acids 1-17) are boxed.

TbMCP8 and TbMCP11 are identical to those of the functionally characterized phosphate carriers Mir1p, Pic2p, and SLC25A3 (Fig. 1B), suggesting a Pi transport function for both TbMCPs. Also phylogenetic analysis supported the predicted Pi transport function for TbMCP8 and TbMCP11 (Fig. 2). As shown previously (Takabatake et al., 1999), phosphate-transporting MCF proteins from vertebrates, insects, plants, fungi and protozoa cluster in distinct clades supported by high bootstrap values (Fig. 2). TbMCP11 clustered specifically with Pi carriers from other related kinetoplastida (*Leishmania infantum*, *T. cruzi* and *T. congolense*) and is branching close to putative Pi carriers from other unicellular eukaryotes, such as the choenoflagellates and chromalveolates. This is in contrast to TbMCP8, which branched outside this group (Fig. 2): the different positions of TbMCP8 and TbMCP11 in the phylogenetic tree is supported by their relatively low sequence similarity (42%), and suggests a divergent evolution of both Pi carriers.

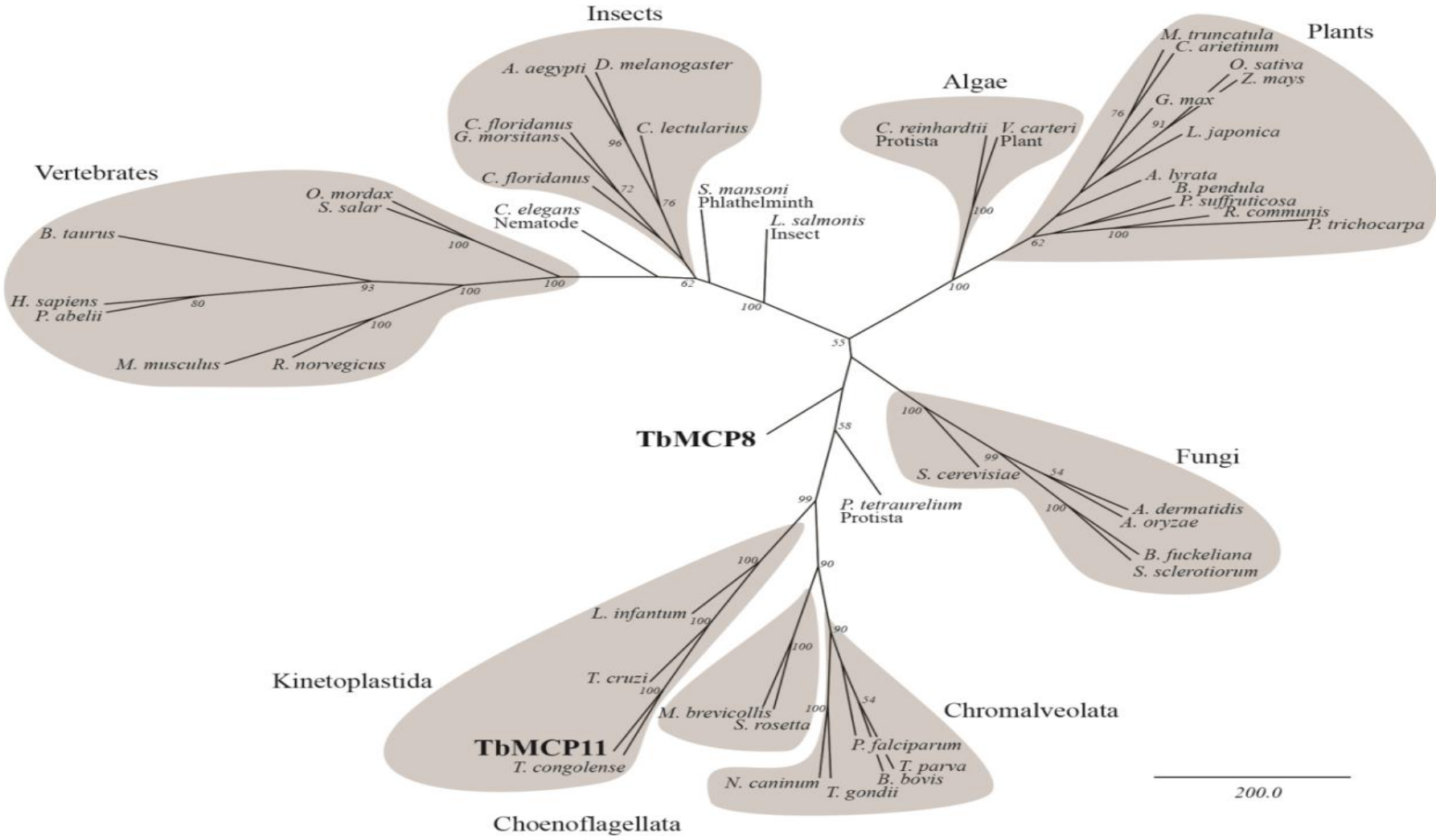
Insects
A. aegypti
D. melanogaster
C. floridanus
G. morsitans
C. lectularius
C. floridanus
Vertebrates
O. mordax
S. salar
B. taurus
H. sapiens
P. abelii
M. musculus
R. norvegicus
C. elegans
Nematode
S. mansoni
Phlathelminth
L. salmonis
Insect
Algae
C. reinhardtii
Protista
V. carteri
Plant
Plants
M. truncatula
C. arietinum
O. sativa
Z. mays
G. max
L. japonica
A. lyrata
B. pendula
P. suffruticosa
R. communis
P. trichocarpa
TbMCP8
P. tetraurelium
Protista
Fungi
S. cerevisiae
A. dermatidis
A. oryzae
B. fuckeliana
S. sclerotiorum
Kinetoplastida
L. infantum
T. cruzi
TbMCP11
T. congolense
Choenoflagellata
M. brevicollis
S. rosetta
Chromalveolata
P. falciparum
T. parva
B. bovis
N. caninum
T. gondii
200.0

Figure 2: Neighbour-joining tree showing the evolutionary relationship between TbMCP8, TbMCP11 and phosphate carrier from other species. Bootstrap values above 50% are showed at the relevant nodes.

3.2 Differential expression of TbMCP11 in *T. brucei*

Expression in *T. brucei* is developmentally regulated at the mRNA level for approximately 2% of its genes (Brems et al., 2005). Northern blot analysis was used to determine whether also *TbMCP8* and *TbMCP11* are differentially expressed in the replicating life cycle stages of *T. brucei*, i.e. the bloodstream form (BSF) and the procyclic form (PCF). For *TbMCP11*, a single hydridizing mRNA band was detected for both BSF and PCF *T. brucei* (Fig. 3A). Its size-length of 2400kb was similar to the *in silico* predicted mRNA size of 2380kb, using the previously described parameters for the estimation of mRNA transcript lengths in *T. brucei* (Benz et al., 2005). Quantification using SRP as a loading control (Fig. 3A) revealed that, compared to the BSF parasite, 3-fold more *TbMCP11* mRNA is present in PCF *T. brucei*. Northern blot analysis using TbMCP8 as a probe failed to detect any mRNA, even when using 20 μg of poly-A^+ purified mRNA (results not shown).

The differential expression of TbMCP11 in BSF and PCF *T. brucei* was confirmed by western blot analysis using the raised TbMCP11 peptide-antibody (this thesis). A single cross-reacting protein band with the expected molecular weight of 34 kDa was detected in both life cycle stages (Fig. 3B). Quantification using tubulin as a loading control (Fig. 3B), revealed that in comparison to the BSF 2.5-fold more TbMCP11 is present in PCF *T. brucei*, which is in agreement with the observed higher levels of *TbMCP11* mRNA in this life cycle stage. Overall, these results suggested a more prominent role of TbMCP11 in PCF *T. brucei*, whereas TbMCP8 is most probably not expressed in, and thus not required for the two replicating life cycle stages of *T. brucei*.

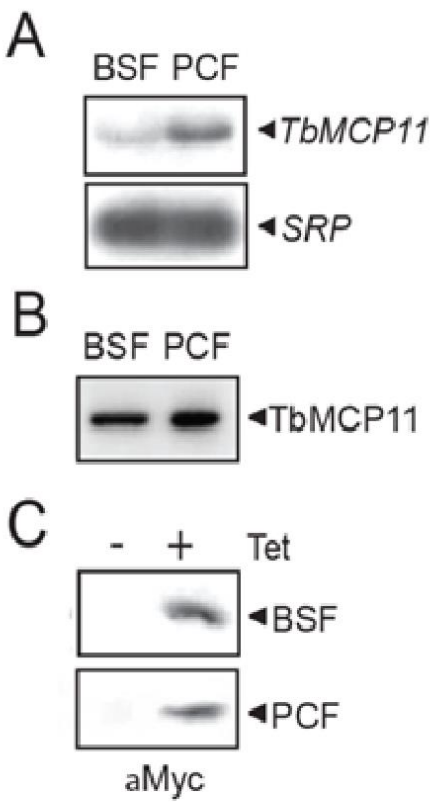
A
BSF PCF
TbMCP11
SRP
B
BSF PCF
TbMCP11
C
- + Tet
BSF
PCF
aMyc

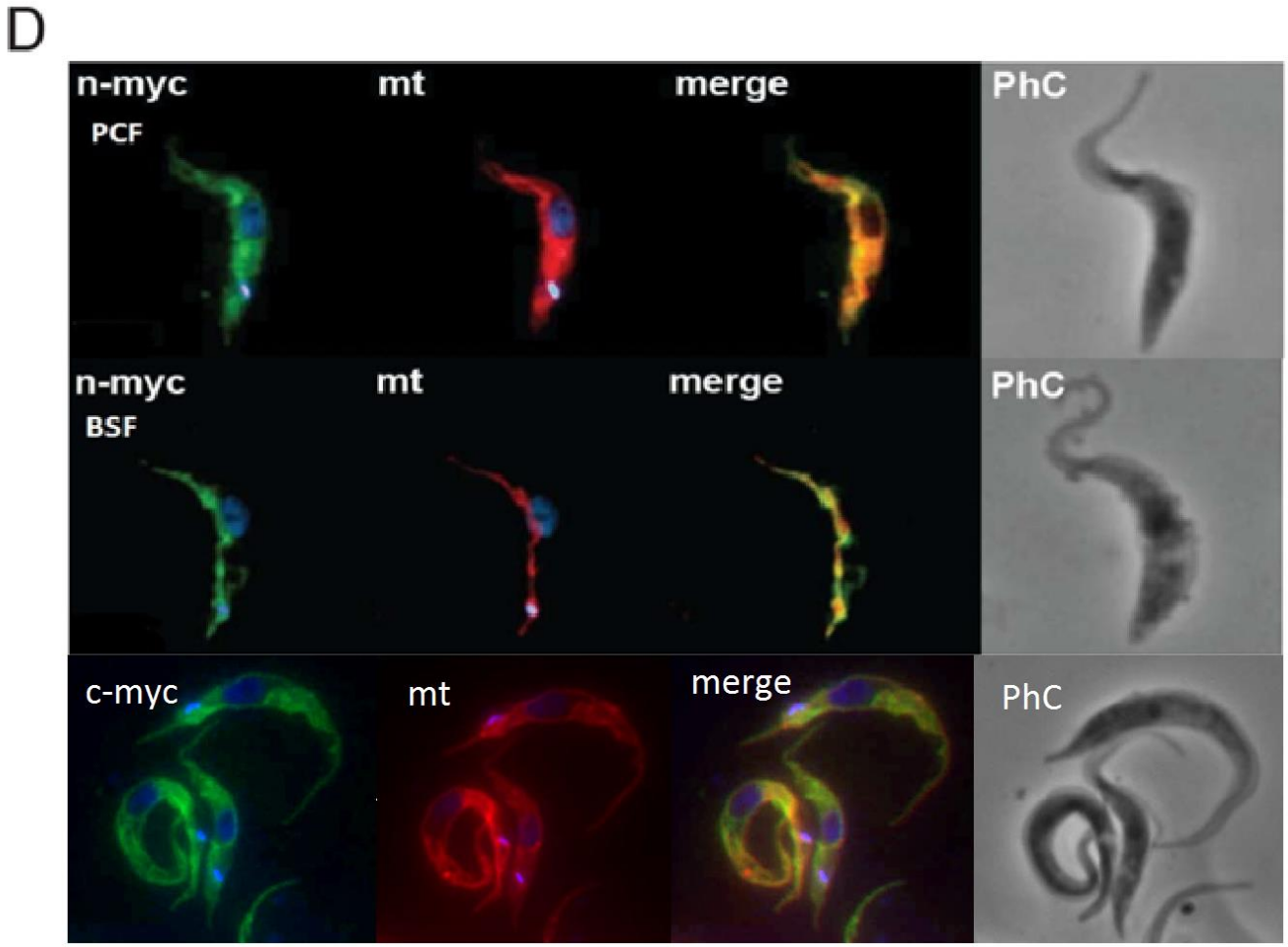
D
n-myc
mt
merge
PhC
PCF
n-myc
mt
merge
PhC
BSF
c-myc
mt
merge
PhC

Figure 3: TbMCP11 is exclusively mtiochondrial and differentially expressed *T.brucei*. A. Northern blot analysis of total RNA in BSF and PCF *T.brucei* using [α^{32}P]-dCTP labelled *TbMCP11* DNA as probe for hybridization.. B. Western blot analysis of BSF and PCF *T.brucei* using αTbMCP11 antibody. C. Western blot analysis the expression of TbMCP11-cmyc upon tetracycline induction using myc antibody. D. Immunofluorescence microscopy of N-terminal myc tagged BSF and PCF using myc antibody (green), Mitotracker (red) staining mitochondrion and DAPI (blue) staining nuclear and kinetoplast DNA.

3.3 TbMCP11 is exclusively mitochondrial in BSF and PCF *T. brucei*

The raised TbMCP11 peptide-antibody was initially used for determining the subcellular localisation of TbMCP11 in BSF and PCF *T. brucei*. However, this antibody appeared not to be suitable for immunofluorescence microscopy (results not shown). Instead, the subcellular location of TbMCP11 was determined by using BSF and PCF *T. brucei* cell-lines expressing a recombinant C-terminal myc-tagged version of TbMCP11 (TbMCP11-cmyc). Western blot analysis using a myc-antibody confirmed the expression of TbMCP11-cmyc upon tetracycline induction (Fig. 3C). Immunofluorescence microscopy using the same antibody revealed specific tubular staining patterns for both PCF and BSF *T. brucei*, which were identical to those obtained for the mitochondrial marker MitoTracker (Fig. 3D, (Vassella et al., 1997)). Similar results were found when using cell lines expressing a recombinant N-terminal myc-tagged version of TbMCP11 (Fig. 3D). These results suggested a mitochondrial location for TbMCP11 in *T. brucei*.

3.4 TbMCP11 functionally complements mitochondrial Pi-carrier deficiency in the yeast Δ*mir1*Δ*pic2*

The *S. cerevisiae* double deletion strain Δ*mir1*Δ*pic2* is deficient in mitochondrial phosphate transport and cannot use its mitochondria for ATP generation (Hamel et al., 2004). As a consequence, Δ*mir1*Δ*pic2* can only grow on a fermentable carbon source such as glucose (YPD medium) (Hamel et al., 2004, Takabatake et al., 2001). The predicted Pi-transport function of TbMCP11 can therefore be assessed by its ability to restore growth of Δ*mir1*Δ*pic2* on a non-fermentable carbon source, such as glycerol (YPG medium) or lactate (YPL medium), which requires functional mitochondria. The open reading frame of *TbMCP11* was cloned into the yeast vector *pYPGK18* (*pYPGK18-TbMCP11*), which allows constitutive expression under control

of a PGK1 promoter (Vaz et al., 2003, Swiegers et al., 2002). The *pYPGK18* vector without an insert was used as a negative control. Δ*mir1*Δ*pic2* was transformed with *pYPGK18* and *pYPGK18-TbMCP11*, and growth of the resulting strains was analysed on YPD, YPG and YPL medium. The *S. cerevisiae* strain BY4741, which is the parental strain of Δ*mir1*Δ*pic2* (Takabatake et al., 2001), was used for comparison of growth on the different media. As expected, BY4741 was able to grow on all media, whereas Δ*mir1*Δ*pic2::pYPGK18* (no insert) was only able to grow on YPD medium (Fig. 4A-C). Growth analysis revealed, however, that expression of TbMCP11 (*pYPGK18-TbMCP11*) was not able to restore growth of Δ*mir1*Δ*pic2* on YPG or YPL medium (Fig. 4B-C). Western blot analysis using the TbMCP11 antibody confirmed the expression and presence of TbMCP11 in Δ*mir1*Δ*pic2::pYPGK18-TbMCP11* (not shown), eliminating the possibility that TbMCP11 maybe was not expressed. Another explanation for the lack of growth could be the insufficient sorting of TbMCP11 to the *S. cerevisiae* mitochondrion. Similar sorting problems have previously been reported for other heterologous mitochondrial proteins when expressed in *S. cerevisae* (van Wilpe et al., 1999). In addition, the mitochondrial ATP/ADP carrier ScAnc2p was shown to be dependent on its N-terminal sequence (amino acids 1-26) for its efficient mitochondrial sorting in *S. cerevisiae* (Truscott et al., 2003, Adrian et al., 1986). Indeed, sequence alignment revealed significant differences in amino acid composition of the N-terminal sequences from TbMCP11, ScPic2p, and ScMir1p (Fig. 1B). Therefore the first 69 nucleotides (coding for amino acids 1-23) of TbMCP11 was substituted with the first 51 nucleotides (coding for amino acids 1-17) of ScPic2p (Fig. 1B), and cloned the resulting *TbMCP11-PIC2*^{nterm} fusion gene in *pYPGK18.* This construct was used for transformation of Δ*mir1*Δ*pic2* and growth of the resulting Δ*mir1*Δ*pic2::TbMCP11-PIC2*^{nterm} strain was analysed on the different

media. Analysis revealed that Δ*mir1*Δ*pic2::TbMCP11-PIC2*^{nterm} strain is now capable of growth on YPG and YPL media (Fig. 4B-C), suggesting that TbMCP11 indeed functions as a mitochondrial Pi-carrier. Growth of Δ*mir1*Δ*pic2::TbMCP11-PIC2*^{nterm} on YPG (Fig. 4B) or YPL medium (Fig. 4C) is however still not optimal when compared to its growth on YPD medium (Fig. 4A) or to the growth of BY4741 on the different media (Fig. 4A-C).

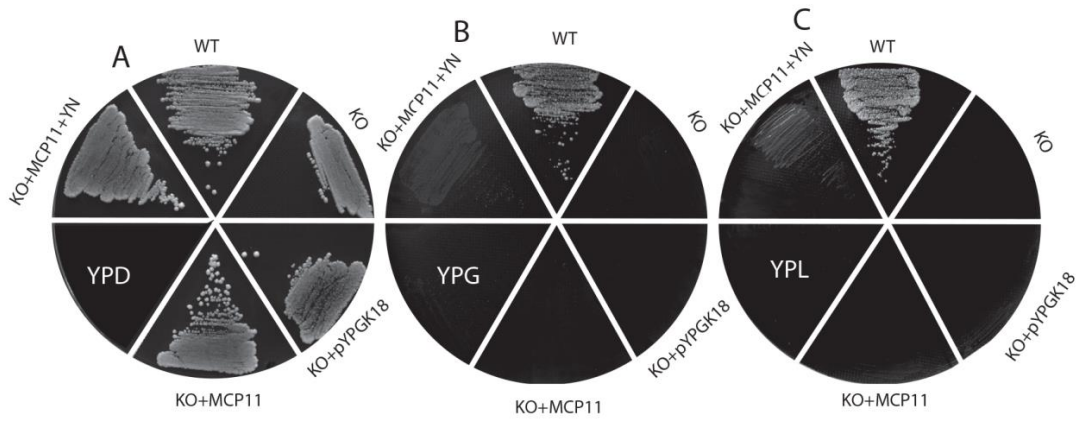

Figure 4: TbMCP11 functionally complement the mitochondrial phosphate carrier in the yeast Δ*mir1*Δ*pic2.* Yeast cell lines growed on YPD medium (A), YPG medium (B), and YPL medium (C). WT, wild type *S. cerevisiae* strain BY4741; KO, phosphate carrier deficient yesat strain Δ*mir1*Δ*pic2;*KO+pYPGK18: phosphate carrier deficient yeast strain Δ*mir1*Δ*pic2* was transformed with empty vector pYPGK18 to obtain Δ*mir1*Δ*pic2::pYPGK18*; KO+MCP11, phosphate carrier deficiency yeast strain Δ*mir1*Δ*pic2* was transformed with pYPGK18 containing TbMCP11; KO+MCP11+YN, phosphate carrier deficiency yeast strain Δ*mir1*Δ*pic2* was transformed with pYPGK18 containing TbMCP11 with the first 69 nucleotides (coding for amino acids 1-23) substituted with the first 51 nucleotides (coding for amino acids 1-17) of ScPic2p.

Further investigation has been done to check whether TbMCP11 and TbMCP11-PIC2^{nterm} were able to restore Pi transport in mitochondria isolated from the different yeast strains. Mitochondria do swell when suspended in a phosphate salt solution (Hamel et al., 2004, Zara et al., 1996). This swelling is caused by mitochondrial phosphate import, leading to an increase of the mitochondrial matrix solute concentration and the subsequent uptake of water. Mitochondria deficient in phosphate transport are unable to swell in the presence of phosphate salt (Hamel et al., 2004, Zara et al., 1996). I used this principle to assess Pi transport in mitochondrial fractions isolated from BY4741 (control), Δ*mir1*Δ*pic2* (Pi carrier deficient), Δ*mir1*Δ*pic2::TbMCP11* and Δ*mir1*Δ*pic2::TbMCP11-PIC2*^{nterm}. The results are summarized in Table 1. The mitochondrial swelling (decrease in absorbance at 545 nm) found for BY4741 mitochondria was set to 100% for comparison. As expected, swelling was reduced to 7% for mitochondria isolated from the Pi-carrier deficient strain Δ*mir1*Δ*pic2*, confirming that mitochondrial phosphate transport indeed makes a substantial contribution to osmotic swelling of mitochondria under the used assay conditions. Expression of TbMCP11 in Δ*mir1*Δ*pic2* resulted in a significant increase (from 7% to 21%) in mitochondrial swelling, whereas expression of TbMCP11-PIC2^{nterm} restored mitochondrial swelling to 100% as found for the BY4741 mitochondria. These results indicated that TbMCP11, and in particular TbMCP11-PIC2^{nterm}, is able to complement Mir1p/Pic2p deficiency in yeast.

Table 1. Mitochondrial swelling in isolated yeast and *T.brucei* mitochondria.

	Cell line - strain	**ΔAbs_{550nm}**	**Swelling (%)**
S. cerevisiae	BY4741 (wildtype)	0.029 ± 0.002	100
	ΔMIR1/ΔPIC2	0.002 ± 0.001	7
	ΔMIR1/ΔPIC2 +TbMCP11	0.006 ±	21

		0.007	
	ΔMIR1/ΔPIC2 +TbMCP11-Pic2p^{nterm}	0.029 ± 0.008	100
PCF *T. brucei*	EATRO1125-T7T	0.149 ± 0.006	100
	TbMCP11^{RNAi} non-induced	0.132 ± 0.008	98
	TbMCP11^{RNAi} induced	0.010 ± 0.007	7

Isolated mitochondria from different yeast strain, PCF *T.brucei* cell line were used to do the mitochondrial swelling assay for assessing mitochodnrial phosphate carrier transport capability. When mitochondria exsit in a higher phoaphate concentraion environment, the phosphate carrier start to transport phosphate into the mitochondrial matrix, which coresponding cause the subsequent uptake of water into mitochondria and finally mitochondria swelling.

3.5 TbMCP11 is essential for growth of PCF, but not BSF T. brucei

Whether the mitochondrial phosphate carrier TbMCP11 is essential for *T. brucei* growth was assessed by the generation of a conventional *TbMCP11* double-knockout cell line for BSF *T. brucei* and by the generation of a RNA interference cell line for PCF *T. brucei*, followed by analysis of their growth phenotype. The BSF TbMCP11 double-knockout cell line Δ*TbMCP11* with the genotype Δ*TbMCP11*::*BSD*/Δ*TbMCP11*::*NEO* was generated by targeted gene replacement, i.e. the sequential replacement of the two *TbMCP11* alleles (*T. brucei* is diploid) via homologous recombination with genes coding for blasticidin resistance (*BSD*) and neomycin resistance (*NEO*). The sequential replacement of both *TbMCP11* alleles was monitored by southern blot analysis (Fig. 5F). Also the corresponding TbMCP11 protein product could not be detected by western blot analysis using the raised TbMCP11 antibody (Fig. 5B). Subsequent growth analysis revealed similar growth

curves for the parental BSF 449 and BSF Δ*TbMCP11* cell lines, which indicated that TbMCP11, and thus mitochondrial phosphate transport, is not required for the growth of BSF *T. brucei* (Fig. 5A).

For PCF *T. brucei*, initially a conventional TbMCP11 double-knockout cell line was attempted to generate using the same targeted gene replacement method as described for BSF *T. brucei*. Although It was able to generate PCF cell lines lacking one *TbMCP11* allele (Δ*TbMCP11*::*BSD*/*TbMCP11*), no viable clones could be obtained upon deletion of the second *TbMCP11* allelle. This failure to generate a viable double-knockout cell line suggested that TbMCP11 expression is required for the growth of PCF *T. brucei*. Alternatively, an RNA interference cell line was generated, which allowed the tetracycline-inducible expression of double-stranded *TbMCP11* mRNA and the concomittant down-regulation of TbMCP11 expression in PCF *T. brucei*. Western blot analysis of the obtained ^{RNAi}*TbMCP11* cell line confirmed that no detectable (below the detection limit of the used method) TbMCP11 was present after 3 days of tetracyline induction (Fig. 5E). RT-PCR using *TbMCP11*-specific primers confirmed the absence of *TbMCP11* mRNA in the obtained PCF *TbMCP11*-RNAi cell lines (Fig. 5C). Growth phenotype analysis using the non-induced ^{RNAi}*TbMCP11* cell line for comparison, revealed that growth of the ^{RNAi}*TbMCP11* cell line gradually slowed down during the first 7 days after tetracycline induction and that growth completely ceased at day 8 (Fig. 5D). TbMCP11 is apparently required for the growth of PCF *T. brucei*, but not for the BSF life cycle stage of the parasite.

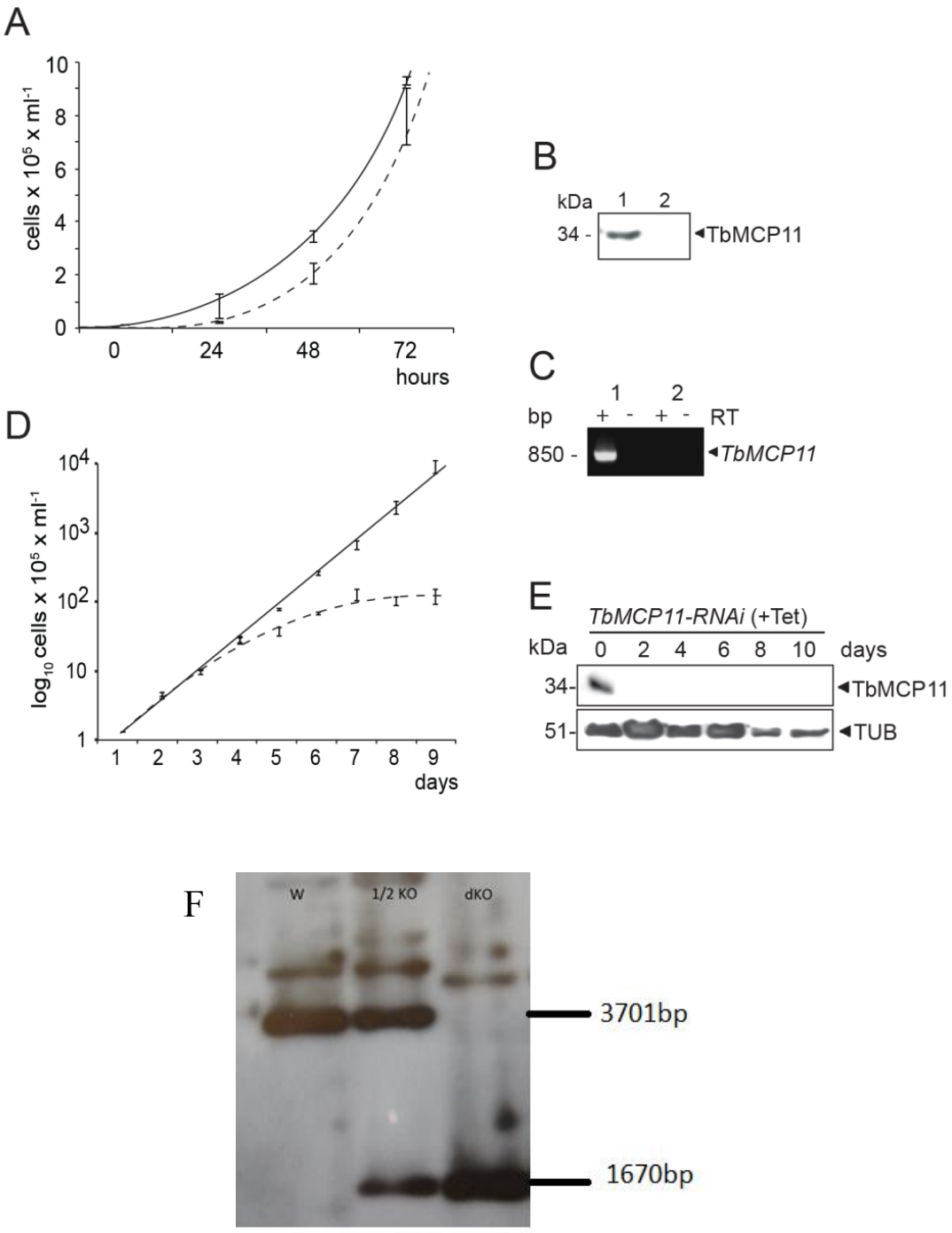

Figure 5: Analysis of depletion of TbMCP11 in both bloodstream and procyclic form *T.brucei*. A. Growth analysis of BSF wild type cell line and TbMCP11 double-knockout cell line Δ*TbMCP11* with the genotype *TbMCP11*::*BSD*/Δ*TbMCP11*::*NEO*. Dash line indicates the growth of Δ*TbMCP11*. Solid line indicates the wild type growth. B. Western blot analysis of wild type BSF (1) and double-knockout Δ*TbMCP11* (2) using αTbMCP11 antibody. C. RT-PCR analysis of mRNA level in wild type PCF (1) and ^{RNAi}*TbMCP11* cell line (2). +, the reaction with reverse

transcriptase. -, without reserves transcriptase (used as control for genome DNA contamination). D. Growth analysis of wild type PCF and ^{RNAi}*TbMCP11* cell line. The growth is showed in log rate. Solid line stands for wild type PCF growth. Dash line stands for ^{RNAi}*TbMCP11* growth. E. Samples were taken every 24 h for western blot analysis of ^{RNAi}*TbMCP11* cell line induced with tetracycline using αTbMCP11 antibody and Tubulin antibody (αTUB). F. Southern blot analysis of knockout Δ*TbMCP11* cell line. In the wild type, BamHI was used to digest the genomic DNA, and only the 3701bp band was expected. In the half knockout, another BamHI site was introdued by replacing TbMCP11 by BSD, so both 3701bp and 1670bp band were expected. In the double-knockout cell line, both of the TbMCP11 allele gene were replaced by BSD or NEO with BamHI site, therefore expected to show only 1670bp band. The bands abouve 3701bp was not expected and is probably due to nonspecific binding. W, wild type; 1/2KO, half knockout cell line; dKO, double-knockout cell line.

3.6 Lack of Pi transport in mitochondria from TbMCP11-depleted PCF *T. brucei*

As described above, yeast mitochondria capable of phosphate transport do swell in the presence of phosphate salt, whereas Pi carrier-deficient mitochondria lack this property (Hamel et al., 2004, Zara et al., 1996). I investigated whether Pi-dependent swelling also occurs for *T. brucei* mitochondria. Mitochondria were isolated from non-induced and TbMCP11-depleted (7d) ^{RNAi}*TbMCP11* trypanosomes. Swelling experiments revealed that also mitochondria from *T. brucei* were capable of swelling in the presence of phosphate salts (Table. 1) Control experiments showed that no mitochondrial swelling occured in the absence of phosphate, indicating that mitochondrial swelling is phosphate dependent (not shown). Analysis of the TbMCP11-depleted *T. brucei* mitochondria revealed a major decrease (93%) in mitochondrial swelling (Table. 1). The observed decrease in swelling (93%) is similar for both the Pi-carrier deficient *S. cerevisiae* Δ*mir1*Δ*pic2* mitochondria and the TbMCP11-depleted mitochondria (Table. 1). These results suggest that TbMCP11 is

most probably responsible for most if not all of the mitochondrial Pi-carrier activity in PCF *T. brucei*.

3.7 Abnormal cell morphology and loss of mitochondrial membrane potential in TbMCP11-depleted PCF *T. brucei*

Substantial changes in cell morphology and cell motility were observed during microscopic examination of the TbMCP11-depleted PCF cell line (Fig. 6A-F). Phase contrast microscopy and scanning electron microscopy revealed that in comparison to the non-induced cell line the morphology of the TbMCP11-depleted (8d after tetracycline-induction) trypanosomes had changed to an elongated, needle-like appearance (Fig. 6F). Staining of nuclear and mitochondrial DNA with DAPI revealed that majority of the cells were multi-nucleated with only a single or no kinetoplast present (Fig. 6E). In addition, increased numbers of cells with fragmentated nuclei were observed (Fig. 6C).

Immunofluorescence microscopy using TbMCP5 antibody revealed the expected mitochondrial (tubular) staining pattern for non-induced PCF ^{RNAi}*TbMCP11* trypanosomes (Fig. 6G). This staining pattern is identical (perfect overlay) to that of αTbMCP5, which specifically labels the mitochondrial ADP/ATP carrier TbMCP5 (Pena-Diaz et al., 2012). Microscopic analysis of TbMCP11-depleted PCF trypanosomes revealed a substantial change in MitoTracker staining, which was not confined to the mitochondrion anymore, but distributed throughout the whole cell (Fig. 6A-E). This result indicated the absence of a mitochondrial membrane potential, which is required for the mitochondrion-specific accumulation of MitoTracker (Vassella et al., 1997, Isenberg and Klaunig, 2000). A similar disruption of the mitochondrial membrane potential can be mimicked by the addition of the ionophore carbonyl cyanide m-chlorophenyl hydrazone (CCCP) (Gallo et al., 1984). Addition of

1 mM CCCP to the non-induced ^{RNAi}*TbMCP11* trypanosomes resulted in a similar loss of mitochondrion-specific Mitotracker staining as observed for the TbMCP11-depleted cell line (Fig. 6G). Overall, these results indicated loss of the mitochondrial membrane potential in PCF *T. brucei* upon depletion of the mitochondrial phosphate carrier TbMCP11. Also notable is that the motility of TbMCP11-depleted PCF cells was very slow or not existing (results not shown).

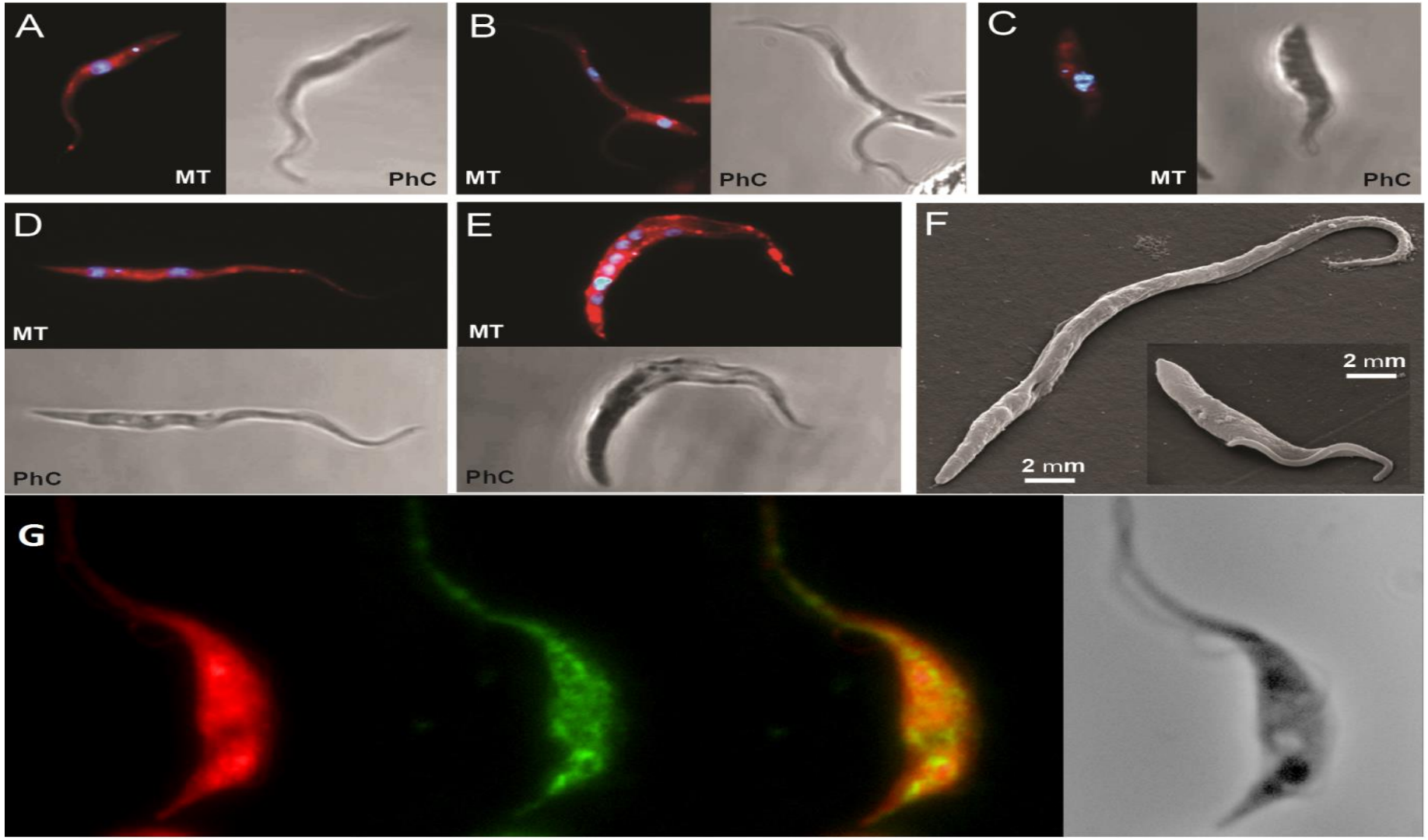
A
MT
PhC
B
MT
PhC
C
MT
PhC
D
MT
PhC
E
MT
PhC
F
2 mm
2 mm
G

Figure 6. TbMCP11 depeleted by RNAi in procyclic form *T.brucei* causes abnormal cell morphology and loss of mitochodnrial membrane potential. After 8 days induced with tetracycline, ^{RNAi}*TbMCP11* cell line stained with Mitotracker (red) and DAPI (blue) (A-E) showed loss of mitochondrial membrane potential (A), stucky cell (B), fractionated nuclear (C), elongated cell (D) and multiple nuclei (E). F. Scanning electron microsocopy (SEM) showed an elongated ^{RNAi}*TbMCP11* cell. The wildtype PCF is on the right lower corner. (G). non-induced ^{RNAi}*TbMCP11* cell cell line treated with 1 mM CCCP showed similar result of lossing mitochondrial membrane potential. The mitochondrion is still in normal shape detected with TbMCP5 antibody (green), while the membrane potential is lost detected with Mitotracker (red). DAPI stained with nuclear and kinetoplast DNA (blue).

3.8 TbMCP11 is required for mitochondrial respiration and ATP production

Isolated *T. brucei* mitochondria were previously shown to produce ATP in a ΔΨ-dependent manner, and in the presence ADP, Pi, and suitable respiratory substrates, such as succinate or α-ketoglutarate (Schneider et al., 2007, Allemann and Schneider, 2000). In the presence of succinate, ATP is produced via oxidative phosphorylation (dependent on respiratory chain), while in the presence of α-ketoglutarate ATP is produced via a combination of oxidative and substrate level phosphorylation (dependent on succinyl-CoA synthetase) (Bringaud et al., 2006). The exchange of mitochondrial ATP for cytosolic ADP is catalysed by the mitochondrial ADP/ATP carrier TbMCP5 (Pena-Diaz et al., 2012). Synthesis and export of ATP results in the depletion of Pi in the mitochondrial matrix, which in turn is replenished by the mitochondrial Pi carrier (Zara et al., 1996, Hamel et al., 2004). This dependence of mitochondrial ATP synthesis on the Pi carrier can be used as a direct assay for determining its presence or activity in isolated mitochondria. For this purpose, mitochondria were isolated from non-induced (control) and TbMCP11-depleted ^{RNAi}*TbMCP11* trypanosomes, and mitochondrial ATP synthesis was determined using succinate or α-ketoglutarate as a substrate (Allemann and Schneider, 2000). As shown in figure 6A, mitochondria isolated from non-induced trypanosomes were capable of producing ATP in the presence of each substrate, indicating that they are indeed "functional". Upon addition of carboxyactractiloside (CATR), a specific inhibitor of the mitochondrial ATP/ADP carrier, no ATP was produced for both substrates (Shabalina et al., 2006). This control experiment confirmed the absence of extra-mitochondrial ATP producing pathways in the isolated mitochondrial fractions: any measured ATP is therefore derived from mitochondrial ATP synthesis (Allemann and Schneider, 2000, Schneider et al., 2007). Also in the absence of Pi, no ATP was

produced, indicating that the isolated mitochondria did not contain any stored Pi (not shown). In another control experiment azide was added, which acts as a specific inhibitor of the respiratory chain and allows discrimination between ATP derived from oxidative phosphorylation or substrate-level phosphorylation (Bowler et al., 2006). In the presence of azide, no mitochondrial ATP production was found when using succinate as a substrate, while for α-ketoglutarate ATP production was reduced to be about 16% of the non-inhibited assay (Fig. 7A). These results were expected since ATP production from succinate exclusively takes place via oxidative phosphorylation (respiratory chain), and thus is completely inhibited in the presence of azide, whereas part (16%) of the ATP produced from α-ketoglutarate results from substrate level phosphorylation, a process which is not affected by azide (Bowler et al., 2006, Vasilyeva et al., 1982). The same ATP production assay was subsequently performed with mitochondria isolated from TbMCP11-depleted trypanosomes. The results revealed that no mitochondrial ATP was produced when using succinate as a substrate, whereas for α-ketoglutarate a substantial reduction in ATP synthesis (>80%) was found compared to the non-induced cell line (Fig. 7A). The residual ATP production found for α-ketoglutarate was ablated upon addition of azide or CATR (Fig. 7A).

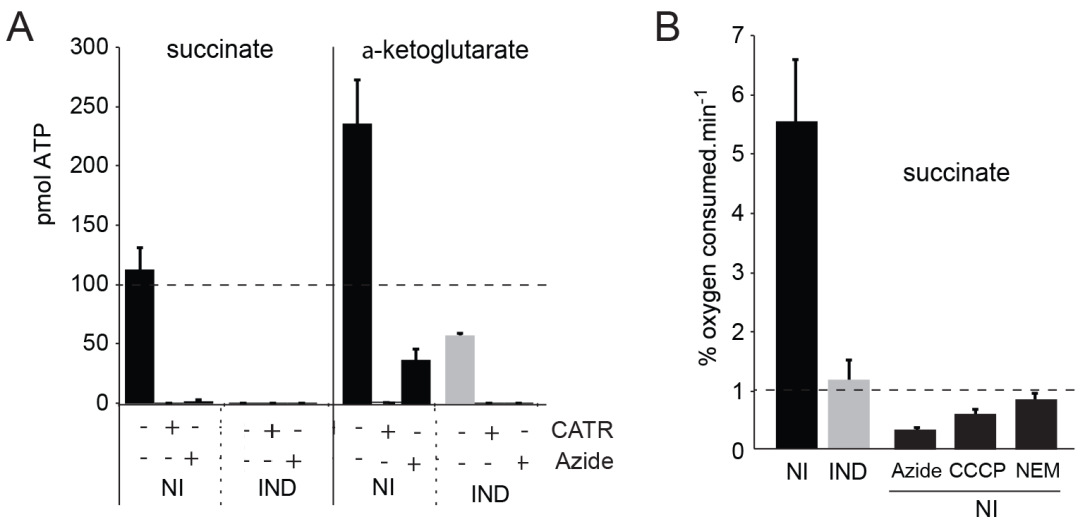

Figure 7: Depletion of TbMCP11 in PCF causes changes in mitochondrial respiration and ATP production. Intact mitochondria were isolated from non-induced (NI) and tetracycline-induced (IND) ^{RNAi}*TbMCP11* cell lines. A. MitochodrialATP production was initiated by addition of succinate or α-ketoglutarate. Inhibitor carboxyatractyloside (CATR) and azide were added into the isolated mitochondria. Data shown were means of >3 independent experiments. B. Oxygen consumption in isolated mitochodria. Succinate was added as substrate. Three inhibitors azide (6.8 mM), carbonyl cyanide m-chlorophenyl hydrazone (CCCP, 1 mM) and N-ethylmaleimide (NEM, 1.5 mM) were added.

Mitochondrial respiration and coupled ATP synthesis requires the consumption of oxygen, which acts as a terminal electron acceptor (Hatefi, 1985, Bienen et al., 1991). Also *T. brucei* was previously shown to consume oxygen during mitochondrial respiration (Beattie and Howton, 1996, Bienen et al., 1991). In addition, an alternative oxidase has been identified, which is oxygen-consuming and is located in the inner mitochondrial membrane of *T. brucei* (Chaudhuri et al., 2006). This alternative oxidase can be specifically inhibited by salicylhydroxamic acid (SHAM), which allows the discrimination between oxygen consumption as a result of mitochondrial respiration or alternative oxidase activity (Chaudhuri et al., 2006). Oxygen consumption was determined for mitochondria isolated from non-induced and TbMCP11-depleted PCF ^{RNAi}*TbMCP11* trypanosomes, with succinate as a substrate and in the absence or presence of SHAM. Control experiments confirmed that in the absence of succinate no oxygen was consumed, while in the presence of succinate oxygen consumption was observed for mitochondria isolated from non-induced PCF ^{RNAi}*TbMCP11* trypanosomes (Fig. 7B). Analysis of mitochondria isolated from TbMCP11-depleted ^{RNAi}*TbMCP11* trypanosomes revealed a substantial decrease (75%) in oxygen consumption (Fig. 7B). A comparable decrease in oxygen consumption was found upon the addition of the mitochondrial respiration inhibitors azide or CCCP to non-induced ^{RNAi}*TbMCP11* cells (Fig. 7B). Overall, these results indicated a key role of the mitochondrial Pi carrier TbMCP11 in mitochondrial respiration and ATP production.

4. Discussion

TbMCP11 shares canonical sequence features with mitochondrial phosphate carriers from other eukaryotes, including the functionally characterised phosphate carriers Pic2p (ScPic2p) and Mir1p (ScMir1p) from *S. cerevisiae*. Heterologous

expression of TbMCP11 or TbMCP11-Pic2p^{nterm} in the phosphate-carrier deficient yeast strain Δ*mir1*Δ*pic2* rescued its mitochondrial swelling capacity in a phosphate-dependent manner. Vice versa, a substantial decrease (>93%) in the phosphate-dependent swelling of PCF *T. brucei* mitochondria was observed upon depletion of TbMCP11. These results confirmed that TbMCP11 indeed functions as a mitochondrial phosphate carrier in *T. brucei*.

Expression of TbMCP11 did however not rescue the growth of Δ*mir1*Δ*pic2* on the non-fermentable substrates glycerol (YPG) and lactate (YPL), while growth on the fermentable substrate glucose was similar to the that of the parental BY4741 strain. I investigated whether this inability to complement growth on a non-fermentable carbon source could be the result of an inefficient sorting of TbMCP11 to the Δ*mir1*Δ*pic2* mitochondrion. The first 26 amino acids of the mitochondrial ADP/ATP-carrier Anc2p from *S. cerevisiae* were previously shown to be essential for an efficient mitochondrial sorting in *S. cerevisiae* (Adrian et al., 1986, Hashimoto et al., 1999). Sequence comparison revealed significant dissimilarities between the N-terminus of TbMCP11 and those of ScMir1p and ScPic2p (see Fig. 1B). To test the inefficient sorting hypothesis, I replaced the first 23 amino acids of TbMCP11 with the first 17 amino acids of ScPic2p. Expression of the TbMCP11-Pic2p^{nterm} fusion protein now resulted in a partial rescue of Δ*mir1*Δ*pic2* growth on both YPG and YPL medium. In addition, a 100% restoration of the phosphate-dependent swelling capacity was observed for Δ*mir1*Δ*pic2* mitochondria when complemented with TbMCP11-Pic2p^{nterm}, whereas with TbMCP11 this swelling capacity was only partially restored. These results confirmed that the inefficient sorting of TbMCP11 to the yeast mitochondria is indeed part of the problem.

However, growth of the TbMCP11-Pic2p^{nterm} -expressing Δ*mir1*Δ*pic2* strain on YPG or YPL medium remains suboptimal and indicated that there are additional problems regarding the function of TbMCP11 in the heterologous yeast host. A possible explanation could be that TbMCP11 has to interact with other proteins to fullfil its physiological function. In mammalian cells, the phosphate carrier is part of a larger protein complex in the inner mitochondrial membrane called the mitochondrial permeability transition pore (MPTP), which further includes the ADP/ATP carrier, the ATP synthase, and the voltage-directed anion channel (VDAC) (Gutierrez et al., 2009, Halestrap, 2009, Halestrap, 2010). A similar complex involved in mitochondrial permeability transition has also been identified in *S. cerevisiae* and other eukaryotes, including plants (Scott and Logan, 2008), amphibians (Hanada et al., 2003) and fish (Krumschnabel et al., 2005). The MPTP is proposed to function as a non-selective pore, which opens in reponse to high matrix calcium concentrations (Lemasters et al., 2009). The sensitivity of the MPTP to calcium is greatly enhanced by oxidative stress or by phosphate and adenine nucleotide depletion (Varanyuwatana and Halestrap, 2012). Opening of the MPTP is activated by binding of phosphate to the mitochondrial phosphate carrier (Leung et al., 2008). However, the exact role of the phosphate carrier in mitochondrial permeability transition is still under debate. The required interaction/cross-talk of TbMCP11 with the heterologous yeast MPTP proteins could be problematic as a result of the existing sequence differences between the phosphate carriers, which in turn could explain the only partial growth complementation in yeast.

TbMCP11 is expressed in both PCF and BSF *T. brucei*, and its 2.5-fold higher abundance in PCF *T. brucei* implies a more important role of the mitochondrial phosphate carrier in this life cycle stage. Two lines of evidence confirmed that

TbMCP11 expression is essential for PCF *T. brucei*: I did not succeed to delete both *TbMCP11* alleles using a conventional double knockout approach, and the down-regulation of TbMCP11 expression by RNA interference resulted in the ablation of trypanosome growth. This, and the fact that no TbMCP8 mRNA could be detected, suggested further that TbMCP11 most probably represents the main and only mitochondrial phosphate carrier in the PCF parasite.

The presence of substantially less TbMCP11 in BSF trypanosomes is in agreement with the current metabolic model of this life cycle stage, which excludes a contribution of the mitochondrion to its cellular ATP provision (Guerra et al., 2006, van Hellemond et al., 2005). Instead, BSF trypanosomes rely exclusively on glycolysis with a concomitant net ATP-production in the cytosol of the parasite (Guerra et al., 2006, Gualdron-Lopez et al., 2012). In addition, the BSF mitochondrion lacks a functional respiratory chain and key enzymes of the TCA cycle (Priest and Hajduk, 1994), and its ATP-synthase level is significantly reduced in comparison to PCF *T. brucei* (Brown et al., 2006). Expression of the mitochondrial ATP synthase is however essential in BSF *T. brucei,* as shown by RNA interference of its α and β subunits, and an important role of this protein in the maintenance of the BSF mitochondrial membrane potential, by pumping protons out of the mitochondrial matrix, has been proposed (Brown et al., 2006). This function of the mitochondrial ATP synthase in BSF *T. brucei* implies a mitochondrial requirement for ATP, which can be provided by the mitochondrial ADP/ATP carrier TbMCP5 (see Chapter II, (Pena-Diaz et al., 2012)). During mitochondrial ATP consumption, ADP and Pi are formed as products, which can be used for subsequent ATP synthesis. This recycling of Pi implies that the bloodstream form mitochondrion is not *per se* dependent on the presence of a mitochondrial phosphate carrier for its function. Indeed, deletion of

both the TbMCP11 allelles in BSF *T. brucei* did not affect its growth, confirming that TbMCP11 and thus mitochondrial phosphate transport is not essential for the BSF parasite.

MitoTracker staining and microscopic analysis of TbMCP11-depleted PCF *T. brucei* revealed that this dye did not accumulate in its mitochondrion, but instead remained exclusively in its cytoplasm. This result indicated a substantial decrease in or even the lack of a mitochondrial membrane potential. Also the phosphate carrier-deficient mitochondrion of Δ*mir1*Δ*pic2* was previously shown to lack a membrane potential (Zara et al., 1996). The lack of a mitochondrial membrane potential is a direct consequence of the important role of the mitochondrial phosphate carrier in oxidative phosphorylation and regulation of mitochondrial permeability transition. Deletion of the mitochondrial phosphate carrier in *S. cerevisiae* resulted in a major decrease in the matrix phosphate levels, the opening of the MPTP, and the concomitant loss of its mitochondrial membrane potential and oxidative phosphorylation capacity (Prieto et al., 1995, Miedlich et al., 2010).

The effect of TbMCP11 depletion on oxidative phosphorylation in *T. brucei* was analysed by *in vitro* ATP-production assays using isolated mitochondria and different metabolic substrates. One of these substrates, i.e. succinate, transfers its electron directly to complex II of the mitochondrial respiratory chain, hereby generating a proton motive force (pmf). This pmf is subsequently used for ATP production by the ATP-synthase complex, which forms an essential part of the oxidative phosphorylation process. The observed absence of mitochondrial ATP production from succinate was therefore expected for TbMCP11-depleted mitochondria, since they lack a functional membrane potential as well as the necessary Pi import required

for ATP synthesis. In contrast to succinate, mitochondrial ATP production from α-ketoglutarate takes place via two different pathways, i.e. oxidative phosphorylation and substrate level phosphorylation (Bringaud et al., 2006, Bochud-Allemann and Schneider, 2002, Schneider et al., 2007). Analysis of the TbMCP11-depleted PCF mitochondria in the presence of α-ketoglutarate revealed a major reduction (84%) in ATP production: this result suggested that the majority of the ATP produced in the PCF mitochondrion is derived from the oxidative phosphorylation of α-ketoglutarate. Also the addition of azide, a potent inhibitor of mitochondrial respiration (Bowler et al., 2006), to parental/non-mutant *T. brucei* mitochondria did result in a 83% decrease of mitochondrial ATP production on the same substrate. These results confirmed that the TbMCP11-depleted mitochondria indeed lack oxidative phosphorylation, which is responsible for about 84% of the ATP production, with the remaining 16% ATP most probably derived from mitochondrial substrate level phosphorylation.

It was further anticipated that a reduced oxidative phosphorylation would also lead to a comparable reduction in respiration and thus oxygen consumption. Comparison of TbMCP11-depleted and non-mutant *T. brucei* mitochondria revealed that the oxygen consumption by the phosphate carrier-deficient mitochondria with succinate as a substrate was reduced to about 20% of its normal non-mutant activity. This result suggests that 80% of the oxygen consumption is due to oxidative phosphorylation, i.e. oxygen consumption by the mitochondrial cytochrome c oxidase present in the respiratory chain complex IV (Gnipova et al., 2012). The remaining oxygen consumption can be attributed to the alternative oxidase (TAO), a cytochrome-independent terminal oxidase present in the mitochondrial electron transport chain of *T. brucei* (Chaudhuri et al., 2006). TAO is mainly known for its vital role in the BSF *T. brucei* energy metabolism by transferring electrons derived from the oxidation of

glycerol-3 phosphate via ubiquinol to oxygen (Chaudhuri et al., 2006). TAO is also expressed, although to lower level, and functional in PCF *T. brucei*, where it is involved in respiration (Chaudhuri et al., 2006). The *T. brucei* alternative oxidase is specifically inhibited by salicylhydroxamic acid (SHAM) (Vanlerberghe and McIntosh, 1997, Chaudhuri et al., 2006). Addition of SHAM to the non-mutant mitochondria resulted in the expected reduction to 84% in oxygen consumption, while the addition of SHAM to the TbMCP11-depleted mitochondria ablated oxygen consumption. These results confirmed that TbMCP11 indeed plays a major role in the oxidative phosphorylation process of PCF *T. brucei*.

Microscopic analysis of the TbMCP11-depleted *T. brucei* cell line revealed further a substantial change in its cellular motility, morphology and nuclear organisation. The motility of TbMCP11-depleted PCF cells was very slow or not existing, when compared to the non-mutant parental trypanosomes. The motility of *T. brucei* is dependent on its flagellum, which is in turn requires ATP for its function (Kohl and Bastin, 2005). The majority of the TbMCP11-depleted trypanosomes showed further an elongated needle-like appaerance, with some of the cells showing an incomplete cellular division. These cells contained either multiple nuclei or a single nucleus showing nuclear fragmentation, next to a single kinetoplast. Overall, these results suggested a failure in kinetoplast replication, which will subsequently lead to a failure in cytokinesis (Gluenz et al., 2011, Jensen and Englund, 2012). The observed nuclear fragmentation indicates the onset of cell death, most probably as a result of the mitochondrial and cellular ATP deficit.

The MCF protein inventory of *T. brucei* includes two predicted mitochondrial phosphate carriers, here TbMCP11, whose function as a phosphate transporter was

confirmed in this study, and TbMCP8 (Colasante et al., 2009). TbMCP8 contains conserved mitochondrial phosphate carrier sequence features, and immunolocalisation studies of ectopically expressed myc-tagged versions of TbMCP8 confirmed the exclusive mitochondrial location of this putative phosphate carrier in both BSF and PCF *T. brucei* (Colasante et al., 2009). Expression studies using northern blot analysis (not shown) and RT-PCR (this study) revealed however that TbMCP8 is not expressed in the analyzed *T. brucei* life cycle stages. Also the double knockout of TbMCP8 in both BSF and PCF *T. brucei* had no effect on the growth of both life cycle stages (results not shown). The phosphate-transporting function of TbMCP8 remains to be experimentally confirmed, and its physiological role in *T. brucei* is yet unknown.

The presence of multiple (mainly pairs) mitochondrial phosphate carriers is not unusual and seems to be a common feature in most eukaryotes (Runswick et al., 1987, Ferreira et al., 1989, Dolce et al., 1991). For example, mammalian cells express two different isoforms from a single gene (Dolce et al., 1994), while the plant *Arabidopsis thaliana* was reported to express three different isoforms (PiC1, PiC2 and PiC3) (Haferkamp and Schmitz-Esser, 2012, Pratt et al., 1991, Stappen and Kramer, 1994). Only two out of three isoforms were experimentally proven. PiC1 is supposed to be the predominant function one (Hamel et al., 2004). The two different mitochondrial phosphate carriers of *S. cerevisiae*, i.e. Pic2p and Mir1p, share only 40% sequence homology and phylogenetic analysis indicated that Pic2p is more related to mitochondrial phosphate carrier sequences from other eukaryotes than to Mir1p found in the same organism (Hamel et al., 2004). Functional analysis revealed that isoform A is highly expressed and predominantly found in heart and muscle, while isoform B is of low abundant and present in all tissues (Fiermonte et al., 1998).

Also TbMCP11 and TbMCP8 share only 42% sequence homology. This dissimilarity in sequence and rapid evolutionary divergence of the different mitochondrial phosphate carrier isoforms suggests different physiological roles (Fiermonte et al., 1998, Hamel et al., 2004). Functional characterisation of the different phosphate carrier isoforms from *S. cerevisiae* revealed that Mir1p represents the major mitochondrial phosphate carrier, whereas Pic2p plays only a minor role (Hamel et al., 2004). Analysis revealed further that the steady state level of Pic2p increases at higher temperature, suggesting that this mitochondrial phosphate carrier is only required under specific environmental stress conditions (Hamel et al., 2004). I have shown here that, in contrast to TbMCP11, TbMCP8 is not expressed in both BSF and PCF *T. brucei*. Whether TbMCP8 is expressed in a different life cycle stage of *T. brucei* or is only expressed under specific environmental conditions remains unclear at this point and is subject to further investigation.

References

ADRIAN, G. S., MCCAMMON, M. T., MONTGOMERY, D. L. & DOUGLAS, M. G. 1986. Sequences required for delivery and localization of the ADP/ATP translocator to the mitochondrial inner membrane. *Mol Cell Biol,* 6**,** 626-34.

ALLEMANN, N. & SCHNEIDER, A. 2000. ATP production in isolated mitochondria of procyclic *Trypanosoma brucei*. *Mol Biochem Parasitol,* 111**,** 87-94.

BARRETT, M. P., BOYKIN, D. W., BRUN, R. & TIDWELL, R. R. 2007. Human African trypanosomiasis: pharmacological re-engagement with a neglected disease. *Br J Pharmacol,* 152**,** 1155-71.

BEATTIE, D. S. & HOWTON, M. M. 1996. The presence of rotenone-sensitive NADH dehydrogenase in the long slender bloodstream and the procyclic forms of *Trypanosoma brucei brucei*. *Eur J Biochem,* 241**,** 888-94.

BELLOFATTO, V. & PALENCHAR, J. B. 2008. RNA interference as a genetic tool in trypanosomes. *Methods Mol Biol,* 442**,** 83-94.

BENZ, C., NILSSON, D., ANDERSSON, B., CLAYTON, C. & GUILBRIDE, D. L. 2005. Messenger RNA processing sites in *Trypanosoma brucei*. *Mol Biochem Parasitol,* 143**,** 125-34.

BIEBINGER, S., WIRTZ, L. E., LORENZ, P. & CLAYTON, C. 1997. Vectors for inducible expression of toxic gene products in bloodstream and procyclic *Trypanosoma brucei*. *Mol Biochem Parasitol,* 85**,** 99-112.

BIENEN, E. J., MATURI, R. K., POLLAKIS, G. & CLARKSON, A. B., JR. 1993. Non-cytochrome mediated mitochondrial ATP production in bloodstream form *Trypanosoma brucei brucei*. *Eur J Biochem,* 216**,** 75-80.

BIENEN, E. J., WEBSTER, P. & FISH, W. R. 1991. Trypanosoma (Nannomonas) congolense: changes in respiratory metabolism during the life cycle. *Exp Parasitol,* 73**,** 403-12.

BOCHUD-ALLEMANN, N. & SCHNEIDER, A. 2002. Mitochondrial substrate level phosphorylation is essential for growth of procyclic *Trypanosoma brucei*. *J Biol Chem,* 277**,** 32849-54.

BOWLER, M. W., MONTGOMERY, M. G., LESLIE, A. G. & WALKER, J. E. 2006. How azide inhibits ATP hydrolysis by the F-ATPases. *Proc Natl Acad Sci U S A,* 103**,** 8646-9.

BREMS, S., GUILBRIDE, D. L., GUNDLESDODJIR-PLANCK, D., BUSOLD, C., LUU, V. D., SCHANNE, M., HOHEISEL, J. & CLAYTON, C. 2005. The transcriptomes of *Trypanosoma brucei* Lister 427 and TREU927 bloodstream and procyclic trypomastigotes. *Mol Biochem Parasitol,* 139**,** 163-72.

BRINGAUD, F., BARRETT, M. P. & ZILBERSTEIN, D. 2012. Multiple roles of proline transport and metabolism in trypanosomatids. *Front Biosci,* 17**,** 349-74.

BRINGAUD, F., RIVIERE, L. & COUSTOU, V. 2006. Energy metabolism of trypanosomatids: adaptation to available carbon sources. *Mol Biochem Parasitol,* 149**,** 1-9.

BRINGAUD, F., ROBINSON, D. R., BARRADEAU, S., BITEAU, N., BALTZ, D. & BALTZ, T. 2000. Characterization and disruption of a new *Trypanosoma brucei* repetitive flagellum protein, using double-stranded RNA inhibition. *Mol Biochem Parasitol,* 111**,** 283-97.

BROWN, G. C. 1992. Control of respiration and ATP synthesis in mammalian mitochondria and cells. *Biochem J,* 284 (Pt 1)**,** 1-13.

BROWN, S. V., HOSKING, P., LI, J. & WILLIAMS, N. 2006. ATP synthase is responsible for maintaining mitochondrial membrane potential in bloodstream form *Trypanosoma brucei*. *Eukaryot Cell,* 5**,** 45-53.

BRUN, R. & SCHONENBERGER 1979. Cultivation and in vitro cloning or procyclic culture forms of *Trypanosoma brucei* in a semi-defined medium. Short communication. *Acta Trop,* 36**,** 289-92.

CHAUDHURI, M., OTT, R. D. & HILL, G. C. 2006. Trypanosome alternative oxidase: from molecule to function. *Trends Parasitol,* 22**,** 484-91.

CHENNA, R., SUGAWARA, H., KOIKE, T., LOPEZ, R., GIBSON, T. J., HIGGINS, D. G. & THOMPSON, J. D. 2003. Multiple sequence alignment with the Clustal series of programs. *Nucleic Acids Res,* 31**,** 3497-500.

COLASANTE, C., ALIBU, V. P., KIRCHBERGER, S., TJADEN, J., CLAYTON, C. & VONCKEN, F. 2006. Characterization and developmentally regulated localization of the mitochondrial carrier protein homologue MCP6 from *Trypanosoma brucei. Eukaryot Cell,* 5**,** 1194-205.

COLASANTE, C., PENA DIAZ, P., CLAYTON, C. & VONCKEN, F. 2009. Mitochondrial carrier family inventory of *Trypanosoma brucei brucei:*

Identification, expression and subcellular localisation. *Mol Biochem Parasitol,* 167**,** 104-17.

DAUM, G., BOHNI, P. C. & SCHATZ, G. 1982. Import of proteins into mitochondria. Cytochrome *b2* and cytochrome *c* peroxidase are located in the intermembrane space of yeast mitochondria. *J Biol Chem,* 257**,** 13028-33.

DAYHOFF, M. O. & ORCUTT, B. C. 1979. Methods for identifying proteins by using partial sequences. *Proc Natl Acad Sci U S A,* 76**,** 2170-4.

DOLCE, V., FIERMONTE, G., MESSINA, A. & PALMIERI, F. 1991. Nucleotide sequence of a human heart cDNA encoding the mitochondrial phosphate carrier. *DNA Seq,* 2**,** 133-5.

DOLCE, V., IACOBAZZI, V., PALMIERI, F. & WALKER, J. E. 1994. The sequences of human and bovine genes of the phosphate carrier from mitochondria contain evidence of alternatively spliced forms. *J Biol Chem,* 269**,** 10451-60.

EID, J. & SOLLNER-WEBB, B. 1991. Stable integrative transformation of *Trypanosoma brucei* that occurs exclusively by homologous recombination. *Proc Natl Acad Sci U S A,* 88**,** 2118-21.

EMBLEY, T. M. & MARTIN, W. 2006. Eukaryotic evolution, changes and challenges. *Nature,* 440**,** 623-30.

ERNSTER, L. & SCHATZ, G. 1981. Mitochondria: a historical review. *J Cell Biol,* 91**,** 227s-255s.

FERREIRA, G. C., PRATT, R. D. & PEDERSEN, P. L. 1989. Energy-linked anion transport. Cloning, sequencing, and characterization of a full length cDNA encoding the rat liver mitochondrial proton/phosphate symporter. *J Biol Chem,* 264**,** 15628-33.

FIERMONTE, G., DOLCE, V. & PALMIERI, F. 1998. Expression in *Escherichia coli*, functional characterization, and tissue distribution of isoforms A and B of the phosphate carrier from bovine mitochondria. *J Biol Chem,* 273**,** 22782-7.

GALLO, R. L., FINKELSTEIN, J. N. & NOTTER, R. H. 1984. Characterization of the plasma and mitochondrial membrane potentials of alveolar type II cells by the use of ionic probes. *Biochim Biophys Acta,* 771**,** 217-27.

GIETZ, R. D. & WOODS, R. A. 2002. Transformation of yeast by lithium acetate/single-stranded carrier DNA/polyethylene glycol method. *Methods Enzymol,* 350**,** 87-96.

GLUENZ, E., POVELONES, M. L., ENGLUND, P. T. & GULL, K. 2011. The kinetoplast duplication cycle in *Trypanosoma brucei* is orchestrated by cytoskeleton-mediated cell morphogenesis. *Mol Cell Biol,* 31**,** 1012-21.

GNIPOVA, A., PANICUCCI, B., PARIS, Z., VERNER, Z., HORVATH, A., LUKES, J. & ZIKOVA, A. 2012. Disparate phenotypic effects from the knockdown of various *Trypanosoma brucei* cytochrome *c* oxidase subunits. *Mol Biochem Parasitol,* 184**,** 90-8.

GUALDRON-LOPEZ, M., BRENNAND, A., HANNAERT, V., QUINONES, W., CACERES, A. J., BRINGAUD, F., CONCEPCION, J. L. & MICHELS, P. A. 2012. When, how and why glycolysis became compartmentalised in the Kinetoplastea. A new look at an ancient organelle. *International journal for parasitology,* 42**,** 1-20.

GUERRA, D. G., DECOTTIGNIES, A., BAKKER, B. M. & MICHELS, P. A. 2006. The mitochondrial FAD-dependent glycerol-3-phosphate dehydrogenase of Trypanosomatidae and the glycosomal redox balance of insect stages of *Trypanosoma brucei* and *Leishmania spp*. *Mol Biochem Parasitol,* 149**,** 155-69.

GUTIERREZ, T., MORRIS, G. & GREEN, D. H. 2009. Yield and physicochemical properties of EPS from Halomonas sp. strain TG39 identifies a role for protein and anionic residues (sulfate and phosphate) in emulsification of n-hexadecane. *Biotechnol Bioeng,* 103**,** 207-16.

HAFERKAMP, I. & SCHMITZ-ESSER, S. 2012. The plant mitochondrial carrier family: functional and evolutionary aspects. *Front Plant Sci,* 3**,** 2.

HALESTRAP, A. P. 2009. What is the mitochondrial permeability transition pore? *J Mol Cell Cardiol,* 46**,** 821-31.

HALESTRAP, A. P. 2010. A pore way to die: the role of mitochondria in reperfusion injury and cardioprotection. *Biochem Soc Trans,* 38**,** 841-60.

HAMEL, P., SAINT-GEORGES, Y., DE PINTO, B., LACHACINSKI, N., ALTAMURA, N. & DUJARDIN, G. 2004. Redundancy in the function of mitochondrial phosphate transport in *Saccharomyces cerevisiae* and *Arabidopsis thaliana*. *Mol Microbiol,* 51**,** 307-17.

HANADA, H., KATSU, K., KANNO, T., SATO, E. F., KASHIWAGI, A., SASAKI, J., INOUE, M. & UTSUMI, K. 2003. Cyclosporin A inhibits thyroid hormone-induced shortening of the tadpole tail through membrane permeability transition. *Comp Biochem Physiol B Biochem Mol Biol,* 135**,** 473-83.

HASHIMOTO, M., SHINOHARA, Y., MAJIMA, E., HATANAKA, T., YAMAZAKI, N. & TERADA, H. 1999. Expression of the bovine heart mitochondrial ADP/ATP carrier in yeast mitochondria: significantly enhanced expression by replacement of the N-terminal region of the bovine carrier by the corresponding regions of the yeast carriers. *Biochimica et biophysica acta,* 1409**,** 113-24.

HATEFI, Y. 1985. The mitochondrial electron transport and oxidative phosphorylation system. *Annu Rev Biochem,* 54**,** 1015-69.

HIRUMI, H. & HIRUMI, K. 1989. Continuous cultivation of *Trypanosoma brucei* blood stream forms in a medium containing a low concentration of serum protein without feeder cell layers. *J Parasitol,* 75**,** 985-9.

HUSON, D. H. 1998. SplitsTree: analyzing and visualizing evolutionary data. *Bioinformatics,* 14**,** 68-73.

ISENBERG, J. S. & KLAUNIG, J. E. 2000. Role of the mitochondrial membrane permeability transition (MPT) in rotenone-induced apoptosis in liver cells. *Toxicol Sci,* 53**,** 340-51.

JENSEN, R. E. & ENGLUND, P. T. 2012. Network news: the replication of kinetoplast DNA. *Annu Rev Microbiol,* 66**,** 473-91.

KENNEDY, E. P. & LEHNINGER, A. L. 1949. Oxidation of fatty acids and tricarboxylic acid cycle intermediates by isolated rat liver mitochondria. *J Biol Chem,* 179**,** 957-72.

KNIRSCH, M., GAWAZ, M. P. & KLINGENBERG, M. 1989. The isolation and reconstitution of the ADP/ATP carrier from wild-type *Saccharomyces cerevisiae*. Identification of primarily one type (AAC-2). *FEBS Lett,* 244**,** 427-32.

KOHL, L. & BASTIN, P. 2005. The flagellum of trypanosomes. *Int Rev Cytol,* 244**,** 227-85.

KRAMER, R. 1996. Structural and functional aspects of the phosphate carrier from mitochondria. *Kidney Int,* 49**,** 947-52.

KRUMSCHNABEL, G., MANZL, C., BERGER, C. & HOFER, B. 2005. Oxidative stress, mitochondrial permeability transition, and cell death in Cu-exposed trout hepatocytes. *Toxicol Appl Pharmacol,* 209**,** 62-73.

KUNJI, E. R. 2004. The role and structure of mitochondrial carriers. *FEBS Lett,* 564**,** 239-44.

LAMOUR, N., RIVIERE, L., COUSTOU, V., COOMBS, G. H., BARRETT, M. P. & BRINGAUD, F. 2005. Proline metabolism in procyclic *Trypanosoma brucei* is down-regulated in the presence of glucose. *J Biol Chem,* 280**,** 11902-10.

LEMASTERS, J. J., THERUVATH, T. P., ZHONG, Z. & NIEMINEN, A. L. 2009. Mitochondrial calcium and the permeability transition in cell death. *Biochim Biophys Acta,* 1787**,** 1395-401.

LEUNG, A. W., VARANYUWATANA, P. & HALESTRAP, A. P. 2008. The mitochondrial phosphate carrier interacts with cyclophilin D and may play a key role in the permeability transition. *J Biol Chem,* 283**,** 26312-23.

MANON, S. & GUERIN, M. 1988. Modifications of oxidative phosphorylations in mitochondria isolated from a mutant of *Saccharomyces cerevisiae.* Possible alterations of the phosphate transport. *Eur J Biochem,* 172**,** 205-11.

MATTHEWS, K. R., ELLIS, J. R. & PATEROU, A. 2004. Molecular regulation of the life cycle of African trypanosomes. *Trends Parasitol,* 20**,** 40-7.

MCBRIDE, H. M., NEUSPIEL, M. & WASIAK, S. 2006. Mitochondria: more than just a powerhouse. *Curr Biol,* 16**,** R551-60.

MICHELS, P. A., BRINGAUD, F., HERMAN, M. & HANNAERT, V. 2006. Metabolic functions of glycosomes in trypanosomatids. *Biochim Biophys Acta,* 1763**,** 1463-77.

MIEDLICH, S. U., ZALUTSKAYA, A., ZHU, E. D. & DEMAY, M. B. 2010. Phosphate-induced apoptosis of hypertrophic chondrocytes is associated with a decrease in mitochondrial membrane potential and is dependent upon Erk1/2 phosphorylation. *J Biol Chem,* 285**,** 18270-5.

OVERATH, P., CZICHOS, J. & HAAS, C. 1986. The effect of citrate/cis-aconitate on oxidative metabolism during transformation of *Trypanosoma brucei. Eur J Biochem,* 160**,** 175-82.

PALADE, G. E. 1952. The fine structure of mitochondria. *Anat Rec,* 114**,** 427-51.

PALMIERI, F. 2004. The mitochondrial transporter family (SLC25): physiological and pathological implications. *Pflugers Arch,* 447**,** 689-709.

PALMIERI, F., PIERRI, C. L., DE GRASSI, A., NUNES-NESI, A. & FERNIE, A. R. 2011. Evolution, structure and function of mitochondrial carriers: a review with new insights. *Plant J,* 66**,** 161-81.

PANIGRAHI, A. K., OGATA, Y., ZIKOVA, A., ANUPAMA, A., DALLEY, R. A., ACESTOR, N., MYLER, P. J. & STUART, K. D. 2009. A comprehensive analysis of *Trypanosoma brucei* mitochondrial proteome. *Proteomics,* 9**,** 434-50.

PANIGRAHI, A. K., ZIKOVA, A., DALLEY, R. A., ACESTOR, N., OGATA, Y., ANUPAMA, A., MYLER, P. J. & STUART, K. D. 2008. Mitochondrial complexes in *Trypanosoma brucei:* a novel complex and a unique oxidoreductase complex. *Mol Cell Proteomics,* 7**,** 534-45.

PENA-DIAZ, P., PELOSI, L., EBIKEME, C., COLASANTE, C., GAO, F., BRINGAUD, F. & VONCKEN, F. 2012. Functional Characterization of TbMCP5, a Conserved and Essential ADP/ATP Carrier Present in the Mitochondrion of the Human Pathogen *Trypanosoma brucei. J Biol Chem,* 287**,** 41861-74.

PRATT, R. D., FERREIRA, G. C. & PEDERSEN, P. L. 1991. Mitochondrial phosphate transport. Import of the H+/Pi symporter and role of the presequence. *J Biol Chem,* 266**,** 1276-80.

PRIEST, J. W. & HAJDUK, S. L. 1994. Developmental regulation of mitochondrial biogenesis in *Trypanosoma brucei. J Bioenerg Biomembr,* 26**,** 179-91.

PRIETO, S., BOUILLAUD, F. & RIAL, E. 1995. The mechanism for the ATP-induced uncoupling of respiration in mitochondria of the yeast *Saccharomyces cerevisiae*. *Biochem J,* 307 (Pt 3)**,** 657-61.

ROBINSON, A. J. & KUNJI, E. R. 2006. Mitochondrial carriers in the cytoplasmic state have a common substrate binding site. *Proc Natl Acad Sci U S A,* 103**,** 2617-22.

RUNSWICK, M. J., POWELL, S. J., NYREN, P. & WALKER, J. E. 1987. Sequence of the bovine mitochondrial phosphate carrier protein: structural relationship to ADP/ATP translocase and the brown fat mitochondria uncoupling protein. *EMBO J,* 6**,** 1367-73.

SAITOU, N. & NEI, M. 1987. The neighbor-joining method: a new method for reconstructing phylogenetic trees. *Mol Biol Evol,* 4**,** 406-25.

SAMBROOK J, F. E., AND MANIATIS T 1989. *Molecular cloning: A Laboratory Manual,* Cold Spring Harbour, New York, Cold Spring Harbour Laboratoay.

SCHNEIDER, A., BOUZAIDI-TIALI, N., CHANEZ, A. L. & BULLIARD, L. 2007. ATP production in isolated mitochondria of procyclic *Trypanosoma brucei. Methods Mol Biol,* 372**,** 379-87.

SCHROERS, A., BURKOVSKI, A., WOHLRAB, H. & KRAMER, R. 1998. The phosphate carrier from yeast mitochondria. Dimerization is a prerequisite for function. *J Biol Chem,* 273**,** 14269-76.

SCOTT, I. & LOGAN, D. C. 2008. Mitochondrial morphology transition is an early indicator of subsequent cell death in *Arabidopsis*. *New Phytol,* 177**,** 90-101.

SHABALINA, I. G., KRAMAROVA, T. V., NEDERGAARD, J. & CANNON, B. 2006. Carboxyatractyloside effects on brown-fat mitochondria imply that the adenine nucleotide translocator isoforms ANT1 and ANT2 may be responsible for basal and fatty-acid-induced uncoupling respectively. *Biochem J,* 399**,** 405-14.

STAPPEN, R. & KRAMER, R. 1993. Functional properties of the reconstituted phosphate carrier from bovine heart mitochondria: evidence for asymmetric orientation and characterization of three different transport modes. *Biochim Biophys Acta,* 1149**,** 40-8.

STAPPEN, R. & KRAMER, R. 1994. Kinetic mechanism of phosphate/phosphate and phosphate/OH- antiports catalyzed by reconstituted phosphate carrier from beef heart mitochondria. *J Biol Chem,* 269**,** 11240-6.

SWIEGERS, J. H., VAZ, F. M., PRETORIUS, I. S., WANDERS, R. J. & BAUER, F. F. 2002. Carnitine biosynthesis in Neurospora crassa: identification of a cDNA coding for epsilon-N-trimethyllysine hydroxylase and its functional expression in *Saccharomyces cerevisiae*. *FEMS Microbiol Lett,* 210**,** 19-23.

TAKABATAKE, R., HATA, S., TANIGUCHI, M., KOUCHI, H., SUGIYAMA, T. & IZUI, K. 1999. Isolation and characterization of cDNAs encoding mitochondrial phosphate transporters in soybean, maize, rice, and Arabidopis. *Plant Mol Biol,* 40**,** 479-86.

TAKABATAKE, R., SIDDIQUE, A. B., KOUCHI, H., IZUI, K. & HATA, S. 2001. Characterization of a *Saccharomyces cerevisiae* gene that encodes a mitochondrial phosphate transporter-like protein. *J Biochem,* 129**,** 827-33.

TRUSCOTT, K. N., VOOS, W., FRAZIER, A. E., LIND, M., LI, Y., GEISSLER, A., DUDEK, J., MULLER, H., SICKMANN, A., MEYER, H. E., MEISINGER, C., GUIARD, B., REHLING, P. & PFANNER, N. 2003. A J-protein is an essential subunit of the presequence translocase-associated protein import motor of mitochondria. *J Cell Biol,* 163**,** 707-13.

VAN HELLEMOND, J. J., OPPERDOES, F. R. & TIELENS, A. G. 2005. The extraordinary mitochondrion and unusual citric acid cycle in *Trypanosoma brucei. Biochem Soc Trans,* 33**,** 967-71.

VAN WILPE, S., BOUMANS, H., LOBO-HAJDU, G., GRIVELL, L. A. & BERDEN, J. A. 1999. Functional complementation analysis of yeast bc1 mutants. A study of the mitochondrial import of heterologous and hybrid proteins. *Eur J Biochem,* 264**,** 825-32.

VANLERBERGHE, G. C. & MCINTOSH, L. 1997. ALTERNATIVE OXIDASE: From Gene to Function. *Annu Rev Plant Physiol Plant Mol Biol,* 48**,** 703-734.

VARANYUWATANA, P. & HALESTRAP, A. P. 2012. The roles of phosphate and the phosphate carrier in the mitochondrial permeability transition pore. *Mitochondrion,* 12**,** 120-5.

VASILYEVA, E. A., MINKOV, I. B., FITIN, A. F. & VINOGRADOV, A. D. 1982. Kinetic mechanism of mitochondrial adenosine triphosphatase. Inhibition by azide and activation by sulphite. *Biochem J,* 202**,** 15-23.

VASSELLA, E., STRAESSER, K. & BOSHART, M. 1997. A mitochondrion-specific dye for multicolour fluorescent imaging of *Trypanosoma brucei. Mol Biochem Parasitol,* 90**,** 381-5.

VAZ, F. M., HOUTKOOPER, R. H., VALIANPOUR, F., BARTH, P. G. & WANDERS, R. J. 2003. Only one splice variant of the human TAZ gene encodes a functional protein with a role in cardiolipin metabolism. *J Biol Chem,* 278**,** 43089-94.

VONCKEN, F., VAN HELLEMOND, J. J., PFISTERER, I., MAIER, A., HILLMER, S. & CLAYTON, C. 2003. Depletion of GIM5 causes cellular fragility, a decreased glycosome number, and reduced levels of ether-linked phospholipids in trypanosomes. *J Biol Chem,* 278**,** 35299-310.

WIRTZ, E., LEAL, S., OCHATT, C. & CROSS, G. A. 1999. A tightly regulated inducible expression system for conditional gene knock-outs and dominant-negative genetics in *Trypanosoma brucei. Mol Biochem Parasitol,* 99**,** 89-101.

ZARA, V., DIETMEIER, K., PALMISANO, A., VOZZA, A., RASSOW, J., PALMIERI, F. & PFANNER, N. 1996. Yeast mitochondria lacking the phosphate carrier/p32 are blocked in phosphate transport but can import preproteins after regeneration of a membrane potential. *Mol Cell Biol,* 16**,** 6524-31.

ZIKOVA, A., SCHNAUFER, A., DALLEY, R. A., PANIGRAHI, A. K. & STUART, K. D. 2009. The F(0)F(1)-ATP synthase complex contains novel subunits and is essential for procyclic *Trypanosoma brucei. PLoS Pathog,* 5**,** e1000436.

Chapter IV

The phosphoarginine energy-buffering system of *Trypanosoma brucei* is essential for survival and involves multiple arginine kinase isoforms with different subcellular locations

The contents of this chapter have been published.

Gao F, Voncken F, Wadforth C, Harley M, Colasante C. 2013. PLoS One.

8(6):e65908

The work presented in this chapter was started with Dr Claudia Colasante, Dr Frank Voncken and Mrs. Cath Wadforth in this laboratory. Dr Claudia Colasante and Dr Frank Voncken did the arginine kinase sequence analysis and started the protein purification and arginine kinase activity assay. Mrs Cath Wadforth helped to preparing medium, buffers and gels. Maggie Harley conducted the HPLC experiment for phosphoarginine synthesis analysis. I carried out the work of *TbAK* RNA interference, flagellar targeting signal analysis of N-terminal extension of TbAK1 using GFP-fusion protein and the following arginine kinase activity assay and growth analysis.

1. Introduction

Virtually all eukaryotes contain energy buffering systems for the regulation of their energy homeostasis in periods of high-energy demand or energy supply fluctuations. The majority of these systems depend on phosphagen kinases that catalyse the reversible and ATP-dependent phosphorylation of guanidino acceptor compounds (Ellington, 2001, Wallimann et al., 1992). The formed high-energy phosphagens are relatively small and highly diffusible molecules that provide fast energy supply when energy consumption becomes critical (Ellington, 2001). In addition, they stabilise the cellular ATP/ADP ratios and function as a temporal and spatial energy buffer in the cell (Wallimann et al., 1992). The two most widely distributed energy buffering systems depend on the phosphorylation of creatine or arginine, with phosphocreatine/creatine kinases predominantly found in vertebrates and sponges, and phosphoarginine/arginine kinases mainly present in invertebrate organisms (Ellington, 2001, Wallimann et al., 1992). Their expression in these multicellular eukaryotes was shown to be tissue specific (Ellington, 2001, Wallimann et al., 1992). Also unicellular eukaryotes contain similar energy buffering systems, with phosphoarginine/ arginine kinase systems described for the ciliates *Paramecium caudatum* and *Tetrahymena pyriformis*, the choanoflagellate *Monosiga brevicollis*, as well as for some Kinetoplastida (Watts and Bannister, 1970, Noguchi et al., 2001, Hoffman and Ellington, Pereira et al., 2000, Pereira et al., Canepa et al., 2011). The Kinetoplastida order contains medically and veterinarily important protozoa, such as *Trypanosoma cruzi*, *Trypanosoma brucei* and *Leishmania major* (Vickerman, 1985). *T. cruzi* is an obligate intracellular parasite and is the causative agent of Chagas disease (Boscardin et al.), while the closely related *Trypanosoma brucei*, an exclusively extracellular parasite, is the causative agent of African trypanosomiasis

(Malvy and Chappuis). Both parasites have a digenetic life cycle and are transmitted by insect vectors (Boscardin et al.) (Malvy and Chappuis). The life cycle of *T. brucei* alternates between the bloodstream form (BSF) found in the blood and tissue fluids of mammals, and the procyclic form (PCF) in the mid-gut of the tsetse fly. During differentiation and the transition from one host to the other, substantial changes in the energy metabolism take place, which allow adaptation of the parasite to the distinct host environments (Matthews, 2005, Bringaud et al., 2006, Fenn and Matthews, 2007, Michels, 1989, van Hellemond et al., 2005). This metabolic transition is accompanied by fluctuations in cellular energy supply and periods of energy shortage, implying the requirement of an energy buffering system. Kinetoplastid arginine kinases have so far only been functionally characterised for *T. cruzi* (Pereira et al., 2011, Canepa et al., 2011). Its genome harbours only one functional arginine kinase-coding gene, i.e. TcCLB.507241.30 (Pereira et al., 2011, Canepa et al., 2011). TcCLB.507241.30 is expressed in the different life cycle stages of *T. cruzi* and is exclusively located in the cytosol of the parasite (Miranda et al., 2009). Exposure of *T. cruzi* epimastigotes to oxidative challenging compounds such as hydrogen peroxide lead to a significantly increased survival capacity upon increased expression of TcCLB.507241.30, suggesting a possible role of this arginine kinase in cellular oxidative stress response (Pereira et al., 2003, Miranda et al., 2006). The genome analysis of the closely related kinetoplastid *T. brucei* contains not one but three different arginine kinase-coding genes, indicating that its energy buffering system is more complex than the one reported for *T. cruzi* (Berriman et al., 2005, Pereira et al., 2011). Here I describe the molecular and functional characterisation of the *T. brucei* phosphoarginine/arginine kinase system, and its important function in the energy metabolism of this kinetoplastid parasite.

2. Materials and methods

2.1 Sequence analysis (performed by Dr Claudia Colasante)

GeneDB (http://www.genedb.org) and NCBI (http://www.ncbi.nlm.nih.gov) accession numbers of the different arginine kinase sequences used for sequence alignment are: TcCLB.507241.30 [*T. cruzi*]; TbAK1, Tb927.9.6170 [*T. brucei*]; TbAK2, Tb927.9.6230 [*Trypanosoma brucei*]; TbAK3, Tb927.9.6290 [*Trypanosoma brucei*]; *C.maenes*, AF167313 [*Carcinus maenas*]; *H.gammarus*, CAA48654.1 [*Homarus gammarus*]; *A.mellifera*, NP_001011603.1 [*Apis mellifera*]; *D.melanogaster*, NP_729446.1 [*Drosophila melanogaster*]; *B.cornutus*, BAA22870.1 [*Batillus cornutus*]; and *O.vulgaris*, BAA95609.1 [*Octopus vulgaris*]. Sequence alignment was obtained using ClustalW2 (www.ebi.ac.uk (Chenna et al., 2003)), which was manually optimized using the Sequence Alignment Editor v2.0a11 program available at http://tree.bio.ed.ac.uk/software.

2.2 Isolation of recombinant TbAK1-nHis (this work has been done jointly with Dr Claudia Colasante)

The open reading frame of *TbAK1* (Tb927.9.6170) was PCR-amplified using the sense primer 5'-GGACGGCATATGGGCTTCGGATCATCAAAA CC-3' and the antisense primer 5'GCTTGCAGGATCCTT CATTTTCATTCGTGGCTACACCGTCTAC-3'. The PCR product was cloned into the bacterial expression vector pET16b (Invitrogen) using the restriction sites *Nde*I and *Bam*HI included in the primer sequences (underlined). Expression from pET16b results in the addition of 10 N-terminal histidine residues to the protein. The resulting plasmid was used for transformation of *E. coli* BL21 (DE3). Protein expression was induced in TB medium supplemented with 10 mM malate and 10 mM pyruvate at 37°C by addition of final concentration at 1 mM of IPTG at an OD_{600nm} of 0.4. The IPTG-induced culture was grown for 3 hours, after which the

bacteria were harvested by centrifugation at 5000x g for 15 minutes. The cell pellet was resuspended in Talon-Binding and Washing Buffer containing 50 mM Na-Phosphate pH 8.0, 300 mM NaCl, 0.01% v/v Tween-20, and protease inhibitor (Roche), lysozyme (200 µg/ml) and DNaseI (10µg/ml), followed by incubation for 30 minutes at 4°C. Cells were lysed using a French Press and intact cells were spun down for 15 minutes at 5000 xg and 4°C. The supernatant was incubated for 30 minutes at 4°C with magnetic Talon Dynabeads, pre-equilibrated in Talon-Binding and Washing Buffer according to the manufacturer's protocol (Dynal Biotech). The supernatant was removed and the dynabeads were washed 5 times with Binding and Washing Buffer. TbAK1-nHis was finally eluted using Talon Elution Buffer (150 mM Imidazole, 50 mM Na-Phosphate buffer pH8.0, 300 mM NaCl, and 0.01% v/v Tween-20).

2.3 Measurement of arginine kinase activity

For the measurement of total cellular arginine kinase activity, cell lysates were prepared by re-suspending $1x10^8$ trypanosomes in 200 µl of 50 mM Tris-HCl pH 7.5 and performing 2 subsequent freeze-thawing cycles. Arginine kinase activity was measured in the forward direction (phosphoarginine formation) using an established coupled enzyme assay (Binder et al., 2001). The assay mixture contained: total trypanosome cell lysate (10 µg protein) or purified TbAK1-nHis protein, 50 mM Tris-acetate pH8.6, 5 mM magnesium acetate, 50 mM ammonium acetate, 0.75 mM phosphoenolpyruvate, 0.45 mM NADH, 0.8 mM ATP, and 2 mM arginine. The assay mixture was incubated at either 37 °C or 28 °C, and the reaction was started by the addition of pyruvate kinase (5 units) and lactate dehydrogenase (5 units). NADH consumption was measured using a spectrophotometer at 340 nm: for each mole of NADH consumed, one mole of phosphoarginine is produced. The data are expressed as mean ± standard deviation.

2.4 Phosphoarginine synthesis and analysis (performed together with Dr Claudia Colasante)

Phosphoarginine was synthesized using the forward arginine kinase reaction (see above) in the presence of purified TbAK1-nHis. Phosphoarginine formation was analysed by HPLC as described previously (performed together with Dr. Claudia Colasante and Maggie Harley) (Viant et al., 2001). The used HPLC configuration consisted of an Agilent 1100 HPLC system including an ALS injector, a DAD detector, a quaternary pump and a fraction collector. Samples were separated on a SP2 Hypersil column (250 mm x 4.6 mm, 5µm particle size) in combination with a Phenomenex guard column containing an ID NH2 cartridge (4 x 3.0mm). Separation was isocratic at 25 °C using 72% (v/v) 20 mM phosphate buffer (pH 2.6) and 28% (v/v) acetonitrile as mobile phase and a flow rate of 1 mL/min. The DAD detector was set at 205 nm, with the reference set to 360 nm. 50 µl of arginine kinase reaction mixture was injected per run. The phosphoarginine-containing peak, with an expected retention time of 5.5 minutes (Viant et al., 2001), was collected and freeze-dried to remove acetonitril. The obtained residue powder was solved in 100 µl ultrapure H_2O and subsequently analysed for the presence of phosphoarginine using the reverse arginine kinase coupled enzyme reaction. The reverse arginine kinase reaction mixture contained: variable amounts of phosphoarginine peak fraction, 50 mM Tris-acetate pH 8.6, 5 mM magnesium acetate, 50 mM ammonium acetate and 1 mM ADP. The reaction was started by addition of 5 µg of the purified TbAK1-nHis enzyme and the formation of ATP was quantified *in situ* using the ATP Bioluminescence CLS II Assay Kit (Roche Applied Science) and a Junior LB9509 tube luminometer (Berthold Technologies).

2.5 Trypanosome culture

Proyclic form (PCF) and bloodstream form (BSF) *Trypanosoma brucei* strain 449 were cultured in MEM-PROS (Overath et al., 1986) and HMI-9 (Hirumi and Hirumi, 1989) medium, respectively. Phleomycin (5 $\mu g.mL^{-1}$) was added to the culture medium to maintain stable expression of the tetracycline repressor from plasmid pHD449 (Biebinger et al., 1997). The PCF cell line EATRO1125.T7T was cultured in SDM79 medium in the presence of G418 (10 $\mu g.mL^{-1}$) and hygromycin (25 $\mu g.mL^{-1}$) to maintain stable expression of the tetracycline repressor and T7 RNA polymerase from plasmids pLew90/Neo and pHD328 (Bringaud et al., 2000). All media were supplemented with 10% (v/v) foetal calf serum (Sigma-Aldrich).

2.6 Western blot analysis

Trypanosome cells were harvested at mid-logarithmic phase densities of $1x10^6$ $cells.mL^{-1}$ (BSF) and $1x10^7$ $cells.mL^{-1}$ (PCF) for protein analysis. 2×10^6 trypanosomes were pelleted for each lane, resuspended in denaturing SDS-containing Laemmli buffer, and the sample denatured for 5 min at 95°C. Proteins were separated on a denaturing 12% sodium dodecylsulfate-containing polyacrylamide gel (SDS-PAGE), and subsequently transferred to a Hybond-P membrane (GE Healthcare Life Sciences) in transfer buffer (39 mM glycine, 48 mM Tris-base, 20% v/v methanol, pH 8.3) for 1 h at 100 V. The membrane was blocked by a 30 min incubation at room temperature in Tris–buffered saline (TBS) containing 0.2% (v/v) Tween 20 (TBS-T) supplemented with 7.5% (w/v) non-fat dry milk with gentle shaking, and subsequently incubated for 1h in TBS-T containing 7.5% milk and the primary antibody (diluted 1:1000). The membrane was then washed once for 15 min, and twice for 5 min in TBS-T, followed by incubation for 45 min at room temperature with the respective secondary antibody (GE Healthcare Life Sciences). The

membrane was washed once for 15 min, and four times for 5 min in TBS-T. Finally, the membrane was processed according to the manufacturer's protocol of the ECL detection kit, followed by exposure to ECL-film (GE Health Care Life Sciences).

2.7 Northern blot analysis

Trypanosome cells were harvested at mid-logarithmic phase densities of $1x10^6$ cells.mL^{-1} (BSF) and $1x10^7$ cells.mL^{-1} (PCF) RNA analysis. Total RNA was isolated from BSF and PCF *T. brucei* strain 449 using the RNeasy Mini Kit (Qiagen). RNA was separated on a denaturing formaldehyde-containing agarose gel, and transferred to a Hybond-N membrane (GE Healthcare). The different *TbAK* 3'-UTRs (300bp downstream of stop codon) were used as DNA-probes for hybridisation. [^{32}P]-dCTP labelled DNA probes were PCR-amplified using 5'-ctaggatccggtgagggtgatgcattgtt-3' (sense) and 5'-ctagg gccctgaacaaccctacaaaatctctctc-3' (antisense) for *TbAK1*; 5'-atcggatccgttctttcctttctttcatacatttcc-3' (sense) and 5'-atcgggcccagaggattcgaaaagcgtaatcgga acagttg-3' (antisense) for *TbAK2*; and 5'-ggacgg aagcttaccatggctacccgcgacgttgctgc-3' (sense) and 5'-gcttgcaggatcccttcgacttct ccagtttgatgagctcaag-3' (anti-sense) for *TbAK3*. RNA blots were pre-hybridized in hybridization solution (5xSSC, 5xDenhardt´s reagent, and 0.5% w/v sodium dodecyl sulphate (SDS)) for 1h at 65°C, followed by the addition of the [^{32}P]-dCTP labelled DNA probes and overnight hybridization at 65°C. The blots were washed at 65°C in subsequently 1x SSC (0.15 M NaCl, 0.015 M sodium citrate) supplemented with 0.1% w/v SDS and 0.1xSSC supplemented with 0.1% w/v SDS, followed by exposure to X-ray film (Kodak).

2.8 Expression of myc-tagged TbAK1-3

The open reading frames of TbAK1-3 were PCR-amplified using genomic DNA from T. brucei strain 449 as template, and the primers 5'-ggacggaagcttac

catgggcttcggatcatcaaaacc-3’ (sense) and 5’-gcttgcaggatccttcattttcattcgtggctacaccgtctac-3’ (antisense) for TbAK1; 5’-ggacggaagcttaccatggctacccgcgacgttgct gc-3’ (sense) and 5’-gcttgcaggatcccaagttcgaaccaa caaatggtttggcgc-3’ (antisense) for TbAK2; and 5’-ggacggaagcttaccatggctacccgcgacgttgctgc-3’ (sense) and 5’-gcttgcaggatcccttcgacttctccagtttgatgagctcaag-3’ (antisense) for *TbAK3*. The restriction enzyme sites *Hin*dIII (sense primers) and *Bam*HI (antisense primers) are underlined and were used for subsequent cloning into the trypanosome expression vectors pHU1 or pHU2 (Colasante et al., 2009). Comparison of the cloned *TbAK1-3* sequences from *T. brucei* strain 449 with the sequences of the corresponding loci in the genome sequence database of *T. brucei* strain 927 (available at http://www.genedb.org) revealed only a few sequence differences at the DNA level, but none in the predicted amino acid sequences. The *T. brucei* expression vectors pHU1 and pHU2 are derived from pHD1700 and pHD1701 (Colasante et al., 2009), respectively, and contain next to the unique *Not*I restriction enzyme cleavage site two additional unique sites, i.e. *Pme*I and *Bcl*I, which can be used for linearization of the plasmids and subsequent trypanosome transfection. Tetracycline-inducible expression from these vectors will result in the addition of a 2xmyc tag to either the C-terminal (pHU1 expression vector) or N-terminal (pHU2 expression vector) end of the expressed protein. The resulting plasmids were used for transfection of PCF and BSF *T. brucei* strain 449, constitutively expressing the tet-repressor (*TETR BLE*) (Biebinger et al., 1997). Trypanosomes were transfected and clonal cell lines isolated as described previously (Biebinger et al., 1997). Trypanosome clones resistant to the hygromycin and bearing a tetracycline-inducible and 2xmyc-tagged ectopic copy of the *TbAK1-3* isoforms were isolated and subsequently analysed by western blotting using a commercial myc

antibody (Roche Applied Science). Expression of the different N-terminal (nmyc) or C-terminal (cmyc) myc-tagged TbAK isoforms was induced by the addition of tetracycline (0.5μg mL^{-1}).

2.9 Immunofluorescence microscopy

PCF and BSF trypanosomes were centrifuged from culture medium at 2,000x g and resuspended in phosphate-buffered saline (PBS) containing 4% w/v paraformaldehyde. Fixed cells were allowed to settle down and attach to poly-L-lysine-coated microscope slides. Immunofluorescent labelling of trypanosomes with 4',6'-diamidino-2-phenylindole (DAPI, DNA-staining) and the different antibodies (see figure legends) was performed as previously described (Voncken et al., 2003) (Colasante et al., 2006, Colasante et al., 2009). Cells were examined using a Leica DM RXA digital de-convolution microscope and images recorded using a digital camera (Hamamatsu).

2.10 RNA interference

Expression of all *TbAK* isoforms was down regulated (silenced) in PCF *T. brucei* by RNA-interference, using the conserved central part of *TbAK1-3* as target sequence. The primers 5'-ggaagcttgacgttgatccggaaggtaa-3' and 5'-cactcgagctctt cattcacccacacgag-3' were used for PCR amplification of the 342 bp sense sequence and the primers 5'-caggatccgacgttgatccggaaggtaa-3' and 5'-cgaagctttcc ctcgagttcactgccttcacaagacg-3' were used for the corresponding 398 bp antisense sequence. The resulting sense and antisense *TbAK* sequences were cloned into the *T. brucei* expression vector *pLew100*, using the unique restriction enzyme sites (underlined) included in the primers (Bringaud et al., 2000). The resulting *pLew100-TbAK* RNAi construct contains a phleomycin resistance gene, with the consecutively cloned sense and antisense *TbAK* target sequences separated by a 50 bp spacer

fragment. Inducible expression is under control of the procyclic acidic repetitive protein (PARP) promoter linked to a prokaryotic tetracycline (tet) operator. The *pLew100-TbAK* RNAi construct was used for transfection of procyclic form *T. brucei* EATRO1125.T7T (Bringaud et al., 2000). The ^{RNAi}*TbAK* cell line was obtained after clonal selection in SDM79 medium containing hygromycin (25 μg.mL^{-1}), neomycin (10 μg.mL^{-1}) and phleomycin (5 μg.mL^{-1}). Addition of tetracycline (0.5 μg.mL^{-1}) will lead to the expression of double-stranded *TbAK* RNA molecules and the concomitant down-regulation (silencing) of all TbAK isoforms.

Depletion of the different TbAK isoforms was assessed at the mRNA level by reverse transcriptase-directed cDNA synthesis and PCR. For this purpose, total RNA (30 μg per sample) was isolated, which was subsequently treated with DNase with final concentration at 10μg/ml at 37°C for 20 minutes to remove contaminating genomic DNA. The reaction was stopped by addition of 8 mM EDTA, followed by an incubation for 20 minutes at 75°C. mRNA was converted to cDNA by using an oligo(dT)18 primer, Maxima Reverse Transcriptase and in the presence of Ribolock RNase inhibitor as described in the manufacturer's protocol (Fermentas). The reverse transcriptase reaction was stopped by incubation at 85°C for 5 minutes. The above described primer combinations were used for the specific PCR-amplification of the different TbAK1-3 isoforms.

2.11 Growth analysis (this work has been done together with Dr Claudia C)

Cultures of PCF and BSF trypanosomes were diluted to a density of 0.5 x 10^6 cells.mL^{-1} and 0.25 x 10^6 cells.mL^{-1}, respectively, at the start of the experiment. Cell densities were determined every 24 hours for a total of 72 hours, using a Neubauer haemocytometer. Expression of the different myc-tagged TbAK isoforms was

induced by addition of tetracycline (0.5 μg.mL^{-1}) to the culture medium 24 hours prior to the start of the experiment. Cell lines were continuously grown in the presence of 0.5μg mL^{-1} tetracycline to maintain expression of the recombinant myc-tagged isoforms. To analyse TbAK expression and growth under oxidative stress conditions, trypanosomes were cultured in the presence of 10 μM (PCF) and 200 μM (BSF) of hydrogen peroxide, respectively.

3. Results

3.1 Sequence analysis

BLASTP sequence analysis, using the *T. cruzi* arginine kinase TcCLB.507241.30 (Pereira et al., 2011) as query, resulted in the identification of three arginine kinase-coding genes in the genome database of *T. brucei* strain Lister 927 (www.genedb.com): Tb927.9.6170, Tb927.9.6230 and Tb927.9.6290, abbreviated to respectively TbAK1, TbAK2 and TbAK3. Alignment (Fig. 1) revealed a high degree of sequence similarity between the different trypanosome arginine kinases (85-99%) and selected arginine kinases from invertebrates, including the crustaceans *Carcinus maenas* (86% similarity to TbAK1) and *Homarus gammarus* (86%), and the insects *Drosophila melanogaster* (84%) and *Apis mellifera* (88%). Sequence analysis showed further that the TbAK1-3 isoforms display a similar protein domain organization as prototypical arginine kinases (Fig. 1), including the presence of an α-helical N-terminal domain of about 100 amino acid residues and a >250 amino acids long C-terminal α/β saddle domain (Ratto et al., 1989, Azzi et al., 2004, Fernandez et al., 2007). The C-terminal domain contains key residues involved in reaction catalysis, while the N-terminal domain regulates access to the catalytic pocket (Ratto et al., 1989, Azzi et al., 2004, Fernandez et al., 2007). Key residues involved in the binding of ATP and the guanidino substrates, as well as the phosphagen kinase active site

signature sequence ‘C-P-x(0,1)-[ST]-N-[ILV]-G-T’ (Prosite motif PDOC00103), are conserved in all analysed sequences (Fig. 1). These results suggested that the TbAK1-3 isoforms function as arginine kinases.

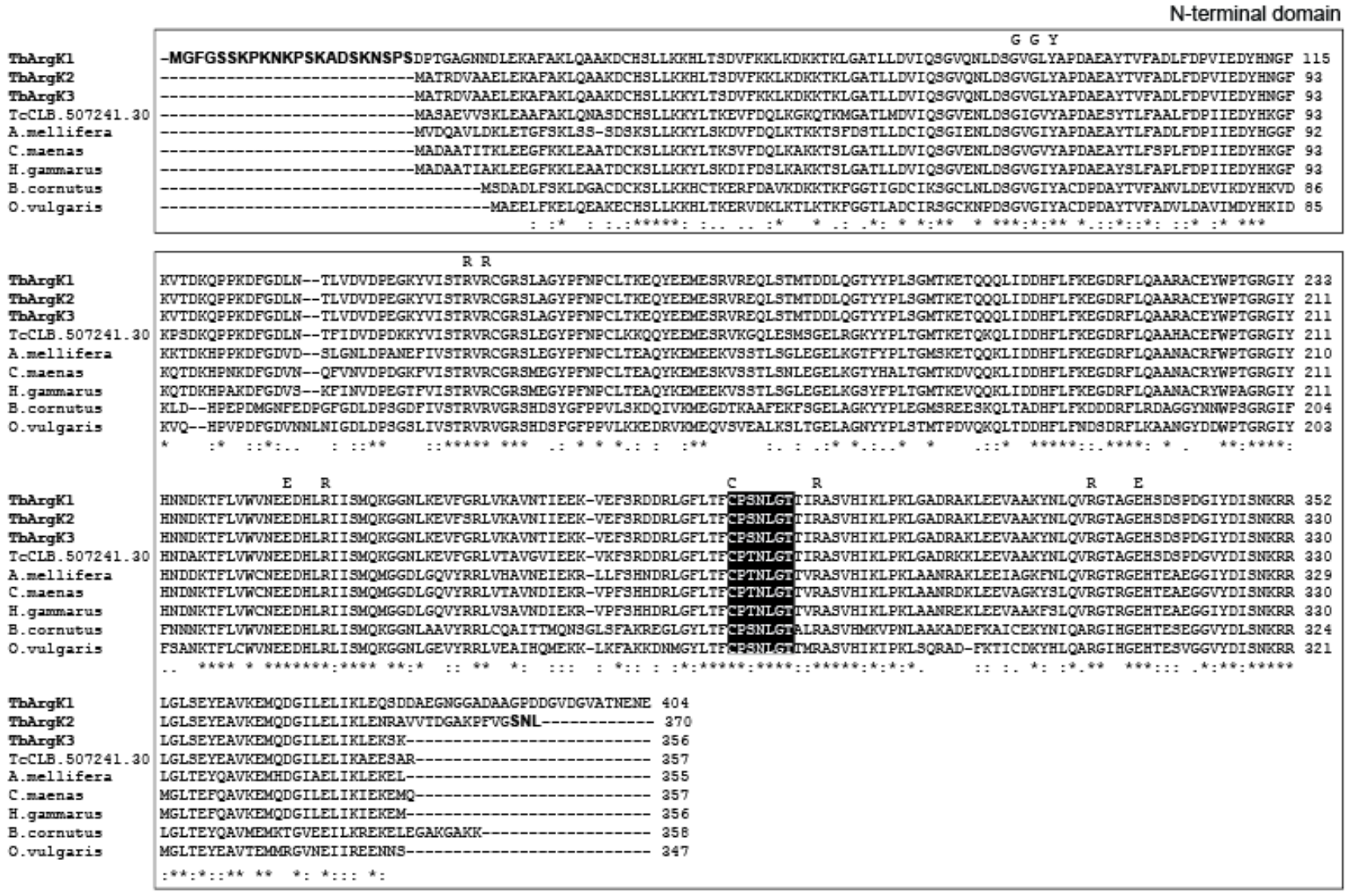
N-terminal domain
G G Y
R R
E R
C R R E
α/β saddle domain

Figure 1: Conserved sequence features of TbAK1-3 and related invertebrate arginine kinases. Sequence alignment of TbAK1-3, *T. cruzi* TcCLB.507241.30, and representative arginine kinases from insects, crustaceans and molluscs. The N-terminal flagellar targeting signal of TbAK1 and the C-terminal PTS1 signal of TbAK2 are shown in bold face. Key residues involved in the binding of ATP and the guanidino substrates are indicated on top of the alignment. The phosphagen kinase active site signature sequence is printed white bold face on a black background. The conserved α-helical N-terminal domain and C-terminal α/β saddle domain are boxed. Identical or similar amino acid residues are represented by respectively (*) and (:), semi-conserved amino acid residues are represented by (.), and gaps are shown as dashes. See Material and Methods for organism names and gene accession numbers.

3.2 Arginine kinase activity of TbAK1

I subsequently confirmed the enzymatic function of the TbAK isoforms. For this purpose, recombinant TbAK1 bearing a N-terminal histidine-tag (TbAK1-nHis) was expressed in the heterologous host *E. coli* BL21 (DE3) and subsequently isolated using Talon-affinity chromatography. SDS-PAGE and coomassie brilliant blue staining of the purified TbAK1-nHis protein fraction revealed a single protein band with the expected molecular size of 55 kDa (Fig. 2A, left panel). Western blot analysis using a His-tag antibody revealed specific staining of the same protein band (Fig. 2A, right panel), thus confirming isolation of the recombinant TbAK1-nHis protein.

The arginine kinase activity of the purified TbAK1-nHis protein was first determined in the phosphoarginine synthesis direction, at temperatures required for growth of the analysed *T. brucei* life cycle stages, here 28°C for PCF and 37°C for BSF *T. brucei*. The results revealed that TbAK1 catalysed the phosphorylation of arginine with a V_{max} of 7.96 ± 0.53 µmol.mg protein^{-1}.min^{-1} at 28°C and 13.05 ± 0.08 µmol.mg protein^{-1}.min^{-1} at 37°C, respectively (Table 1). The optimum reaction temperature was found to be 37°C, with only 57% of its activity remaining at 28°C (Table 1). I further determined the different K_m values for the recombinant TbAK1 protein (Fig. 3). The arginine concentration was set to 3 mM for determination of K_m^{ATP}, while for determination of K_m^{arg} the ATP concentration was set to 0.8 mM. Comparison with published data revealed that the specific activity and K_m values of TbAK1 were similar to those previously reported for the recombinant *T. cruzi* arginine kinase, i.e. a K_m^{ATP} of 10-16 µmol.mg protein^{-1}.min^{-1} and K_m^{arg} of 0.3 mM, respectively (Pereira et al., 2000). The pH optimum for TbAK1 was about 8.0 (not shown). Similar to previously characterized arginine kinases from other eukaryotes, also TbAK1 was

specific for arginine and was unable to catalyse the phosphorylation of creatine (not shown).

The synthesis of phosphoarginine by TbAK1 was further analysed by HPLC using a SP2 Hypersil column (Viant et al., 2001). The expected elution times for arginine and phosphoarginine are 3.3 and 5.5 min, respectively (Viant et al., 2001). Analysis of the resulting elution patterns revealed that in the absence of TbAK1-nHis no phosphoarginine was formed (Fig. 2B, left panel), whereas in its presence an additional peak was found with the expected elution time of 5.5 min for phosphoarginine (Fig. 2B, right panel). This peak was collected (elution range 5.2-5.8 min) and further analysed using a coupled arginine kinase assay in the direction of phosphoarginine dephosphorylation and ATP synthesis. The enzyme assay mix contained ADP and the eluted HPLC fractions as substrates, as well as the purified recombinant TbAK1-nHis enzyme. ATP formation was measured using a firefly luciferase-dependent ATP detection kit. The results confirmed that the HPLC peak at 5.5 min indeed contained phosphoarginine, since ATP was only synthesized in the presence of TbAK1-nHis and ADP (Fig. 2C). As expected, a linear correlation was found between the volume of HPLC eluate and the amount of ATP produced (Fig. 2C). No ATP was generated during control experiments, i.e. where no TbAK1-nHis or heat-inactivated TbAK1-nHis was added during the phosphoarginine synthesis reaction (not shown) or in the absence of HPLC eluate (Fig. 2C). These results confirmed that TbAK1 indeed catalyses the reversible phosphorylation of arginine.

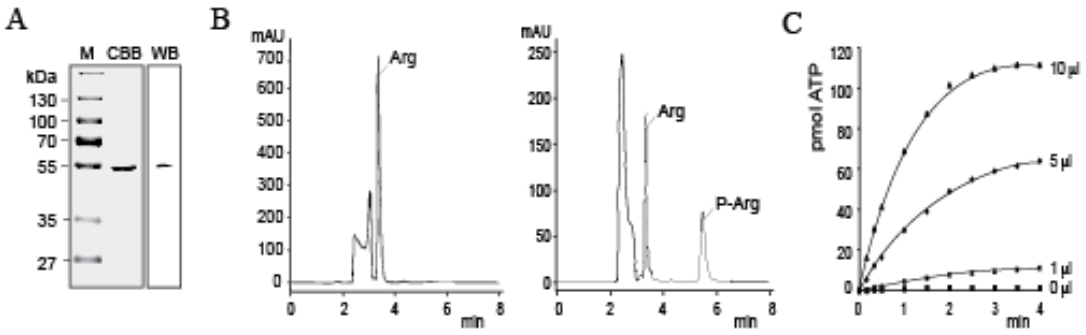

Figure 2: TbAK1-nHis catalysis the reversible phosphorylation of arginine (taken from (Voncken et al., 2013). **A**. TbAK1-nHis was expressed in *E. coli* BL21 (DE3) and subsequently isolated using Talon affinity chromatography. Left panel: SDS-PAGE and coomassie brilliant blue (CBB) staining revealed a single protein band (~55kDa) in the purified TbAK1-nHis protein fraction. Right panel: western blot (WB) analysis using a commercial His-tag antibody stained the same protein band (arrow). **B**. HPLC analysis of reaction products formed in the absence (left panel) and presence (right panel) of purified TbAK1-nHis. Elution time of arginine and phosphoarginine are 3.3 and 5.5 minutes, respectively. **C**. Reverse arginine kinase reaction catalysed by recombinant TbAK1-nHis and using ADP (1mM) and increasing volumes (0-10 µl) of the collected phosphoarginine fraction as substrate. ATP formation from phospharginine was measured using a firefly luciferase-dependent ATP detection kit. Abbreviations are: M, molecular weight marker; kDa, kilodalton.

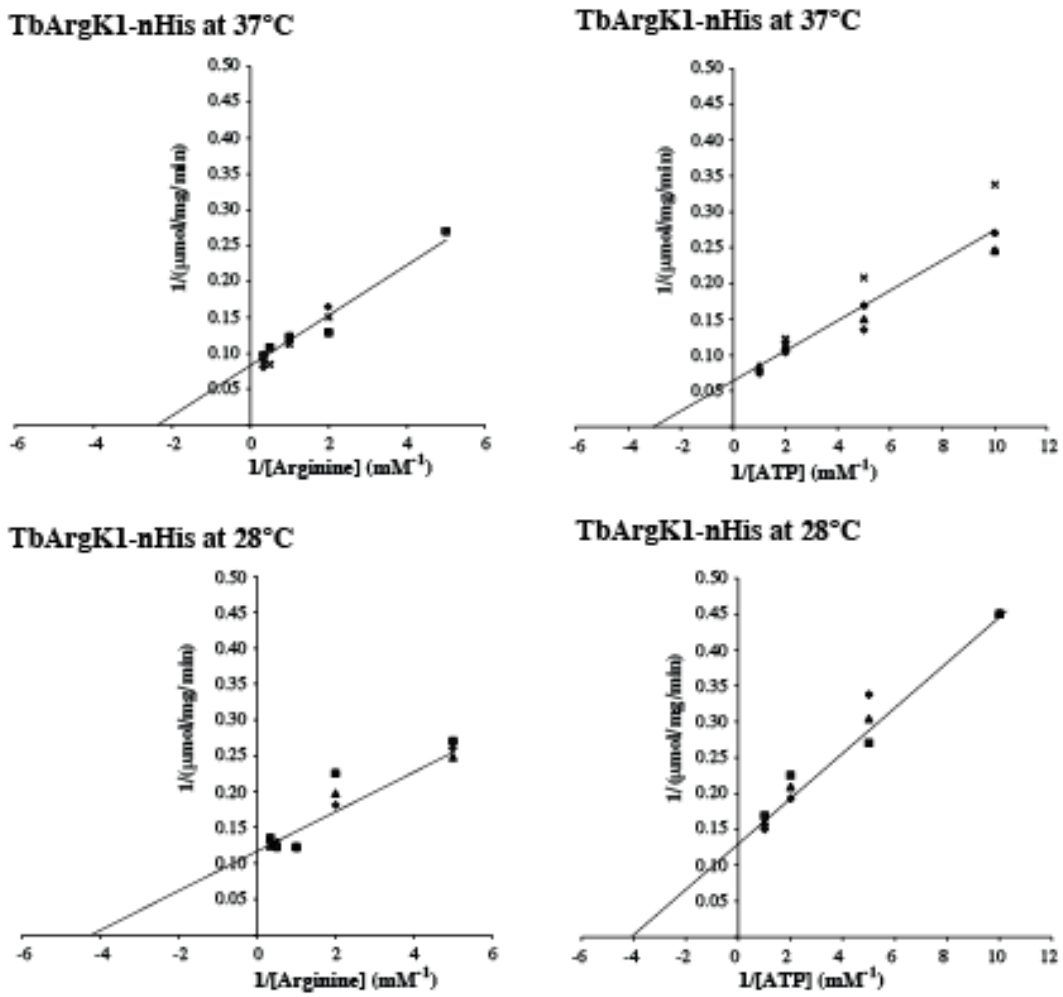

Figure 3: Lineweaver-Burk plots used for the determination of the different Michaelis-Menten constants, here K_m^{ATP} and K_m^{arg}, and the maximum velocity (V_{max}) for the phosphoarginine synthesis catalysed by TbAK1-nHis at respectively 28°C and 37°C (taken from (Voncken et al., 2013)). Arginine kinase activity was measured in the forward phosphoarginine producing direction. Values and standard deviations are derived from >3 independent experiments.

3.3 Subcellular location of TbAK1-3

Arginine kinases were previously reported to be associated with different subcellular compartments (Watts and Bannister, 1970, Hird and Robin, 1985, Chamberlin, 1997, Noguchi et al., 2001, Hoffman and Ellington). The *T. cruzi* arginine kinase

TcCLB507241.30 was shown to be exclusively cytosolic, which is in agreement with the absence of identifiable subcellular targeting signals (Miranda et al., 2009). Sequence alignment revealed that TbAK1 contains distinct N- and C-terminal extensions of respectively 22 and 26 amino acid residues, when compared to TbAK2-3 and TcCLB507241.30 (Fig. 1). Sequence analyses using the SignalP, MITOPROT, Predotar, PSORT and TargetP programs (available at http://www.expasy.ch) however failed to attribute any specific subcellular targeting function to these extensions. Also TbAK3, the smallest TbAK isoform, lacks any recognisable subcellular targeting signals (Fig. 1). This in contrast to TbAK2, which contains a conserved type 1 peroxisomal targeting signal (PTS1) at its carboxy-terminal end, i.e. the tri-peptide 'SNL' (Fig. 1). This tripeptide is sufficient for peroxisomal targeting in eukaryotes (Sommer and Wang, 1994, Amery et al., 1998) and its presence in TbAK2 suggested a glycosomal location in *T. brucei*.

Because of the high amino acid sequence similarity of TbAK1-3, no isoform-specific antibodies could be raised. We therefore decided to analyse their subcellular location by expressing recombinant N- or C-terminal myc-tagged protein versions and detecting them by using a myc-tag antibody. Western blot analysis confirmed the successful expression of myc-tagged TbAK1-3 in the generated BSF and PCF *T. brucei* cell lines (see insets Fig. 4 and Fig. 5).

Immunofluorescence microscopy of the same cell lines revealed that the subcellular localisation of TbAK1 and TbAK2 was dependent on the position of the added myc-tag (Fig. 4A-B, Fig. 5). TbAK2-nmyc was found exclusively in the glycosomes of PCF and BSF *T. brucei* (Fig. 4A-B), as expected from the presence of the C-terminal PTS1 signal (see above, and Fig. 1). Addition of a myc-tag to the C-terminal end of

this arginine kinase (TbAK2-cmyc) resulted in a flagellar location instead (suppl. Fig. 2). This 'failure' to target TbAK2 to the glycosome was anticipated since any sequence addition to a PTS1 signal disrupts its targeting function (Gould et al., 1989). This result confirmed further that the tripeptide 'SNL' indeed functions as a glycosome-targeting signal.

Immunofluorescence microscopy of *T. brucei* cell lines expressing TbAK1-cmyc (Fig. 4A-B) showed that this arginine kinase is flagellar. Addition of the myc-tag to the N-terminus (TbAK1-nmyc) redirected this protein to the cytosol instead, suggesting the presence of an N-terminal flagellar targeting signal. We subsequently assessed whether the N-terminal extension of TbAK1 can independently function as a flagellar targeting signal. For this purpose, a PCF *T. brucei* cell line was generated that expressed a GFP-fusion protein (Nterm-TbAK1/GFP) containing the first 22 amino acids of TbAK1 at its N-terminus. A *T. brucei* cell line expressing only GFP was used as a control. Immunofluorescence microscopy revealed that Nterm-TbAK1/GFP was exclusively located in the flagellum (Fig. 4D), whereas the native GFP was exclusively found in the cytosol (Fig. 4C). This result confirmed that the 22 amino acid long N-terminal extension of TbAK1 functions as a flagellar targeting signal in *T. brucei*.

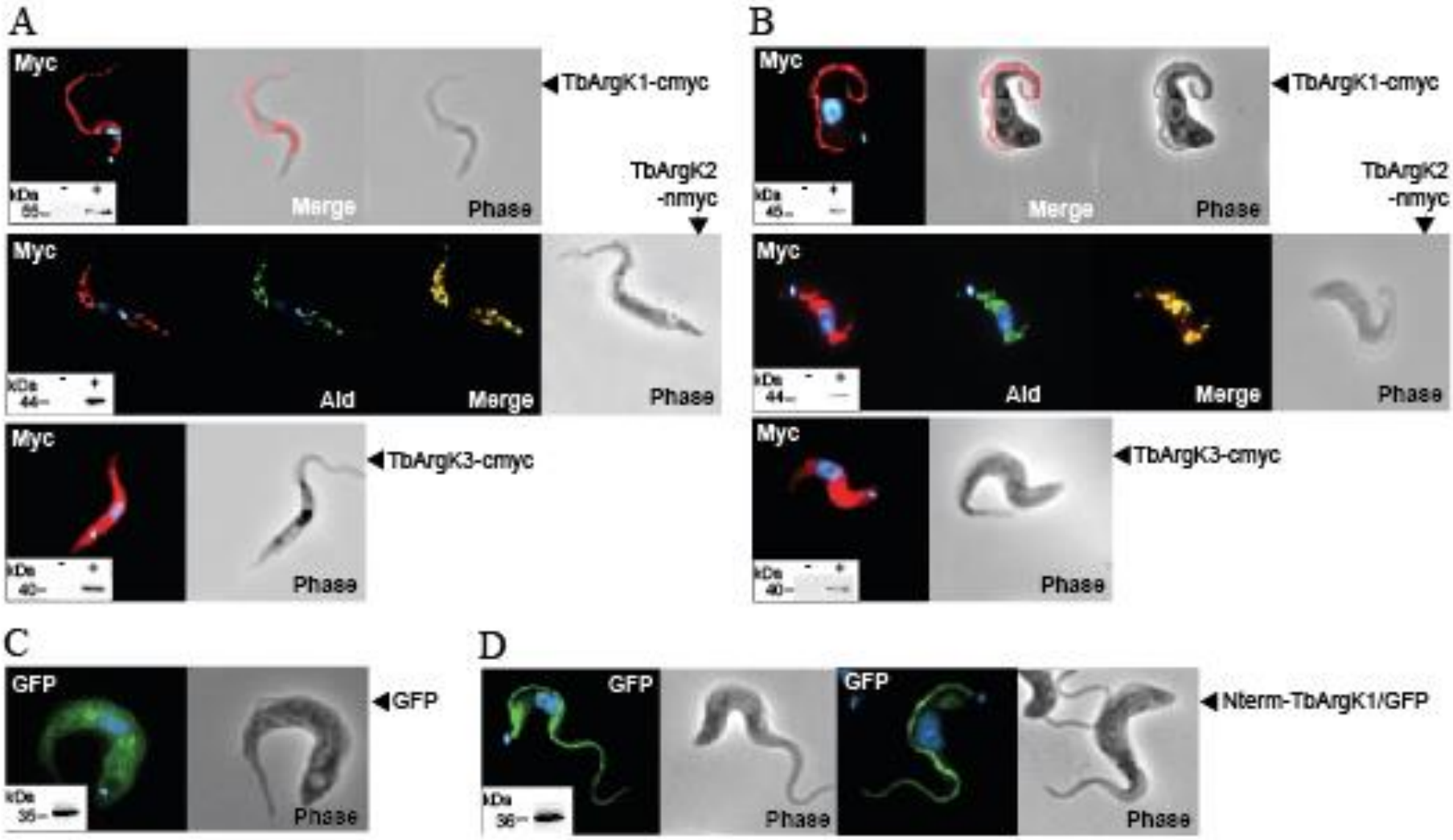
A
Myc
Merge
Phase
TbArgK1-cmyc
TbArgK2
-nmyc
Myc
Ald
Merge
Phase
Myc
Phase
TbArgK3-cmyc
B
Myc
Merge
Phase
TbArgK1-cmyc
TbArgK2
-nmyc
Myc
Ald
Merge
Phase
Myc
Phase
TbArgK3-cmyc
C
GFP
Phase
GFP
D
GFP
Phase
GFP
Phase
Nterm-TbArgK1/GFP

Figure 4: TbAK1-3 isoforms have different subcellular locations in *T. brucei* (adapted from Voncken et al., 2013). **A** and **B**: Immunofluorescence microscopy of PCF (A) and BSF (B) *T. brucei* cell lines expressing different myc-tagged TbAK isoforms (red). Glycosomes (green) were detected using a polyclonal antibody directed against the glycosomal marker protein aldolase (Lorenz et al., 1998), while the nucleus and kinetoplast were stained (blue) with the DNA-binding dye DAPI. The merge (overlay) shows the co-localisation of TbAK2-nmyc and the glycosomal aldolase. Insets in A and B: western blot analysis of the different cell lines grown in the absence (-, non-induced) or presence (+, induced) of tetracycline (0.5µg mL^{-1}), and using a commercial myc-antibody. For western blot analysis, cells were harvested 24 hours after induction and $2x10^6$ trypanosomes were analysed per gel lane. Abbreviations: Phase, phase-contrast. **C** and **D**: Immunofluorescence microscopy of the *T. brucei* PCF cell lines expressing GFP (C) and Nterm-TbAK1/GFP (D). GFP is visualized by its natural auto-fluorescence, while the nucleus and kinetoplast were stained (blue) with the DNA-binding dye DAPI. Insets in C and D: western blot analysis of the different constitutively expressing cell lines, using a commercial GFP-antibody.

Immunofluorescence microscopy of BSF and PCF cell lines expressing myc-tagged TbAK3 revealed that this arginine kinase was located in the cytosol, regardless whether the myc-tag was added to its N- or C-terminus (Fig. 4A-B, Fig. 5). A cytosolic location of TbAK3 is in agreement with the absence of any identifiable targeting signals in its deduced amino acid sequence. Overall, the results indicated that in *T. brucei* each TbAK isoform is located in a different subcellular compartment.

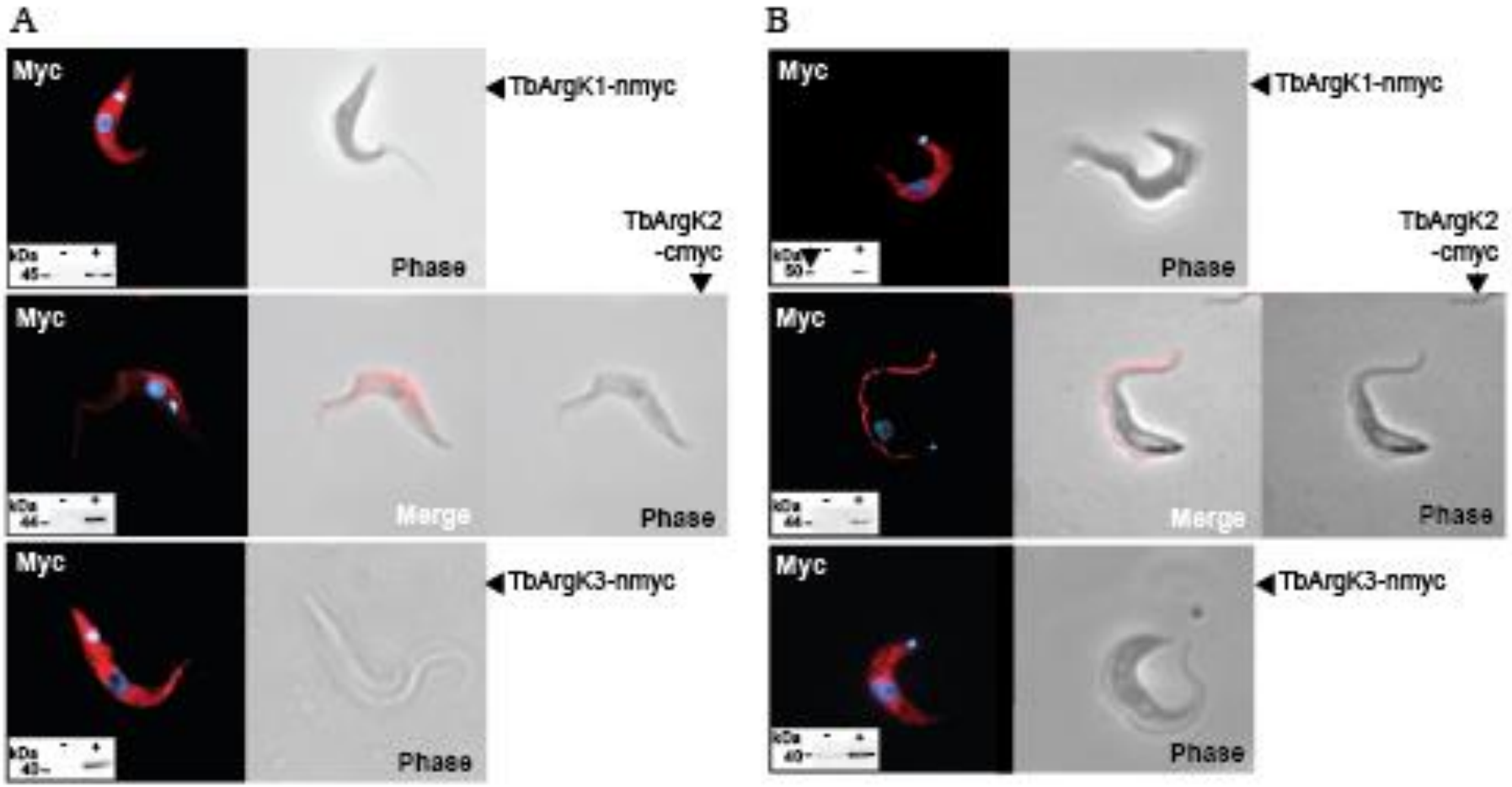
A
Myc
Phase
TbArgK1-nmyc
TbArgK2
-cmyc
Myc
Merge
Phase
Myc
Phase
TbArgK3-nmyc
B
Myc
Phase
TbArgK1-nmyc
TbArgK2
-cmyc
Myc
Merge
Phase
Myc
Phase
TbArgK3-nmyc

Figure 5: Immunofluorescence microscopy of PCF (A) and BSF (B) *T. brucei* cell lines expressing myc-tagged TbAK1-3 (red) (adapted from Voncken et al., 2013). The nucleus and kinetoplast were stained (blue) with the DNA-binding dye DAPI. Insets in A and B: western blot analysis of the different cell lines grown in the absence (-, non-induced) or presence (+, induced) of tetracycline (0.5 μg mL^{-1}), and using a commercial myc-antibody. For western blot analysis, cells were harvested 24 hours after induction and $2x10^6$ trypanosomes were analysed per gel lane. Abbreviations: Phase, phase-contrast.

3.4 Life cycle stage-dependent expression

In *T. brucei*, expression of approximately 2% of genes is developmentally regulated at the mRNA level (Brems et al., 2005). Northern blot analysis was used to investigate whether this is also the case for the dTbAK isoforms. The open reading frames of *TbAK1-3* display >85% nucleotide sequence identity and can therefore not be used as specific DNA probes. Instead, their highly variable 3' untranslated regions (UTRs) were used as gene-specific probes. The results revealed a single cross-hybridising mRNA band for each of the *TbAK* genes in both BSF and PCF *T. brucei* (Fig. 6a). The observed size-lengths of these mRNAs, here 2.1kb (*TbAK1*), 1.8kb (*TbAK2*) and 2.0kb (*TbAK3*), were similar to the *in silico* predicted mRNA transcript sizes of 2.3kb, 1.8kb and 2.2kb, respectively, using the previously described parameters for the calculation of mRNA transcript lengths in *T. brucei* (Benz et al., 2005). The *TbAK* mRNA levels were quantified by hybridizing the same northern blots with the signal recognition particle (SRP) DNA probe, which is routinely used for normalisation of mRNA expression levels in *T. brucei* (Colasante et al., 2007). Quantification revealed that (1) *TbAK1* mRNA is 2.5-fold more abundant in PCF *T. brucei*, (2) *TbAK2* mRNA is 2.8-fold more abundant in BSF *T. brucei*, and (3) *TbAK3* mRNA is 1.5-fold more abundant in PCF *T. brucei* (Fig. 6A). The results obtained for *TbAK2* correlate well with previously published microarray analysis results, which revealed about 2.1-fold more *TbAK2* mRNA in BSF *T. brucei*, when compared to the PCF (Brems et al., 2005).

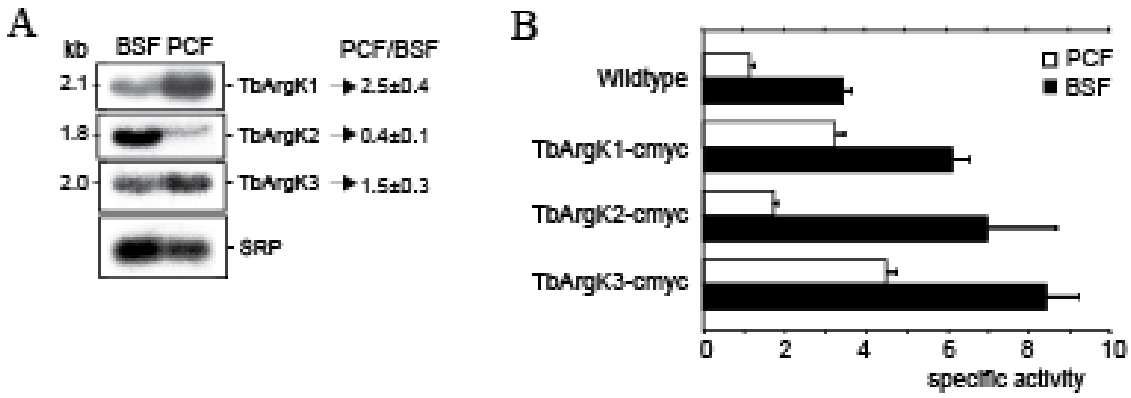

Figure 6: TbAK1-3 are differentially expressed**. A.** Northern blot analysis of total RNA (10μg per lane) isolated from bloodstream form (BSF) and procyclic form (PCF) *T. brucei* (taken from Voncken et al., 2013). The *TbAK1-3* 3'UTRs were used as DNA probes to detect the respective mRNA transcripts, while the signal recognition particle (SRP) was used as a loading control (Colasante et al., 2007). Numbers represent the relative mRNA ratios (PCF/BSF) calculated from pixel intensities of the different mRNA bands (ImageJ: http://rsb.info.nih.gov/ij/) after normalisation against SRP, and represent the mean from 3 independent experiments. **B**. Specific arginine kinase activities in total cell lysates from 'wildtype' and TbAK-overexpressing bloodstream form (BSF, white bars) and procyclic form (PCF, black bars) *T. brucei* cell lines. Specific arginine kinase activity was determined in the forward (phosphoarginine synthesis) direction using 2 mM arginine and 0.8 mM ATP as substrates, and using 10μg of protein (total cell-lysate) per assay. Values are the means of at least three independent experiments.

As mentioned above, no isoform-specific antibodies were raised due to the sequence similarities of TbAK1-3. This excluded the possibility to assess the expression of the different TbAK isoforms at the protein level. Instead, I measured the total arginine kinase activity in cell extracts derived from 'wildtype' PCF and BSF *T. brucei* cell lines. Comparison revealed substantial differences in specific arginine kinase activity depending on the developmental stage of the parasite: for BSF *T. brucei* a specific arginine kinase activity of 3.43 ± 0.22 µmol x min^{-1} x mg^{-1} was observed, while for PCF *T. brucei* a 3-fold lower specific activity of 1.14 ±0.12 µmol x min^{-1} x mg^{-1} was found (Table 1). Comparison with previously published data showed that the specific arginine kinase activities for PCF *T. brucei* Lister 449 (this paper) were about 4-fold higher than those previously reported for *T. brucei* (unknown procyclic form strain in (Pereira et al., 2002)), and 12-fold higher than those found for *T. cruzi* epimastigotes (Pereira et al., 2002).

Table 1: K_m and V_{max} values of the TbAK1-nHis arginine kinase activity (adapted from Voncken et al., 2013)

		28°C	**37°C**
$\boldsymbol{K_m}$	ATP	0.23±0.03	0.32±0.06
	Arginine	0.24±0.05	0.48±0.07
$\boldsymbol{V_{max}}$	ATP/Arginine	7.96±0.53	13.96±2.32

K_m and maximum velocity (V_{max}) values are shown in mM and µmol/mg/min, respectively. The results are the mean from three individual exprenments.

3.5 Overexpression, oxidative stress and growth

Increased expression of TcCLB.507241.30 in *T. cruzi* significantly improved its survival (growth) capacity under standard and oxidative-challenging culture conditions (Pereira et al., 2003). Here I investigated whether also the TbAK1-3 isoforms play a similar role in *T. brucei*. For this experiment the same cell lines expressing myc-tagged TbAK1-3 were used as for the immunolocalisation studies shown in Fig. 3A-B. The expected higher arginine kinase activity in these TbAK-myc over-expressing cell lines was confirmed by enzyme analysis, which showed an overall >1.3-fold increase in total arginine kinase activity, when compared to the 'wildtype' *T. brucei* cell line (Fig. 6B). Subsequent growth analysis revealed an overall >1.5-fold increase in the growth rates of the PCF TbAK-myc over-expressing cell lines (Fig. 7A), suggesting that an increased arginine kinase activity was beneficial to PCF trypanosome growth. For the TbAK-overexpressing BSF *T. brucei* cell lines, however, the growth rates either did not significantly increase (TbAK1-2) or revealed a major decrease, as shown for TbAK3 (Fig. 7B). A higher arginine kinase activity evidently does not benefit growth of the BSF trypanosome, and is even detrimental in case of an increased cytosolic arginine kinase activity.

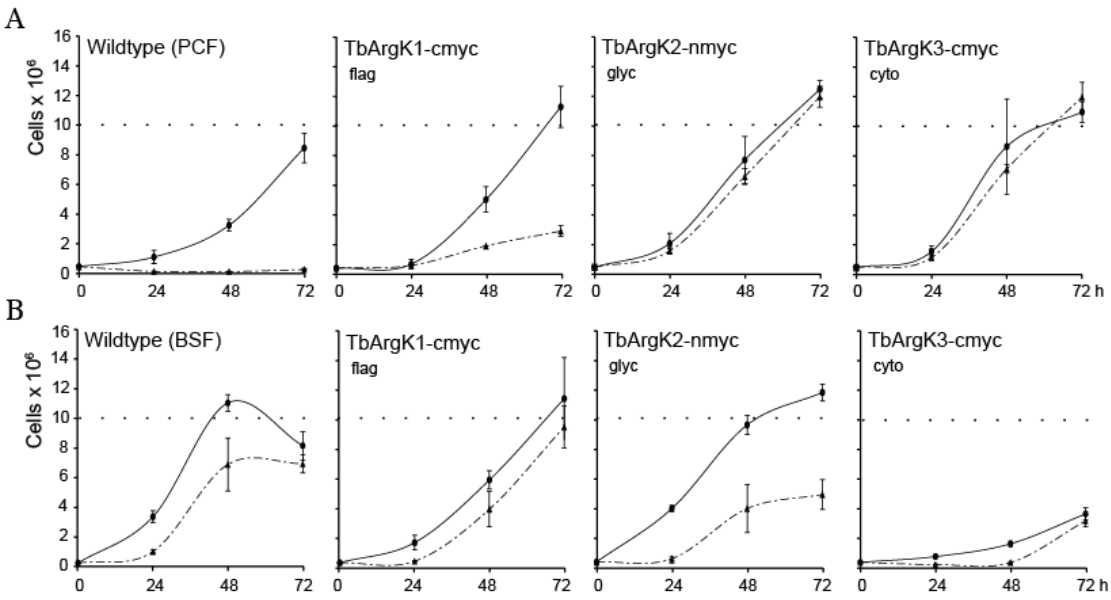

Figure 7. Growth analysis of *T. brucei* cell lines overexpressing TbAK1-3. Growth curves of 'wildtype' and TbAK-overexpressing PCF (**A**) and BSF (**B**) cell-lines under standard (solid lines) and hydrogen peroxide-challenged (dashed lines) culture conditions (adapted from Voncken et al., 2013). Overexpression of TbAK1-3 was induced by addition of 0.5 μg.ml^{-1} tetracycline 24 hours before the start of the experiment. PCF trypanosomes were oxidatively challenged with 10 μM of hydrogen peroxide, while BSF trypanosomes were challenged with 200 μM of hydrogen peroxide. Cell densities were determined every 24 hours, for a total of 72 hours. Each growth curve represents the means of at least 3 independent experiments. Abbreviations: flag, flagellar; glyc, glycosomal; cyto, cytosolic.

The same cell lines were subsequently exposed to increasing concentrations (0-250 μM) of hydrogen peroxide in order to assess their capacity to handle oxidative stress. The hydrogen peroxide concentrations required for causing a growth defect were determined empirically for the different cell lines (not shown). Growth analysis revealed that 'wildtype' PCF *T. brucei* completely ceased growth within 24 hours after exposure to 10 μM of hydrogen peroxide (Fig. 7A). This growth defect was completely reversed upon the overexpression of glycosomal TbAK2 or cytosolic TbAK3, whereas overexpression of the flagellar TbAK1 resulted in only a partial

reversal of this growth defect. Increasing the hydrogen peroxide concentration to >15 µM was invariably lethal for all analysed PCF cell lines (not shown). In contrast, BSF *T. brucei* appeared to be far more resistant to oxidative stress than PCF trypanosomes: only a minor growth defect was observed in the presence of 200 µM of hydrogen peroxide for the 'wildtype' BSF cell line (Fig. 7B). The larger capacity of BSF *T. brucei* to withstand oxidative stress is in agreement with its 3-fold higher cellular arginine kinase activity. Addition of 250 µM of hydrogen peroxide was however lethal for all analysed BSF cell-lines (cells died). Notably, the reduced growth of 'wildtype' BSF trypanosomes in the presence of 200 µM of hydrogen peroxide could not be reversed by overexpression of any of the TbAK1-3 isoforms (Fig. 7B).

3.6 Silencing of TbAK expression

Whether arginine kinase activity is essential for *T. brucei* growth was assessed by RNA interference (RNAi). For this purpose, a tetracycline-inducible PCF *TbAK-RNAi* cell line was generated, which allowed the silencing of all three TbAK isoforms in a single step. The *TbAK1-3* mRNA levels were monitored by RT-PCR using the isoform-specific PCR primers. The outcomes of the control experiments were as expected, and showed that: (1) no TbAK1 PCR-product was produced in the absence of reverse transcriptase, (2) the non-related gene TbMCP11 (Colasante et al., 2009) could be amplified from cDNA, and (3) the expected PCR products were found for all TbAK isoforms when using mRNA from the PCF 'wildtype' cell line (Fig. 8A). The results for the induced *TbAK-RNAi* cell line revealed that no PCR product could be detected after 6 days of tetracycline induction (shown in Fig. 8A), which suggested a major decrease in *TbAK* mRNA levels (below detection limit of used method). Accordingly, no arginine kinase activity could be detected when analysing cell

extracts from the same induced *TbAK-RNAi* cell line. This result confirmed the successful silencing of TbAK expression. Growth analysis revealed that under standard culture conditions the growth rate of the TbAK-depleted cell line had decreased to about 10% of the 'wildtype' cell line (Fig. 8B). Moreover, addition of 0.025 µM of hydrogen peroxide to the TbAK-depleted cell line was found to be lethal, while growth of the 'wildtype' cell line decreased to about 50% of its original capacity (Fig. 8C). Overall, the TbAK-depleted cell line became >40-fold more sensitive to hydrogen peroxide. Our results confirmed that arginine kinase activity is required for *T. brucei* growth under standard culture conditions, and is even essential when the parasite is exposed to elevated oxidative stress.

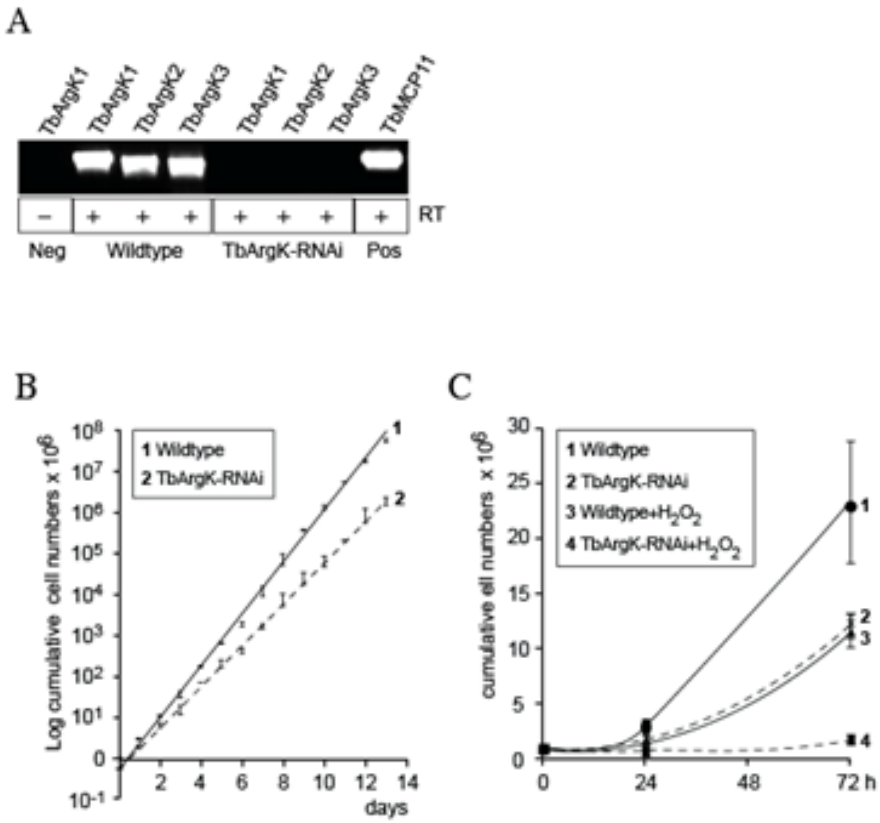

Figure 8: Silencing of TbAK1-3 expression in PCF *T. brucei* (adapted from Voncken et al., 2013). **A**. TbAK isoform-specific PCR of the 'wildtype' PCF cell line (lanes 2-

4), and the derived ^{RNAi}*TbAK* cell line (lanes 5-7) cultured for 6 days in the presence of tetracycline (0.5 μg.ml^{-1}). Prior to PCR, mRNA was converted to cDNA by reverse transcriptase (RT). No TbAK1 PCR-product was found in the absence (-) of reverse transcriptase (lane 1), indicating that the mRNA samples were not contaminated with genomic DNA. PCR of the non-related gene TbMCP11 (lane 8, (Colasante et al., 2009)) was used as a positive control for cDNA synthesis. B. Cumulative growth curves of the 'wildtype' PCF cell line (solid line) and the induced ^{RNAi}*TbAK* cell line (dashed line) showing an 18-fold difference in cell density after 12 days under standard culture conditions. **C**. Cumulative growth curves of PCF 'wildtype' cell line (solid lines) and the derived ^{RNAi}*TbAK* cell line (dashed lines), grown for 72 h under standard and oxidative challenging culture conditions. The ^{RNAi}*TbAK* cell line was induced with tetracycline for 6 days prior to the start of this growth experiment, ensuring complete silencing of all TbAK isoforms (see A.). For the oxidative-challenging culture conditions, 0.025 μM of hydrogen peroxide was added to the culture medium.

4. Discussion

Phosphagens like phosphoarginine are relatively small molecules with larger diffusion coefficients than ATP. In addition, they are metabolically 'inert' and can be stored in the cell without affecting the overall ATP/ADP balance, which is critical for the regulation of many metabolic processes (Ellington, 2001). Phosphagens are therefore the molecules of choice for energy transport and buffering in highly polarised eukaryotic cells (Ellington, 2001). The involved kinases are often located near sites of high ATP turnover, allowing the transfer of energy from a source of ATP production to a site of ATP consumption (Wallimann et al., 1992, Ellington, 2001). Several models have been postulated in which the spatial (subcellular) distribution of phosphagen kinases plays a crucial role in intracellular energy transport as well as in the control and regulation of ATP-dependent enzymes and pathways in the different

subcellular compartments (Wallimann et al., 1992). Also the energy metabolism of *T. brucei* is highly compartmentalised, with ATP-producing pathways located in the glycosome, mitochondrion and cytosol (van Hellemond et al., 2005, Michels et al., 2006, Bringaud et al., 2006). The relative contribution of these subcellular compartments to the overall ATP production is dependent on the developmental stage of the parasite. ATP production in BSF *T. brucei* depends primarily on substrate-level phosphorylation during glycolysis, with the first 7-9 enzymes of this pathway compartmentalised in the glycosome (Michels et al., 2006). This in contrast to PCF *T. brucei*, which primarily depends on mitochondrial degradation of proline, and concomitant substrate-level and oxidative phosphorylation for its ATP generation (van Hellemond et al., 2005, Bringaud et al., 2006).

Evidence has been provided that *T. brucei* expresses 3 functional arginine kinases, with each isoform located in a different subcellular compartment: TbAK3 is exclusively cytosolic, while TbAK1 and TbAK2 are found in the flagellum and glycosome, respectively. The different subcellular locations of TbAK1 and TbAK2 are dependent on specific signal sequences, whose targeting function was disrupted by the proximate addition of a myc-tag. Disruption of a C-terminal PTS1 signal by sequence extension, as is the case for TbAK2-cmyc, was previously shown to abolish peroxisomal targeting in other eukaryotes (29). Interestingly, TbAK2-cmyc did not localise to the cytosol as expected, but to the flagellum instead. Sequence analysis failed to identify any flagellar targeting signals in TbAK2. Putative N-terminal flagellar targeting sequences have previously been proposed for other *T. brucei* proteins, but their exact amino acid sequence composition remains elusive (Snapp and Landfear, 1999, Pullen et al., 2004, Bouvier et al., 2006). This in contrast to TbAK1: localisation studies revealed that the first 22 amino acids of this protein were

sufficient to target GFP to the trypanosome flagellum. Comparison to the N-terminal sequences of other flagellar *T. brucei* proteins (not shown) did not reveal any sequence similarities. The N-terminal extension of TbAK1 apparently represents a novel trypanosome flagellar targeting signal. How to explain the flagellar sorting of TbAK2-cmyc, which lacks such a N-terminal extension? TbAK1 and TbAK2 are very similar in sequence, apart from the obvious N- and C-terminal extensions present in TbAK1 (see Fig. 1). Most organellar proteins require specific targeting signals in order to reach their subcellular destinations. However, there are a number of known exceptions where proteins without obvious targeting signals are still transported to specific subcellular compartments. This can be achieved through oligomer formation with proteins bearing a specific targeting signal. Such 'piggy-backing' protein transport mechanism has been reported for various peroxisomal, glycosomal, glyoxysomal and vacuolar proteins (Glover et al., 1994, Lee et al., 1997, Subramani, 2002). Similar to the structurally and functionally related creatine kinases, also some arginine kinases were found to form heterodimers (Wright-Weber et al., 2006). A possible heterodimer formation of the flagellar TbAK1 with TbAK2-cmyc could be an explanation for the observed flagellar localisation of TbAK2 upon ablation of its glycosome-targeting signal. However, the evident that further investigation is required regarding the nature of the TbAK1 flagellar targeting sequence as well as the putative heterodimer formation of TbAK1 and TbAK2. The proposed glycosomal location of TbAK2 is corroborated by organelle proteomics, which identified this arginine kinase isoform as a glycosomal constituent during protein mass-spectrometric analysis of highly purified *T. brucei* glycosomes (Colasante et al., 2006).

The different subcellular locations of TbAK1-3 suggest that they play an important role in the control and regulation of ATP-dependent enzymes and pathways in the different subcellular compartments. Northern blot analysis revealed that expression of the glycosomal TbAK2 is 2.8-fold upregulated in BSF *T. brucei*, indicating a more important role in this life cycle stage of the parasite. This result correlates well with the crucial role of the glycosome in the BSF energy metabolism (Michels et al., 2006). However, the general accepted model is that there is no net ATP synthesis in this organelle, with glycolysis-derived ATP primarily produced in the cytosol (Michels et al., 2006). If no net ATP-production occurs in the glycosome, why would this organelle then require a phosphoarginine/arginine kinase-dependent energy buffering system? The *T. brucei* glycosome further contains several adenylate kinases, which were proposed to play a role in the maintenance of the glycosomal ATP/ADP balance and the removal of AMP by the reversible conversion of ATP and AMP to 2 molecules of ADP (Ginger et al., 2005). The presence of both adenylate kinase and TbAK2 and in BSF and PCF glycosomes implicates that under certain conditions either a surplus or deficit of ATP can exist in this organelle, which again could be counter-balanced by the presence of a phosphoarginine/arginine kinase energy buffering system.

Northern blot analysis revealed further a significantly up-regulated expression of the cytoplasmic TbAK3 (1.5-fold) and flagellar TbAK1 (2.5-fold) in PCF *T. brucei*, suggesting a more prominent role of both TbAK isoforms in this life cycle stage of the parasite. PCF *T. brucei* is primarily depending on ATP-generation in the mitochondrion (van Hellemond et al., 2005, Bringaud et al., 2006). The mitochondrial ATP is exported to the cytosol via the ATP/ADP-carrier, which is located in the mitochondrial inner membrane (Colasante et al., 2009). In the cytosol,

ATP could be converted to phosphoarginine by the cytoplasmic TbAK3 to serve as a highly mobile cellular energy carrier and local energy buffer. *T. brucei* is a flagellate protozoan and is depending on its flagellum for cell motility, cell division and survival (Ralston et al., 2009). Flagellar mobility consumes significant quantities of ATP and provision of the more bulky ATP across the *T. brucei* flagellum is rather difficult due to the flagellar length, compact protein structure, and the narrow connection between flagellum and cytosol (Nevo and Rikmenspoel, 1970, Mitchell et al., 2005, Fridberg et al., 2007). The *T. brucei* flagellum contains further enzymes that are normally associated with the mitochondrial and glycosomal energy metabolism, such as enolase, pyruvate kinase, phosphoglycerate mutase, and adenylate kinase (Ginger et al., 2005, Hart et al., 2009, Oberholzer et al.). These enzymes are proposed to function in the maintenance of the flagellar energy homeostasis (Mitchell et al., 2005, Ginger et al., 2005). The channelling of phosphagens between mitochondrion and flagellum was previously described for spermatozoa of the sea urchin *Strongylocentrotus purpuratus*, with mitochondrial and flagellar creatine kinases representing respectively ATP source and ATP sink (Tombes and Shapiro, 1985). Also the phosphoarginine system of *P. caudatum* was reported to be involved in the supply of energy to the cilia (Noguchi et al., 2001). Here, we propose a similar spatial energy-buffering system for *T. brucei,* with the cytosolic TbAK3 acting as a phosphoarginine source and the flagellar TbAK1 providing ATP to fuel flagellar motility.

An important function of the phosphagen/ phosphagen kinase system is the provision of energy in periods of increased energy-demand or during energy fluctuations (Ellington, 2001, Wallimann et al., 1992). Increased expression of TcCLB.507241.30 in *T. cruzi* epimastigotes or the heterologous expression of the same phosphagen

kinase in either *Escherichia coli* or *Saccharomyces cerevisiae* resulted in a substantially increased resistance to oxidative challenging compounds (Canonaco et al., 2002, Pereira et al., 2003, Canonaco et al., 2003). Vice versa, an increased cellular arginine kinase activity was measured upon exposure of *T. cruzi* epimastigotes to hydrogen peroxide (Miranda et al., 2006). These findings suggested an important role of the phosphoarginine/arginine kinase system in oxidative stress response, a process that inherently consumes substantial amounts of ATP and eventually can lead to ATP-depletion (Tiwari et al., 2002, Agalakova and Gusev, 2012). Also the different developmental stages of the exclusively extracellular parasite *T. brucei* are constantly exposed to oxidative stress, predominantly as a result of the innate immune response of its different hosts, but also as a consequence of its own unusual, partly aerobic fermentative, energy metabolism (Krieger et al., 2000, Turrens, 2004, MacLeod et al., 2007b, Macleod et al., 2007a, Saleh et al., 2009). In particular BSF *T. brucei* lives in an environment, i.e. the mammalian bloodstream, in which oxidative stress factors are highly abundant (Turrens, 2004). It is therefore not surprising that BSF *T. brucei* is far more resistant (about 20-fold) against an oxidative challenge with hydrogen peroxide than PCF trypanosomes. Measurement of total arginine kinase activity indeed revealed a substantially higher specific arginine kinase activity in BSF *T. brucei*, which correlated well with its increased capacity to withstand oxidative stress. Similar to *T. cruzi*, a substantially increased oxidative stress resistance was observed upon the increased expression of the different TbAK isoforms in PCF *T. brucei*. Vice versa, PCF *T. brucei* became highly sensible to oxidative stress upon RNAi and complete depletion of all of its arginine kinase activity. Overexpression of TbAKs in BSF *T. brucei*, however, did not result in the expected increase in oxidative stress resistance, but lead to an overall inhibition of

trypanosome growth under standard culture conditions. A possible explanation for this phenomenon could be that an increased expression of arginine kinase disturbs the cellular ATP/ADP ratio: BSF *T. brucei* already displays about 3-fold more arginine kinase activity than PCF trypanosomes, and an even further increase of this activity could potentially affect its cellular availability of ATP.

A number of important questions are remaining, which require further investigation. For example, why does *T. brucei* express 3 different arginine kinase isoforms with specific subcellular localisations, whereas the related kinetoplastid *T. cruzi* contains only a single cytoplasmic arginine kinase? Or, what is the individual contribution of each TbAK isoform to the spatial energy-buffering system of *T. brucei*? Is each of the different TbAK isoforms required for trypanosome survival (growth) and/or differentiation? Future research will focus on the depletion of the individual TbAK isoforms by gene deletion in the different life cycle stages of T. brucei in order to gain more insight into their specific physiological roles.

References

AGALAKOVA, N. I. & GUSEV, G. P. 2012. Fluoride induces oxidative stress and ATP depletion in the rat erythrocytes in vitro. *Environmental toxicology and pharmacology,* 34**,** 334-337.

AMERY, L., BREES, C., BAES, M., SETOYAMA, C., MIURA, R., MANNAERTS, G. P. & VAN VELDHOVEN, P. P. 1998. C-terminal tripeptide Ser-Asn-Leu (SNL) of human D-aspartate oxidase is a functional peroxisome-targeting signal. *Biochem J,* 336 (Pt 2)**,** 367-71.

AZZI, A., CLARK, S. A., ELLINGTON, W. R. & CHAPMAN, M. S. 2004. The role of phosphagen specificity loops in arginine kinase. *Protein Sci,* 13**,** 575-85.

BENZ, C., NILSSON, D., ANDERSSON, B., CLAYTON, C. & GUILBRIDE, D. L. 2005. Messenger RNA processing sites in *Trypanosoma brucei. Mol Biochem Parasitol,* 143**,** 125-34.

BERRIMAN, M., GHEDIN, E., HERTZ-FOWLER, C., BLANDIN, G., RENAULD, H., BARTHOLOMEU, D. C., LENNARD, N. J., CALER, E., HAMLIN, N. E., HAAS, B., BOHME, U., HANNICK, L., ASLETT, M. A., SHALLOM, J., MARCELLO, L., HOU, L., WICKSTEAD, B., ALSMARK, U. C., ARROWSMITH, C., ATKIN, R. J., BARRON, A. J., BRINGAUD, F., BROOKS, K., CARRINGTON, M., CHEREVACH, I., CHILLINGWORTH, T. J., CHURCHER, C., CLARK, L. N., CORTON, C. H., CRONIN, A., DAVIES, R. M., DOGGETT, J., DJIKENG, A., FELDBLYUM, T., FIELD, M. C., FRASER, A., GOODHEAD, I., HANCE, Z., HARPER, D., HARRIS, B. R., HAUSER, H., HOSTETLER, J., IVENS, A., JAGELS, K., JOHNSON, D., JOHNSON, J., JONES, K., KERHORNOU, A. X., KOO, H., LARKE, N., LANDFEAR, S., LARKIN, C., LEECH, V., LINE, A., LORD, A., MACLEOD, A., MOONEY, P. J., MOULE, S., MARTIN, D. M., MORGAN, G. W., MUNGALL, K., NORBERTCZAK, H., ORMOND, D., PAI, G., PEACOCK, C. S., PETERSON, J., QUAIL, M. A., RABBINOWITSCH, E., RAJANDREAM, M. A., REITTER, C., SALZBERG, S. L., SANDERS, M., SCHOBEL, S., SHARP, S., SIMMONDS, M., SIMPSON, A. J., TALLON, L., TURNER, C. M., TAIT, A., TIVEY, A. R., VAN AKEN, S., WALKER, D., WANLESS, D., WANG, S., WHITE, B., WHITE, O., WHITEHEAD, S., WOODWARD, J., WORTMAN, J., ADAMS, M. D., EMBLEY, T. M., GULL, K., ULLU, E., BARRY, J. D., FAIRLAMB, A. H., OPPERDOES, F.,

BARRELL, B. G., DONELSON, J. E., HALL, N., FRASER, C. M., et al. 2005. The genome of the African trypanosome *Trypanosoma brucei. Science,* 309**,** 416-22.

BIEBINGER, S., WIRTZ, L. E., LORENZ, P. & CLAYTON, C. 1997. Vectors for inducible expression of toxic gene products in bloodstream and procyclic *Trypanosoma brucei*. *Mol Biochem Parasitol,* 85**,** 99-112.

BINDER, M., MAHLER, V., HAYEK, B., SPERR, W. R., SCHOLLER, M., PROZELL, S., WIEDERMANN, G., VALENT, P., VALENTA, R. & DUCHENE, M. 2001. Molecular and immunological characterization of arginine kinase from the Indianmeal moth, *Plodia interpunctella*, a novel cross-reactive invertebrate pan-allergen. *J Immunol,* 167**,** 5470-7.

BOSCARDIN, S. B., TORRECILHAS, A. C., MANARIN, R., REVELLI, S., REY, E. G., TONELLI, R. R. & SILBER, A. M. 2011. Chagas' disease: an update on immune mechanisms and therapeutic strategies. *J Cell Mol Med,* 14**,** 1373-84.

BOUVIER, L. A., MIRANDA, M. R., CANEPA, G. E., ALVES, M. J. & PEREIRA, C. A. 2006. An expanded adenylate kinase gene family in the protozoan parasite *Trypanosoma cruzi. Biochim Biophys Acta,* 1760**,** 913-21.

BREMS, S., GUILBRIDE, D. L., GUNDLESDODJIR-PLANCK, D., BUSOLD, C., LUU, V. D., SCHANNE, M., HOHEISEL, J. & CLAYTON, C. 2005. The transcriptomes of *Trypanosoma brucei Lister 427* and *TREU927* bloodstream and procyclic trypomastigotes. *Mol Biochem Parasitol,* 139**,** 163-72.

BRINGAUD, F., RIVIERE, L. & COUSTOU, V. 2006. Energy metabolism of trypanosomatids: adaptation to available carbon sources. *Mol Biochem Parasitol,* 149**,** 1-9.

BRINGAUD, F., ROBINSON, D. R., BARRADEAU, S., BITEAU, N., BALTZ, D. & BALTZ, T. 2000. Characterization and disruption of a new *Trypanosoma brucei* repetitive flagellum protein, using double-stranded RNA inhibition. *Molecular and biochemical parasitology,* 111**,** 283-97.

CANEPA, G. E., CARRILLO, C., MIRANDA, M. R., SAYE, M. & PEREIRA, C. A. 2011. Arginine kinase in Phytomonas, a trypanosomatid parasite of plants. *Comp Biochem Physiol B Biochem Mol Biol,* 160**,** 40-3.

CANONACO, F., SCHLATTNER, U., PRUETT, P. S., WALLIMANN, T. & SAUER, U. 2002. Functional expression of phosphagen kinase systems

confers resistance to transient stresses in *Saccharomyces cerevisiae* by buffering the ATP pool. *J Biol Chem,* 277**,** 31303-9.

CANONACO, F., SCHLATTNER, U., WALLIMANN, T. & SAUER, U. 2003. Functional expression of arginine kinase improves recovery from pH stress of *Escherichia coli*. *Biotechnol Lett,* 25**,** 1013-7.

CHAMBERLIN, M. 1997. Mitochondrial arginine kinase in the midgut of the tobacco hornworm (*Manduca sexta*). *J Exp Biol,* 200**,** 2789-96.

CHENNA, R., SUGAWARA, H., KOIKE, T., LOPEZ, R., GIBSON, T. J., HIGGINS, D. G. & THOMPSON, J. D. 2003. Multiple sequence alignment with the Clustal series of programs. *Nucleic Acids Res,* 31**,** 3497-500.

COLASANTE, C., ELLIS, M., RUPPERT, T. & VONCKEN, F. 2006. Comparative proteomics of glycosomes from bloodstream form and procyclic culture form *Trypanosoma brucei brucei*. *Proteomics,* 6**,** 3275-93.

COLASANTE, C., PENA DIAZ, P., CLAYTON, C. & VONCKEN, F. 2009. Mitochondrial carrier family inventory of *Trypanosoma brucei brucei*: Identification, expression and subcellular localisation. *Mol Biochem Parasitol,* 167**,** 104-17.

COLASANTE, C., ROBLES, A., LI, C. H., SCHWEDE, A., BENZ, C., VONCKEN, F., GUILBRIDE, D. L. & CLAYTON, C. 2007. Regulated expression of glycosomal phosphoglycerate kinase in *Trypanosoma brucei. Mol Biochem Parasitol,* 151**,** 193-204.

ELLINGTON, W. R. 2001. Evolution and physiological roles of phosphagen systems. *Annu Rev Physiol,* 63**,** 289-325.

FENN, K. & MATTHEWS, K. R. 2007. The cell biology of *Trypanosoma brucei* differentiation. *Curr Opin Microbiol,* 10**,** 539-46.

FERNANDEZ, P., HAOUZ, A., PEREIRA, C. A., AGUILAR, C. & ALZARI, P. M. 2007. The crystal structure of *Trypanosoma cruzi* arginine kinase. *Proteins,* 69**,** 209-12.

FRIDBERG, A., BUCHANAN, K. T. & ENGMAN, D. M. 2007. Flagellar membrane trafficking in kinetoplastids. *Parasitol Res,* 100**,** 205-12.

GINGER, M. L., NGAZOA, E. S., PEREIRA, C. A., PULLEN, T. J., KABIRI, M., BECKER, K., GULL, K. & STEVERDING, D. 2005. Intracellular positioning of isoforms explains an unusually large adenylate kinase gene family in the parasite *Trypanosoma brucei*. *J Biol Chem,* 280**,** 11781-9.

GLOVER, J. R., ANDREWS, D. W. & RACHUBINSKI, R. A. 1994. *Saccharomyces cerevisiae* peroxisomal thiolase is imported as a dimer. *Proc Natl Acad Sci U S A,* 91**,** 10541-5.

GOULD, S. J., KELLER, G. A., HOSKEN, N., WILKINSON, J. & SUBRAMANI, S. 1989. A conserved tripeptide sorts proteins to peroxisomes. *J Cell Biol,* 108**,** 1657-64.

HART, S. R., LAU, K. W., HAO, Z., BROADHEAD, R., PORTMAN, N., HUHMER, A., GULL, K., MCKEAN, P. G., HUBBARD, S. J. & GASKELL, S. J. 2009. Analysis of the trypanosome flagellar proteome using a combined electron transfer/collisionally activated dissociation strategy. *J Am Soc Mass Spectrom,* 20**,** 167-75.

HIRD, F. J. & ROBIN, Y. 1985. Studies on phosphagen synthesis by mitochondrial preparations. *Comp Biochem Physiol B,* 80**,** 517-20.

HIRUMI, H. & HIRUMI, K. 1989. Continuous cultivation of *Trypanosoma brucei* blood stream forms in a medium containing a low concentration of serum protein without feeder cell layers. *J Parasitol,* 75**,** 985-9.

HOFFMAN, G. G. & ELLINGTON, W. R. 2011. Arginine kinase isoforms in the closest protozoan relative of metazoans. *Comp Biochem Physiol Part D Genomics Proteomics,* 6**,** 171-7.

KRIEGER, S., SCHWARZ, W., ARIYANAYAGAM, M. R., FAIRLAMB, A. H., KRAUTH-SIEGEL, R. L. & CLAYTON, C. 2000. Trypanosomes lacking trypanothione reductase are avirulent and show increased sensitivity to oxidative stress. *Mol Microbiol,* 35**,** 542-52.

LEE, M. S., MULLEN, R. T. & TRELEASE, R. N. 1997. Oilseed isocitrate lyases lacking their essential type 1 peroxisomal targeting signal are piggybacked to glyoxysomes. *Plant Cell,* 9**,** 185-97.

LORENZ, P., MAIER, A. G., BAUMGART, E., ERDMANN, R. & CLAYTON, C. 1998. Elongation and clustering of glycosomes in *Trypanosoma brucei* overexpressing the glycosomal Pex11p. *EMBO J,* 17**,** 3542-55.

MACLEOD, E. T., DARBY, A. C., MAUDLIN, I. & WELBURN, S. C. 2007a. Factors affecting trypanosome maturation in tsetse flies. *PLoS One,* 2**,** e239.

MACLEOD, E. T., MAUDLIN, I., DARBY, A. C. & WELBURN, S. C. 2007b. Antioxidants promote establishment of trypanosome infections in tsetse. *Parasitology,* 134**,** 827-31.

MALVY, D. & CHAPPUIS, F. 2011. Sleeping sickness. *Clin Microbiol Infect,* 17**,** 986-95.

MATTHEWS, K. R. 2005. The developmental cell biology of *Trypanosoma brucei. J Cell Sci,* 118**,** 283-90.

MICHELS, P. A. 1989. The glycosome of trypanosomes: properties and biogenesis of a microbody. *Exp Parasitol,* 69**,** 310-5.

MICHELS, P. A., BRINGAUD, F., HERMAN, M. & HANNAERT, V. 2006. Metabolic functions of glycosomes in trypanosomatids. *Biochim Biophys Acta,* 1763**,** 1463-77.

MIRANDA, M. R., BOUVIER, L. A., CANEPA, G. E. & PEREIRA, C. A. 2009. Subcellular localization of *Trypanosoma cruzi* arginine kinase. *Parasitology,* 136**,** 1201-7.

MIRANDA, M. R., CANEPA, G. E., BOUVIER, L. A. & PEREIRA, C. A. 2006. *Trypanosoma cruzi*: Oxidative stress induces arginine kinase expression. *Exp Parasitol,* 114**,** 341-4.

MITCHELL, B. F., PEDERSEN, L. B., FEELY, M., ROSENBAUM, J. L. & MITCHELL, D. R. 2005. ATP production in *Chlamydomonas reinhardtii* flagella by glycolytic enzymes. *Mol Biol Cell,* 16**,** 4509-18.

NEVO, A. C. & RIKMENSPOEL, R. 1970. Diffusion of ATP in sperm flagella. *J Theor Biol,* 26**,** 11-8.

NOGUCHI, M., SAWADA, T. & AKAZAWA, T. 2001. ATP-regenerating system in the cilia of *Paramecium caudatum*. *J Exp Biol,* 204**,** 1063-71.

OBERHOLZER, M., LANGOUSIS, G., NGUYEN, H. T., SAADA, E. A., SHIMOGAWA, M. M., JONSSON, Z. O., NGUYEN, S. M., WOHLSCHLELGEL, J. A. & HILL, K. L. 2011. Independent analysis of the flagellum surface and matrix proteomes provides insight into flagellum signaling in mammalian-infectious *Trypanosoma brucei*. *Mol Cell Proteomics*.

OVERATH, P., CZICHOS, J. & HAAS, C. 1986. The effect of citrate/cis-aconitate on oxidative metabolism during transformation of *Trypanosoma brucei. Eur J Biochem,* 160**,** 175-82.

PEREIRA, C. A., ALONSO, G. D., IVALDI, S., SILBER, A. M., ALVES, M. J., TORRES, H. N. & FLAWIA, M. M. 2003. Arginine kinase overexpression improves *Trypanosoma cruzi* survival capability. *FEBS Lett,* 554**,** 201-5.

PEREIRA, C. A., ALONSO, G. D., PAVETO, M. C., IRIBARREN, A., CABANAS, M. L., TORRES, H. N. & FLAWIA, M. M. 2000. *Trypanosoma cruzi* arginine kinase characterization and cloning. A novel energetic pathway in protozoan parasites. *J Biol Chem,* 275**,** 1495-501.

PEREIRA, C. A., ALONSO, G. D., TORRES, H. N. & FLAWIA, M. M. 2002. Arginine kinase: a common feature for management of energy reserves in African and American flagellated trypanosomatids. *J Eukaryot Microbiol,* 49**,** 82-5.

PEREIRA, C. A., BOUVIER, L. A., CAMARA MDE, L. & MIRANDA, M. R. 2011. Singular features of trypanosomatids' phosphotransferases involved in cell energy management. *Enzyme Res,* 2011**,** 576483.

PULLEN, T. J., GINGER, M. L., GASKELL, S. J. & GULL, K. 2004. Protein targeting of an unusual, evolutionarily conserved adenylate kinase to a eukaryotic flagellum. *Mol Biol Cell,* 15**,** 3257-65.

RALSTON, K. S., KABUTUTU, Z. P., MELEHANI, J. H., OBERHOLZER, M. & HILL, K. L. 2009. The *Trypanosoma brucei* flagellum: moving parasites in new directions. *Annu Rev Microbiol,* 63**,** 335-62.

RATTO, A., SHAPIRO, B. M. & CHRISTEN, R. 1989. Phosphagen kinase evolution. Expression in echinoderms. *Eur J Biochem,* 186**,** 195-203.

SALEH, M. A., AL-SALAHY, M. B. & SANOUSI, S. A. 2009. Oxidative stress in blood of camels (Camelus dromedaries) naturally infected with *Trypanosoma evansi. Vet Parasitol,* 162**,** 192-9.

SNAPP, E. L. & LANDFEAR, S. M. 1999. Characterization of a targeting motif for a flagellar membrane protein in *Leishmania enriettii*. *J Biol Chem,* 274**,** 29543-8.

SOMMER, J. M. & WANG, C. C. 1994. Targeting proteins to the glycosomes of African trypanosomes. *Annu Rev Microbiol,* 48**,** 105-38.

SUBRAMANI, S. 2002. Hitchhiking fads en route to peroxisomes. *J Cell Biol,* 156**,** 415-7.

TIWARI, B. S., BELENGHI, B. & LEVINE, A. 2002. Oxidative stress increased respiration and generation of reactive oxygen species, resulting in ATP depletion, opening of mitochondrial permeability transition, and programmed cell death. *Plant physiology,* 128**,** 1271-81.

TOMBES, R. M. & SHAPIRO, B. M. 1985. Metabolite channeling: a phosphorylcreatine shuttle to mediate high energy phosphate transport between sperm mitochondrion and tail. *Cell,* 41**,** 325-34.

TURRENS, J. F. 2004. Oxidative stress and antioxidant defenses: a target for the treatment of diseases caused by parasitic protozoa. *Mol Aspects Med,* 25**,** 211-20.

VAN HELLEMOND, J. J., OPPERDOES, F. R. & TIELENS, A. G. 2005. The extraordinary mitochondrion and unusual citric acid cycle in *Trypanosoma brucei. Biochem Soc Trans,* 33**,** 967-71.

VIANT, M. R., ROSENBLUM, E. S. & TJEERDEMA, R. S. 2001. Optimized method for the determination of phosphoarginine in abalone tissue by high-performance liquid chromatography. *J Chromatogr B Biomed Sci Appl,* 765**,** 107-11.

VICKERMAN, K. 1985. Developmental cycles and biology of pathogenic trypanosomes. *Br Med Bull,* 41**,** 105-14.

VONCKEN, F., GAO, F., WADFORTH, C., HARLEY, M. & COLASANTE, C. 2013. The Phosphoarginine Energy-Buffering System of *Trypanosoma brucei* Involves Multiple Arginine Kinase Isoforms with Different Subcellular Locations. *PLoS One,* 8.

VONCKEN, F., VAN HELLEMOND, J. J., PFISTERER, I., MAIER, A., HILLMER, S. & CLAYTON, C. 2003. Depletion of GIM5 causes cellular fragility, a decreased glycosome number, and reduced levels of ether-linked phospholipids in trypanosomes. *J Biol Chem,* 278**,** 35299-310.

WALLIMANN, T., WYSS, M., BRDICZKA, D., NICOLAY, K. & EPPENBERGER, H. M. 1992. Intracellular compartmentation, structure and function of creatine kinase isoenzymes in tissues with high and fluctuating energy demands: the 'phosphocreatine circuit' for cellular energy homeostasis. *Biochem J,* 281 (Pt 1)**,** 21-40.

WATTS, D. C. & BANNISTER, L. H. 1970. Location of arginine kinase in the cilia of *Tetrahymena pyriformis*. *Nature,* 226**,** 450-1.

WRIGHT-WEBER, B., HELD, B. C., BROWN, A. & GROSSMAN, S. H. 2006. Immunological and physical comparison of monomeric and dimeric phosphagen kinases: Some evolutionary implications. *Biochim Biophys Acta,* 1760**,** 364-71.

Chapter V

Discussion and Conclusion

Discussion

The mitochondrion plays an important role in the cellular energy (ATP) provision of virtually all eukaryotes (Henze and Martin, 2003). This also includes *Trypanosoma brucei*, although the importance of mitochondrial ATP production in this parasite seems to be restricted to mainly the procyclic form (Bochud-Allemann and Schneider, 2002;Schneider et al., 2007). Its TCA (Krebs) cycle does not contribute to ATP production in the conventional way (van Weelden et al., 2003), and mitochondrial ATP is mainly produced by substrate level and oxidative phosphorylation using the amino acid proline as the main energy-providing substrate (Bochud-Allemann and Schneider, 2002;Bringaud et al., 2012). Oxidative phosphorylation is in PCF *T. brucei* driven by the proton motive force generated by the electron transport chain (functional complexes I-IV) and terminal alternative oxidase (TAO), and the proton-pumping ATP-synthase complex located in the mitochondrial inner membrane (Njogu et al., 1980). To maintain the cellular energy provision, the produced ATP has to be exported from the mitochondrial matrix in exchange for ADP and Pi from the cytosol. It has been shown in this PhD thesis that in PCF *T. brucei* this exchange is facilitated by two MCF proteins, i.e. the ADP/ATP carrier TbMCP5 (Chapter II) and the phosphate carrier TbMCP11 (Chapter III) located in the mitochondrial inner membrane.

The MCF inventory of *T. brucei* includes next to TbMCP5 another putative ADP/ATP carrier, i.e. TbMCP15, with significant sequence similarity to TbMCP5 and functionally characterised ADP/ATP carriers from other eukaryotes (Chapter II) (Colasante et al., 2009). Comprehensive sequence analysis confirmed that TbMCP5 contains canonical ADP/ATP carrier sequence features (Colasante et al., 2009;Kunji,

2004), whereas they are not conserved in TbMCP15. Heterologous expression in the *ANC*-deficient yeast strain *JL1Δ2Δ3u*$^{-}$ (Clemencon et al., 2008) revealed that only TbMCP5 was able to restore its growth on the non-fermentable carbon source lactate. These results suggest that TbMCP15 does not function as a classical ADP/ATP carrier. Subsequent transport studies using TbMCP5-complemented *JL1Δ2Δ3u*$^{-}$ mitochondria confirmed that TbMCP5 has similar biochemical properties and ADP/ATP-exchange kinetics as Anc2p, the prototypical ADP/ATP carrier of *S. cerevisiae* (Chapter II, (Pena-Diaz et al., 2012)). Immunofluorescence microscopy and western blot analysis confirmed further that TbMCP5 is exclusively mitochondrial and is differentially expressed with 4.5-fold more TbMCP5 present in the procyclic form then in the bloodstream form. Silencing of TbMCP5 expression in PCF *T. brucei* revealed that this ADP/ATP carrier is essential for parasite growth, particularly when depending on proline for energy generation. Moreover, ADP/ATP-exchange in isolated PCF *T. brucei* mitochondria was eliminated upon depletion TbMCP5, which indicated that TbMCP5 is the main or even the only ADP/ATP exchanger present in the PCF *T. brucei* mitochondrion. The mitochondrial transport function and physiological role of TbMCP15 remains unclear at this point, and requires further investigation.

Next to the phosphate carrier TbMCP11, the *T. brucei* MCF protein inventory includes another putative phosphate carrier, i.e. TbMCP8, with significant sequence similarity to TbMCP11 and functionally characterized phosphate carriers from other eukaryotes (Chapter III) (Colasante et al., 2009). Expression analysis (mRNA level) revealed however that TbMCP8 is not expressed in BSF or PCF *T. brucei*. This in contrast to TbMCP11, which is expressed in both life cycle stages, with 2.5-fold more TbMCP11 present in the procyclic form. Analysis of the TbMCP11-depleted BSF

Δ*TbMCP11* and PCF *TbMCP11-RNAi* cell lines revealed that this phosphate carrier is not required for growth of the BSF, but that it is essential for the growth of PCF *T. brucei*. Depletion of TbMCP11 (*TbMCP11-RNAi*) resulted in loss of the mitochondrial membrane potential and the ablation of mitochondrial ATP production in PCF *T. brucei*. Expression of TbMCP11 in the phosphate carrier-deficient *S. cerevisiae* deletion strain Δ*Mir1*Δ*Pic2* (Hamel et al., 2004) partly restored its growth on the non-fermentable carbon sources lactate and glycerol. TbMCP11 expression further restored swelling of the phosphate carrier-deficient Δ*Mir1*Δ*Pic2* and *T. brucei TbMCP11-RNAi* mitochondria in a phosphate-dependent fashion, confirming its predicted phosphate transport function. The level of functional complementation of the mitochondrial phosphate transport function in yeast was dependent on the presence of a host-specific mitochondrial targeting sequence in TbMCP11. Overall, these results confirmed that TbMCP11 functions as the main or even the only mitochondrial phosphate carrier in PCF *T. brucei*.

The increased TbMCP5 and TbMCP11 levels, and the fact that both MCF proteins are essential in PCF *T. brucei,* is in agreement with the important role of the mitochondrion in this life cycle stage, i.e. the provision of ATP to the rest of the cell. This implies that in PCF *T. brucei*, TbMCP5 most probably mainly functions in the export of mitochondrial ATP to the cytosol, while TbMCP11 most probably functions in the import of cytosolic phosphate into the mitochondrial matrix.

In contrast to PCF *T. brucei*, the BSF *trypanosome* relies exclusively on glycolysis and a concomitant ATP-production in the cytosol of the parasite (Michels et al., 2000;Opperdoes, 1987). Its mitochondrion lacks a functional respiratory chain and key enzymes of the TCA cycle (van Hellemond et al., 2005), and has reduced ATP-

synthase levels in comparison to PCF *T. brucei* (Schnaufer et al., 2005;Brown et al., 2006). This argues for a less significant role of the BSF mitochondrion in cellular ATP provision, and in agreement with this, significantly lower levels of TbMCP5 (Chapter II) and phosphate carrier TbMCP11 are present in its mitochondrion (Chapter III). Depletion of the mitochondrial ATP-synthase activity in BSF *T. brucei* by RNA interference revealed an essential role of this enzyme in the maintenance of the mitochondrial membrane potential (Schnaufer et al., 2005;Brown et al., 2006). This in turn implies a mitochondrial requirement for ATP, which drives the proton-pumping function of the ATP-synthase. The ADP/ATP carrier TbMCP5 could fulfill this function and play an important role in the import of cytosolic glycolysis-derived ATP into the mitochondrial matrix of BSF *trypanosomes*. Such import would not only support the maintenance of the mitochondrial membrane potential, but would also provide energy for essential anabolic metabolism in the BSF mitochondrion (van Hellemond et al., 2005). That TbMCP5 plays such a physiological role in BSF *T. brucei* has still to be proven, but preliminary experiments showed that BSF *T. brucei* ceased its growth and mitochondrial ATP-production upon the addition of the specific ADP/ATP carrier inhibitor carboxyatractyloside (not shown in this thesis), which suggests an essential role of TbMCP5 in this life cycle stage. The ADP formed in the mitochondrial matrix will be exported during ADP/ATP exchange, whereas the fate of the formed Pi, which also has to be exported from the mitochondrial matrix, is still unclear at this point. The double knockout of TbMCP11 had however no effect on BSF growth, which suggests that this phosphate carrier is not required in this life cycle stage (Chapter III). Whether this mitochondrial phosphate export is driven by a different MCF protein or is maybe even not required at all, is not clear at this point and requires further investigation. Preliminary experiments showed further that this

phosphate transport function is certainly not taken over by the putative phosphate carrier TbMCP8, which is the only other predicted phosphate carrier in the *T. brucei* MCF protein inventory (Colasante et al., 2009). Its expression is however not induced/up-regulated in the TbMCP11-deficient BSF and PCF *T. brucei* cell lines (not shown in this thesis). The transport function and physiological role of TbMCP8, and whether TbMCP8 is expressed in a different life cycle stage of *T. brucei* or is only expressed under specific environmental conditions, remains unclear at this point and is subject to further investigation.

The cellular energy homeostasis in virtually all eukaryotic cells is dependent on a phosphagen energy-buffering system, which in periods of high-energy demand or energy supply fluctuations can provide the cell with essential ATP (Ellington, 2001). The phosphoarginine/arginine kinase-dependent energy buffering system of the kinetoplastid parasite *Trypanosoma brucei* consists of three highly similar arginine kinase isoforms, i.e. TbAK1-3 (Chapter IV). Localisation studies using recombinant myc-tagged protein versions revealed that each isoform is located in a specific subcellular compartment of *T. brucei*: TbAK1 is exclusively found in the flagellum, TbAK2 in the glycosome, and TbAK3 in the cytosol of the parasite. The flagellar location of TbAK1 is dependent on a 22 amino acid long N-terminal extension, which apparently functions as a flagellar targeting signal in *T. brucei*. The glycosomal location of TbAK2 is in agreement with the presence of a conserved peroxisomal targeting signal, the C-terminal tripeptide ‘SNL’ (Sommer and Wang, 1994;Amery et al., 1998). TbAK3 lacks any apparent targeting sequences and is accordingly located in the cytosol of the parasite.

Expression analysis revealed that each TbAK isoform is differentially expressed in BSF and PCF *T. brucei*, while the total cellular arginine kinase activity was 3-fold higher in BSF trypanosomes. The differential expression of the TbAK1-3 isoforms and their different subcellular locations in *T. brucei* indicates a substantial change in the temporal and spatial energy requirements during parasite differentiation. The expression of the flagellar arginine kinase TbAK1 and cytosolic arginine kinase TbAK3 was significantly up regulated in PCF *T. brucei*, suggesting an increased arginine kinase activity in the parasite's cytosol and flagellum. PCF trypanosomes initially develop and multiply in the midgut of the tsetse fly, after which they migrate through the peritrophic membrane into the ectoperitropic space, followed by the proventriculus, the foregut, and finally the salivary glands (Matthews et al., 2004;Ralston et al., 2009). This migration of PCF *T. brucei* in the Tsetse fly requires significant motility, which in turn implies the constant provision of sufficient ATP to the flagellum (see (Ralston et al., 2009) references therein). Since no ATP is produced in the flagellum (Ralston et al., 2009), it is reasonable to assume that TbAK1 is predominantly working in the ATP-forming direction, i.e. converting phosphoarginine and ADP into arginine and ATP, thereby fuelling flagellar motility. In PCF *T. brucei*, the mitochondrion is the predominant source of ATP (Kohl and Bastin, 2005), which is exported to the cytosol by TbMCP5 (Chapter II). In the cytosol, ATP will be either directly consumed or temporary stored as phosphoarginine, which is catalysed by the cytosolic arginine kinase TbAK3. Phosphoarginine can subsequently diffuse to the flagellum and fuel motility through ATP provided by TbAK1 activity.

Expression analysis revealed further that in BSF *T. brucei* the glycosomal arginine kinase TbAK2 was abundantly expressed (Chapter IV). In BSF *T. brucei*, ATP is

predominantly produced by glycolysis (Michels et al., 2000;Opperdoes, 1987). The latest metabolic model suggests a balanced ATP production and consumption in the glycosome, with net ATP primarily produced in the cytosol (Bakker et al., 1997). In addition, it has been shown that no ADP/ATP exchange takes place in the glycosome (Bakker et al., 1997). The physiological function of TbAK2 in the glycosome is not clear at this point, apart from the formation of a putative glycosomal energy buffering system. It is feasible that under certain physiological conditions either a surplus or deficit of ATP can exist in the glycosome (van Weelden et al., 2005). The resulting glycosomal ADP/ATP imbalance would negatively affect the glycolytic pathway in the glycosome, and the survival of the BSF parasite. The presence of a phosphoarginine/arginine kinase (TbAK2) energy buffering system in the glycosome would prevent this. The *T. brucei* glycosome contains further several adenylate kinases, which catalyse the reversible conversion of AMP and ATP to 2 molecules of ADP (Opperdoes et al., 1981). The removal of the waste product AMP is essential since its accumulation would inhibit biosynthesis. The presence of both adenylate kinases and TbAK2 in the BSF glycosome argues for the existence of a glycosomal energy buffering system, which most probably plays an important role in the maintenance of the glycosomal ATP/ADP balance.

Overexpression of TbAK1-3 particularly improved PCF *T. brucei* growth during oxidative challenges with hydrogen peroxide, whereas elimination of the total cellular arginine kinase activity by RNA interference significantly affected PCF growth under standard culture conditions and was even lethal in the presence of hydrogen peroxide. These results suggested that the phosphoarginine/arginine kinase system plays an important role in oxidative stress response. The different developmental stages of *T. brucei* are constantly exposed to oxidative stress as a result of the innate immune

response of its different hosts, but also as a consequence of its own unusual, partly aerobic fermentative energy metabolism. In particular the mammalian bloodstream is highly abundant in oxidative stress factors (Turrens, 2004). Measurement of total cellular arginine kinase activity indeed revealed a substantially higher specific arginine kinase activity in BSF *T. brucei*, which correlated well with its substantially increased capacity to withstand oxidative stress.

In addition, I have done the mitochondrial proteomics analysis for both bloodstream and procyclic form *Trypanosoma brucei.* The results showed most enzymes required for TCA cycle were found in the mitochondrion of both bloodstream and procyclic form *Trypanosoma brucei.* Furthermore the mitochondrial ATP production assay has been done with different substrates for TCA cycle. The preliminary results showed that the bloodstream form of *T.brucei* still produced a certain amount of ATP although at much lower levels compare with procyclic form *T.brucei.* These results need to be repeated to gain a reliable estimate of mitochondrial ATP production assay in the bloodstream form of *T.brucei.* In the future, depletion of TbMCP5 in the bloodstream form *Trypanosoma brucei* could be done for further studying the mitochondrion function in bloodstream form *T.brucei.*

Conclusions

The mitochondrial carrier family proteins TbMCP5 and TbMCP11 are essential for the maintenance of the energy homeostasis in *T. brucei* by facilitating respectively ADP/ATP-exchange and phosphate transport in its mitochondrion. *T. brucei* contains in addition an essential phosphoarginine-dependent energy buffering system consisting of multiple arginine kinase isoforms (TbAK1-3) in different subcellular

compartments. This system plays a key role in the maintenance of the energy homeostasis in the different life cycle stages of *T. brucei*.

References

AMERY, L., BREES, C., BAES, M., SETOYAMA, C., MIURA, R., MANNAERTS, G. P. & VAN VELDHOVEN, P. P. 1998. C-terminal tripeptide Ser-Asn-Leu (SNL) of human D-aspartate oxidase is a functional peroxisome-targeting signal. *Biochem J,* 336 (Pt 2)**,** 367-71.

BAKKER, B. M., MICHELS, P. A., OPPERDOES, F. R. & WESTERHOFF, H. V. 1997. Glycolysis in bloodstream form *Trypanosoma brucei* can be understood in terms of the kinetics of the glycolytic enzymes. *J Biol Chem,* 272**,** 3207-15.

BOCHUD-ALLEMANN, N. & SCHNEIDER, A. 2002. Mitochondrial substrate level phosphorylation is essential for growth of procyclic *Trypanosoma brucei*. *J Biol Chem,* 277**,** 32849-54.

BRINGAUD, F., BARRETT, M. P. & ZILBERSTEIN, D. 2012. Multiple roles of proline transport and metabolism in trypanosomatids. *Front Biosci,* 17**,** 349-74.

BROWN, S. V., HOSKING, P., LI, J. & WILLIAMS, N. 2006. ATP synthase is responsible for maintaining mitochondrial membrane potential in bloodstream form *Trypanosoma brucei*. *Eukaryot Cell,* 5**,** 45-53.

CLEMENCON, B., REY, M., DIANOUX, A. C., TREZEGUET, V., LAUQUIN, G. J., BRANDOLIN, G. & PELOSI, L. 2008. Structure-function relationships of the C-terminal end of the Saccharomyces cerevisiae ADP/ATP carrier isoform 2. *J Biol Chem,* 283**,** 11218-25.

COLASANTE, C., PENA DIAZ, P., CLAYTON, C. & VONCKEN, F. 2009. Mitochondrial carrier family inventory of *Trypanosoma brucei* brucei: Identification, expression and subcellular localisation. *Mol Biochem Parasitol,* 167**,** 104-17.

ELLINGTON, W. R. 2001. Evolution and physiological roles of phosphagen systems. *Annu Rev Physiol,* 63**,** 289-325.

HAMEL, P., SAINT-GEORGES, Y., DE PINTO, B., LACHACINSKI, N., ALTAMURA, N. & DUJARDIN, G. 2004. Redundancy in the function of mitochondrial phosphate transport in Saccharomyces cerevisiae and Arabidopsis thaliana. *Mol Microbiol,* 51**,** 307-17.

HENZE, K. & MARTIN, W. 2003. Evolutionary biology: essence of mitochondria. *Nature,* 426**,** 127-8.

KOHL, L. & BASTIN, P. 2005. The flagellum of trypanosomes. *Int Rev Cytol,* 244**,** 227-85.

KUNJI, E. R. 2004. The role and structure of mitochondrial carriers. *FEBS Lett,* 564**,** 239-44.

MATTHEWS, K. R., ELLIS, J. R. & PATEROU, A. 2004. Molecular regulation of the life cycle of African trypanosomes. *Trends Parasitol,* 20**,** 40-7.

MICHELS, P. A., HANNAERT, V. & BRINGAUD, F. 2000. Metabolic aspects of glycosomes in trypanosomatidae - new data and views. *Parasitol Today,* 16**,** 482-9.

NJOGU, R. M., WHITTAKER, C. J. & HILL, G. C. 1980. Evidence for a branched electron transport chain in *Trypanosoma brucei*. *Mol Biochem Parasitol,* 1**,** 13-29.

OPPERDOES, F. R. 1987. Compartmentation of carbohydrate metabolism in trypanosomes. *Annu Rev Microbiol,* 41**,** 127-51.

OPPERDOES, F. R., MARKOS, A. & STEIGER, R. F. 1981. Localization of malate dehydrogenase, adenylate kinase and glycolytic enzymes in glycosomes and

the threonine pathway in the mitochondrion of cultured procyclic trypomastigotes of *Trypanosoma brucei*. *Mol Biochem Parasitol,* 4**,** 291-309.

PENA-DIAZ, P., PELOSI, L., EBIKEME, C., COLASANTE, C., GAO, F., BRINGAUD, F. & VONCKEN, F. 2012. Functional characterization of TbMCP5, a conserved and essential ADP/ATP carrier present in the mitochondrion of the human pathogen *Trypanosoma brucei*. *J Biol Chem,* 287**,** 41861-74.

RALSTON, K. S., KABUTUTU, Z. P., MELEHANI, J. H., OBERHOLZER, M. & HILL, K. L. 2009. The *Trypanosoma brucei* flagellum: moving parasites in new directions. *Annu Rev Microbiol,* 63**,** 335-62.

SCHNAUFER, A., CLARK-WALKER, G. D., STEINBERG, A. G. & STUART, K. 2005. The F1-ATP synthase complex in bloodstream stage trypanosomes has an unusual and essential function. *EMBO J,* 24**,** 4029-40.

SCHNEIDER, A., BOUZAIDI-TIALI, N., CHANEZ, A. L. & BULLIARD, L. 2007. ATP production in isolated mitochondria of procyclic *Trypanosoma brucei. Methods Mol Biol,* 372**,** 379-87.

SOMMER, J. M. & WANG, C. C. 1994. Targeting proteins to the glycosomes of African trypanosomes. *Annu Rev Microbiol,* 48**,** 105-38.

TURRENS, J. F. 2004. Oxidative stress and antioxidant defenses: a target for the treatment of diseases caused by parasitic protozoa. *Mol Aspects Med,* 25**,** 211-20.

VAN HELLEMOND, J. J., OPPERDOES, F. R. & TIELENS, A. G. 2005. The extraordinary mitochondrion and unusual citric acid cycle in *Trypanosoma brucei*. *Biochem Soc Trans,* 33**,** 967-71.

VAN WEELDEN, S. W., FAST, B., VOGT, A., VAN DER MEER, P., SAAS, J., VAN HELLEMOND, J. J., TIELENS, A. G. & BOSHART, M. 2003. Procyclic *Trypanosoma brucei* do not use Krebs cycle activity for energy generation. *J Biol Chem,* 278**,** 12854-63.

VAN WEELDEN, S. W., VAN HELLEMOND, J. J., OPPERDOES, F. R. & TIELENS, A. G. 2005. New functions for parts of the Krebs cycle in procyclic *Trypanosoma brucei*, a cycle not operating as a cycle. *J Biol Chem,* 280**,** 12451-60.

Appendix 1, medium used for *T.brucei* culture

1. MEM-Pros (Minimum Essential Medium for procyclic Trypanosomes)

Proline-free MEM-Pros medium

	g/5L
$CaCl_2$. $2H_2O$	1.375
KCl	2.0
$MgSO_4$. $7H_2O$	2.0
NaCl	34.0
NaH_2PO_4. H_2O	0.70
HEPES	35.70
L-Arginine-HCl	0.63
L-Cystine	0.12
L-Glutamine	1.46
L-Histidine-HCl. H_2O	0.21
L-Isoleucine	0.26
L-Leucine	0.26
L-Lysine	0.365
L-Methionine	0.075
L-Phenylalanine	0.50
L-Threonine	0.24
L-Tryptophane	0.05
L-Tyrosine	0.50
L-Valine	0.23
Adenosin	0.12
Ornithin-HCl	0.10

Non-essential amino acids

	mg/5L
Glycine	37.50
L-Alanine	44.50

L-Asparagine	66.00
L-Aspartic Acid	66.50
L-Glutamic Acid	73.50
L-Serine	52.50

Components of proline-free MEM-Pros medium are dissolved in 4 L ultra-pure H_2O. pH is adjusted to 7.4 with 10M NaOH. 50 mL MEM-Vitamins, 50 mg Phenol Red and 20ml X5 non-essential amino acids are then added to the solution. pH is adjusted to 7.4 again and the medium is brought to 5 L volume with ultra pure H_2O. After filter-sterilizing, the medium is divided in 450 mL aliquots in sterile glass bottles and placed at 4°C. Before use, phleomycin (0.5 µg/ml), FCS (10%), haemin (7.5 µg/ml), Penicillin/Streptomycin (50 units/ml) and proline (5mM) are filtered to each bottle.

2. HMI-9 medium. (Bloodstream trypanosomes culture medium)

	g/10L
Iscove's modified Dulbecco's medium (Gibco-BRL #42200)	176.6
Sodium bicarbonate	30.24
Hypoxanthine	1.36
Sodium pyruvate	1.10
Thymidine	0.39
Bathocuprone sulfate	0.28

Components are mixed and adjusted to pH 7.5 with 10M NaOH. The medium is filter-sterilized, divided in 450 mL aliquots in sterile glass bottles and kept at -20°C. Before use, the medium in each bottle is completed with 50 mL FCS, 2.5mL 100mM L-Cysteine solution (prepared just before use), 7 µl β-mercaptoethanol, 5 µl phleomycin (20 mg/ml stock) and 5 mL Penicillin/Streptomycin stock (stock concentration, 5000 U/mL, 5mg/mL).

3. SDM-79/80 medium (for procyclic form trypanosomes)

	Amount/10L
MEM (Earl's) Powder	70.0 g
Media 199 powder	20.0 g
50 × MEM essential amino acids	80.0 ml
100 × MEM non-essential a.a.	60.0 ml
Glucose (Anhydrous)	10.0 g (depleted for SDM 80)
HEPES (sodium salt)	80.0 g
MOPS (free acid)	50.0 g
Sodium Bicarbonate	20.0 g
Sodium pyruvate	1.0 g
DL- Alanine	2000 mg
L-Arginine	1000 mg
L-Glutamine	3000 mg
DL-Methionine	700 mg
L-Phenylalanine	800 mg
L-Proline	6000 mg
DL-Serine	600 mg
Taurine	1600 mg
DL-Threonine	3500 mg
L-Tyrosine	1000 mg
Guanosine	100 mg
Folic acid	40 mg
D(+)glucosamine hydrochloride	500 mg
p-Aminobenzoic acid	20 mg
Biotin	2 mg
BME vitamin solution 100 ×	100 ml

Components are mixed and brought to 10 L. pH is adjust to 7.4 with 10M NaOH. The medium is filter-sterilized, divided in 450 mL aliquots in sterile glass bottles and kept at 4°C. Before use, the medium in each bottle is completed with 10% FCS, 50 units/ml Penicillin/Streptomycin.

Appendix 2, medium used for yeast culture.

1. YNB - yeast nitrogen broth medium

	Amount/L
Yeast nitrogen base without amino acids	6.7g
10 × yeast synthetic dropout solution (containing all standard amino acids with 76 mg/L concentration except Leucine with 380mg/L, adenine 18 mg/L, inositol 76 mg/L and p-aminobenzoic acid 8 mg/L) (Sigma)	100ml

Add water (for making plate add 2% agar) and adjust the pH to 5.8, and autoclave. After the medium cool to about 55 °C, then add sterile glucose to 2%.

2. YPD- yeast extract peptone dextrose medium

	Concentration
Yeast extract	1% (w/v)
Peptone	2% (w/v)
Glucose	2% (w/v)

3. YPG – yeast extract peptone glycerol medium

	Concentration
yeast extract	1% (w/v)
peptone	2% (w/v)
glycerol	3% (w/v)

4. YPL – yeast extract peptone lactate medium

	Concentration
yeast extract	1% (w/v)
peptone	2% (w/v)
lactate	2% (w/v)

Adjust the pH to 5.5 using KOH, then autoclave.

Appendix 3, yeast strains used for transformation

Statin name	genotype
Saccharomyces cerevisiae BY4741 (kindly provided by Dr. Johannes A. Mayr)	MATa; his3Δ 1; leu2Δ 0; met15Δ 0; ura3Δ 0
Saccharomyces cerevisiae JL1Δ2Δ3u^{-} (from Dr. Ludovic Pelosi)	Source strain is W303 (Matα *leu*2-3,112 *his*3-11 *ade*2-1 *trp*1-1 *ura*3-1). JL-1-3 (*W303-1B anc1*::*LEU2 anc2*::*HIS3 anc3*::*URA3)* is derived from W303. *JL1Δ2Δ3u*$^{-}$ (JL-1–3 Δ*anc2*::*HIS3* Δ[269–975]*anc3*) is derived from JL-1-3
Saccharomyces cerevisiae strain Δ*mir1*Δ*pic2* (kindly provided by Dr. Johannes A. Mayr)	Source strain BMA64 is a diploid homozygous for *ade2–1, ura3–1, his3–11,-15,* Δ*trp1, leu 2–3,-112. MIR1,* a 933-bp *Hin*cII fragment was replaced by a 1162 bp *Pvu*II fragment carrying the *TRP1* gene. For *PIC2*, a 913 bp *Bgl*II-*Pst*I fragment was replaced by a 2751 bp *Nsi*I-*Bam*HI fragment carrying the *LEU2* gene. Trp + or Leu + diploids were depleted for single mutant strain. Double mutant strain was constructed by crossing the two single mutants.